BEST AVAILABLE IMAGES

Defective images within this document are accurate representations of the original documents submitted by the applicant.

Defects in the images may include (but are not limited to):

- BLACK BORDERS
- TEXT CUT OFF AT TOP, BOTTOM OR SIDES
- FADED TEXT
- ILLEGIBLE TEXT
- SKEWED/SLANTED IMAGES
- COLORED PHOTOS
- BLACK OR VERY BLACK AND WHITE DARK PHOTOS
- GRAY SCALE DOCUMENTS

IMAGES ARE BEST AVAILABLE COPY.

As rescanning documents *will not* correct images, please do not report the images to the Image Problem Mailbox.

I hereby certify that this correspondence is being deposited with the United States Postal Service as first class mail in an envelope addressed to: Commissioner of Patents and Trademarks, Washington, D.C. 20231 on May 1, 1996

Dan T. Stinchcomb

Declaration of Dan T. Stinchcomb, Ph.D.

1. I am the Director of Biology at Ribozyme Pharmaceuticals, Inc. in Boulder Colorado. I have worked in the field of Ribozymes since 1993. My *Curriculum Vitae* is attached (Appendix A).

2. I have reviewed the specification of patent application entitled "Modified Ribozymes", US Serial No. 08/434,547 and related divisional applications–Serial Nos. 08/434,506; and 08/434,533. Following is my analysis of the efficacy of "Modified Ribozymes" *in vivo* and the potential application of ribozymes as therapeutic agents.

3. The application describes ribozymes having "catalytic" activity and "enhanced stability against chemical and enzymatic degradation." Modification of ribozymes at the sugar 2'-position with a "modifier group" such as halo, azido, sulfhydryl, amino, mono-substituted amino and disubstituted amino groups, have been shown to enhance the stability of ribozymes against nuclease degradation without affecting the ability of these modified ribozymes to cleave target RNA. One of the main purposes for enhancing the stability of ribozymes inside a cell is to improve their effectiveness as a therapeutic agent and/or as a "biocatalyst."

4. The potential for using ribozymes as therapeutic agents to diagnose and treat variety of diseases is well recognized and has been the subject of active research for the past ten years (for a review see Christoffersen and Marr, 1995 *J. Med. Chem.* 38, 2023; copy enclosed as Exhibit 1).

5. While no *in vivo* data is provided in the above-captioned application, examples discussed in this declaration, and in the art, amply support the use of approaches described in the application, to successfully synthesize nuclease-stable ribozymes for sequence-specific cleavage of RNA in a cell culture or an animal model system. I believe that cell culture and animal data showing efficacy of chemicaliy-modified ribozymes is reasonably predictive of their utility as a therapeutic agent.

6. Unmodified RNA is unstable in biological sera. Thus, a significant challenge in using ribozymes as drugs is to modify the RNA chemically to increase ribozyme stability while retaining ribozyme catalytic activity. A number of structural modifications have been applied to oligonucleotides in general to enhance nuclease resistance, as described in the application. The majority of this work has been carried out with hammerhead ribozymes since their small size makes them amenable to chemical synthesis and modification. Similar modifications can be readily introduced into other ribozyme motifs such as the hairpin ribozyme by adopting the teachings of the above application.

7. Chemically synthesized (and nuclease-stable) ribozymes can be directly delivered to cells and tissues using a variety of approaches known in the art (for a review see Exhibit 1). For example, ribozymes delivered by intra-articular injection have been shown to cleave target mRNA in synovial tissues (Flory *et al.* 1995, *Proc. Natl. Acad. Sci.*, 93, 754; Exhibit 2). Formulation of ribozymes in a gel form has been successfully employed to deliver ribozymes to the cornea of the eye [Ayers *et al.* 1995, *J. Controlled Rel.* (in press); Exhibit 3]. Ribozymes have also been successfully incorporated into poly L-lactic acid polymers and their delayed release in *vitro* has been documented (Lewis *et al.* 1995 *J. Cell. Biochem.* S19A, 227; Exhibit 4). There are a number of additional approaches described in the art that can be readily adopted to deliver ribozymes into a cell. The choice of delivery system can be readily made by carrying out routine and standard experiments well known in the art.

8. Following are a few examples of chemically-modified ribozyme efficacy in cell culture and animal models. These examples demonstrate the general utility of the chemically-modified ribozymes as potential therapeutic agents, as disclosed in the application.

Ribozyme Efficacy In Cell Culture Model Systems:

9. *Ribozymes Targeting MDR-1*: Chemically synthesized DNA/RNA chimeric ribozymes have been used to cleave *MDR-1* mRNA (Kiehntopf *et al.*, 1994, *EMBO. J.* 13, 4645; Exhibit 5). *MDR-1* encodes a phosphoglycoprotein

that can cause multiple drug resistance (MDR) in cancer cells. In this case, the hammerhead ribozyme contained DNA sequences in its binding arms and 2'-deoxy-2'-fluoro pyrimidine nucleotides in the ribozyme catalytic core and stem-loop II region. Ribozymes modified with 2'-deoxy-2'-fluoro groups are specifically described in the above-referenced applications and are known to increase nuclease resistance of the ribozymes (see also Exhibit 6). Ribozymes were delivered to cells as complexes with a cationic lipid. After treatment, drug resistant cell lines showed reduced expression of the *MDR-1* gene product, reduced ability to export rhodamine and increased sensitivity to the anti-neoplastic drug, vindesine. Interestingly, the DNA/RNA chimeric ribozymes showed enhanced efficacy relative to an all RNA ribozyme or an antisense phosphorothioate DNA control; an inactive all RNA ribozyme had no effect on gene expression or drug resistance. Synthetic chemically-modified ribozymes directed against *MDR-1* may provide a means of reversing drug resistance that can be observed in cancer patients during chemotherapy.

I performed or had performed on my behalf, the experiments discussed in Sections 10-13, *infra*.

10. *Ribozymes Targeting c-myb:* Coronary angioplasty is widely used to surgically treat atherosclerosis. Unfortunately, 35-45% of angioplasty patients develop restenosis or reocclusion of the treated vessel within 6 months of the operation. Restenosis after angioplasty is associated with activation and proliferation of underlying smooth muscle cells. The hyperproliferation and excessive matrix deposition by these cells contribute to a reduction in the diameter of the lumen and eventual occlusion of the vessel. Ribozymes capable of inhibiting smooth muscle cell activation and proliferation could be used therapeutically to reduce intimal thickening and restenosis.

The proto-oncogene, c-*myb* is thought to be a critical regulator of smooth muscle cell proliferation. Ribozymes with optimal activity were synthesized using the nuclease-stable ribozyme motif described in the application and by Beigelman *et al.*, 1995 *J. Biol. Chem.* 270, 25702; Exhibit 6). The hammerhead ribozymes contained either 1) 2′-*C*-allyl substitution at U_4 position, five ribose residues, four phosphorothioate linkages between

nucleotides in the 5′-binding arm, an inverted 3′-3′-linked nucleotide at the 3′-terminus, and 2'-*O*-methyl substitutions at all the other positions; 2) or 2′-deoxy-2'-amino substitution at U_4 and U_7 positions, five ribose residues, four phosphorothioate linkages between nucleotides in the 5′-binding arm, an inverted 3′-3′-linked nucleotide at the 3′-terminus and 2'-*O*-methyl substitutions at all the other positions. Ribozymes modified with 2'-deoxy-2'-amino groups are specifically described in the above-referenced applications and are known to increase nuclease resistance of the ribozymes (see also Exhibit 6).

The nuclease-stable ribozymes were applied to serum-starved smooth muscle cells as complexes with the cationic lipid, DOSPA. Active ribozymes effectively blocked serum-stimulated cell proliferation [Figures 2-6 of Jarvis *et al.,* 1996 *RNA* (in press), Exhibit 7; and Figures 3-6 of Jarvis *et al.,* 1996 (submitted for publication); Exhibit 11]. Inactive ribozymes or active ribozymes with scrambled binding arm sequences had little effect on cell proliferation. Ribozymes without modifications that render them stable to nucleases failed to dramatically inhibit cell proliferation. Thus, optimal inhibition of proliferation was sequence-specific and required a nuclease-stable catalytic core capable of cleaving the target mRNA. Indeed, when c-*myb* mRNA levels were measured by a quantitative polymerase chain reaction technique, the active ribozyme significantly reduced cellular levels of its target mRNA. The ability of these synthetic, nuclease-resistant ribozymes to inhibit smooth muscle cell proliferation raises the possibility of locally delivering ribozymes to vessel walls immediately following angioplasty procedures. Prevention of smooth muscle cell activation and proliferation by such ribozymes directed against c-*myb* may reduce the incidence of restenosis that occurs after coronary angioplasty.

11. *Ribozymes Targeting HIV-1 RNA:* Ribozymes with optimal activity were synthesized using the nuclease-stable ribozyme motif described in the application and by Beigelman *et al.,* 1995 *J. Biol. Chem.* 270, 25702; Exhibit 6). The hammerhead ribozymes contained the 2′-deoxy-2'-amino substitution at U4 and U7 positions, and an inverted 3′-3′ nucleotide at the 3′-terminus. Ribozymes modified with 2'-deoxy-2'-amino groups are specifically described in the above-referenced applications.

The nuclease-stable ribozymes, targeted against human immunodeficiency virus (HIV) LTR, were applied to $CD4^+$ 293 cells as complexes with calcium phosphate. The cells were then infected with HIV-1 and the level of viral protein, p24, production was measured at 6 days post infection. As shown in Exhibit 8, active 568 hammerhead ribozymes (Active 568 HH) effectively decreased HIV-1 p24 protein production at two different ribozyme concentrations of 3 and 6 μg. A decrease in HIV-1 p24 protein production is indicative of inhibition of HIV-1 replication. Inactive ribozymes (Inactive 568 HH), as expected, had little effect on p24 production since they are not capable of cleaving the target RNA. Thus, inhibition of viral replication was sequence-specific and required a nuclease-stable catalytic core capable of cleaving the target mRNA. The ability of these synthetic, nuclease-resistant ribozymes to inhibit HIV replication indicates the possibility of using ribozymes as potential anti-viral agents.

Ribozyme Efficacy in Animal Model Systems:

12. *Ribozyme efficacy in the Rabbit Knee model:* Osteoarthritis is a debilitating disease in which loss of cartilage can cause severe pain and incapacitation. The degradation of cartilage in osteoarthritic patients is correlated with excessive production of the matrix metalloproteinase, stromelysin. Nuclease-resistant ribozymes have been shown to reduce their stromelysin mRNA when injected into the synovium of rabbit knees (Flory *et al.* 1995; Exhibit 2).

The hammerhead ribozymes used in this study contained 1) 2′-*C*-allyl substitution at U_4 position, five ribose residues, four phosphorothioate linkages between nucleotides in the 5′-binding arm, an inverted 3′-3′-linked nucleotide at the 3′-terminus and 2'-*O*-methyl substitutions at all the other positions; 2) 2′-deoxy-2'-amino substitution at U_4 and U_7 positions, five ribose residues, four phosphorothioate linkages between nucleotides in the 5′-binding arm, an inverted 3′-3′-linked nucleotide at the 3′-terminus and 2'-*O*-methyl substitutions at all the other positions; 3) 2′-*C*-allyl substitution at U_4 position, five ribose residues, an inverted 3′-3′-linked nucleotide at the 3′-terminus and 2'-*O*-methyl substitutions at all the other positions; or 4) 2′-deoxy-2'-amino substitution at U_4 and U_7 positions, five ribose residues, an

inverted 3´-3´-linked nucleotide at the 3´-terminus and 2'-*O*-methyl substitutions at all the other positions. Ribozymes modified with 2'-deoxy-2'-amino groups and phosphorothioate substitutions are specifically described in the above-referenced applications and are known to increase nuclease resistance of the ribozymes (see also Exhibit 6).

Nuclease-stable ribozymes directed against the mRNA encoding stromelysin were injected in physiological saline solution and were shown to accumulate intact in synovial tissue. Twenty four hours after ribozyme administration, IL-1α was injected into the joint to induce stromelysin mRNA expression. Tissues were harvested 6 hours after IL-1α induction, synovial RNA was extracted and stromelysin mRNA was quantified by Northern or RNase protection analysis. Intra-articular injection of active ribozymes significantly reduced synovial levels of stromelysin mRNA (Figures 4-6 of Exhibit 2). Inactive or irrelevant ribozymes had no effect. Active ribozymes with several different chemical modifications (including the 2'-deoxy-2'-amino modifications described in the application), to provide nuclease-resistance, and targeting several different ribozyme cleavage sites in stromelysin mRNA were efficacious *in vivo*. Thus, nuclease-resistant ribozymes can specifically cleave target mRNAs *in vivo*. These experiments demonstrate the feasibility of using small, chemically synthesized ribozymes to impact gene expression in animal models of human disease. Furthermore, these ribozymes may be useful in reducing the active joint degradation that occurs in patients with osteoarthritis.

13. *Ribozyme efficacy in rat corneal model:* Vascular endothelial growth factor (VEGF) is a potent mitogen for endothelial cells and plays a role in several pathological conditions such as proliferative retinopathy and solid tumor growth. VEGF stimulates vascular endothelial cell growth and proliferation of new blood vessels *via* two transmembrane receptors, *Flt-1* and KDR.

As a novel approach to the regulation of abnormal angiogenesis, we have designed and tested ribozymes that are targeted to *Flt-1* and *KDR* mRNAs. Reduction of VEGF receptor mRNAs by ribozyme cleavage should lead to a reduced level of receptor protein and a subsequent decrease in

disease-related angiogenesis. All ribozymes used in these studies were prepared synthetically and are chemically stabilized with "modifier" groups, such as 2'-*C*-allyl and 2'-deoxy-2'-amino (specifically described in the above-referenced applications), to protect them from degradation.

We have identified a number of ribozymes targeted to both receptor mRNAs that are capable of significantly reducing VEGF-stimulated growth of human microvascular endothelial cells in culture. For example, as shown in Exhibit 12, hammerhead ribozymes targeted against two sites (site 1358 and 4229) within the *Flt-1* mRNA were synthesized with chemical modifications and tested in a cell-proliferation assay. The hammerhead ribozymes contained either 1) 2´-*C*-allyl substitution at U_4 position, five ribose residues, four phosphorothioate linkages between nucleotides in the 5´-binding arm, an inverted 3´-3´-linked nucleotide at the 3´-terminus and 2'-*O*-methyl substitutions at all the other positions (2'-*C*-allyl ribozymes); 2) or 2´-deoxy-2'-amino substitution at U_4 and U_7 positions, five ribose residues, four phosphorothioate linkages between nucleotides in the 5´-binding arm, an inverted 3´-3´-linked nucleotide at the 3´-terminus and 2'-*O*-methyl substitutions at all the other positions (2'-Amino ribozymes). Ribozymes modified with 2'-deoxy-2'-amino groups are specifically described in the above-referenced applications and are known to increase nuclease resistance of the ribozymes (see also Exhibit 6). Nuclease-stable hammerhead ribozymes targeted to both sites within *Flt-1* RNA were able to significantly inhibit VEGF-induced proliferation of human microvascular endothelial cells. The specificity of ribozyme action was demonstrated in that Fibroblast Growth Factor (FGF)-stimulated cell growth was completely unaffected by treatment with ribozymes targeting *Flt-1* VEGF receptor mRNAs.

Greater than 90% inhibition of VEGF-induced cell proliferation was observed when ribozymes directed against both *Flt-1* and KDR receptors were tested in combination. Control ribozymes, either catalytically inactive ribozymes or active ribozymes targeted to unrelated RNAs, had little or no effect on VEGF-stimulated cell growth.

Studies using a rat corneal model of angiogenesis in which VEGF protein and the chemically-stabilized ribozymes were co-delivered on a

nitrocellulose filter disk surgically implanted into the cornea have been carried out. Fluorescently-labeled ribozyme accumulated in the limbus region in or near the microvascular endothelial cells of the pericorneal vessels from which corneal neovascularization occurs. A significant portion of ^{32}P-labeled ribozyme remained intact in the eye for at least 72 hours. These two observations indicate that ribozymes accumulate and persist in the target tissue when administered in this manner.

In further studies using the same VEGF/ribozyme administration method described above, a synthetic chemically-stabilized hammerhead ribozyme (the ribozyme contained 2′-*C*-allyl substitution at U_4 position, five ribose residues, four phosphorothioate linkages between nucleotides in the 5′-binding arm, an inverted 3′-3′-linked nucleotide at the 3′-terminus and 2'-*O*-methyl substitutions at all the other positions) targeting site 4229 within *Flt-1* mRNA (Active 4229 HH) inhibited VEGF-induced angiogenesis by greater than 50% relative to corneas treated with either VEGF alone or VEGF and a catalytically inactive ribozyme (Inactive 4229 HH; Exhibit 9). These results indicate that ribozyme catalysis is required for anti-angiogenic activity. Eyes treated with ribozyme alone (*i.e.* no VEGF) showed no angiogenic response (Exhibit 9). This work suggests a therapeutic role for ribozymes in diseases characterized by VEGF-related neovascularization.

14. *Ribozyme efficacy in newborn mice:* Amelogenin (AMEL) is a highly conserved group of protein necessary for mammalian enamel "biomineralization". Lyngstadaas *et al.*, 1995, *EMBO. J.* 14, 5224 (Exhibit 10), have recently shown that a locally administered chemically-modified hammerhead ribozyme (the ribozymes were substituted with 2'-*O*-allyl groups to enhance nuclease resistance) is capable of cleaving amelogenin RNA in newborn mice resulting in "a prolonged and specific arrest of amelogenin synthesis" and a subsequent inhibition of normal mineralized enamel formation (Figures 3-4 of Exhibit 10). The authors state in the abstract on page 5224 that: "[T]hese results demonstrate that synthesized ribozymes can be highly effective in achieving both timed and localized 'knock out' of important gene products *in vivo*, and suggest new possibilities for suppression of gene expression for research and therapeutic purposes."

15. The examples discussed in this declaration provide ample support for the general utility and enablement of using the approaches, described and claimed in the application, to successfully synthesize chemically-modified ribozyme that are nuclease stable and catalytically active. These ribozymes are capable of specifically cleaving target RNA in a variety of cell culture and animal model systems As described in the application, it is now possible to design *trans*-cleaving ribozymes, synthesize and stabilize them chemically, deliver them to cells, and test them for efficacy in an ever increasing number of cell and animal models. The efficay of ribozymes in cell culture and animal models are reasonably predictive of the utility of ribozymes as therapeutic agents. These results strongly suggest that the therapeutic benefits of synthetic chemically-modified ribozymes in humans will most certainly be realized.

I hereby certify that all statements made herein of my own knowledge are true and that all statements made on information and belief are believed to be true; and further that these statements were made with the knowledge that willful false statements and the like so made are punishable by fine or imprisonment, or both, under Section 1001 of Title 18 of the United States Code and that such willful false statements may jeopardize the validity of the application or any patents issued thereon.

Date: April 30 1996

Dan T. Stinchcomb

Dan T. Stinchcomb, Ph.D.

Appendix A

Dan T. Stinchcomb

DIRECTOR OF BIOLOGY RESEARCH

Harvard University	B.A.	1976	Biology
Stanford University	Ph.D.	1981	Biochemistry

1981-1984	Postdoctoral Fellow, University of Colorado, Boulder, CO
1984-1987	Assistant Professor, Harvard University, Boston, MA
1987-1988	Associate Professor, Harvard University, Boston, MA
1988-1990	Scientist, Research & Development, Synergen, Inc., Boulder, CO
1990-1993	Senior Scientist, Research & Development, Synergen, Inc., Boulder, CO
1993-1994	Senior Scientist, Ribozyme Pharmaceuticals, Inc., Boulder, CO
1994-present	Director, Biology Research, Ribozyme Pharmaceuticals, Inc., Boulder, CO

Research Experience

Over fourteen years of post-doctoral research experience in the biological sciences, including seven years in the biotechnology industry. Skilled in conceiving, managing, and completing new research projects aimed towards the development of human pharmaceuticals. Established and directed effective research teams in diverse areas, including gene therapy, cell biology, molecular genetics, and biochemistry. Particular expertise in the delivery of RNA and DNA to cells *in vitro* and *in vivo*, HIV gene therapy, cardiovascular disease, and cytokines and cell surface molecules involved in inflammation and cell-cell communication.

Publications

Robert Tjian, Dan Stinchcomb, and Richard Losick. 1974. Antibody directed against *Bacillus subtilis* σ factor purified by sodium dodecyl sulfate slab gel electrophoresis. J. Biol. Chem. 250: 8824-8828.

Kevin Struhl, Dan T. Stinchcomb, Stewart Scherer, and Ronald W. Davis. 1979. High frequency transformation of yeast: autonomous replication of hybrid DNA molecules. Proc. Natl. Acad. Sci. USA 76: 1035-1039.

Dan Stinchcomb, Kevin Struhl, and Ronald W. Davis. 1979. Isolation and characterization of a yeast chromosomal replicator. Nature 282: 39-43.

Ronald W. Davis, Tom St. John, Kevin Struhl, Dan Stinchcomb, Stewart Scherer, and Mike McDonell. 1979. Structural and functional analysis of the *his3* gene and

galactose inducible sequences in yeast. In: Eukaryotic Gene Regulation (R. Axel, T. Maniatis, and C. Fred Fox, eds.), pp. 51-55. Academic Press, New York.

David Botstein, S. Carl Falco, Sue E. Stewart, Miles Brennan, Stewart Scherer, Dan T. Stinchcomb, Kevin Struhl, and Ronald W. Davis. 1979. Sterile host yeast (SHY): A eukaryotic system of biological containment for recombinant DNA experiments. Gene 8: 17-24.

Kevin Struhl, Dan T. Stinchcomb, and Ronald W. Davis. 1980. A physiological study of functional expression in *Escherichia coli* of the cloned yeast imidazole glycerol-phosphate dehydratase gene. J. Mol. Biol. 136: 291-307.

Dan T. Stinchcomb, Marjorie Thomas, Jeffrey Kelly, Eric Selker, and Ronald W. Davis. 1980. Eukaryotic DNA segments capable of autonomous replication in yeast. Proc. Natl. Acad. Sci. USA 77: 4559-4563.

Robert T. Elder, Thomas P. St. John, Dan T. Stinchcomb, and Ronald W. Davis. 1980 Studies on the transposable element TY1 of yeast: I. RNA homologous to Ty1. Cold Spring Harbor Symp. Quant. Biol. 45: 581-584.

Dan T. Stinchcomb, Carl Mann, Eric Selker, and Ronald W. Davis. 1981. DNA sequences that allow the replication and segregation of yeast chromosomes. In: Structure and DNA Interactions of Replication Origins. ICN-UCLA Symposia on Molecular and Cellular biology, Volume XXI (Dan S. Ray and C. Fred Fox, eds.), Academic Press, New York.

Dan T. Stinchcomb, Carl Mann, and Ronald W. Davis. 1982. Centromeric DNA from *Saccharomyces cervisiae* J. Mol. Biol. 158: 157-179.

Dan T. Stinchcomb, Craig Mello, and David I. Hirsh. 1985. *Caenorhabditis elegans* DNA that directs segregation in yeast cells. Proc. Natl. Acad. Sci. USA 82: 4167-4171.

Dan T. Stinchcomb, Jocelyn Shaw, and David I. Hirsh. 1985. Extrachromosomal DNA transformation of *C. elegans*. In: Banbury Report 20: Genetic Manipulation of the Early Mammalian Embryo. Cold Springs Harbor Press, Cold Spring Harbor, New York.

David I. Hirsh, Kenneth J. Kemphues, Dan T. Stinchcomb, and Richard Jefferson. 1985. Genes affecting early development in *C. elegans*. Cold Spring Harbor Symp. Quant. Biol. 50: 69-78.

Dan T. Stinchcomb, Jocelyn Shaw, Steve Carr, and David I. Hirsh. 1985. Extrachromosomal DNA transformation of *Caenorhabditis elegans*. Mol. Cell. Biol. 5: 3484-3496.

David Hirsh, George Cox, James Kramer, Dan Stinchcomb and Richard Jefferson. 1985. Structure and expression of the collagen genes of *C. elegans*. Annals of the New York Academy of Sciences 460: 163-171.

Craig C. Mello, James M. Kramer, Dan Stinchcomb, and Victor Ambros. 1991. Efficient gene transfer in *C. elegans*: extrachromosomal maintenance and integration of transforming sequences. EMBO Journal 10: 3959-3970.

B. Anne Croy, Larry J. Guilbert, Melissa A. Brown, Nicholas M. Gough, Dan T. Stinchcomb, Nancy Reed, and Thomas G. Wegmann. 1991. Characterization of cytokine production by the metrial gland and granulated metrial gland cells. J. Reprod. Immunol. 19, 149-166.

Diane J. Levitan, Lynn Boyd, Craig C. Mello, Kenneth J. Kemphues and Dan T. Stinchcomb. 1994. par-2, a gene required for blastomere asymmetry in *C. elegans*, encodes zinc-finger and ATP-binding motifs. Proc. Natl. Acad. Sci. USA 91, 6108-6112.

James D. Thompson, Dennis Macejak, Larry Couture, and Dan T. Stinchcomb. 1995. Ribozymes in gene therapy. Nature Medicine 1, 277-278.

James D. Thompson, David F. Ayers, Terra Malmstrom, Timothy L. McKenzie, Louis Ganousis, Bharat Chowrira, Larry Couture, and Dan T. Stinchcomb. 1995. Improved accumulation of recombinant RNAs expressed from a tRNA-based RNA polymerase III promoter. Nucleic Acids Research 23, 2259-2268.

Tod M. Woolf, Jennifer M. Chase, and Dan T. Stinchcomb. 1995. Toward the therapeutic editing of mutated RNA sequences. Proc. Natl. Acad. Sci. USA 92, 8298-8302.

Dan T. Stinchcomb. 1995. Constraining the cell cycle: regulating cell division and differentiation by gene therapy. Nature Medicine 1, 1004-1006.

Nassim Usman and Dan T. Stinchcomb. 1995. Design, synthesis, and function of therapeutic hammerhead ribozymes. In RNA Catalysis. F. Eckstein and D. Lilley, eds. Nucleic Acids and Molecular Biology 10, in press.

Thale Jarvis, Laverna Alby, Amber Beaudry, Francine E. Wincott, Leonid Beigelman, Antony DiRenzo, Jim McSwiggen, Nassim Usman, and Dan T. Stinchcomb. 1996. Inhibition of smooth muscle cell proliferation by ribozymes that cleave *c-myb* mRNA. Submitted.

Tod M. Woolf, Suzy Brown, Jennifer Chase, Antony DiRenzo, Danuta Tracz, Fran Wincott, Nassim Usman, and Dan T. Stinchcomb. 1996. Modifications required for effective binding of cellular mRNA targets by RNA oligonucleotides. In preparation.

Thale Jarvis, Francine Wincott, Leonid Beigelman, Laverna Alby, Antony DiRenzo, John Gustofson, Jim McSwiggen, Nassim Usman, and Dan T. Stinchcomb. 1996. RNA modifications that enhance ribozyme activity in cells. In preparation.

Larry Couture and Dan T. Stinchcomb. 1996. Ribozymes in gene therapy: the promises and the pitfalls. Trends in Genetics, in preparation.

Published Patents

Dan T. Stinchcomb, Marjorie Thomas, and Ronald W. Davis. Eukaryotic autonomously replicating segment used with specific gene to form hybrid DNA to enhance stable integration of gene into chromosome of eukaryotic host.

J. Dayer, M. J. Milhausen, and D. T. Stinchcomb. T-cell membrane monocyte inducing proteins-tmip-1 and tmip-2- induce expression of cytokine(s): for treatment of diseases caused by dysfunctional or deficiency of T-cells, in cancer therapy and in listeriosis.

B. Chowrira, K. G. Draper, J. McSwiggen, D. T. Stinchcomb, and J. D. Thompson. Enzymatic nucleic acid cleaves RNA of an immunodeficiency virus - useful for treating an acquired immunodeficiency disease, and in a vector to immunise against infection with HIV-1

Inventor on eight patent applications covering ribozyme inhibition of gene expression.

Exhibit 1

Reprinted from Journal of Medicinal Chemistry, 1995, 38.

Ribozymes as Human Therapeutic Agents

Ralph E. Christoffersen* and J. Joseph Marr

Ribozyme Pharmaceuticals, Inc., Boulder, Colorado 80301

Received November 22, 1994

I. Introduction

The protein encoded by a particular gene normally corresponds to an RNA sequence considerably shorter than the sequence transcribed from that gene. This is due to the fact that genes typically contain several exons (expressed sequences) separated by a series of introns (intervening sequences). When the RNA is transcribed from a gene, the corresponding intron sequences are spliced out and the exons are ligated in a transesterification reaction. The newly spliced series of exons is then translated into the appropriate proteins.

In the early 1980s Cech and his colleagues discovered that certain RNA splicing reactions are catalyzed by RNA. It was unequivocally demonstrated that certain intervening sequences (Group I) were inherently capable of catalyzing RNA splicing reactions to give rise to mature RNA. Cech termed such RNA molecules, possessing enzymatic activity, "ribozymes".[1-3] These RNA enzymes have now been found in a wide variety of biological systems. By suitable chemical or molecular manipulation, ribozymes can be engineered either to bind specifically to external desired RNA sequence targets and cleave them, thereby inhibiting a gene function, or to ligate new pieces of RNA onto the target by trans splicing to create a new gene function. Therein lies their therapeutic potential.

In less than 15 years since the initial discovery by Cech and Altman,[1-3] the fundamental importance of catalytic RNA (ribozymes) in chemistry and biology has become apparent. The demonstration that RNA plays an active catalytic role in the production of proteins from DNA and is not merely a "passive" participant has caused a major paradigm shift in the role of RNA in chemistry and biology. Furthermore, th availability of "catalytic RNA" to carry out processes previously reserved only for protein enzymes has caused a rethinking of the role RNA may have played in evolution.[4-10]

Ribozymes provide a broad and enabling technology applicable to human disease diagnosis and therapy, agriculture, and animal health.[11] Correspondingly, research interest in ribozymes has grown exponentially over the past several years (Figure 1). Over 500 articles were published through the end of 1993 on various aspects of ribozymes and their role in chemistry, biology, and medicine.

The broad potential of ribozyme technology is due to the fact that a ribozyme will, in principle, selectively bind and cleave any target RNA. Thus, highly specific control of gene expression by ribozyme cleavage and consequent nuclease destruction of mRNA fragments can be contemplated, as illustrated in Figure 2.

In the diagnosis and treatment of human diseases, the sequence-specific enzymatic activity, and the relative ease with which a lead ribozyme can be designed have substantial advantages that may translate into low side effects, high potency, and substantially reduced drug discovery time. Ribozymes are applicable in principle to any disease where a specific protein or virus can be linked to disease etiology.

Translation of this potential into a new class of human therapeutic agents is coupled with technical challenges. In this review, the current status of efforts to demonstrate how ribozymes can be used to treat human diseases will be considered along with identification of remaining issues and possible future directions.

II. Chemistry and Biology of Ribozymes

A. Types f Ribozymes. Ribozymes were identified first by their ability to splice introns out of mRNA when an RNA precursor of *Tetrahymena thermophila* was

0022-2623/95/1838-2023$09.00/0

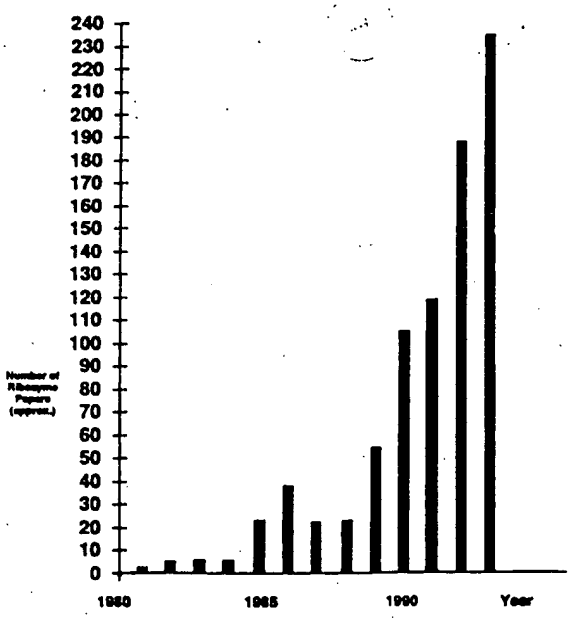

Figure 1. Annual growth of ribozyme publications.

found to be self-splicing.[1,2] Additional studies extended the kinds of self-splicing ribozymes from Group I to Group II introns[12–15] found predominantly in fungal mitochondria. Modification of the *Tetrahymena* self-splicing intron by deleting the first 19 nucleotides created an important change; it converted the self-cleaving ribozyme into one acting on an *external* RNA (or DNA) substrate. The ribozyme was acting "in *trans*". Thus, the group I intron can be engineered to catalyze a sequence-specific reaction. Group I introns also have been found in cyanobacteria[19] and slime mold[20] (Figure 3).

Group I ribozymes range in size from 200 to 1000 nucleotides (Figure 4). They require a U in the target sequence 5′ to the cleavage site, and bind 4–6 nucleotides at the 5′ side.

RNAse P is a ribonucleoprotein consisting of approximately 375 nt of RNA plus a small polypeptide. The RNA portion cleaves tRNA precursors to produce the mature tRNA.[3]

The VS ribozyme is derived from a satellite RNA (VS) of certain natural isolates of *Neurospora*. This ribozyme differs from the others shown in Figure 4 in that it will cleave double-stranded RNA.[21] These three ribozymes are all large, relative to the others, and any applications involving these large ribozymes must necessarily be those which utilize gene therapy methods.

The "Hammerhead" (HH) and "Hairpin" (HP) ribozyme motifs were originally identified in plant viroids and virusoids;[22–26] the Hepatitis Delta Virus (HDV) ribozyme was found in a satellite RNA of human hepatitis B virus.[27,28] Each of these was identified in a self-cleaving form and has been converted to cleave external RNA substrates as well.[25,29–34]

The ability to design ribozymes against selected external RNA targets has expanded their therapeutic potential. Hammerhead ribozymes can be modified in their binding arms to be complementary to any target RNA which contains a UH (where H is any nucleotide but guanosine). The optimum length of the binding arms appears to be 7/7 nucleotides on the 3′- and 5′-ends of the rib[illegible]. For the HP ribozyme, four nucleotides on th[illegible]de and a variable number on the 3′ side of the cleavage site can be modified. In the HDV ribozyme only 7 nucleotides at the 5′ side of the cleavage site need be changed to alter the specificity (Figure 4). Since these ribozymes are relatively small, they can be made by chemical synthesis or produced by viral or nonviral vectors. This ability to modify the binding arms of ribozymes to complement the sequences within a given RNA potentially endows ribozymes with a therapeutic specificity heretofore not possible.

Increasing the length of the complementary binding sequences in the ribozyme should improve the specificity of binding. A recognition sequence of approximately 15 nucleotides—7 in the 3′- and 5′-arms and one at the catalytic core—should be optimal for recognition, specificity, and turnover. This nucleotide length may be unique in the human genome; however, this does not take into account the bias in the genetic code, particularly in regions that are transcribed as mRNA. Nevertheless, this target size of 15 nucleotides will assure reasonable uniqueness and, therefore, therapeutic specificity, that will be assessed as candidate ribozymes appear in therapeutics.[35,36] It may not be desirable to extend the recognition sequence beyond 15 nucleotides since, beyond that point, the binding affinity increases to the point where the off-rate of the cleaved product from the enzyme is too slow to permit efficient catalysis and nonspecific effects also may occur.[37]

B. Mechanism of Action. Ribozymes cleave their target using either a transesterification or hydrolysis mechanism (Figure 3). In the cleavage reaction the formation of a 2′,3′ cyclic phosphate and 5′-hydroxyl are typical products. If the ribozyme is present in excess, as is often the case in practice, but at a concentration that is not saturating with respect to the substrate, the cleavage rate is determined by the second-order rate constant k_{cat}/K_m. Values of approximately 10^8 M^{-1} min^{-1} are frequently observed.[30] If the substrate is in excess, and at saturating concentrations, ribozymes are rate-limited by release of the product.[38] Improvements in ribozyme turnover may result from research to modify ribozymes in a way to increase product release from the complex.

C. Ribozyme Evolution. Techniques to alter or improve ribozyme function, generally known as directed *in vitro* evolution, have been devised.[39–45] By maintaining diversity throughout multiple generations and selectively amplifying those ribozymes with a specific property of interest, the *Tetrahymena* ribozyme was evolved into a Group I intron that cleaved DNA targets in addition to RNA.[39]

In a different application of *in vitro* evolution, Lorsch and Szostak[45] created a random pool of 10^{15}–10^{16} RNA molecules containing an ATP-binding domain and identified five RNAs capable of acting as 5′-kinases and two 2′-kinases. This broadened the scope of ribozyme formation further to include polynucleotide kinase activity. The inherent potential of ribozymes to bind and act on many kinds of substrates coupled with selective methods to amplify and refine these new activities will lead to the development of many new ribozyme functions.

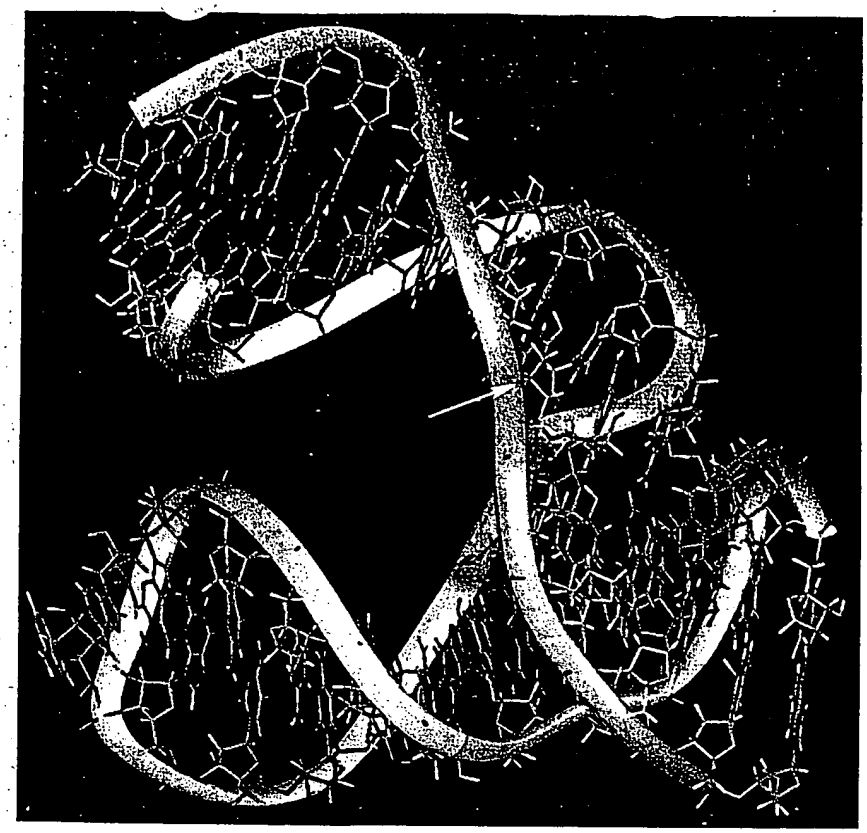

Figure 2. Crystallographic representation of a ribozyme binding to its substrate. This model was constructed from the coordinates determined by Pley, H. W.; Flaherty, K. M.; McKay, D. B. *Nature* **1994**, *372*, 68–74. The figure was kindly supplied by Dr. James McSwiggen, RPI, Inc. The cleavage site occurs on the substrate at the point designated by the arrow. The substrate lies in a vertical orientation in apposition to the binding arms of the ribozyme.

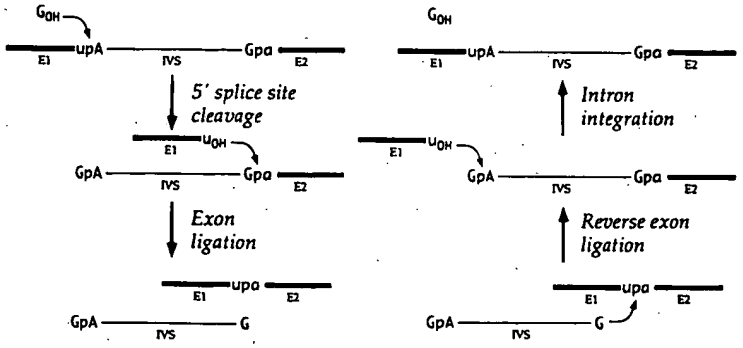

Figure 3. Splicing of group I introns: forward and reverse reactions. The letter E refers to exons and IVS refers to the intervening sequence. The three-letter sequence, such as Gpa or GpA, refers to two nucleotides connected by a phosphodiester bond. In the forward reaction, attack of the required GTP cofactor at the 5′-splice site releases the 5′-exon. The 5′-exon then attacks the 3′-splice site resulting in exon ligation and excision of the IVS. The reverse reaction follows the same pathway in the opposite direction. After binding of the ligated exon RNA in the active site of the linear IVS, attack of the 3′-terminal OH of the IVS on the phosphate at the splice junction results in the addition of the 3′-exon to the 3′-end of the IVS. In the second step, the 3′-hydroxyl of the 5′-exon attacks the phosphate of the first phosphodiester bond of the IVS, releasing G and joining the 5′-exon to the 5′-end of the IVS. Exon sequences are in lower case; IVS sequences in upper case. The authors are indebted to Dr. John Burke of the University of Vermont for this figure.

III. Proof of Principle

To demonstrate the potential of ribozymes, their abilities to cleave mRNA targets must be correlated with biochemical and physiological changes that result from target cleavage. Many studies now have been published which illustrate these proofs of principle.

In a study of HH ribozymes in monkey (COS1) cells,[46] ribozymes designed against chloramphenicol acetyltransferase (CAT) were cloned into a mammalian expression vector and electroporated into the cells. They specifically suppressed CAT expression up to 60% relative to an inactive ribozyme and a corresponding antisense control.

In another study, DNA encoding a ribozyme-tRNA construct was microinjected into the nucleus of frog oocytes.[47] It remained largely in the nucleus, but small

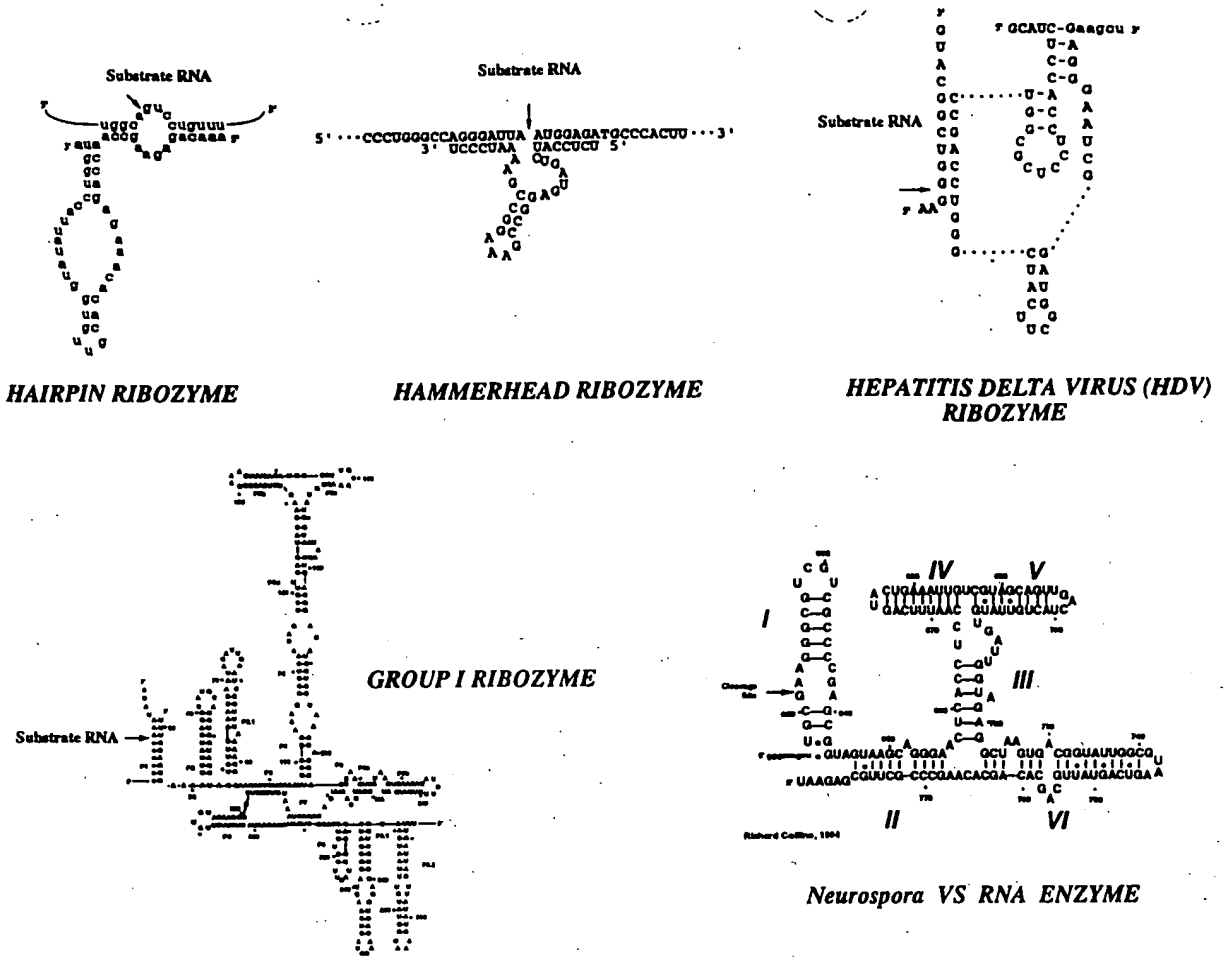

Figure 4. General structures of representative ribozymes. The *Tetrahymena thermophila* self-splicing group I intron structure as proposed by Cech *et al.* (Cech, T. R.; Damberger, S. H.; Gutell, R. R. *Struct. Biol.* **1994**, *1*, 273–280). Arrows indicate the 5′ and 3′ splice-sites. Lower case letters = exons; thick lines = connections where arrowheads show 5′ → 3′; P1, etc. = conserved paired regions; thin lines = tertiary structure. For the Hammerhead, Hairpin, and Hepatitis Delta Virus ribozymes, arrows indicate the site of RNA cleavage. N can be A, U, G, or C; N′ is a nucleotide complementary to N; H is A, U, or C; Y is any pyrimidine. The secondary structure of the Hairpin ribozyme–substrate complex as proposed by Berzal-Herranz *et al.* (Berzal-Herranz, A.; Joseph, S.; Chowrira, B. M.; Butcher, S.; Burke, J. M. *EMBO J.* **1993**, *12*, 2567–2574). The secondary structure of a Hammerhead ribozyme–substrate complex as proposed by Long and Uhlenbeck, (Long, D. M.; Uhlenbeck, O. C. *FASEB J.* **1993**, *7*, 25–30). The secondary structure of a Hepatitis Delta Virus ribozyme-substrate complex as proposed by Perrota and Been, 1992 (supra). The structure of the *Neurospora VS* ribozyme as proposed by Guo, H. C. T. and Collins, R. A. (Guo, H. C. T.; Collins, R. A. *EMBO J.* **1995**, *14*, 368–376).

amounts were transported to the cytoplasm. Reduction of the co-injected U7snRNA target, present in the cytoplasm, was observed after 10 and 20 h.

The studies of L'Huiller *et al.*[48] demonstrated the specificity of a ribozyme directed against α-lactalbumin. Saxena and Ackerman[49] demonstrated that injection of a ribozyme directed against 28S RNA cleaved the 28S RNA but not related RNA. This showed that the ribozyme could detect its substrate among other RNAs present in the cell. Cleavage products for that substrate were found. Other studies at the cellular level now have been reported, and it is clear that the question of cell culture "proof of principle" for ribozymes has been answered affirmatively.[50–52]

Several studies of ribozyme function *in vivo* have been reported. Among the more definitive and dramatic examples is a study in *Drosophila*.[53] Transgenic eggs were generated which carried a ribozyme against the *fushi tarazu* (*ftz*) gene under the control of a heat-inducible promoter. These investigations distinguished the two developmental phases of the *ftz* gene, using timed heat-induction of the ribozyme. Induction of the ribozyme against the first of these development phases, production of a seven-stripe cuticle pattern, created cuticle defects in larvae. Activation of the ribozyme in other eggs later during neurogenesis inhibited central nervous system development without disturbing the antecedent cuticle pattern. These experiments demonstrated that specific induction of ribozymes at different points in *Drosophila* development is possible, that activation of the ribozyme causes the same phenotypic mutations in segmentation and neurogenesis that occur in known *ftz* mutations, and that the presence of the ribozyme caused no other biological or biochemical damage to the organism.

In another study, a plasmid carrying a ribozyme against β_2-microglobulin was injected into the male pronucleus of fertilized oocytes.[54] Seven transgenic

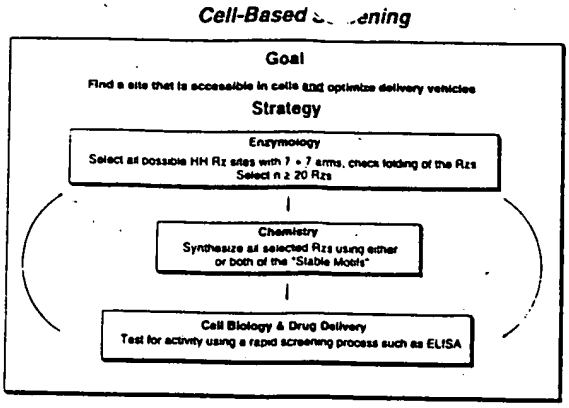

Figure 5. Ribozyme testing scheme.

animals were used to establish three ribozyme-expressing families. Ribozymes were expressed in the lung, kidney, and spleen. Ribozyme expression was accompanied by a reduction of mRNA β_2 microglobulin greater than 90% in the lungs of individual mice; smaller reductions were observed in kidney and spleen. Such a study not only provides convincing proof of principle *in vivo* but also confirms that continued expression of a ribozyme directed against a nonessential function will not result in any obvious toxicity in an animal.

IV. Ribozyme Design and Selection

A. Identification of Active Ribozymes. Identification of a lead ribozyme is a much simpler and shorter process than that required for most chemically synthesized small molecules. Knowledge of the relevant gene sequences and, therefore, its mRNA sequence, is sufficient. Ribozyme targets within the mRNA and the flanking sequences required to assure selectivity can be identified rapidly with existing computer methods. Once these putative ribozyme sites are identified, ribozyme recognition sequences are reviewed to determine whether the arms will fold improperly and bind to one another or to the catalytic core. Those which have the potential to do so are eliminated.[55,56]

At this point one can either determine availability of these potential sites to ribozyme cleavage *in vitro* using an RNAse H assay or move directly to a cell-based tissue culture assay. Before the availability of chemically stabilized ribozymes (see IV.B) *in vitro* screening using the RNAse H assay was employed. In this assay, DNA oligonucleotides are synthesized to be comparable in size to the ribozyme and complementary to the RNA sequences around the putative ribozyme sites. These are mixed with a long RNA substrate, and an excess of RNAse H is added. This enzyme cleaves the RNA strand at the ends of the DNA–RNA heteroduplex. The mixture is analyzed by gel electrophoresis. Sites on the target RNA where the DNA oligomer has bound will be cleaved, and that site is presumed to accessible to a ribozyme. We have found this assay to be have a predictive value of about 80% with respect to the activity of ribozymes in cell culture and animals.

Since the advent of chemically stabilized ribozymes, we have abandoned the RNAse H assay. In its place, we make those ribozymes which are predicted not to fold upon themselves and assay these directly in a tissue culture system in which the ability of the ribozyme to eliminate a biological activity is assessed. This provides a more realistic assessment of the ability of a ribozyme to attack its target mRNA in a cell. This system is more reproducible and has more relevance to the function of that ribozyme in an animal model. We consider it to be the screening method of choice (Figure 5).

B. Stability of Ribozymes in Biological Milieu. Unmodified RNA is unstable in biological systems. This is a significant challenge to establishing ribozymes as human therapeutics.

A number of structural modifications have been applied to synthetic oligonucleotides to enhance nuclease resistance.[57-61] Substitution of the 2′-*O*-Me-modified nucleotide at all positions in a hammerhead ribozyme except G5, G8, A9, A15.1, and G15.2 gives rise to a catalytically active molecule, but with a significantly decreased k_{cat} value.[61] However, these molecules showed a 1000-fold increase in stability as compared to an all-RNA ribozyme. In another investigation, a persubstituted 2′-*O*-allyl-containing ribozyme with ribose residues at positions U4, G5, A6, G8, G12, and A15.1 retained 20% of the catalytic activity of an all-RNA ribozyme. As in the previous case, the stability of this ribozyme was increased, with 30% of the material intact after 2 h compared to a less than 1 min half-life for the all-RNA ribozyme.[62]

Two phosphorothioate linkages at C3 and U4, with replacement of U7 by adenosine or guanosine in a phosphorothioate-DNA/RNA chimera further stabilize the molecule, but the catalytic activities of these chimeras are significantly reduced.[63] Substitution of all the pyrimidine nucleotides in a HH ribozyme by their 2′-amino or 2′-fluoro analogs resulted in a 1200-fold increased stability in rabbit serum but also gave a 25–50-fold decrease in activity compared to an unmodified ribozyme.

Beigelman *et al.*[64,65] constructed a considerably improved stable HH motif by utilizing selected modification of approximately 32 2′-modified sugars. Most of these were substituted as 2′-*O*-Me residues as described above. The remaining 2′ modifications were introduced at positions U4 or U7. Two of these ribozymes, U4- and U7-2′-amino and U4-2′-*C*-allyl, have wild-type catalytic activity and a 5–8 h half-life in human serum. The addition of a 3′–3′-linked dT or an abasic nucleoside to the 3′ terminus of these ribozymes increases their half-lives in serum to greater than 72 h (Figure 6).

The positions for these particular modifications were determined by analysis of the products of ribozyme degradation in human serum. The presence of 2′-O-Me residues protected their respective bases from exonuclease and endonuclease degradation. The predominant exonuclease in human serum cleaves from the 3′-end of the oligomer. However, there remained some residual exonuclease degradation even after 2′-O-Me substitution. For this reason the inverted T was added to convert the 3′-end into a 5′-"like"-end, which eliminated susceptibility to the 3′-exonuclease. The other vulnerable sites were the two internal pyrimidines in the U4 and U7 positions of the catalytic core, since endonucleases are more effective against pyrimidine linkages than against purine linkages. Modifications at the 2′-positions of U4 and U7 eliminated this susceptibility.

At this time, the best U4/U7 2′-modifications are

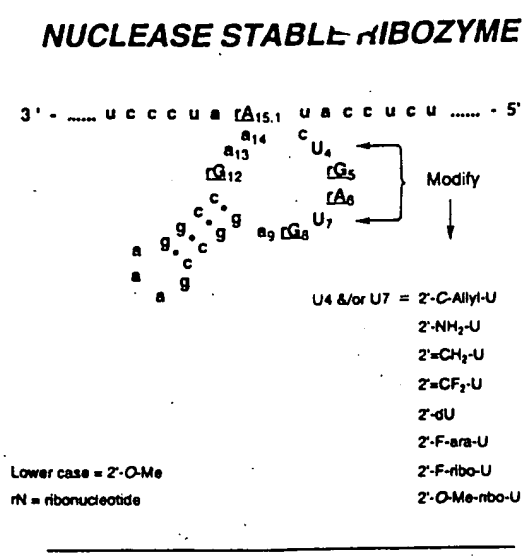

U4/U7 (2'/2')	$t_{1/2}$ Activity (min)	$t_{1/2}$ Stability (min)	$\beta = t_S/t_A \times 10$
OH/OH	1	0.1	1
O-Me/*O*-Me	4	260	650
ara-F/*O*-Me	5	>500	>1000
O-Me/NH_2	5	500	1000
NH_2/NH_2	2	300	1500
C-Allyl/*O*-Me	3	>500	>1700
C-Allyl/*O*-Me + IT	3	4320	14,400
NH_2/NH_2 + IT	2	4320	21,600

Figure 6. Modifications which confer increased stability to ribozymes. The lower section shows the increase in net activity conferred by the modifications compared to the unmodified (all RNA) ribozyme. The second column indicates the time required to cleave one-half of the substrate in solution under standard conditions (Tris, 50 mM, pH 7.5; $MgCl_2$, 10 mM; substrate, 1 nM; ribozyme at three concentrations: 8, 40, and 100 nM). The third column lists the time for one-half of the ribozyme to be destroyed in human serum at 37 °C. The fourth column is the ratio of the third column to the second. The fourth column is the ratio of the third column to the second which provides a measure of the relative stability–activity values of the ribozymes. The multiplier of 10 is included to relate the ribozymes to a unit stability–activity value for the unmodified molecule.

amino/amino and *C*-allyl/OMe. These provide more than a 1500-fold increase in biological activity and stability as compared to the unmodified ribozyme. An additional increase to 14 000–21 000 for each of these motifs was achieved by introducing 3'-3'-linked T to the 3'-end of the ribozyme (Figure 6). Such extended stability in human serum coupled with the retention of activity should allow use of synthesized ribozymes for exogenous delivery in various therapeutic settings.

V. Delivery of Ribozymes to Cells

There are two general methods of delivering oligonucleotides; incorporation into a viral or nonviral vector of DNA which codes for the oligonucleotide, or use of a chemically-synthesized ribozyme, either coupled physically or chemically to a lipid or other molecule or delivered as a "free" ribozyme. In the former, transfection or infection (plasmid or viral) of the cell depends upon an artificial means of increasing cell permeability or the inherent characteristics of the virus. In the latter, the molecule complexed to the ribozyme makes use of either a nonspecific entry mechanism (as with a lipid carrier) or a somewhat more specific entry method such as receptor-mediated endocytosis.

A. Exogenous Delivery. Many lipid vehicles have been studied for use in exogenous delivery of oligonucleotides. For example, liposomes (bilamellar lipid spheres of approximately 100–500 nm diameter) can encapsulate relatively large quantities of drug molecules either within their aqueous interiors or dissolved into the hydrocarbon regions of their bilayers.[66,67] Liposomes also protect their contents from renal filtration and degradation by serum enzymes.[68] When attached to the proper antibody or other ligand, liposomes can sometimes be directed to a tissue depending on the ability of the ligand to facilitate cell-specific attachment and entry.[69–72]

Despite these advantages, there are obstacles to the use of liposomes as delivery vehicles. Unmodified liposomes do not survive long in systemic circulation since they are removed rapidly by macrophages of the reticuloendothelial system. Such uptake may be avoided partially by modifying the character of the lipids in the bilayer or by a poly(ethylene glycol) coating to prevent nonspecific adsorption of serum proteins and therefore nonspecific recognition of liposomes by macrophages.[73–75] In addition, in general it is not possible to target liposomes to a specific tissue. This has been partially surmounted by the use of receptor-mediated endocytosis where, for example, a liposome has been attached to folic acid *via* the distal end of a few lipid-conjugated poly(ethylene glycol) (PEG) molecules on the liposome surface.[76]

An alternative method which appears to have greater potential is the use of cationic lipids. These are materials which contain a nonpolar long-chain fatty acid, usually C16 or C18, complexed to a cationic polyamine such as spermidine. These lipids, although they aggregate under some conditions when mixed with oligonucleotides, are believed to complex with the oligonucleotide in such a way that it is not internalized into a liposome-type structure. Supporting this concept is the demonstration that oligonucleotides complexed with cationic lipids are susceptible to nucleases whereas those within liposomes are not.

Many investigations to date have utilized DNA–cationic lipid complexes to deliver oligonucleotides to cells.[77–84] It appears that these lipid–DNA complexes have relatively little toxicity if used in low concentrations. At higher concentrations there is evidence of toxicity following intravenous injection in mice.[83] Modification of the lipid carrier reduced the toxicity at lipid and DNA concentrations up to 1000-fold higher than those used previously.[83] Based on these results, DNA–lipid formulations or ribozyme–lipid formulations are being considered as possible delivery vehicles for exogenous oligonucleotide human therapy. Nevertheless, the rules developed for the delivery of DNA via cationic lipids may not apply to small pieces of RNA. Larger circular pieces of replicating RNA behave similar to DNA when delivered with cationic lipids. Smaller pieces of RNA, less than 500 nucleotides, were not taken up under these circumstances (P. Felgner, personal communication). Our internal studies have also dem-

onstrated that a given lipid pr... ation may serve well in one cell type but not in another.

Intracellular localization after passage across the cell membrane also needs to be considered. For example, even if large numbers of ribozymes are delivered to a particular cell type (as many as several million can be delivered), many of the ribozymes appear trapped within the endosomal compartment of the cell. Certain ribozymes, when microinjected into a cell, will appear in the nucleus almost immediately. When the same ribozymes are delivered with a lipid vehicle, they are trapped in the endosome. This paradox of having large quantities of ribozymes in the cell with little biological activity has led to the conclusion that the choice of lipid vehicles will vary with target cell. Even with cell type optimization, release from the endosome cannot be guaranteed.

Another aspect of intracellular localization also needs to be considered, i.e., co-localization of ribozyme with its intended mRNA target. While this may be possible without intervention, Sullenger and Cech[85] have found that inclusion of a retroviral packaging signal as part of the ribozyme gave 90% reduction of titer of a targeted retrovirus, presumably because in cell culture the ribozyme was co-localized in the nucleus with its viral genomic RNA target. At the same time, the ribozyme had no effect on the same target localized in the cytoplasm. In another method of enhancing ribozyme activity,[86] it was shown in the test tube that the cleavage rate of a HH ribozyme can be enhanced 10–20-fold upon addition of the NC protein of HIV-1, which also enhanced the ability of the ribozyme to discriminate between cleavage of RNA oligonucleotides with differing sequences. Hence, delivery of a ribozyme to the same cellular compartment as the target, either through chemical modification of the ribozyme or otherwise associating it with a "localization" or "enhancement" factor, can be expected to increase the rate at which the ribozyme finds its target and hence increase its effectiveness.

While the use of lipids and other factors to enhance exogenous delivery and effectiveness of oligonucleotides is encouraging, the process for designing such lipids still remains somewhat empirical and must be decided experimentally for each ribozyme in each cell of interest.

B. Endogenous (Vector) Delivery. All studies of viral delivery of ribozymes to date have utilized retroviruses (see below). Other viruses also offer potential for ribozyme gene therapy, e.g., adenovirus, adeno-associated virus, and others.

Retroviral vectors possess several properties of interest. For example, they will transfect and express therapeutic genes in disease-susceptible cells, have no contaminating helper virus, and integrate into the genome of the cell.[87] In viral diseases such as HIV, these characteristics can be used to advantage, i.e., the integrated ribozyme expression unit would be expected to replicate continuously and, when expressed, compete with both infection and replication of wild-type HIV.

Adeno-associated virus (AAV), since it is nonpathogenic and able to transfect diverse cell types, is another attractive vector for ribozyme delivery. A vector consisting only of the *cis*-acting terminal repeats of AAV was established by Samulski.[87] This type of vector has been used to express the TAR antisense from an internal Rous sarcoma v... long terminal repeat, and blocked HIV replication after challenge. A more than 1000-fold reduction in reverse transcriptase activity was seen by day seven post challenge.[87] AAV also has been used to transform $CD34^+$ cells with a transduction efficiency of approximately 80% in the presence of interleukin 3 and granulocyte/macrophage-colony-stimulating factor.[87]

Adenovirus also has been studied as a vector for the delivery of oligonucleotides. It is a DNA virus which enters cells through binding of adenovirus with its cell-surface receptor and transfer into endocytic vesicles.[88–91] Adenoviruses can be used to express genes as well as to enhance delivery of various large molecules such as dextrans, proteins, and plasmid DNA linked to ligands, whether it is replication-competent or replication-deficient.[92,93] The mechanism for enhanced delivery by replication-deficient adenovirus is not clear but involves release of materials from the endocytic vesicle to the cytoplasm. This characteristic has been utilized by Gao *et al.*[94] to deliver genes to airway epithelium *via* an adenovirus–polysine–DNA complex.

Viral delivery of ribozymes and other oligonucleotides is at an early stage of development, and investigations to date in therapeutic settings are described below. While any of the viral vectors is applicable in principle, more experience is needed. For example, targeting ribozyme-containing vectors to particular tissues or cells may be important. This may be accomplished via a physical method such as an aerosol to the lung epithelium, to a target tissue *ex vivo* such as bone marrow which is then reinfused, by widespread delivery *via* a vector such as adeno-associated virus which would infect many cells and tissues, or by intracellular targeting.[85]

Other nonviral vector approaches also have been used to deliver plasmids and/or DNA. However, it appears that there is no single lipid formulation which will suffice for all cell types, whether it is for a synthetic ribozyme or a vector-delivered ribozyme. For example, San *et al.*[83] showed a significant variation in the amount of DNA expression from one cell type to another. This varied from 1% conversion (transfection efficiency) of MCA205 cells to 15% in human melanoma cells to 55% in 293 cells.

IV. Therapeutic Applications

Therapeutic applications of ribozymes are potentially quite broad but have thus far been applied to situations involving inhibition of overexpression of a gene. The gene target may be foreign, as in a viral infection, or may be a normal gene which has undergone mutation such as an activated protooncogene.

The most obvious areas of therapy at this time are viral infections, both acute and chronic; cancer where an oncogene product is known; and various disease states where overexpression of a particular gene is associated with a disease state. Examples of the latter include restenosis and other cardiovascular diseases, transplant rejection, osteoarthritis, and immunological diseases. This review will concentrate on examples from viral infections and cancer.

A. Viral Diseases. One of the earliest descriptions of the activity of ribozymes against viral diseases was that of Sarver *et al.*[95] In that investigation, cleavage of HIV sequences in a cell-free system by HH ribozymes was demonstrated. Also, in human cells stably express-

ing a HH ribozyme targeted to t[illegible]g transcript, a substantial reduction in *gag* RI[illegible]lative to non-ribozyme-expressing cells was seen. This reduction in RNA was reflected in a reduction in p24 antigen levels of approximately 98%.

To measure long-term effects of ribozyme expression, the growth curve of cells constitutively expressing an anti-HIV ribozyme was followed for 10 days, and no impairment of cell growth was observed.[95] Longer term toxicity studies have shown that ribozyme-containing cells behave as their control non-ribozyme-expressing counterparts when followed for nine months.[96]

A subsequent study[97] used a HH ribozyme designed against a conserved region within the 5′-leader sequence of HIV RNA. This was selected because it is present on all HIV RNAs and is essential for viral transcription, transactivation and translation. Thus, cleavage at this site would be expected to produce a small 5′ fragment to act as a competitive inhibitor of replication, transactivation, and translation. In addition, HIV enhances transcription by a feedback mechanism involving the viral *tat* protein. Therefore, ribozymes were expressed not only in a constitutive manner, but also in a *tat*-inducible manner under the control of a fusion *TK*-transactivation-responsive (TAR) promoter. This allowed the ribozyme to be upregulated in the presence of HIV replication in the cell.

The results of this study demonstrated that stable MT_4 transformants which express the ribozyme under the control of the herpes simplex virus thymidine kinase promoter were only modestly resistant to HIV infection. Virus production was simply delayed. In cells allowing ribozyme expression under control of the simian virus 40 or cytomegalovirus promoter, the rate of HIV multiplication was decreased slightly and virus production was delayed about 2 weeks. The highest level of resistance was observed in MT_4 cells transformed with a vector containing the TAR promoter to allow ribozyme expression in a *tat* inducible manner. No HIV production was observed 22 days after infection of these cells. The results of this study not only corroborated the foregoing and those of others[98] but also illustrated the importance of high expression levels of the ribozyme in HIV-infected cells. An inducible promoter that upregulates the ribozyme in the presence of this infection may enhance efficacy even further.

A similar strategy was described by Yu *et al.*[99] These investigators designed a HP ribozyme to cleave the 5′-leader sequence of HIV. Expression of the HP ribozyme under the control of a β-actin promoter inhibited HIV expression in a transient expression system. In a followup investigation,[100] the human $tRNA^{VAL}$ gene and the adenovirus VA1 gene promoter, both transcribed by RNA polymerase III (pol III), were used as expression cassettes for the HP ribozyme. Because of the small size, high rate of transcription, and broad expression in various tissues, pol III transcription units have been used more broadly thus far for expressing ribozymes than pol II promoters.[101–103] The Yu *et al.*[100] investigation demonstrated that the HP ribozyme expressed from a pol III promoter inhibited HIV expression up to 95% in a transient transfection assay. The authors also showed that the HIV RNA cleavage products were degraded with high specificity.

Both the studies by Weerasinghe *et al.*[97] and Yu *et al.*[100] support the cr[illegible]sion that, by cleaving at the 5′-leader sequence, t[illegible]zyme removes the RNA cap so that the mRNA is po[illegible]y translated and probably more quickly degraded. Moreover, the 5′-leader sequence is highly conserved among most HIV isolates and therefore is a theoretically more important therapeutic target. Of available HIV strains, only "MN" contains one nucleotide substitution in the 5′-leader sequence cleaved by a hairpin ribozyme. There are differences among some HIV strains in other portions of the 5′-leader.[104]

The latter authors also used a retroviral vector to deliver the ribozyme, and demonstrated 70–95% inhibition of several strains of HIV. In these experiments, p24 was analyzed after 24 h, and it is not clear if this particular strategy would be effective in a longer assay. Nevertheless, it supports the earlier work of Weerasinghe *et al.*[97] and adds a second ribozyme motif for potential use against HIV.

In an interesting variation, a ribozyme was created by inserting a 22-nucleotide catalytic HH domain into an antisense RNA of 413 nucleotides directed against the 5′-leader/*gag* region of HIV.[105] This left 129 nucleotides on the 5′-flanking sequence and 284 nucleotides on the 3′-flanking sequence. The rationale for the experiment was to prevent the ribozyme from dissociating after binding and cleaving the target, and thereby discern whether catalysis conferred a significant advantage to antisense RNA. An inactivated ribozyme, which did not cleave the substrate, and the catalytically active ribozyme were transfected into human sw480 cells along with infectious proviral HIV DNA. HIV replication was analyzed by measurement of RNA and by ELISA. The presence of the catalytically active region conferred a 4–7-fold greater inhibition of HIV replication as compared to the antisense and the inactive mutant. Both kinetic and structural studies indicated that the ability to form double strands was not changed in using ribozymes and suggested that the ability to cleave target RNA was a critical prerequisite for the observed increase of inhibition of replication of HIV.

The investigations described above clearly demonstrate the ability of ribozymes to inhibit replication of HIV in cell culture. The inhibition varies from several days to several weeks. One of the possible ways to augment inhibition further is to use promoters which ensure high copy numbers in the cell and/or inducible promoters which are activated by the presence of the viral target.

There are several other methods that may be useful in increasing the activity of ribozymes against HIV, e.g., addition of a protein which facilitates catalysis or the use of multiple ribozymes. For example, a study by Bertrand and Rossi[106] demonstrated that addition of certain RNA binding proteins enhanced the ribozyme cleavage reaction. Some of these activities were dependent upon the ribozyme–substrate hybrid length. Certain proteins, heterogeneous nuclear RNP, A1, and the HIV nucleocapsid protein (NCp7), inhibit the reaction of shorter duplexes. NCp7 also inhibits the cleavage of longer duplexes (17–20bp). Both of the latter enhance the turnover of ribozymes by increasing the rate of product dissociation when the products are bound with 7bp or less. Since A1 is though to interact with

most mRNAs *in vivo*, it may enhance intracellular activity of ribozymes.

Another way to enhance ribozyme effectiveness in solution is through the use of multiple ribozymes.[107] In this investigation, the ribozymes were flanked by *cis*-acting ribozymes at both the 5′- and the 3′-ends so that, upon transcription, multiple ribozymes were trimmed and liberated independently. When levels of ribozyme expression were examined, the amount of transcript was proportional to the number of units connected in tandem. The activities of these ribozymes were also proportional to the number of units. The activities of connected-type ribozymes reached a plateau at values of about $n = 3$. In the tandem *cis*-cleaving ribozymes, $n = 1-10$, their results indicated that the multiple ribozyme expression system could generate independent ribozymes specific for different target sites *in vitro* without sacrificing the activity of any individual ribozyme.

A multiple ribozyme transcript may be more active against HIV in cells than the corresponding individual ribozymes.[108] A transcription unit containing nine ribozymes (a "nonaribozyme") was more active than transcripts with fewer catalytic units. The individual ribozymes were arranged in tandem. The multitarget ribozymes retained the specificity of monoribozymes but were more efficient per ribozyme RNA copy and remained active when part of a large transcript.

In one investigation an anti-HIV ribozyme was found to be less effective than the corresponding antisense.[109] This is the only study which has shown this; the reason is not clear.

The above provides encouragement regarding the potential use of ribozymes in the management of HIV infection. Therapeutic efficacy will require high efficiency of transfection or transduction of the gene coding for the ribozyme. This is attainable in tissue culture but has not yet been demonstrated in humans. An *ex vivo* treatment of hematopoietic stem cells may allow this goal to be realized but will depend to a great degree on the nature of the viral vector. This is a field of science still in its infancy, and the optimum choice of viral vector is not currently apparent. In addition, experiments which have reported activity of ribozymes against HIV have used low multiplicities of infection (the ratio of input virus to cells), usually on the order of 10^{-3}. At higher multiplicities, ribozyme protection often disappears. The reduction in virus titer is measured by percent inhibition, but an effective therapeutic will require a reduction of several orders of magnitude. Finally, ribozymes must compete against the best therapeutic agents currently in clinical medicine. Ribozymes and antisense agents have not yet received a thorough comparison with these small molecules. While none of these objections constitute an impassable hurdle, they remain important considerations when evaluating the potential usefulness of ribozymes in this disease.

Ribozyme inhibition of other viruses also has been studied. Xing and Whitton[110] prepared ribozymes which cleave the RNA genome of lymphocytic choriomeningitis virus (LCMV), a prototype arenavirus. Several sites on the LCMV genome were cleaved efficiently in *trans* in solution. The efficiency of the cleavage was site-dependent, and the authors showed that the secondary structure at the target site could abolish ribozyme cleavage. Computer-assisted analysis indicated that much of the LCMV genome may be involved in base pairing which would render it similarly resistant to ribozyme attack. The remaining open regions lacked a GUC target site, but there were several alternative sites available which could be cleaved: AUC, CUC, and AUU. They further demonstrated that an anti-LCMV ribozyme expressed in tissue culture cells diminished viral RNA levels and reduced infectious virus yield approximately 100-fold.[111] This effect was shown to be specific since yields of related arenavirus were not similarly curtailed.

Thus, activity of ribozymes against viruses has been clearly demonstrated in solution and in cells. The challenge now is to arrange appropriate promoters and multiple ribozymes as needed and direct them to highly conserved sequences to achieve the appropriate therapeutic result.

B. Inhibition of Oncogene Function. The crucial differences between normal cells and cancer cells appear to stem from discrete changes in specific genes controlling proliferation and tissue homeostasis. Many cancer-related genes have been discovered which are implicated in the natural history of human cancer because they are consistently found to be mutated in tumors. They fall into two descriptive categories: tumor-suppressor genes and oncogenes.

Oncogenes are evolutionary conserved and have been identified because they induce cellular transformation either when naturally incorporated into a retrovirus or when their DNA is transfected into tissue culture cells. Most of the known oncogenes were originally isolated as viruses containing genes of nonprimate origin. These genes are mutations of protooncogenes which are normally found in cells and are activated during embryogenesis or specific tissue regeneration or cell growth. The mutation, which may be a point mutation, alters the property of the corresponding protein and thereby induces uncontrolled cell growth. Since they are overexpressed and produce RNA which is distinguishable from the protooncogene, oncogenes are potentially excellent targets for ribozyme therapeutic activity.

By delivering phosphorothioate antisense oligomers with the cationic lipid lipofectin, Monia *et al.*[112] demonstrated a 5-fold discrimination between a point mutation in the 12th codon of H-*ras* and the wild-type (WT) H-*ras* target sequence. The authors also showed that discrimination correlated with and was limited by the difference in thermodynamic stability of the hybrids formed between mutants or WT sequences. Because of the sequence requirements of ribozyme cleavage, a ribozyme targeted to this site should have greater discrimination between mutated and wild-type genes than antisense molecules that rely on differences in thermodynamic stability or an RNase H mechanism.

This same 12th codon mutation (GGC to GUC) in H-*ras* creates a consensus HH ribozyme target site.[113] An H-*ras*-dependent cell line was stably transformed with a β-actin expression vector encoding a HH ribozyme. Isolated clones showed reduced H-*ras* expression and reduced rates of cell proliferation. The study demonstrated a decrease in the H-*ras* RNA and a corresponding decrease in the protein derived from H-*ras* expression, p21. The cell lines transformed by the anti-H-*ras* ribozyme were examined for their ma-

lignant potential in athymic (mice. The ribozyme described above was designe cleave the mRNA of the H-*ras* gene expressed in human bladder carcinoma EJ cells. DNA encoding the ribozyme was cloned into a mammalian expression vector and transfected into these cells. The cell data described above provided convincing evidence *in vitro* that the ribozyme could inactivate the H-*ras* gene product. These same cell lines were then injected by an orthotopic (transurethral) implantation model to recapitulate the invasive potential of bladder carcinoma. The EJ transfected cells preserved the malignant phenotype in these mice and caused highly invasive tumors and death due to high tumor burden.

In contrast, in the EJ clones transfected with the ribozyme-expressing vector there was a dramatic reduction in the malignant phenotype. The tumors displayed limited invasive capacity and there was a significant increase in survival, approximately double that of the control cells (a medium of 75 days *vs* a medium of 47 days). Histology of the bladders demonstrated that control tumors consisted of cells with highly invasive properties with nests of neoplastic cells dispersed throughout the tubules of the normal kidney. In contrast, the ribozyme clones produced tumor nodules that compressed surrounding tubules of the normal kidney but with no evidence of invasion in the vascular spaces. Tumor-bearing mice alive at 86–90 days had ribozymes present as detected by the PCR assay. Thus, this experiment demonstrated the ability of a ribozyme directed against H-ras mRNA to reverse the phenotypic expression H-*ras* *in vitro* and *in vivo*.

Ribozymes can inhibit the transformation of NIH 3T3 cells by the activated c-Ha-*ras* gene.[114,115] Plasmids containing the ribozyme-encoding genes were expressed under the control of the long-terminal repeats of Rouse sarcoma virus in NIH 3T3 cells transfected with the c-Ha-*ras* gene. These ribozymes inhibited the formation of cell foci by about 50% by cleaving the oncogene mRNA. In addition, when the activated c-Ha-*ras* gene was cotransfected with the ribozyme-encoding gene, colonies were isolated which were morphologically different from those containing only the c-Ha-*ras* gene.

The c-*fos* gene has been implicated in signal transduction, DNA synthesis, and resistance to anti-neoplastic agents.[116] It is one of the earliest known genes activated in response to mitogenic stimuli. Its interaction with the oncogene *jun* and the DNA binding activity of the *fos-jun* heterodimer suggest that fos functions as a transcriptional activator. The linkage between expression of c-*fos* and DNA synthesis genes is supported by data that cisplatin administration leads to a sequential induction of c-*fos* followed by a dTMP synthase and DNA polymerase.[117] A ribozyme was constructed to a site in c-*fos* mRNA, and it was demonstrated that activation of the fos ribozyme resulted in decreased c-*fos* gene expression, increased sensitivity to chemotherapeutic agents (including cisplatin), and a significant decrease in dTMP synthase, DNA polymerase β, topoisomerase I, and hMTII-A gene expression (human metallothionein).[116–119]

Snyder *et al.*[120] demonstrated ribozyme-mediated inhibition of *bcr/abl* gene expression in a cell line which was positive for the Philadelphia chromosome. The Philadelphia chromosome results from a reciprocal translocation en chromosomes 9 and 22 and is found in over patients with chronic myelogenous leukemia (CML). This translocation results in the transposition of the cellular (c-*abl*) gene from its usual position on chromosome 9 to chromosome 22.[121,122] Transposition of c-*abl* into the *BCR* gene results in the creation of an abnormal fusion gene termed *bcr-abl*. The mRNA transcript resulting from the fusion gene is translated into a p210 protein with augmented tyrosine kinase activity. This $p210^{bcr/abl}$ protein and its corresponding RNA are found in virtually all patients with CML and in about 50% of patients with Philadelphia-chromosome-positive acute lymphoblastic leukemia.

In this study a ribozyme was directed against the junction sequence in *bcr/abl*. The DNA encoding this ribozyme was incorporated into a plasmid and transfected into EM-2 cells (a CML-derived cell line) using a liposome vehicle. The ribozyme decreased levels of detectable *bcr/abl* mRNA in these cells, inhibited expression of the *bcr/abl* gene product, $p210^{bcr/abl}$, completely, and inhibited cell growth by 84%, significantly more than an antisense oligonucleotide. There was no significant inhibition by liposome vector alone, sense oligonucleotide, or unrelated ribozyme. Wright *et al.*[123] also demonstrated ribozyme-mediated cleavage of *bcr/abl*. This ribozyme transcript was tested against a synthetic substrate which covered the translocation sequence. This study confirmed the activity of a ribozyme against the translocation sequence and also showed that cleavage of the normal *bcr* occurred but at a reduced efficiency compared to the *bcr/abl* substrate. A similar study by Shore *et al.*[124] also showed ribozyme-mediated cleavage of the *bcr/abl* oncogene transcript. These investigators designed a ribozyme to cleave a GUU triplet adjacent to the junction of the cBCR and cABL fused genes. The ribozyme efficiently cleaved the RNA transcript *in vitro*. To determine the effect of constitutive expression of the ribozyme on the gene product, the ribozyme cDNA sequence was inserted into different retroviral expression vectors. Introduction of the recombinant retroviruses into the CML blast crisis cell line K562 resulted in the elimination of the p210 protein kinase activity in several single-cell clones infected with the ribozyme expression cassette.

Cantor *et al.*[125] developed a ribozyme that cleaves *rex/tax* mRNA and inhibited bovine leukemia virus expression. The transactivating protein, tax, stimulates the long terminal repeat to promote viral transcription and may be involved in tumorigenesis. Rex is involved in the transition from early expression of regulatory proteins to later expression of viral structural proteins. A ribozyme designed against both target sequences cleaved more than 80% of the target RNA *in vitro*. Synthetic DNA encoding the ribozyme was cloned into an expression vector and transfected into bovine leukemia virus-infected bat lung cells. Intracellular cleavage of the *rex/tax* mRNA was confirmed by reverse transcriptase PCR. In cells expressing the ribozyme, viral expression was inhibited significantly as measured by bovine leukemia virus core protein p24 (61% inhibition) and reverse transcriptase activity (92% inhibition).

Future Aspects

As demonstrated above, control of gene expression using ribozymes holds the potential to provide an

important new paradigm for ...an therapeutics. In the past several years, substantial progress has been made in translating this potential into reality. Cell culture and *in vivo* efficacy have been demonstrated in a number of systems, and therapeutic applications in viral diseases and cancer have been initiated. However, to complete this process, a number of issues need to be resolved. The current status of these issues, both for ribozymes and other oligonucleotide therapeutic approaches, is discussed below.

A. Specificity. One of the features that distinguishes oligonucleotide-based therapies from other approaches is the high degree of selectivity that is available, at least in principle. Differences are becoming apparent in the translation into practice of ribozyme, antisense, 2′,5′-polyadenosine oligonucleotide and other techniques. (The 2′,5′-polyadenosine guide sequence serves to activate a latent RNAse (RNAse L) in the cell which cleaves double-stranded RNA.[126-128]) One of the particular advantages of ribozymes is, as noted by Herschlag[36] and others,[57] the length of a target sequence of 15 nucleotides which may be unique in the human genome. Herschlag also showed that, for ribozymes and other oligonucleotide therapeutics that act through binding an RNA target followed by cleavage by an additional enzyme, adding bases to a recognition sequence ultimately reduces discrimination, since cleavage occurs virtually every time the target RNA or a mismatched RNA is bound. This occurs despite the weaker binding of the mismatched RNA because dissociation is too slow to allow the ribozyme to discriminate between the target RNA and a mismatched RNA.

The Herschlag conclusions are supported in the study of Goodchild and Kohli.[129] They demonstrated that ribozymes designed to cleave sequences specific to viral RNA (HIV) may be better antiviral agents than larger antisense oligonucleotides. By reducing the base pair formed with the substrate from 20 to 12, they showed that the rate of cleavage *in vitro* increased 10-fold. Deletions within the stem–loop structure in the ribozyme also increased the initial rate of the reaction.

Specificity mismatches near the core not only reduce binding but have an additional negative effect on cleavage. To give an extreme example, matched arms but with a mismatch at the "U" of "UH" site gives no cleavage by a hammerhead ribozyme; the corresponding antisense molecule presumably is not much affected.

Limited specificity is found in most antisense DNA oligomers, which typically contain 20 nucleotides or more.[57] This is particularly true in the case of DNA antisense oligonucleotides comprised of phosphorothioate linkages. To illustrate this point, Woolf and coworkers[126] demonstrated in an oocyte that, as mismatches in an antisense molecule were introduced, the oligomer continued to inhibit its primary target but showed nonspecific inhibition of other targets as well. Since oligonucleotides beyond the length of 15 will increase the number of mismatch recognition opportunities, the appearance of nonspecific effects for oligonucleotides having more than 15 nucleotides is not surprising.

In the case of ribozymes, available internal data on hammerhead ribozymes indicates that the optimum length of recognition arms is 6–7 nucleotides on each side of the catalytic core. Therefore, experimental evidence curr... available is consistent with the Herschlag theoretical analysis.[36] Thus, with optimum recognition sequences in ribozymes long enough to recognize a target sequence uniquely but not requiring additional nucleotides for activity, nonspecific effects are minimized.

B. Kinetic Considerations. Kinetic considerations may also be important in the effective translation of oligonucleotide therapeutics into reality. In the case of antisense approaches, the DNA–RNA hybrid may be cleaved by activated RNase H. However, this process requires a trimolecular mechanism involving sequential or simultaneous association of the antisense molecule, the target RNA, and the RNAase in order to achieve cleavage. For this to be an efficient mechanism, the third component of the reaction, i.e., the requisite cleaving enzyme, must be present at saturating concentrations relative to the binary complex. This is difficult to assure in general for all cell types of interest, but studies to date[57] suggest that these enzymes may be present in sufficient abundance to carry out the reactions in some cases. Similar conclusions apply for the 2–5A approach,[127,128] where activation of RNAse L is required to cleave the target in the 2-5A–target complex.

Ribozymes do not require a separate enzymatic component for cleavage of the target. Only the bimolecular complex of ribozyme and target plus Mg^{2+} are needed, since both recognition and cleavage are incorporated into the same molecule. Demonstration of the extent of therapeutic advantage that this provides to ribozymes will presumably become evident as animal and human clinical studies are carried out.

C. Cleavage and Turnover. The ability of ribozymes to cleave their target enzymatically provides at least three significant potential advantages as therapeutics: their mechanism of action which destroys the substrate, multiple turnover to increase potency, and increased specificity when compared to small molecules or antisense therapeutic agents.

To demonstrate the importance of target cleavage, the experiment of Homann and co-workers is relevant.[105] They incorporated the catalytic domain of a HH ribozyme into a 413 nucleotide antisense RNA directed against the 5′-leader/gag region of HIV. The presence of the catalytically active RNA resulted in a 4–7-fold greater inhibition of HIV replication as compared to the parental antisense and the inactive mutant. Using ribozyme turnover to increase potency is at an earlier stage. The study by L'Huiller *et al.*[48] demonstrated cleavage products in cells but also showed a requirement for a ribozyme excess of approximately 1000:1 relative to the substrate. The ribozyme appeared to be functioning as a catalytic agent but was present in substrate quantities. This may be due to a relatively slow turnover rate.

D. Delivery. One of the issues of importance to effective exogenous delivery of ribozymes has been satisfactorily resolved, i.e., the creation of chemically modified ribozymes with both significant activity and long lifetimes in human serum. However, issues of lipid choice, targeting of specific cell types or organs, avoidance of sources of drug elimination such as the kidney, intracellular localization of ribozyme with its target, and increase of effective ribozyme delivery to cells through

challenges.

In the field case of ve delivery, the questions which remain are common to the field of gene therapy. The optimum viral vector is not clear; experience to date is largely limited to retroviral vectors. Optimization of ribozyme activity by modification of the transcription unit also provides opportunities for improvement.[130,131] Delivery of vectors is also an issue; whether *ex vivo* delivery of viral vectors will be sufficient or whether systemic delivery is necessary is not clear. Creation of satisfactory vectors to transfect CD34+ or stem cells is still in its infancy. Whether nonviral vectors can be utilized is not clear. Finally, reduction in production costs and long-term safety questions remain to be answered.

E. Therapeutic Potential. The therapeutic possibilities for ribozymes in clinical medicine are many. The mRNA for any protein which is causative in a disease is a potential ribozyme target. Similarly, microorganisms, especially viruses, since they are the pathogenic agents in infectious processes are likely targets for ribozyme therapy. In each of these general examples, it is the specificity of the ribozyme which is so important in therapy. The ability to eliminate a specific mRNA in a cell without damage to other normal cellular RNA molecules is a significant advance in therapeutics and one which may not apply to other therapeutic modalities.

Chemically synthesized ribozymes can be delivered to a variety of target organs or tissues topically. For example, the direct application of a ribozyme to the arterial wall may be used to modify the restenotic process after angioplasty. The target in this instance would be one of the gene products associated with smooth muscle cell proliferation which is activated by the angioplasty procedure. One could also inject a synthetic ribozyme into a joint space to suppress an inflammatory process by eliminating a particular cytokine or enzyme in that process. A viral infection in the lung, especially one confined to the bronchial epithelium, could be treated by aerosolization of a chemically synthesized ribozyme. The duration of action of the stable ribozyme should be sufficient to treat a viral infection of 4–6 days.

Ribozymes delivered by a vector will be of more use in systemic diseases, infectious or noninfectious, and diseases of a chronic nature, local or systemic, where long-term expression of the ribozyme is important. The most prominent example is the use of a ribozyme against HIV to eliminate the virus from the stem cells in the bone marrow. This could permit the reconstitution of the immune system with cells resistant to HIV. A leukemic process due to the presence of a new gene product, such as *bcr–abl* in chronic myelogenous leukemia, is a natural target for a ribozyme since the RNA product of the fusion gene is not found in normal cells and is known to be causative in the disease. Oncogenes associated with other types of neoplasia, which result from the mutation of a protooncogene, similarly are good potential targets since the new gene product also is not found in the normal adult cell. The list of potential applications is as long as the list of new gene products associated with viral diseases, neoplastic diseases, chronic inflammatory conditions, cardiovascular diseases, gene overproduction of an aberrant protein.

Acknowledgment. The authors would like to express their appreciation to T. Cech, N. Usman, B. Chowrira, and D. Stinchcomb for helpful comments and suggestions.

Biographies

Ralph E. Christoffersen obtained his Ph.D. degree in Physical Chemistry from Indiana University, Bloomington, IN, in 1964. After postdoctoral experience at the University of Nottingham, England, and Iowa State University in Ames, he joined the faculty of the Department of Chemistry at the University of Kansas. In 1972 he was appointed Professor of Chemistry and in 1979 became Vice Chancellor for Academic Affairs. In 1981, he joined Colorado State University as President, and when he left in 1983 to join the Upjohn Company in Kalamazoo as Director of Biotechnology, was Professor of Chemistry. In 1989, he left the position of Vice President, Discovery Research at Upjohn, to join Smith-Kline Beecham as Senior Vice President, Research. In 1992, he became President and CEO of Ribozyme Pharmaceuticals in Boulder, CO.

J. Joseph Marr obtained his M.D. degree from Johns Hopkins in 1964 and completed an M.S. in Research in Microbiology at the St. Louis University Graduate School. After six years at Washington University School of Medicine, he became Professor in Medicine and Microbiology at the St. Louis University School of Medicine and reached the rank of Vice Chairman. In 1982, he joined the University of Colorado Health Sciences Center as Professor of Medicine and Biochemistry, Director of the Clinical Laboratories, and Head, Division of Infectious Diseases and the Division of Laboratory Medicine. In 1989 he joined G. D. Searle as Senior Vice President, Discovery Research. Since 1993, he has been Vice President, R & D, and CSO at Ribozyme Pharmaceuticals in Boulder, CO.

References

(1) Cech, T. R.; Zaug, A. J.; Grabowski, P. J. *In vitro* Splicing of the Ribosomal RNA Precursor of *Tetrahymena*: Involvement of a Guanosine Nucleotide in the Excision of the Intervening Sequence. *Cell* **1981**, *29*, 487–496.
(2) Kruger, K.; Grabowski, P. J.; Zaug, A. J.; Sands, J.; Gottschling, D. F.; Cech, T. R. Self-splicing RNA: Autoexcision and Autocyclization of the Ribosomal RNA Intervening Sequence of *Tetrahymena*. *Cell* **1982**, *31*, 147–157.
(3) Guerrier-Takada, C.; Gardiner, K.; Marsh, T.; Pace, N.; Altman, S. The RNA Moiety of Ribonuclease P Is the Catalytic Subunit of the Enzyme. *Cell* **1983**, *35*, 849–857.
(4) Cech, T. R. Self-splicing RNA: Implications for Evolution. *Int. Rev. Cytol.* **1985**, *93*, 3–22.
(5) Darnell, J. S.; Doolittle, W. F. Speculations on the Early Course of Evolution. *Proc. Natl. Acad. Sci. U.S.A.* **1986**, *83*, 1271–1275.
(6) Cech, T. R. A Model for the RNA-catalyzed Replication of RNA. *Proc. Natl. Acad. Sci. U.S.A.* **1986**, *83*, 4360–4363.
(7) Joyce, G. F.; Schwartz, A. W.; Miller, S. L.; Orgel, L. E. The Case for An Ancestral Genetic System Involving Simple Analogues of the Nucleotides. *Proc. Natl. Acad. Sci. U.S.A.* **1987**, *84*, 4398–4402.
(8) Cech, T. R. RNA Chemistry. Ribozyme Self-replication? *Nature* **1989**, *339*, 507–508.
(9) Doudna, J. A.; Szostak, J. W. RNA-catalyzed Synthesis of Complementary-strand RNA. *Nature* **1989**, *339*, 519–522.
(10) Cech, T. R. The Efficiency and Versatility of Catalytic RNA: Implications for An RNA World. *Gene* **1993**, *135*, 33–36.
(11) For a review of ribozyme development, see: Cech, T. R. Ribozyme Engineering. *Curr. Opin. Struct. Biol.* **1992**, *2*, 605–609.
(12) Cech, T. R. The Generality of Self-splicing RNA: Relationship to Nuclear mRNA Splicing. *Cell* **1986**, *44*, 207–210.

(13) Peebles, C. L.; Perlman, P. S.; [illegible]burg, K. L.; Petrillo, M. L.; Tabor, J. H.; Jarrell, K. A.; [illegible]A.-L. A Self-splicing RNA Excises an Intron Lariat. *Cell* 1986, *44*, 213–223.
(14) Van der Veen, R. T.; Arnberg, A. C.; Van der Horst, G.; Bonen, L.; Tabak, H. F.; Grivell, L. A. Excised Group II Introns in Yeast Mitochondria Are Lariats And Can Be Formed By Self-splicing *In Vitro*. *Cell* 1986, *44*, 225–234.
(15) Michel, F.; Umesono, K.; Ozeki, H. Comparative and Functional Anatomy of Group II Catalytic Introns – A Review. *Gene* 1989, *82*, 5–30.
(16) Zaug, A. J.; Kent, J. R.; Cech, T. R. A Labile Phosphodiester Bond at the Ligation Junction in A Circular Intervening Sequence. *Science* 1984, *224*, 574–578.
(17) Zaug, A. J.; Cech, T. R. The Intervening Sequence RNA of *Tetrahymena* Is An Enzyme. *Science* 1986, *231*, 470–475.
(18) Zaug, A. J.; Been, M. D.; Cech, T. R. The *Tetrahymena* Ribozyme Acts Like An RNA Restriction Endonuclease. *Nature* 1986, *324*, 429–433.
(19) Xu, M.-Q.; Kathe, S. D.; Goodrich-Blair, H.; Nierzwicki-Bauer, S. A.; Shub, D. A. Bacterial Origin of Chloroplast Intron: Conserved Self-Splicing Group I Introns in Cyanobacteria. *Science* 1990, *250*, 1566–1570.
(20) Johansen, S.; Vogt, V. M. An Intron in the Nuclear Ribosomal DNA of Didymium iridis Codes for a Group I Ribozyme and a Novel Ribozyme That Cooperate in Self-Splicing. *Cell* 1994, *76*, 725–734.
(21) Guo, H. C. T.; Collins, R. A. Efficient *trans*-cleavage of a stem-loop RNA substrate by a ribozyme derived from *Neurospora VS* RNA. *EMBO J.* 1995, *14*, 368–376.
(22) Prody, G. A.; Bakos, J. T.; Buzayan, J. M.; Schneider, I. R.; Bruening, G. Autolytic Processing of Dimeric Plant Virus Satellite RNA. *Science* 1986, *231*, 1577–1580.
(23) Hutchins, C. J.; Rathjen, P. D.; Forster, A. C.; Symons, R. H. Self-cleavage of Plus And Minus RNA Transcripts of Avocado Sunblotch Viroid. *Nucl. Acids Res.* 1986, *14*, 3627–3640.
(24) Uhlenbeck, O. C. A Small Catalytic Oligoribonucleotide. *Nature* 1987, *328*, 596–600.
(25) Forster, A. C.; Symons, R. H. Self-cleavage of Virusoid RNA Is Performed By The Proposed 55-Nucleotide Active Site. *Cell* 1987, *50*, 9–16.
(26) Edington, B. V.; Nelson, R. S. Utilization or Ribozymes in Plants. *Gene Regulation: Biology of Antisense RNA and DNA*. Erickson, R. P., Izant, J. G., Eds.; Raven Press: New York, 1992; pp 209–221.
(27) Sharmeen, L.; Kuo, M. Y. P.; Dinter-Gottlieb, G.; Taylor, J. Antigenomic RNA of Human Hepatitis Delta Virus Can Undergo Self-Cleavage. *J. Virol.* 1988, *62*, 2674–2679.
(28) Wu, H.-N.; Lin, Y.-J.; Lin, F.-P.; Makino, S.; Chang, M.-F.; Lai, M. M. C. Human Hepatitis Delta Virus RNA Subfragments Contain An Autocleavage Activity. *Proc. Natl. Acad. Sci. U.S.A.* 1989, *86*, 1831–1835.
(29) Haseloff, J.; Gerlach, W. L. Simple RNA Enzymes with New and Highly Specific Endoribonuclease Activities. *Nature* 1988, *334*, 585–591.
(30) Hampel, A.; Tritz, R.; Hicks, M.; Cruz, P. "Hairpin" Catalytic RNA Model: Evidence for Helices and Sequence Requirement for Substrate RNA. *Nucl. Acids Res.* 1990, *18*, 299–304.
(31) Feldstein, P. A.; Buzayan, J. M.; Bruening, G. Two Sequences Participating in the Autolytic Processing of Satellite Tobacco Ringspot Virus Complementary RNA. *Gene* 1989, *82*, 53–61.
(32) Perrotta, A. T.; Been, M. D. A Pseudoknot-Like Structure Required for Efficient Self-Cleavage of Hepatitis Delta Virus RNA. *Nature* 1991, *350*, 434–436.
(33) Branch, A. D.; Robertson, H. D. Efficient *Trans* Cleavage and A Common Structural Motif for the Ribozymes of the Human Hepatitis Delta Agent. *Proc. Natl. Acad. Sci. U.S.A.* 1991, *88*, 10163–10167.
(34) Perrotta, A. T.; Been, M. D. Cleavage of Oligoribonucleotides By A Ribozyme Derived from the Hepatitis Delta Virus RNA Sequence. *Biochemistry* 1992, *31*, 16–21.
(35) Helene, C.; Toulme, J. J. Specific Regulation of Gene Expression by Antisense, Sense, and Antigene Nucleic Acids. *Biochim. Biophys. Acta* 1990, *1049*, 99–125.
(36) Hearst, J. E. A Photochemical Investigation of the Dynamics of Oligonucleotide Hybridization. *Annu. Rev. Phys. Chem.* 1988, *39*, 291–315.
(37) Herschlag, D. Implications of Ribozyme Kinetics for Targeting the Cleavage of Specific RNA Molecules *in Vivo*: More Isn't Always Better. *Proc. Natl. Acad. Sci. U.S.A.* 1991, *88*, 6921–6925.
(38) Young, B.; Herschlag, D.; Cech, T. R. Mutations in a Nonconserved Sequence of the Tetrahymena Ribozyme Increase Activity and Specificity. *Cell* 1991, *67*, 1007–1019.
(39) Beaudry, A. A.; Joyce, G. F. Directed Evolution of an RNA Enzyme. *Science* 1992, *257*, 635–641.
(40) Green, R.; Szostak, J. W. Selection of a Ribozyme that Functions as a Superior Template in a Self-Copying Reaction. *Science* 1992, *258*, 1910–1915.
(41) Lehman, N.; Joyce, G. F. Evolution *In Vitro* of an RNA Enzyme with Altered Metal Dependence. *Nature* 1993, *361*, 182–185.
(42) Pan, R.; U[illegible]. O. C. *In Vitro* Selection of RNAs that Undergo Aut[illegible]tic Cleavage with Pb^{2+}. *Biochemistry* 1992, *31*, 3887–3895.
(43) Bartel, D. P.; Szostak, J. W. Isolation of New Ribozymes from a Large Pool of Random Sequences. *Science* 1993, *261*, 1411–1418.
(44) Prudent, J. R.; Uno, T.; Schultz, P. G. Expanding the Scope of RNA Catalysis. *Science* 1994, *264*, 1924–1927.
(45) Lorsch, J. R.; Szostak, J. W. *In vitro* Evolution of New Ribozymes with Polynucleotide Kinase Activity. *Nature* 1994, *371*, 31–36.
(46) Cameron, F. H.; Jennings, P. A. Specific Gene Suppression by Engineered Ribozymes in Monkey Cells. *Proc. Natl. Acad. Sci. U.S.A.* 1989, *86*, 9139–9143.
(47) Cotten, M.; Birnstiel, M. L. Ribozyme Mediated Destruction of RNA *in vivo*. *EMBO J.* 1989, *8*, 3861–3866.
(48) L'Huillier, P. J.; Davis, S. R.; Bellamy, A. R. Cytoplasmic Delivery of Ribozymes Leads to Efficient Reduction in α-lactalbumin mRNA Levels in C1271 Mouse Cells. *EMBO J.* 1992, *11*, 4411–4418.
(49) Saxena, S. K.; Ackerman, E. J. Ribozymes Correctly Cleave a Model Substrate and Endogenous RNA *In Vivo*. *J. Biol. Chem.* 1990, *265*, 17106–17109.
(50) Inokuchi, Y.; Yuyama, N.; Hirashima, A.; Nishikawa, S.; Ohkawa, J.; Taira, J. A Hammerhead Ribozyme Inhibits the Proliferation of an RNA Coliphage SP in *E. Coli*. *J. Biol. Chem.* 1994, *269*, 11361–11366.
(51) Efrat, S.; Leiser, M.; Wu, Y.-J.; Fusco-DeMane, D.; Emran, O. A.; Surana, M.; Jetton, T. L.; Magnuson, M. A.; Weir, G.; Fleischer, N. Ribozyme-Mediated Attenuation of Pancreatic β-Cell Glucokinase Expression in Transgenic Mice Results in Impaired Glucose-Induced Insulin Secretion. *Proc. Natl. Acad. Sci. U.S.A.* 1994, *91*, 2051–2055.
(52) Steinecke, P.; Herget, T.; Schreier, P. H. Expression of a Chimeric Ribozyme Gene Results in Endonucleolytic Cleavage of Target mRNA and A Concomitant Reduction of Gene Expression *In Vivo*. *EMBO J.* 1992, *11*, 1525–1530.
(53) Zhao, J. J.; Pick, L. Generating Loss-of-function Phenotypes of the *fushi tarazu* Gene with a Targeted Ribozyme in *Drosophila*. *Nature* 1993, *365*, 448–451.
(54) Larsson, S.; Hotchkiss, G.; Andang, M.; Nyholm, T.; Inzumza, J.; Jansson, I.; Ahrlund-Richter, L. Reduced β2-microglobulin mRNA Levels in Transgenic Mice Expressing a Designed Hammerhead Ribozyme. *Nucl. Acids Res.* 1994, *22*, 2242–2248.
(55) Zuker, M. On Finding All Suboptimal Foldings of an RNA Molecule Science 1989, *244*, 48–52.
(56) Christoffersen, R. E.; McSwiggen, J. A.; Konings, D. Application of Computational Technologies to Ribozyme Biotechnology Products. *J. Mol. Struct. (THEOCHEM)* 1994, *311*, 273–284.
(57) Beaucage, S. L.; Iyer, R. P. The Functionalization of Oligonucleotides *via* Phosphoramidite Derivatives. *Tetrahedron* 1993, *49*, 6123–6194.
(58) Milligan, J. F.; Matteucci, M. D.; Martin, J. C. Current Concepts in Antisense Drug Design. *J. Med. Chem.* 1993, *36*, 1923–1937.
(59) Pieken, W. A.; Olsen, D. B.; Benseler, F.; Aurup, H.; Eckstein, F. Kinetic Characterization of Ribonuclease Resistant 2'-modified Hammerhead Ribozymes. *Science* 1991, *253*, 314–317.
(60) Scaringe, S. A.; Franklyn, C.; Usman, N. Chemical Synthesis of Biologically Active Oligoribonucleotides Using β-cyanoethyl Protected Ribonucloside Phosphoramidites. *Nucl. Acids Res.* 1990, *18*, 5433–5441.
(61) Yang, J.-H.; Usman, N.; Chartrand, P.; Cedergren, R. J. Minimum Ribonucleotide Requirement for Catalysis by the RNA Hammerhead Domain. *Biochemistry* 1992, *31*, 5005–5009.
(62) Paolella, G.; Sproat, B. S.; Lamond, A. I. Nuclease-resistant Ribozymes with High Catalytic Activity. *EMBO J.* 1992, *11*, 1913–1919.
(63) Shibahara, S.; Mukai, S.; Morisawa, H.; Nakashima, H.; Kobayashi, S.; Yamamoto, N. Inhibition of Human Immunodeficiency Virus (HIV-1) Replication by Synthetic Oligo-RNA Derivatives. *Nucl. Acids Res.* 1989, *17*, 239–252.
(64) Beigelman, L.; Karpeisky, A.; Usman, N. Synthesis of 1-Deoxy-D-Ribofuranose Phosphoramidite and the Incorporation of Abasic Nucleotides in Stem-Loop II of a Hammerhead Ribozyme. *Bioorg. Med. Chem. Lett.* 1994, *4*, 1715–1720.
(65) Usman, N.; Beigelman, L.; Draper, K.; Gonzalez, C.; Jensen, K.; Karpeisky, A.; Modak, A.; Matulic-Adamic, J.; DiRenzo, A.; Haeberli, P.; Tracz, D.; Grimm, S.; Wincott, F.; McSwiggen, J. Chemical Modification of Hammerhead Ribozymes: Activity and Nuclease Resistance. *Biochemistry*, in press.
(66) Lichtenberg, D.; Liposomes: Preparation, Characterization, and Preservation. *Methods Biochem. Anal.* 1988, *33*, 337–468.
(67) Litzinger, D. C.; Huang, L. Phosphatidylethanolamine Liposomes: Drug Delivery, Gene Transfer and Immunodiagnostic Applications. *Biochim. Biophys. Acta* 1992, *1113*, 201–227.
(68) Mayer, L. D.; Tai, L. C. L.; Ko, D. S. C.; Masin, D.; Ginsberg, R. S.; Cullis, P. R.; Bally, M. B. Influence of Vesicle Size, Lipid Composition, and Drug-to-Lipid Ratio on the Biological Activity of Liposomal Doxorubicin in Mice. *Cancer Res.* 1989, *49*, 5922–5930.

ability of Ganglioside-Stabilized ...ylphosphatidylethanolamine Liposomes. *Biochim. Bio... ...ta* **1992**, *1104*, 179–187.
(70) Leserman, L. D.; Weinstein, J. N. ...menthal, R.; Terry, W. D. Receptor-mediated Endocytosis of antibody-opsonized liposomes by tumor cells. *Proc. Natl. Acad. Sci. U.S.A.* **1980**, *77*, 4089–4093.
(71) Berinstein, N.; Matthay, K. K.; Papahadjopoulos, D.; Levy, R.; Sikic, B. I. Antibody-Directed Targeting of Liposomes to Human Cell Lines: Role of Binding and Internalization of Growth Inhibition. *Cancer Res.* **1987**, *47*, 5954–5959.
(72) Milhaud, P. G.; Machy, P.; Lebleu, B.; Leserman, L. Antibody-targeted Liposomes Containing poly(rI)-poly(rC) Exert a Specific Antiviral and Toxic Effect on Cells Primed with Interferons α/β or γ. *Biochim. Biophys. Acta* **1989**, *987*, 15–20.
(73) Moghimi, S. M.; Patel, H. M. Opsonophagocytosis of Liposomes by Peritoneal Macrophages and Bone Marrow Reticulendothelial Cells. *Biochim. Biophys. Acta* **1992**, *1135*, 269–274.
(74) Papahadjopoulos, D.; Allen, T. M.; Gabizon, A.; Mayhew, E.; Matthay, K.; Huang, S. K.; Lee, K.-D.; Woodle, M. C.; Lasic, D. D.; Redemann, C.; Martin, F. J. Sterically stabilized liposomes: Pronounced improvmenets in blood clearance, tissue distribution and therapeutic index of encapsulated drugs against implanted tumors. *Proc. Natl. Acad. Sci. U.S.A.* **1991**, *88*, 11460–11464.
(75) Klibanov, A. L.; Maruyama, K.; Beckerleg, A. M.; Torchilin, V. P.; Huang, L. Activity of amphipathic poly(ethylene glycol) 5000 to prolong the circulation time of liposomes depends on the liposome size and is unfavorable for immunoliposome binding to target. *Biochim. Biophys. Acta* **1991**, *1062*, 142–148.
(76) Lee, R. J.; Low, P. S. Delivery of Liposomes into Cultured KB Cells *via* Folate Receptor-mediated Endocytosis. *J. Biol. Chem.* **1994**, *269*, 3198–3204.
(77) Nabel, E. G.; Plautz, G.; Boyce, F. M.; Stanley, J. C.; Nabel, G. J. Recombinant gene expression *in vivo* within endothelial cells of the arterial wall. *Science* **1989**, *244*, 1342–1344.
(78) Nabel, E. G.; Plautz, G.; Nabel, G. J. Site-specific Gene Expression *In Vivo* By Direct Gene Transfer into the Arterial Wall. *Science* **1990**, *249*, 1285–1288.
(79) Nabel, G. J.; Nabel, E. G.; Yang, Z.-Y.; Fox, B. A.; Plautz, G. E.; Gao, X.; Huang, L.; Shu, S.; Gordon, D.; Chang, A. E. Direct Gene Transfer with DNA Liposome Complexes in Melanoma: Expression, Biologic Activity and Lack of Toxicity in Humans. *Proc. Natl. Acad. Sci. U.S.A.* **1993**, *90*, 11307–11311.
(80) Plautz, G. E.; Yang, Z.; Wu, B.; Gao, X.; Huang, L.; Nabel, G. J. Immunotherapy of malignancy by *in vivo* gene transfer into tumors. *Proc. Natl. Acad. Sci., U.S.A.* **1993**, *90*, 4645–4649.
(81) Stewart, M. J.; Plautz, G. E.; Del Buono, L.; Yang, Z. Y.; Xu, L.; Gao, X.; Huang, L.; Nabel, E. G.; Nabel, G. J. Gene Transfer *in Vivo* with DAN-liposome Complexes: Safety and Acute Toxicity in Mice. *Human Gene Ther.* **1992**, *3*, 267–275.
(82) Zhu, N.; Liggitt, D.; Liu, Y.; Debs, R. Systemic Gene Expression after Intravenous DNA Delivery into Adult Mice. *Science* **1993**, *261*, 209–211.
(83) San, H.; Yang, Z.-H.; Pompili, V. J.; Jaffe, M. L.; Plautz, G. E.; Xu, L.; Felgner, J. H.; Wheeler, C. J.; Felgner, P. L.; Gao, X.; Huang, L.; Gordon, D.; Nabel, G. J.; Nabel, E. G. Safety and Short-Term Toxicity of a Novel Cationic Lipid Formulation for Human Gene Therapy. *Human Gene Ther.* **1993**, *4*, 781–788.
(84) Plautz, G. E.; Wu, B.-Y.; Gao, X.; Huang, L.; Nabel, G. J. Gene Transfer *In Vivo* with DNA-liposome Complexes: Lack of Autoimmunity and Gonadal Localization. *Human Gene Ther.* **1992a**, *3*, 649–656.
(85) Sullenger, B. A.; Cech, T. R. Tethering Ribozymes to a Retroviral packaging Signal for Destruction of Viral RNA. *Science* **1993**, *262*, 1566–1569.
(86) Tsuchihashi, A.; Khosla, M.; Herschlag, D. Protein Enhancement of Hammerhead Ribozyme Catalysis. *Science* **1993**, *262*, 99–102.
(87) Samulski, R. J. Adeno-associated virus: Integration at a Specific Chromosomal Locus. *Curr. Opin. Genet. Dev.* **1993**, *3*, 74–80.
(88) Seth, P.; Rosenfeld, M.; Higginbotham, J.; Crystal, R. G. Mechanism of Enhancement of DNA Expression Consequent to Cointernalization of a Replication-Deficient Adenovirus and Unmodified Plasmid DNA. *J. Virol.* **1994**, 933–940.
(89) FitzGerald, D. J. P.; Padmanabhan, R.; Pastan, I.; Willingham, M. C. Adenovirus-induced Release of Epidermal Growth Factor and Pseudomonas Toxin into the Cytosol of KB Cells During Receptor-mediated Endocytosis. *Cell* **1983**, *32*, 607–617.
(90) Seth, P.; FitzGerald, D.; Willingham, M.; Pastan, I. Pathway of Adenovirus Entry into Cells. in *Virus Attachment and Entry into Cells*; Colwell, R., Lonberg-Holm, K., Eds.; American Society for Microbiology: Washington, D.C., 1986.
(91) Otero, M. J. and Carrasco, L. Proteins Are Co-internalized with Virion Particles During Early Infection. *Virology* **1987**, *160*, 75–80.
T.; Biruntiel ...High Efficiency Receptor-mediated Delivery of Small a... ...e 48 Kilobase Gene Constructs Using the Endosome-d... ...on Activity of Defective or Chemically Inactivated Adenovirus Particles. *Proc. Natl. Acad. Sci. U.S.A.* **1992**, *89*, 6094–6098.
(93) Curiel, D. T.; Agarwal, S.; Wagner, E.; Cotten, M. Adenovirus enhancement of transferrin-polylysine-mediated gene delivery. *Proc. Natl. Acad. Sci. U.S.A.* **1991**, *88*, 8850–8854.
(94) Gao, L.; Wagner, E.; Cotten, M.; Agarwal, S.; Harris, C.; Romer, M.; Miller, L.; Hu, P.-C.; Curiel, D. Direct *In Vivo* Gene Transfer to Airway Epithelium Employing Adenovirus-Polylysine-DNA Complexes. *Human Gene Ther.* **1993**, *4*, 17–24.
(95) Sarver, N.; Cantin, E. M.; Chang, P. S.; Zaia, J. A.; Ladne, P. A.; Stephens, D. A.; Rossi, J. J. Ribozymes as Potential Anti-HIV-1 Therapeutic Agents. *Science* **1990**, *247*, 1222–1225.
(96) Rossi, J. J.; Sarver, N. Catalytic Antisense RNA (Ribozymes): Their Potential and Use as Anti-HIV-1 Therapeutic Agents. *Innovations in Antiviral Development and the Detection of Virus Infection*; Block, T.; Ed.; Plenum Press: New York, 1992; pp 95–109.
(97) Weerasinghe, M.; Liem, S. E.; Asad, S.; Read, S. E.; Joshi, S. Resistance to Human Immunodeficiency Virus Type 1 (HIV-1) Infection in Human CD4+ Lymphocyte-Derived Cell Lines Conferred by Using Retroviral Vectors Expressing an HIV-1 RNA-Specific Ribozyme *J. Virol.* **1991**, *65*, 5531–5534.
(98) Dropulic, B.; Lin, N. H.; Martin, M. A.; Jean, K. T. Functional Characterization of a U5 Ribozyme: Intracellular Suppression of Human Immunodeficiency Virus Type I Expression. *J. Virol.* **1992**, *66*, 1432–1441.
(99) Yu, M.; Ojwang, J.; Yamada, O.; Hampel, A.; Rapapport, J.; Looney, D.; Wong-Staal, F. A Hairpin Ribozyme Inhibits Expression of Diverse Strains of Human Immunodeficiency Virus Type I. *Proc. Natl. Acad. Sci. U.S.A.* **1993**, *90*, 6340–6344.
(100) Ojwang, J. O.; Hampel, A.; Looney, D. J.; Wong-Staal, F.; Rappaport, J. Inhibition of Human Immunodeficiency Virus Type 1 Expression by a Hairpin Ribozyme. *Proc. Natl. Acad. Sci. U.S.A.* **1992**, *89*, 10802–10806.
(101) Sullenger, B. A.; Lee, T. C.; Smith, C. A.; Ungers, G. E.; Gilboa, E. Expression of Chimeric tRNA-driven Antisense Transcripts Renders HIV3T3 Cells Highly Resistant to Moloney Murine Leukemia Virus Replication. *Mol. Cell. Biol.* **1990**, *10*, 6512–6523.
(102) Sullenger, B. A.; Gallardo, H. F.; Ungers, G. E.; Gilboa, E. Overexpression of TAR Sequences Renders Cells Resistant to Human Immunodeficiency Virus Replication. *Cell* **1990**, *63*, 601–608.
(103) Jennings, P. A.; Molloy, P. L. Inhibition of SV40 Replicon Function by Engineered Antisense RNA Transcribed by RNA Polymerase III. *EMBO J.* **1987**, *6*, 3043–3047.
(104) Myers, G.; Korber, B.; Berzofsky, J. A.; Smith, R. F.; Pavlakis, G. N. *Human Retroviruses and AIDS*; Theoretical Biology and Biophysics: Los Alamos, 1992.
(105) Homann, M.; Tzortzakaki, S.; Rittner, K.; Sczakiel, G.; Tabler, M. Incorporation of the Catalytic Domain of a Hammerhead Ribozyme into Antisense RNA Enhances its Inhibitory Effect on the Replication of Human Immunodeficiency Virus Type 1. *Nucl. Acids Res.* **1993**, *21*, 2809–2814.
(106) Bertrand, E. L.; Rossi, J. J. Facilitation of Hammerhead Ribozyme Catalysis by the Nucleocapsid Protein of HIV-1 and the Heterogeneous Nuclear Ribonucleoprotein A1. *EMBO J.* **1994**, *13*, 2904–2912.
(107) Ohkawa, J.; Yuyama, T.; Nishikawa, S.; Taira, K. Importance of independence in riboryme reactions: kinetic behavior of trimmed and of simply connected multiple ribozymes with potential activity against human immunodeficiency virus. *Proc. Natl. Acad. Sci. U.S.A.* **1993**, *90*, 11302–11306.
(108) Chen, C.-J.; Banerjea, A. C.; Harmison, G. G.; Haglund, K.; Schubert, M. Multitarget-ribozyme Directed to Cleave at up to Nine Highly Conserved Hiv-1 Env RNA Regions Inhibits HIV-1 Replication – Potential Effectiveness Against Most Presently Sequenced Hiv-1 Isolates. *Nucl. Acids Res.* **1992**, *20*, 4581–4589.
(109) Lo, K. M. S.; Biasolo, M. A.; Dehni, G.; Palu, G.; Haseltine, W. A. Inhibition of Replication of HIV-1 by Retroviral Vectors Expressing *tat*-Antisense and Anti-*tat* Ribozyme RNA. *Virology* **1992**, *190*, 176–183.
(110) Xing, Z.; Whitton, J. L. Ribozymes Which Cleave Arenavirus RNAs: Identification of Susceptible Target Sites and Inhibition by Target Site Secondary Structure. *J. Virol.* **1992**, *66*, 1361–1369.
(111) Xing, Z.; Whitton, J. L. An Anti-Lymphocytic Choriomeningitis Virus Ribozyme Expressed in Tissue Culture Cells Diminishes Viral RNA Levels and Leads to a Reduction in Infectious Virus Yield. *J. Virol.* **1993**, *67*, 1840–1847.
(112) Monia, B. P.; Johnston, J. F.; Ecker, D. J.; Zounes, M. A.; Lima, W. F.; Frier, S. M. Selective Inhibition of Mutant Ha-*ras* messenger RNA Expression by Antisense Oligonucleotides. *J. Biol. Chem.* **1992**, *267*, 19954–19962.

(113) Kashani-Sabet, M.; Funato, T.; Jiao, L.; Wang, W.; Yoshida, E.; Kashfinn, B. I.; S ,Γ.; Wu, A. M.; Moreno, J. G.; Traweek, S. T.; Ahlering, T. ..., Scanlon, K. J. Reversal of the Malignant Phenotype by an Anti-*ras* Ribozyme. *Antisense Res. Dev.* **1992**, *2*, 3–15.
(114) Koizumi, M.; Kamiya, H.; Ohtsuka, E. Ribozymes Designed to Inhibit Transformation of NIH3T3 Cells by the Activated c-Ha-*ras* Gene. *Gene* **1992**, *117*, 179–184.
(115) Koizumi, M.; Kamiya, H.; Ohtsuka, E. Inhibition of c-Ha-*ras* Gene Expression by hammerhead ribozymes containing a Stable C(UUCG)G Hairpin Loop. *Biol. Pharm. Bull.* **1993**, *16*, 879–883.
(116) Scanlon, K. J.; Jiao, L.; Funato, T.; Wang, W.; Tone, T.; Rossi, J. J.; and Kashani-Sabet. Ribozyme-mediated cleavage of c-*fos* mRNA reduces gene expression of DNA synthesis enzymes and metallothionein. *Proc. Natl. Acad. Sci. U.S.A.* **1991**, *88*, 10591–10595.
(117) Kashani-Sabet, M.; Wang, M.; Scanlon, K. J. Cyclosporin A Suppresses Cisplatin-induced c-*fos* gene Expression in Ovarian Carcinoma Cells. *J. Biol. Chem.* **1990**, *265*, 11285–11288.
(118) Rauscher, F. J., III; Cohen, D. R.; Curran, T.; Bos, V. J.; Vogt, P. K.; Bohmann, D.; Tjian, T.; Franza, B. R., Jr.; Cyclosporin A Suppresses Cisplatin-induced c-*fos* Gene Expression in Ovarian Carcinoma Cells. *Science* **1988**, *240*, 1010–1016.
(119) Funato, R.; Yoshida, E.; Jiao, L.; Tone, T.; Kashani-Sabet, M.; Scanlon, K. J. The Utility of An Anti-*fos* Ribozyme in Reversing Cisplatin Resistance in Human Carcinomas. *Adv. Enzyme Regul.* **1992**, *32*, 195–209.
(120) Snyder, D. S.; Wu, Y.; Wang, J. L.; Rossi, J. J.; Swiderski, P.; Kaplan, B. E.; Forman, S. J. Ribozyme-mediated Inhibition of *bcr-abl* Gene Expression in a Philadelphia Chromosome-Positive Cell Line. *Blood* **1993**, *82*, 600–605.
(121) Heisterkamp, N.; Stephenson, J. R.; Groffen, J.; Hansen, P. F.; De Klein, A.; Baartram, C. R.; Grosveld, G. Localization of the c-*abl* Oncogene Adjacent to a *trans*location Break Point in Chronic Myelocytic Leukaemia. *Nature* **1983**, *306*, 239.
(122) Bartram, C. R.; De Klein, A.; Hagemeijer, A.; van Agthoven, T.; van Kessel, A. G.; Bootsma, D.; Grosveld, G.; Ferguson-Smith, M. A.; Davies, T.; Stone, M.; Heisterkamp, N.; Stephenson, J. R.; Groffen, J. *Trans*location of c-*abl* Oncogene Correlates with the Presence of a Philadelphia Chromosome in Chronic Myelotic Leukaemia. *Nature* **1983**, *306*, 277.
(123) Wright, L.; ,S. B.; Milliken, S.; Biggs, J.; Kearney, P. Ribozyme-m. , cleavage of the bcr/abl transcript expressed in chronic myeloid leukemia. *Exp. Hematol.* **1993**, *21*, 1712–1718.
(124) Shore, S. K.; Nabissa, P. M.; Reddy, E. P. Ribozyme-mediated Cleavage of the *bcr/abl* Oncogene Transcript: *In Vitro* Cleavage of RNA and *in Vivo* Loss of p^{210} Protein-kinase Activity. *Oncogene* **1993**, *8*, 3183–3188.
(125) Cantor, G. H.; McElwain, T. F.; Birkebak, T. A.; Palmer, G. H. Ribozyme Cleaves *rex/tax* mRNA and Inhibits Bovine Leukemia Virus Expression. *Proc. Natl. Acad. Sci. U.S.A.* **1993**, *90*, 10932–10936.
(126) Woolf, T. M.; Melton, D. A.; Jennings, C. G. B. Specificity of Antisense Oligonucleotides *In Vivo*. *Proc. Natl. Acad. Sci. U.S.A.* **1992**, *89*, 7305–7309.
(127) Torrence, P. F.; Maitra, R. K.; Lesiak, K.; Khamnei, S.; Zhou, A.; Silverman, R. H. Targeting RNA for Degradation with a (2'-5')oligoadenylate-antisense Chimera. *Proc. Natl. Acad. Sci. U.S.A.* **1993**, *90*, 1300–1304.
(128) Maran, A.; Maitra, R. K.; Kumar, A.; Dong, B.; Xiao, W.; Li, G.; Williams, B. R. G.; Torrence, P. F.; Silverman, R. H. Blockage of NF-κB Signaling by Selective Ablation of an mRNA Target by 2–5A Antisense chimeras. *Science* **1994**, *265*, 789–792.
(129) Goodchild, J.; Kohli, V. Ribozymes That Cleave An RNA Sequence from Human Immunodeficiency Virus: the Effect of Flanking Sequence on Rate. *Arch. Biochem. Biophys.* **1991**, *284*, 386–391.
(130) Taylor, N. R.; Rossi, J. J. Ribozyme-mediated Cleavage of an HIV-1 *gag* RNA: The Effects of Nontargeted Sequences and Secondary Structure on Ribozyme Cleavage Activity. *Antisense Res. Devel.* **1991**, *1*, 173–186.
(131) Chowrira, B. M.; Pavco, P. A.; McSwiggen, J. A. *In vitro* and *in vivo* Comparison of Hammerhead, Hairpin and Hepatitis Delta Virus Self-processing Ribozyme Cassettes. *J. Biol. Chem.* **1994**, *269*, 25856–25864.

JM9407872

Nuclease-resistant ribozymes decrease stromelysin mRNA levels in rabbit synovium following exogenous delivery to the knee joint

CRAIG M. FLORY*†, PAMELA A. PAVCO‡, THALE C. JARVIS‡, MARK E. LESCH*, FRANCINE E. WINCOTT‡, LEONID BEIGELMAN‡, STEPHEN W. HUNT III*, AND DENIS J. SCHRIER*

*Department of Immunopathology, Parke-Davis Pharmaceutical Research, Division of Warner-Lambert Company, Ann Arbor, MI 48105; and ‡Ribozyme Pharmaceuticals Inc., Boulder, CO 80301

Communicated by Pedro Cuatrecasas, Parke-Davis Pharmaceutical Research, Ann Arbor, MI, September 25, 1995

ABSTRACT **Catalytic RNA molecules, or ribozymes, have generated significant interest as potential therapeutic agents for controlling gene expression. Although ribozymes have been shown to work *in vitro* and in cellular assays, there are no reports that demonstrate the efficacy of synthetic, stabilized ribozymes delivered *in vivo*. We are currently utilizing the rabbit model of interleukin 1-induced arthritis to assess the localization, stability, and efficacy of exogenous antistromelysin hammerhead ribozymes. The matrix metalloproteinase stromelysin is believed to be a key mediator in arthritic diseases. It seems likely therefore that inhibiting stromelysin would be a valid therapeutic approach for arthritis. We found that following intraarticular administration ribozymes were taken up by cells in the synovial lining, were stable in the synovium, and reduced synovial interleukin 1α-induced stromelysin mRNA. This effect was demonstrated with ribozymes containing various chemical modifications that impart nuclease resistance and that recognize several distinct sites on the message. Catalytically inactive ribozymes were ineffective, thus suggesting a cleavage-mediated mechanism of action. These results suggest that ribozymes may be useful in the treatment of arthritic diseases characterized by dysregulation of metalloproteinase expression.**

The discovery that certain RNA species possess autocatalytic activity (1–3) has generated significant interest in the potential therapeutic use of catalytic RNA molecules, or ribozymes, in controlling gene expression (4). Naturally occurring ribozymes come in a variety of structural motifs (5). Although most ribozymes evolved to cleave their target sequences in cis, ribozymes have also been shown to function in trans (6, 7). Thus, ribozymes have exceptionally broad potential as therapeutic agents for the selective control of gene expression. Of the naturally occurring ribozymes, the hammerhead (8) is the smallest of the known ribozyme motifs and therefore the most amenable to chemical synthesis. It is also well characterized with respect to kinetic parameters and optimal target sequence, and potential cleavage sites are abundant on most messages.

To develop therapeutic ribozymes, significant research has been devoted to improving catalytic activity, developing nuclease resistance, and optimizing the intracellular delivery of both synthetic and expressed ribozymes (8–11). Synthetic ribozymes have shown efficacy in cell culture in reducing the expression of tumor necrosis factor-α (12), bcr-abl (13), and MDR-1 (14). These studies utilized either chemically synthesized chimeric ribozymes with DNA binding arms to increase nuclease resistance or *in vitro* transcribed ribozymes that are protected in part from degradation by being complexed with cationic lipids. We have used ribozymes that contain novel modifications that allow significant catalytic activity while substantially enhancing their nuclease resistance (15).

There are only a few examples of ribozyme activity *in vivo*, and these involve expression of the ribozyme as a transgene either in *Drosophila* (16) or in mice (17, 18). Demonstration of *in vivo* efficacy represents an important advance in the development of synthetic ribozymes as therapeutic agents.

The matrix metalloproteinases (MMPs) are a group of enzymes that degrade extracellular matrix components such as the collagens, gelatins, proteoglycans, and fibronectin (19). Although MMPs play an important role in embryogenesis and normal tissue remodeling (20), abnormal expression may contribute to such disease processes as atherosclerosis (21), cancer (22), and arthritis (23). Stromelysin (MMP3) may be a key mediator in arthritic diseases. It degrades proteoglycans and a broad spectrum of other matrix components (19), and it can readily degrade cartilage *in vitro* (24). Stromelysin also has the capacity to activate the proenzyme forms of collagenase (25), and the 72- (26) and 92-kDa (27) gelatinases, thus initiating a proteinase cascade. Unlike normal synovial fibroblasts, those derived from osteoarthritic or rheumatoid synovium produce high levels of stromelysin and collagenase upon stimulation (28). Most relevant, however, is the marked upregulation of stromelysin and other MMPs seen in articular tissues from patients with osteo- or rheumatoid arthritis (29, 30). It seems likely therefore that inhibiting stromelysin would be a valid therapeutic approach for arthritis.

In the rabbit, injection of human recombinant interleukin 1α (IL-1α) into the knee joint leads to leukocyte accumulation in the joint space, loss of proteoglycan from the articular cartilage, and release of proteoglycan fragments into the synovial fluid (31). An increase in the levels of the MMPs stromelysin and collagenase in the rabbit articular tissues also occurs after stimulation with IL-1 (32, 33). These attributes make it an appropriate model for assessing the role of proteases involved in the pathophysiology of joint disease. We are using this model to assess the localization, stability, and efficacy of exogenous antistromelysin hammerhead ribozymes. These ribozymes are modified to enhance their resistance to nucleolytic degradation (34). We found that ribozymes are taken up by cells in the synovial lining after intraarticular administration. The ribozymes demonstrate good stability in the synovium and can significantly reduce the synovial levels of IL-1-induced stromelysin mRNA. Catalytically inactive ribozymes had little effect on stromelysin mRNA levels. This report demonstrates efficacy of an exogenous synthetic ribozyme *in vivo*.

MATERIALS AND METHODS

Ribozyme Synthesis and Sequences. Ribozymes were synthesized and purified as described by Wincott et al. (35). The

The publication costs of this article were defrayed in part by page charge payment. This article must therefore be hereby marked "*advertisement*" in accordance with 18 U.S.C. §1734 solely to indicate this fact.

Abbreviations: MMP, matrix metalloproteinase; IL, interleukin.

†To whom reprint requests should be addressed.

hammerhead ribozyme motif used in this study contains binding arms (7–8 nt), which can anneal to the stromelysin message, and an invariant core sequence (22 nt) required for catalytic activity. Ribozymes designated as inactive contain the same binding arm sequences as their active counterparts but have two mutations in the core that eliminate cleavage activity. Scrambled ribozymes have the catalytically active core, but the arm sequence is scrambled to eliminate binding to the target sequence.

The sequences of the ribozymes used are given below. Ribozymes are named for their position of cleavage in the human stromelysin sequence. In cases in which the rabbit site was not homologous with human, the rabbit-specific ribozyme is indicated with an R. Lowercase indicates 2′-*O*-methyl nucleotides, uppercase indicates 2′-hydroxyl (ribo) nucleotides, T indicates 3′-3′ inverted thymidine (iT), and µ indicates 2′-amino at positions U4 and U7.

Site 1049, active:	5′-gaaggaacµGAµGaggccgaaaggccGaaAgauggcT
Site 1049, inactive:	5′-gaaggaacµuAµGaggccgaaaggccGauAgauggcT
Site 1049, scrambled:	5′-ugaagagcµGAµGaggccgaaaggccGaaAcggaagT
Site 1363, active:	5′-cuucaaacµGAµGaggccgaaaggccGaaAcagcauT
Site 1366R, active:	5′-augcuuccµGAµGaggccgaaaggccGaaAaaacagT
Site 1410, active:	5′-aaacacccµGAµGaggccgaaaggccGaaAcuguguT
Site 883, active:	5′-cuggaggccµGAµGaggccgaaaggccGaaAcagguucT
Site 1489R, active:	5′-ugccuuccµGAµGaggccgaaaggccGaaAuacaccT

Unless otherwise indicated, backbone linkages are phosphodiester. These ribozymes are designated U4, U7 NH2, and 3′-iT. In some cases, the ribozymes contained four phosphorothioate linkages at the 5′ end (designated U4, U7 NH2, 4 5′ P=S, and 3′-iT). An alternative chemistry of ribozyme 1049 was also used in which position U4 was 2′-*C*-allyl, position U7 was 2′-*O*-methyl, and five phosphorothioate linkages were included on both the 5′ and 3′ ends (U4 *C*-allyl, 5&5 P=S). The catalytic cleavage activity of all of the ribozymes was verified on a complementary short substrate by standard methods; inactive ribozymes did not exhibit any detectable cleavage activity under these conditions (data not shown).

In Vivo Localization and Stability of Ribozymes Delivered Intraarticularly. Male New Zealand White rabbits (3–4 kg) were anesthetized with ketamine·HCl/xylazine and injected intraarticularly with ≈15 × 10^6 cpm (corresponding to 30 ng) of ^{32}P internally labeled ribozyme combined with 10 µg of unlabeled ribozyme in a total vol of 0.5 ml of phosphate-buffered saline (PBS). At various times thereafter, animals were euthanized, the knee joints were lavaged, and synovial tissue was removed, weighed, and either snap frozen for sectioning and autoradiography or placed in Trizol reagent (GIBCO/BRL) for RNA extraction. After initial homogenization of the synovial tissues for RNA extraction, an aliquot was removed to estimate cpm per mg of synovial tissue (assuming that 20% of the synovium was harvested). After extraction of total RNA from the synovial tissue, equal amounts of RNA were run on a denaturing 5% acrylamide gel and the gel was exposed to x-ray film for densitometric quantitation.

In Situ Hybridization. *In situ* hybridization studies were carried out using full-length antisense RNA probes generated by *in vitro* transcription of linearized pRC/CMV plasmid (Invitrogen) containing an ≈1500-bp rabbit stromelysin cDNA (gift of C. Brinckerhoff, Dartmouth Medical School). Samples of synovial tissue were removed, snap frozen in liquid nitrogen, and stored at −80°C. Frozen sections (4–6 µm) were placed on poly(L-lysine)-treated slides and stored at −20°C. Modifications of previously described methods were used (36).

Efficacy Studies. Rabbits were anesthetized with ketamine·HCl/xylazine and injected intraarticularly through the suprapatellar ligament of both knees with various amounts of ribozyme in 0.5 ml of PBS or in PBS alone. Twenty-four hours after ribozyme administration, each rabbit received 25 ng of recombinant human IL-1α (Genzyme) in one knee and vehicle (PBS/0.2% fetal bovine serum) in the other. The synovium was harvested 6 hr after IL-1 infusion, snap frozen in liquid nitrogen, and stored at −80°C.

Table 1. Distribution of radioactivity after intraarticular administration of radiolabeled ribozyme

	Time after ribozyme administration	Synovial tissue*	Synovial RNA	Synovial lavage fluid
Exp. 1	4 hr	4.0	0.03	0.17
	24 hr	3.0	0.32	0.01
Exp. 2	24 hr	5.6	0.32	ND
	3 days	3.0	0.33	ND
	7 days	1.2	0.19	ND

^{32}P internally labeled ribozyme (15 × 10^6 cpm; corresponding to 30 ng) was mixed with 10 µg of unlabeled ribozyme before intraarticular injection. Numbers reflect percentage recovery of total administered radioactivity and represent mean values from three separate animals. ND, not determined.

*Assessed by determining radioactivity of an aliquot after the initial homogenization with Trizol.

RNA Analysis. Total RNA was extracted from synovial tissue with Trizol reagent and analyzed by Northern blotting as described (36). After probing with a full-length antisense RNA probe to stromelysin (see above), the blots were stripped and reprobed with a 100-nt complementary RNA probe to 18S rRNA (Ambion, Austin, TX) to normalize for loading and extraction efficiency. After autoradiography, levels of stromelysin and 18S rRNA were quantified on a scanning densitometer and the data were normalized to the 18S values. In some experiments, RNA was analyzed by both Northern blot analysis and RNase protection (P.A.P., unpublished data). The results were essentially the same when assessed by either method.

RESULTS

Delivery of Ribozymes to Rabbit Synovial Tissues. For these studies, ribozyme labeled with ^{32}P at one internal position was administered directly into the intraarticular space. The fate of the labeled ribozyme was assessed 4 and 24 hr postribozyme administration in the first experiment, and 1, 3, and 7 days after administration in the second. The percentage of labeled ribozyme remaining in the synovial tissue remained relatively constant between 4 and 24 hr (Table 1, Exp. 1). In the total RNA fraction, however, there was a 10-fold increase in associated radioactivity during the same time period.§ Between 1 and 7 days, there was a 2-fold drop in the total RNA radioactivity and a 4-fold drop in synovial radioactivity (Table 1, Exp. 2). Autoradiographic analysis of the synovial tissue at 24 hr demonstrated that the bulk of the radioactivity was associated with the synovial lining and was intracellular (Fig. 1*A*).

The integrity of the labeled ribozyme extracted with the total synovial RNA at the various times is also shown in Fig. 1. At 4 hr no degradation products could be detected, and by 24 hr the ribozyme remained 80–90% intact (Fig. 1*B*). There were no consistent differences in either the amount or the integrity of labeled ribozyme extracted from IL-1-treated and nontreated knees. The substantial increase in labeled ribozyme present at 24 vs. 4 hr noted above was readily apparent. Fig. 1*C* shows ribozyme integrity at 1, 3, and 7 days. Even after

§These results may be explained by recent studies which indicate that fluorescent ribozyme present in synovial cells 4 hr after administration is mostly endosomal, while at 24 hr there is a more diffuse cytoplasmic fluorescence (data not shown). Therefore, although the total amount present in the tissues may have been similar at 4 and 24 hr (as assessed by total tissue homogenates), at 4 hr the endosomal ribozymes may have been lost in the RNA extraction if the endosomes were not disrupted during the homogenization procedure.

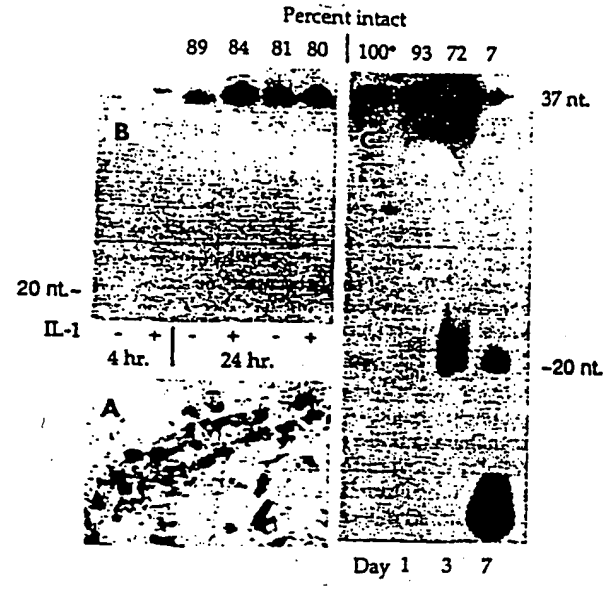

FIG. 1. (*A*) Localization of labeled ribozyme in synoviocytes 24 hr after intraarticular injection. ^{32}P internally labeled ribozyme (15×10^6 cpm; corresponding to 30 ng) was mixed with 10 μg of unlabeled ribozyme before injection. (×340.) (*B*) Stability of labeled ribozyme in synovial tissue 4 and 24 hr after intraarticular administration. Total RNA from synovium (10 μg per lane) was run on a 5% acrylamide/urea gel to assess integrity of the labeled ribozyme. (*C*) Stability of labeled ribozyme in synovial tissue 1, 3, and 7 days after intraarticular administration. The ~20-nt fragment noted in Fig. 2 is the predicted result of endonucleolytic cleavage at two of the unmodified ribonucleotides in the core. *, Sample of ribozyme prior to injection.

7 days, a small amount of full-length ribozyme was still present in synovial tissue.

Stromelysin Expression in Synovial Tissues of IL-1-Treated Rabbit Knees. The kinetics of stromelysin expression after intraarticular injection of 25 ng of IL-1α was assessed by Northern blot (Fig. 2). IL-1 induced a marked but transient increase in the levels of stromelysin mRNA that peaked 6 hr post-IL-1 infusion and returned to near baseline by 24 hr. Saline alone induced a minor but variable increase in strome-

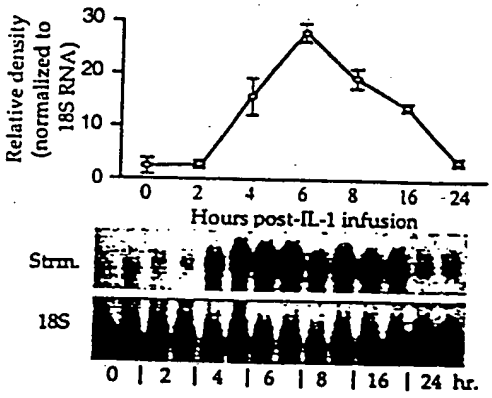

FIG. 2. Kinetics of stromelysin expression after intraarticular injection of 25 ng of IL-1α. Total RNA was extracted from synovial tissue and analyzed by Northern blotting. After probing with a full-length antisense RNA probe to stromelysin, the blots were stripped and reprobed with a 100-nt complementary RNA probe to 18S rRNA to control for equal loading. After autoradiography, stromelysin and 18S rRNA message levels were quantified on a scanning densitometer, and the data were normalized to the 18S values.

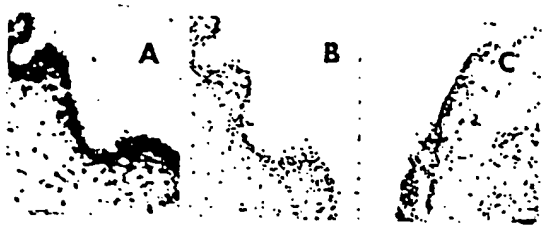

FIG. 3. *In situ* hybridization analysis of stromelysin expression synovial tissue after intraarticular injection of 25 ng of recombina IL-1α. (*A*) IL-1-stimulated tissues hybridized with antisense compl mentary RNA probe. (*B*) IL-1-stimulated tissues with sense probe. ((Control tissues from saline-injected knees hybridized with antisen probe. (×100.)

lysin expression, which followed the same kinetics (data n shown).

Stromelysin mRNA present in IL-1-induced synovial tissu was also visualized by *in situ* hybridization. Fig. 3*A* illustrat the high level of stromelysin expression observed in th synovial lining from IL-1-treated joints and its absence in th underlying tissue. An adjacent section of IL-1-treated tissu incubated with the sense RNA probe was completely negativ (Fig. 3*B*). Fig. 3*C* shows the much reduced expression observe in control, saline-injected knees. Little or no expression wa observed in untreated knees (data not shown).

Reduction in Stromelysin mRNA Levels by Intraarticula Delivery of Synthetic Ribozymes. Delivery studies (Fig. 1 demonstrated that peak intact ribozyme levels were observe in the synovium 24 hr after injection. Therefore, we chose t administer ribozyme 24 hr before IL-1 stimulation for th efficacy studies. The synovial tissue was harvested for RN analysis 6 hr post-IL-1 infusion, the peak of induced strome lysin mRNA levels (Fig. 2).

A representative dose–response curve for ribozyme 104 (U4, U7 NH2, and 3′-iT) demonstrated a significant reductio in stromelysin message at both the 100 and 300 μg per kne dose of active ribozyme (Fig. 4). At a 1.0-mg dose, the efficac of the active ribozyme was unchanged or slightly reduced fron that seen with the 100-μg dose (data not shown). This ri bozyme had been tested on numerous occasions and resulte in an average 60% reduction (ranging from 20% to 80%) i stromelysin message levels compared to the level observed i control, vehicle-treated animals. The inactive ribozyme con trol retains binding arms identical to the active version bu

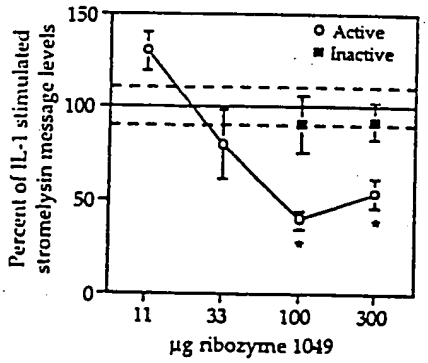

FIG. 4. Dose–response curve of reduction in synovial stromelysin mRNA levels by intraarticular injection of ribozyme 1049, U4, U7 NH2, and 3′-iT. Percentage reduction in IL-1-induced stromelysin message was calculated by using the message level in synovium from saline-injected, non-IL-1-treated joints as the baseline. Data represent two experiments with a total of four animals per dose. Dashed lines represent standard error of IL-1-treated controls. *, Statistically significant difference from IL-1-treated controls ($P < 0.05$).

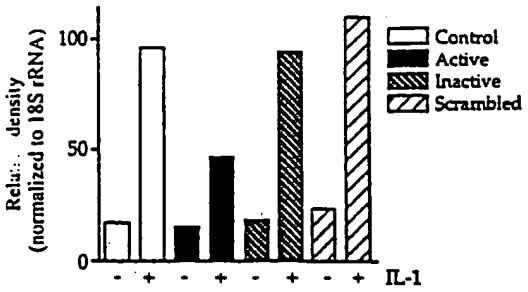

FIG. 5. Reduction in synovial stromelysin mRNA levels by intraarticular injection of ribozyme 1049, U4 C-allyl, and 5&5 P=S. Active, inactive, and scrambled ribozymes were tested in parallel. Results from a single animal for each ribozyme are given.

...ains a mutated catalytic domain, thus allowing binding to the target sequence but preventing cleavage. There was no significant inhibition of stromelysin mRNA levels by the inactive ribozyme control at any dose.

A number of different chemically modified nucleotides have been developed that confer significant resistance to nucleolytic degradation when incorporated into ribozymes (33). Fig. 5 shows the activity of an alternative stabilized chemical motif targeting the same site, ribozyme 1049. Comparison of Figs. 4 and 5 shows that the two modified ribozymes demonstrate ...lar efficacy. Fig. 5 also includes a scrambled ribozyme ...ontrol in which the binding arm sequence of the active ribozyme has been rearranged so that it can no longer bind to its target site on stromelysin mRNA. Like the inactive control, it fails to inhibit stromelysin expression in the synovium. Taken together, these two controls indicate that the ribozyme must bind to and cleave its target site in order to affect the mRNA levels.

The effects of ribozymes that target several different sites in stromelysin message are compiled in Fig. 6. It is clear from ...se data that not all of the sites tested are equally amenable ...ibozyme-mediated cleavage, probably because sites are not equally accessible to ribozyme binding. Ribozymes to sites 1489R and 883 were consistently ineffective, 1410 has shown variable efficacy, and ribozymes to sites 1049, 1366R, and 1363 have shown consistent and relatively equal efficacy. Inactive versions of several of these ribozymes have been tested and have consistently failed to inhibit stromelysin expression (data not shown). A comparison of ribozymes with different 5' end

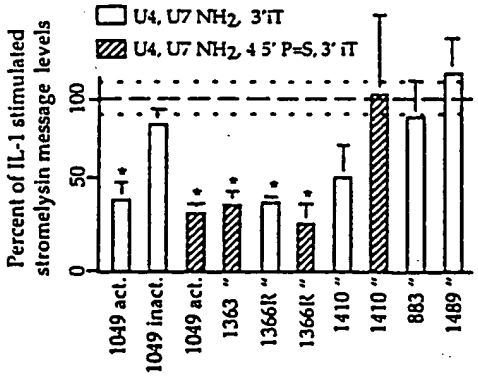

FIG. 6. Reduction in synovial stromelysin mRNA levels by intraarticular injection of ribozymes. Combined data from multiple experiments comparing activity of ribozymes of two different stabilization chemistries and ribozymes directed against different sites on the message. Dotted lines represent standard error of IL-1-treated controls. *, Statistically significant difference from IL-1-treated controls ($P < 0.05$).

modifications (with and without phosphorothioate linkages) is also contained within these data. In general, ribozymes containing phosphorothioate linkages at the 5' end show similar efficacy compared to non-phosphorothioate-containing ribozymes.

DISCUSSION

We have shown that nuclease-resistant ribozymes injected intraarticularly in rabbits were taken up in the synovial lining and remained ~90% intact at 1 day and 70% intact at 3 days postadministration. Administration of ribozymes directed against stromelysin mRNA resulted in a significant reduction in the levels of IL-1-induced stromelysin message in the synovium. This effect was demonstrated with ribozymes recognizing several distinct sites on the message and with ribozymes of different stabilization chemistries. Although ribozymes to all of the sites were shown to be catalytically active in biochemical assays, several were ineffective *in vivo*. This demonstrates the need for an empirical determination of appropriate target sites. RNA secondary structure or association with cellular proteins may affect target site accessibility. In general, ribozymes that contain mutations that render them inactive were ineffective in reducing stromelysin mRNA levels, thus supporting a cleavage mechanism for ribozyme activity. These results suggest that ribozymes may be useful in the treatment of arthritic diseases characterized by dysregulation of metalloproteinase expression.

Ribozymes have shown potential as a viable approach for the treatment of malignancies and AIDS. In the area of cancer, ribozymes to several different targets have been developed that are capable of reversing the transformed phenotype and reducing cell proliferation or tumorigenicity (13, 37, 38). A variety of ribozymes targeting human immunodeficiency virus have also been reported (39–41). Thus, a body of literature is emerging that illustrates the therapeutic potential for ribozymes in a broad spectrum of disease conditions.

The initial findings that synthetic DNA oligonucleotides (42) or antisense sequences expressed intracellularly (43) could interfere with gene expression have stimulated considerable research in the area of antisense therapeutics. Poor specificity with DNA oligonucleotides has, however, been a recurrent problem with the antisense strategy (44–46). The lack of efficacy observed with inactive ribozyme controls in this study is evidence of a high degree of specificity by ribozymes. In addition, it provides strong support for a cleavage-mediated mechanism of action.

The therapeutic potential of stromelysin ribozymes in the treatment of arthritis remains to be determined. Experiments to evaluate the impact of stromelysin reduction on cartilage proteoglycan levels remain to be done. We do not yet know whether the enzyme levels decrease concordantly with the mRNA or the degree of enzyme reduction necessary to see a therapeutic effect. Because multiple metalloproteinases may be involved in the pathogenesis of arthritis, there may be an advantage in targeting more than one enzyme. In addition, several delivery issues must be addressed. For example, chondrocytes, as well as synoviocytes, produce stromelysin after IL-1 stimulation. We are assessing the relative contribution of these enzyme sources to cartilage proteoglycan loss as well as the ribozyme uptake by these tissues. For chronic conditions such as arthritis, sustained release approaches would be beneficial, and several are under consideration.

1. Kruger, K., Grabowski, P. J., Zaug, A. J., Sands, J., Gottschling, D. E. & Cech, T. R. (1982) *Cell* 31, 147–157.
2. Zaug, A. J., Grabowski, P. J. & Cech, T. R. (1983) *Nature (London)* 301, 578–583.
3. Guerrier-Takada, C., Gardiner, K., Marsh, T., Pace, N. & Altman, S. (1983) *Cell* 35, 849–857.

4. Christoffersen, R. E. & Marr, J. J. (1995) *J. Med. Chem.* 38, 2023–2037.
5. Castanotto, D., Rossi, J. J. & Deshler, J. O. (1992) *Crit. Rev. Eukaryotic Gene Expression* 2, 331–357.
6. Zaug, A. J., Been, M. D. & Cech, T. R. (1986) *Nature (London)* 324, 429–431.
7. Uhlenbeck, O. C. (1987) *Nature (London)* 328, 596–600.
8. Symons, R. H. (1994) *Curr. Biol.* 4, 322–330.
9. Cech, T. R. (1992) *Curr. Biol.* 2, 605–609.
10. Heidenreich, O., Benseler, F., Fahrenholz, A. & Eckstein, F. (1994) *J. Biol. Chem.* 269, 2131–2138.
11. Yang, J. H., Usman, N., Chartrand, P. & Cedergren, R. J. (1992) *Biochemistry* 31, 5005–5009.
12. Sioud, M., Natvig, J. B. & Forre, O. (1992) *J. Mol. Biol.* 223, 831–835.
13. Snyder, D. S., Wu, Y., Wang, J. L., Rossi, J. J., Swiderski, P., Kaplan, B. E. & Forman, S. J. (1993) *Blood* 2, 600–605.
14. Kiehntopf, M., Brach, M. A., Licht, T., Petschauer, S., Karawajew, L., Kirschning, C. & Herrmann, F. (1994) *EMBO J.* 13, 4645–4652.
15. Usman, N., Beigelman, L., Draper, K., Gonzalez, C., Jensen, K., Karpeisky, A., Modak, A., Matulic-Adamic, J., DiRenzo, A., Haeberli, P., Tracz, D., Grimm, S., Wincott, F. & McSwiggen, J. (1994) *Nucleic Acids Symp. Ser.* 31, 163–164.
16. Zhao, J. J. & Pick, L. (1993) *Nature (London)* 365, 448–451.
17. Larsson, S., Hotchkiss, G., Andang, M., Nyholm, T., Inzunza, J., Jansson, I. & Ahrlund-Richter, L. (1994) *Nucleic Acids Res.* 22, 2242–2248.
18. Efrat, S., Leiser, M., Wu, Y. J., Fusco-DeMane, D., Emran, O., Surana, M., Jetton, T., Magnuson, M. A., Weir, G. & Fleischer, N. (1994) *Proc. Natl. Acad. Sci. USA* 91, 2051–2055.
19. Woessner, J. F. (1991) *FASEB J.* 5, 2145–2154.
20. Werb, Z., Alexander, C. M. & Adler, R. R. (1992) *Matrix Suppl.* 1, 337–343.
21. Henney, A. M., Wakeley, P. R., Davies, M. J., Foster, K., Hembry, R., Murphy, G. & Humphries, S. (1991) *Proc. Natl. Acad. Sci. USA* 88, 8154–8158.
22. Stetler-Stevenson, W. G., Aznavoorian, S. & Liotta, L. A. (1993) *Annu. Rev. Cell Biol.* 9, 541–573.
23. Murphy, G. & Hembry, R. M. (1992) *J. Rheumatol. Suppl.* 32, 61–64.
24. Bonassar, L. J., Frank, E. H., Murray, J. C., Paguio, C. G., Moore, V. L., Lark, M. W., Sandy, J. D., Wu, J. J., Eyre, D. R. & Grodzinsky, A. J. (1995) *Arthritis Rheum.* 38, 173–183.
25. Suzuki, K., Enghild, J. J., Morodomi, T., Salvesen, G. & Nagase, H. (1990) *Biochemistry* 29, 10261–10270.
26. Miyazaki, K., Umenishi, F., Funahashi, K., Koshikawa, N., Yasumitsu, H. & Umeda, M. (1992) *Biochem. Biophys. Res. Commun.* 185, 852–859.
27. Ogata, Y., Enghild, J. J. & Nagase, H. (1992) *J. Biol. Chem.* 267, 3581–3584.
28. Brinckerhoff, C. E. & Auble, D. T. (1990) *Ann. N.Y. Acad. Sci.* 580, 355–374.
29. Hembry, R. M., Bagga, M. R., Reynolds, J. J. & Hamblen, D. L. (1995) *Ann. Rheum. Dis.* 54, 25–32.
30. Okada, Y., Shinmei, M., Tanaka, O., Naka, K., Kimura, A., Nakanishi, I., Bayliss, M. T., Iwata, K. & Nagase, H. (1992) *Lab. Invest.* 66, 680–690.
31. Pettipher, E. R., Higgs, G. A. & Henderson, B. (1986) *Proc. Natl. Acad. Sci. USA* 83, 8749–8753.
32. Mehraban, F., Kuo, S., Riera, H., Chang, C. & Moskowitz, R. W. (1994) *Arthritis Rheum.* 37, 1189–1197.
33. Hutchinson, N. I., Lark, M. W., MacNaul, K. L., Harper, C. Hoerner, L. A., McDonnell, J., Donatelli, S., Moore, V. & Bayne, E. K. (1992) *Arthritis Rheum.* 35, 1227–1233.
34. Beigelman, L., McSwiggen, J., Draper, K., Gonzalez, C., Jensen K., Karpeisky, A., Modak, A., Matulic-Adamic, J., DiRenzo, A. Haeberli, P., Sweedler, D., Tracz, D., Grimm, S., Wincott, F. Thackaray, V. G. & Usman, N. (1995) *J. Biol. Chem.* 270 25702–25708.
35. Wincott, F., DiRenzo, A., Shaffer, C., Grimm, S., Tracz, D. Workman, C., Sweedler, D., Gonzalez, C., Scaringe, S. & Usman N. (1995) *Nucleic Acids Res.* 23, 2677–2684.
36. Flory, C. M., Jones, M. L. & Warren, J. S. (1993) *Lab. Invest.* 69 396–404.
37. Funato, T., Shitara, T., Tone, T., Jiao, L., Kashani-Sabet, M. & Scanlon, K. J. (1994) *Biochem. Pharmacol.* 48, 1471–1475.
38. Kobayashi, H., Dorai, T., Holland, J. F. & Ohnuma, T. (1994 *Cancer Res.* 54, 1271–1275.
39. Yu, M., Poeschla, E., Yamada, O., Degrandis, P., Leavitt, M. C. Heusch, M., Yees, J., Wong-Staal, F. & Hampel, A. (1995 *Virology* 206, 381–388.
40. Ventura, M., Wang, P., Franck, N. & Saragosti, S. (1994 *Biochem. Biophys. Res. Commun.* 203, 889–898.
41. Zhou, C., Bahner, I. C., Larson, G. P., Zaia, J. A., Rossi, J. & Kohn, D. B. (1994) *Gene* 149, 33–39.
42. Zamecnik, P. C. & Stephenson, M. L. (1978) *Proc. Natl. Acad Sci. USA* 75, 280–284.
43. Izant, J. G. & Weintraub, H. (1984) *Cell* 36, 1007–1015.
44. Wagner, R. W. (1994) *Nature (London)* 372, 333–335.
45. Bennett, C. F., Condon, T. P., Grimm, S., Chan, H. & Chiang, M (1994) *J. Immunol.* 152, 3530–3540.
46. Villa, A. E., Guzman, L. A., Poptic, E. J., Labhasetwar, V. D'Souza, S., Farrell, C. L., Plow, E. F., Levy, R. J., DiCorlete P. E. & Topol, E. J. (1995) *Circ. Res.* 76, 505–513.

ELSEVIER

Journal of Controlled Release 00 (1995) 000–000

journal of controlled release

Polyacrylic acid mediated ocular delivery of ribozymes

Deborah Ayers [a], Jon M. Cuthbertson [a], Ken Schroyer [b], Sean M. Sullivan [1 a,*]

[a] Department of Drug Delivery Ribozyme Pharmaceuticals, Inc., Boulder, CO 80301, USA

[b] Department of Pathology University of Colorado Health Sciences Center, Denver, CO, USA

Received 29 September 1994; revised 16 January 1995; accepted 28 July 1995

Abstract

A catalytic RNA (ribozyme) was formulated with polyacrylic acid (Carbopol®) for ocular delivery in mice. In vitro experiments showed that the ribozyme could be loaded into the polymer in the gel state and be released from the polymer upon collapse of the gel by addition of cations. The ribozyme was formulated with polyacrylic acid and administered to mouse eyes. 5–10-fold greater retention of ribozyme was obtained compared to ribozyme alone. Further characterisation of the formulation showed greater ribozyme accumulation when applied as a liquid rather than a gel. Two independent methods were used to show that the ribozymes were internalized rather than adsorbed to the surface of the eye. The first involved the treatment of the mouse eyes with micrococcal nuclease after ribozyme administration. Less than 50% of the ribozyme was removed by nuclease. The second method visualized ribozyme localization within the tissue by autoradiography using ^{33}P-labeled ribozyme. The results showed that the ribozyme was localized in the outer layers of the corneal epithelium 10 min after administration. 30 min after administration, grains were localized over the lower epithelial layers and into matrix. The kinetics of ribozyme accumulation showed that uptake peaked 30 min after administration and the ribozyme levels persisted in the ocular tissue for 3 h after administration. Ocular retention of the ribozyme was linear over the dose range of 42–833 μM with a constant 0.5% Carbopol® concentration, thus showing that the highest concentration of the ribozyme did not exceed the loading capacity of the polymer. These results demonstrate the potential for polyacrylic acid to be a controlled release drug delivery vehicle for ribozymes to epithelium.

Keywords: Polyacrylic acid; Ribozymes; Corneal epithelium; Drug delivery; Controlled release

1. Introduction

Development of oligonucleotide based therapeutics has rapidly progressed over the last several years. The rationale has been to specifically inhibit the synthesis of a key protein responsible for maintaining a disease state. An oligonucleotide 20–25 nucleotides in length is designed to bind with sequence specificity to an intracellular target RNA. Hybridization leads to translational arrest or triggers ribonuclease H degradation of the target RNA. These types of therapeutics include antisense DNA and ribozymes. There have been several examples where antisense DNA has been used both in vitro and in vivo to inhibit protein expression and produce a biological endpoint [1–4]. In vivo efficacy of antisense DNA required the assistance of delivery vehicles, such as pluronic gels, cationic lipids or ligand derivatized polylysine, to decrease the effective dose [5–10] compared to administration of the antisense DNA alone [11].

* Corresponding author. Tel. 510-748-3053; Fax 510-769-8533.

[1] Present address: Somatix Therapy Corporation, 850 Marina Village Parkway, Alameda, CA 94501, USA.

SSDI 0168-3659(95)00117-4

Development of ribozyme based therapeutics may also require assistance of a delivery vehicle to gain entry into a diseased tissue and cell. The target strategy is similar to antisense with the difference being that a ribozyme can catalytically cleave the target RNA in the absence of intracellular enzymes leaving the target RNA permanently inactive for protein synthesis. There are examples that show ribozyme mediated reduction of specific mRNA levels and protein levels yielding a biological endpoint. These include prevention of HIV proliferation [12,13] and inhibition of cell proliferation by bcr-abl transformed cells [14,15]. There is one in vivo report of ribozyme activity that involved expression of the ribozyme to inhibit the expression of a specific gene [16]. The first step towards achieving in vivo ribozyme activity with chemically synthesized ribozymes is to show that ribozymes are taken up by the appropriate tissue. One approach is to formulate the ribozyme in a delivery vehicle capable of creating a controlled release depot at the site of administration, such as polyacrylic acid.

Polyacrylic acid has the unique property of being a liquid at pH 5 and a gel at pH 7. Permeation of cations into the gelled polymer collapses the gel back to a liquid [17]. In terms of a drug delivery vehicle, it is ideal for ocular delivery of ribozymes to the corneal epithelium. The ribozyme/polymer formulation binds to the surface of the corneal epithelium. The ribozyme is released as cations from the tear fluid and secretion from the epithelial cells collapse the gel to a liquid. The first step toward determining the feasibility of this system as a potential therapeutic was to assess ribozyme retention by a tissue and determine which cell types accumulated the ribozymes. The mouse eye was designed as a model system for evaluation of the ribozyme/Carbopol® formulation. Hence, this report describes the in vivo characterization of ribozyme accumulation in mouse corneal epithelium using polyacrylic acid as the delivery vehicle.

2. Materials and methods

2.1. Reagents

Phosphoramidites were purchased from Chemgenes, Waltham, MA. Carbopol® 974, Pemulen® TR1 and TR2 were obtained from B.F. Goodrich, OH. [γ-^{32}P]ATP and [γ-^{33}P]ATP were purchased from Dupont-NEN, Wilmington, DE.

2.2. DNA synthesis and radiolabeling

RNA was synthesized on an ABI 394 Synthesizer according to the method of Scaringe et al. [18]. The ribozyme sequence was 5′-GCGUCUCUGAUGAG-GUCCGA-AAGGACCGAAACGGUC-3′ and contained five 2′-*O*-methyl ribose nucleotides at the 5′- and 3′-ends of the ribozyme. The ribozyme was labeled by adding a 2-fold excess of [γ-^{32}P]ATP with 5 units of T4 polynucleotide (ATP:5′-dephosphopolynucleotide 5′-phosphotransferase) kinase (EC 2.7.1.78) (United States Biochemical Corporation, Cleveland, OH). Unincorporated radiolabel was separated from the radiolabeled ribozyme using a 1 ml Sephadex (Pharmacia, NJ) G-25 superfine spin column equilibrated with diethylpyrocarbonate treated water.

2.3. In vitro compatibility of polyacrylic acid and ribozymes

A 1% stock of Carbopol® 974 in water was prepared by vortexing the polyacrylic acid into solution and hydrating the polyacrylic acid overnight at room temperature. Gel formation and release of RNA was tested prior to in vivo testing. ^{32}P-labeled ribozyme was formulated with polyacrylic acid in the liquid phase, pH 5. Carbopol® concentrations ranged from 0.05 to 0.5% with the ribozyme concentration held constant at 1 mg/ml. A 50 μl aliquot was placed on a piece of parafilm. The sample either remained as a liquid or was converted to a gel by the addition of 2 μl of 2 N ammonium hydroxide into the droplet using a 10 μl Hamilton syringe. The parafilm was washed with a stream of water and the wash was counted. The water wash was followed by a phosphate-buffered saline (PBS: 140 mM NaCl, 2.7 mM KCl, 10 mM sodium phosphate, pH 7.4) wash and the PBS wash was counted. The PBS was mixed with 95% formamide, loaded on to a 20% polyacrylamide denaturing gel and analyzed for intact ribozyme.

Ficoll flotation was performed by mixing the ribozyme and Carbopol® together to yield a final concentration of 0.5% Carbopol® and 1 mg/ml of ribozyme. The ribozyme was labeled at the 5′-end with

[^{32}P]ATP. 50 μl was neutralized with ammonium hydroxide to form the gel. The gel was overlaid with 1 ml of 30% Ficoll in water. This was overlaid with 1 ml of 10% Ficoll followed by 1 ml of water. The gradient was centrifuged at 3000 rpm in a desk top centrifuge for 15 min. The gradients were fractionated into 0.5 ml aliquots and analyzed for radioactivity.

2.4. *In vivo administration of ribozymes*

Polyacrylic acid was hydrated overnight with diethylpyrocarbonate treated water at a concentration of 1%. Equal volumes of 1% Carbopol® and radiolabeled ribozyme were mixed to yield a final concentration of 0.5% Carbopol®, pH 5. Short term anesthesia was used to anesthetize the mice during Carbopol/ribozyme administration. The mice remained anesthetized for 20–30 min after administration. 2 μl of the mixture was applied to each mouse eye using a P2 pipetman (Gilson, Emeryville, CA). The mice were killed by cervical dislocation. The eyes were surgically removed, washed three times in PBS and placed in 100 μl of 95% formamide. The eyes were frozen in liquid nitrogen and thawed at room temperature three times. 40 μl was applied to a 20% acrylamide sequencing gel. The amount of intact ribozyme was quantitated using a PhosphoImager (Sunnyvale, CA). For autoradiography of tissue sections, the eyes were fixed in 3% glutaraldehyde and embedded in paraffin. The eyes were sliced in 5 μm sections and stained with standard hematoxalin/erythromycin or overlaid with photographic emulsion (Kodak NTB 2.26, Rochester, NY). The sections were exposed to the photographic emulsion for 8 days prior to development.

3. Results and discussion

3.1. *In vitro characterization of ribozyme/polyacrylic acid compatibility*

Ribozyme/Carbopol® was determined using a simple assay. ^{32}P-Labeled ribozyme was formulated with Carbopol® and applied to a piece of parafilm at pH 4.5. Washing the parafilm with a jet of water completely removed the ribozyme. Neutralization of the ribozyme/Carbopol® solution with ammonium hydroxide produced a gel. Ammonium hydroxide was used preferentially to avoid the introduction of sodium ions which could interfere with gel formation. Washing the gelled sample with water did not remove any ribozyme from the parafilm. Washing the same sample with phosphate-buffered saline (PBS) completely removed the ribozyme from the parafilm. The ribozyme obtained from the PBS wash was applied to a 20% polyacrylamide denaturing gel and shown to be 100% intact. The ribozyme also retained 100% substrate cleavage activity (data not shown). This model system was simple in design but showed that the ribozyme could be loaded into the polymer in the gel state and released upon addition of cations. The released ribozyme was not degraded and remained catalytically active, thus showing compatibility between the two components.

An independent assay was used to check the in vitro loading capacity of the polyacrylic acid. This assay relied on buoyant density of the polymer in the gel state. The ribozyme was mixed with polyacrylic acid and neutralized to pH 7. The gel was overlaid with a discontinuous Ficoll gradient composed of 30%, 10% Ficoll and water. After centrifugation, the radioactivity was counted at the 10% Ficoll/water interface. 75% percent of the ^{32}P-CPMs were localized at the interface when the formulation was a gel. Less than 5% of the ^{32}P-CPMs were at the interface when the Carbopol®/ribozyme formulation was a liquid. Several polyacrylic acid based polymers were tested with the parafilm assay. These included Pemulens® TR-1 and TR-2, Carbopol® 940 and Carbopol® A-52 and Carbopol® 974. The gel formed by Carbopol® 974 appeared to have the most mechanical strength and was tested for in vivo delivery. The assessment of mechanical strength was based solely on physical appearance.

3.2. *In vivo administration of ribozyme/polyacrylic acid to mouse eyes*

Accumulation of intact RNA in the mouse eye was tested using RNA alone and RNA formulated with Carbopol® 974. Carbopol®/RNA was applied to the mouse eye in the liquid state and the gel state. The amount of intact RNA retained by the mouse eye was assayed 3 and 10 min after application. The eyes were washed in water, saline or washed with saline followed by treatment with micrococcal nuclease for 1 min. The water wash was designed to remove ribozyme loosely associated with the eye. The PBS wash should collapse

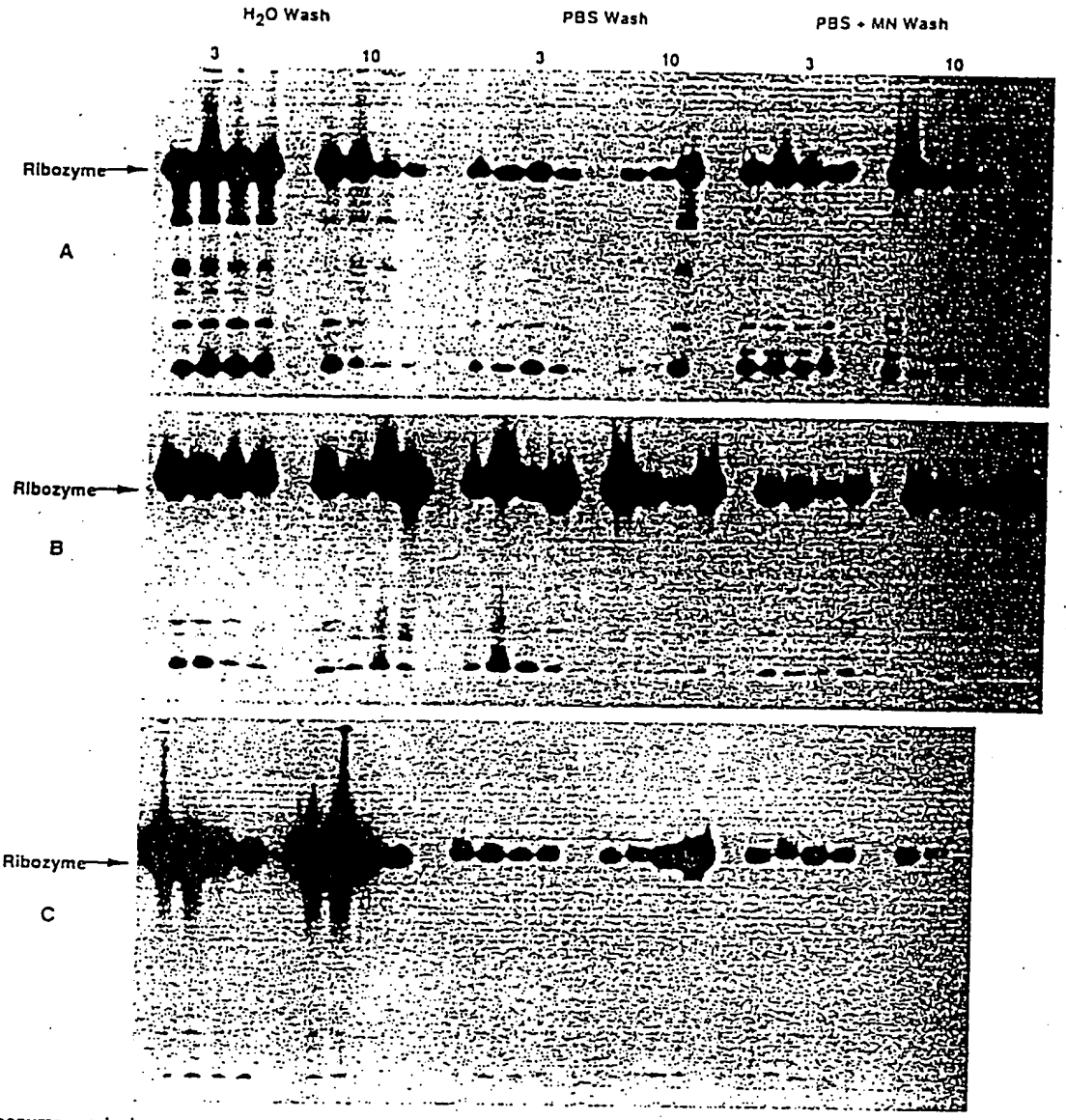

Fig. 1. Ribozyme uptake by mouse corneal epithelium: Effect of gel vs liquid for ribozyme/polyacrylic acid formulation. A 2 μl dose of 42 mM ribozyme was applied to mouse eyes by itself or formulated with 0.5% polyacrylic acid. The ribozyme/polyacrylic acid was applied as a liquid or a gel. The ribozyme was radiolabeled at the 5'-end with [γ-^{32}P]ATP. The total RNA was extracted from the mouse eye and analyzed on a 20% polyacrylamide/urea gel. Each lane represents extraction from one eye.

the gel releasing the ribozyme/Carbopol™ from the surface of the eye, and the PBS wash followed by treatment with micrococcal nuclease should remove ribozyme bound to the eye in the absence of Carbopol™ 974 leaving only the internalized ribozyme. The amount of micrococcal nuclease added was sufficient to completely digest the ribozyme within 1 min. The results are shown in Fig. 1. Panel A is RNA alone; panel B is RNA with Carbopol™ 974 in the fluid state (pH 5); and panel C is RNA with Carbopol® 974 in the gel state (pH 7). The amount of ribozyme retained by the eye when applied in the absence of polyacrylic acid (panel A) was approximately 1% of the offered dose. This value was the same for both the 3 and 10 min time points. Ribozyme formulated with polyacrylic acid in the liquid state showed 3–5-fold more ribozyme in the eye compared to the free control. Panels B and C show a comparison of ocular ribozyme retention when

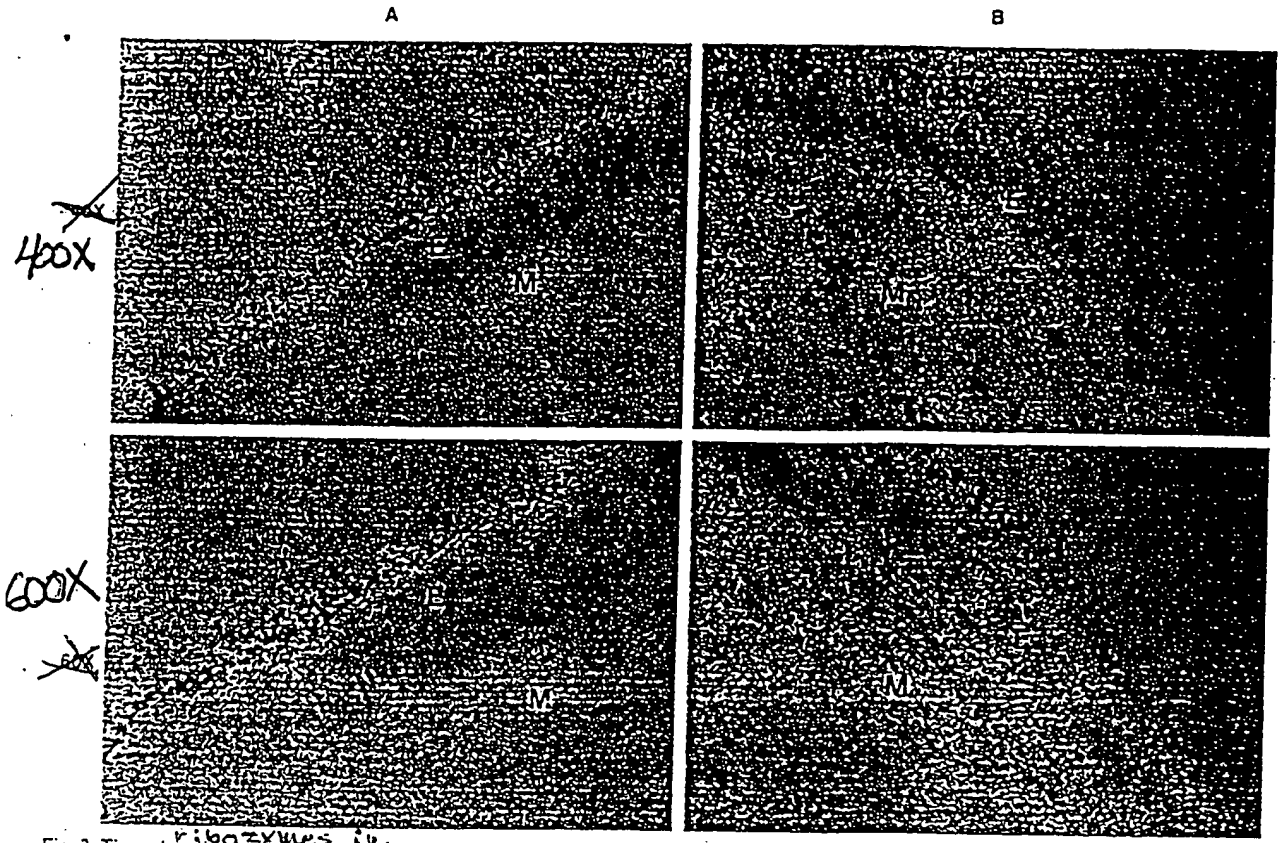

Fig. 2. Tissue localization of mouse eyes. A 2 μl dose of 42 μM ribozyme, 0.5% polyacrylic acid dose was applied to mouse eyes. The ribozyme was radiolabeled at the 5'-end with [γ-^{33}P]ATP. The eyes were harvested after 10 and 30 min, fixed with glyceraldehyde, embedded in paraffin and cut into 5 mm sections. The sections were overlaid with photographic emulsion and exposed for 3 days. ~~The 40× and 60× refer to the magnification of the objective.~~ The epithelium is designated by 'E' and the matrix by 'M'.

applied as a liquid or a gel, respectively. More ribozyme was retained by the eye when applied as a gel. However, micrococcal nuclease treatment showed that more ribozyme was internalized when applied as a liquid. The implication was that the ribozyme was protected due to internalization of the ribozymes into the tissue. These results showed that Carbopol™ 974 was able to yield a higher level of ribozyme retention by the mouse eye compared to ribozyme alone. Application of this formulation as a liquid achieved better penetration into the tissue.

3.3. Tissue distribution of ribozymes in mouse eyes

The above results showed that the RNA accumulated in the eye and indirectly showed that the RNA had been internalized. Ribozyme internalization was more clearly shown using ^{33}P-labeled RNA followed by autoradiography of the tissue sections. ^{33}P has the advantage of low level radiation yielding discrete silver grains upon exposure to a photographic emulsion. The isotope was incorporated into the ribozyme at the 5'-end without altering the chemical structure of the ribozyme, and formulated in 0.5% Carbopol®. The ribozyme/polyacrylic acid was administered to two eyes. One eye was sectioned and analyzed by autoradiography for localization of the ribozyme. Total RNA was extracted from the other eye and analyzed by gel electrophoresis to show that the silver grains represented intact ribozyme. The autoradiographs are shown in Fig. 2. Sections were processed 10 min and 30 min after administration. The sections are shown at 400× and 600×. 10 min after administration, the silver grains were localized in the outermost layers of the corneal epithelium. 30 min after administration, the grains were also found in lower cell layers and in the matrix

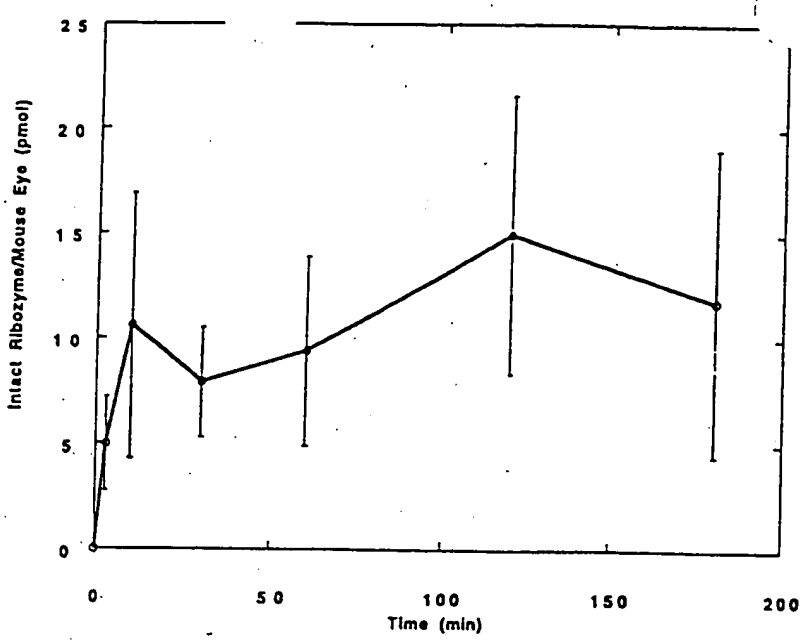

Fig. 3. Kinetics of ribozyme uptake. 2 μl of 42 μM ribozyme/0.5% polyacrylic acid, pH 5 was applied to mouse eyes. At each time point, the total RNA was extracted from the eyes, analyzed on a 20% acrylamide/urea gel and the amount of intact ribozyme was quantitated using a PhosphorImager. Each data point represents 6 eyes.

between the epithelium and the endothelium. Total RNA extraction showed that 80% of the delivered ribozyme was intact verifying that the silver grains represented ribozyme distribution and not reasimilated radiolabel. These results showed that with time, the

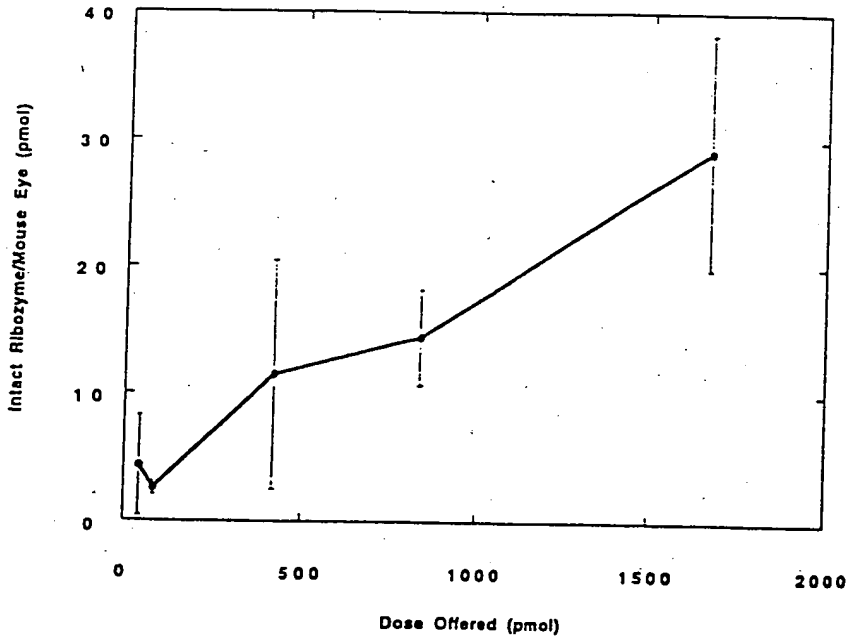

Fig. 4. Dose dependent ocular accumulation of ribozymes. Increasing concentrations of ribozyme were formulated with 0.5% polyacrylic acid. 2 μl of each dose was applied to the mouse eyes. Eyes were harvested 30 min after administration and the total RNA was extracted. The RNA was analyzed using a 20% acrylamide/urea gel and quantitated using a PhosphorImager. Each data point represents an average of 6 eyes.

corneal epithelium

3.4. Long-term accumulation of ribozym... ...ouse eyes

Characterization of the ribozyme distribution within the corneal epithelium showed that the ribozyme continued to accumulate 30 min after administration. Ribozyme accumulation was measured over a 3 h period using a 1 μg ribozyme/0.5% polyacrylic acid dose to determine the peak time for accumulation. The results are shown in Fig. 3. RNA uptake peaked between 10 and 30 min after administration and remained at that level for the duration of the time course. These results were consistent with the previous observations that the ribozyme continued to accumulate in the mouse eyes 10–30 min after administration. Intact ribozyme persisted in the tissue for up to 3 h after administration.

3.5. Polyacrylic acid loading capacity of ribozymes

The loading capacity of Carbopol® 974 was tested in vivo by formulating the ribozyme/ Carbopol® in such a way that the Carbopol® concentration was held constant at 0.5% and the ribozyme concentration was increased from 42 to 833 μM. 2 μl was applied to each eye yielding a range of 0.5–20 μg of ribozyme applied to each eye. The eyes were harvested 30 min after administration and the cells of the tissue were lysed by freeze-thawing the tissue in the presence of formamide. This procedure was shown to release a minimum of 90% of the radioactivity associated with the eye. 40 μl of the 100 μl lysate was analyzed by 18% polyacrylamide urea gel and quantitated using a PhosphoImager. The results are shown in Fig. 4. A linear relationship was observed between the offered ribozyme dose and the percentage retained by the eyes. These results showed that the ribozyme loading capacity of the Carbopol® was not exceeded by the 833 μM ribozyme dose. The dose curve for RNA accumulation was linear over the range tested yielding 5% of offered dose retained by the eye.

4. Conclusions

The results from this study demonstrated the utility of Carbopol® 974, a polyacrylic acid based controlled

zymes. The tested ribozyme w... ...ot degraded in the presence of the polymer, the ri... ...le retained its catalytic activity after being relea... from the polymer and the polymer was able to increase ocular retention 5–10-fold compared to unformulated ribozyme. The degree of ribozyme accumulation in the absence of Carbopol® 974 was surprising in lieu of the chemical composition of the ribozyme, a negatively charged polymer with a molecular mass of approximately 12 kDa. It suggested that a transport process existed for the ribozyme whether it be facilitated transport, passive diffusion or endocytosis. In vitro characterization of ribozyme uptake by primary tissue culture cells has show that ribozymes can be taken up by cells with 50% of the internalized ribozymes being localized in the cytoplasm (unpublished observation). The process was inefficient yielding approximately 0.5% of the offered dose being taken up over a dose range of 0.5–5 μM. Similar results have been reported for antisense DNA [19–21]. Even though this process is inefficient, these observations showed that ribozyme can get into cells and once inside, the ribozyme can gain access to the cytoplasm. By increasing the residence time of the ribozyme in the eye or creating a localized depot adsorbed to the surface of the eye, this transport process could then be used to transport ribozymes into the corneal epithelium. This is, in part, the explanation for the enhanced uptake by the Carbopol formulated ribozyme.

The fact that the ribozyme had been transported into the cells was verified by two independent observations. The first involved the comparison of the gel state formulation vs. the liquid state formulation shown in Fig. 1. The last set of conditions in each panel contained a micrococcal nuclease treatment of the eyes prior to extraction. This condition was designed to digest any ribozyme adsorbed to the cell surface. The control was verified by showing that the ribozyme was completely digested under the specified conditions (unpublished result). For each of the formulations, there was remaining ribozyme after this treatment with the gel state formulation yielding the greatest amount of intact ribozyme. There is always the argument that micrococcal nuclease access to the ribozyme could have been restricted when adsorbed to the surface of the eye. However, internalization and also paracellular transport was observed in the autoradiography imaging of the eye

showed that a minimum of 80% of the [illegible]P represented intact ribozyme. Hence, the maj[illegible]of silver grains in the autoradiography was intact ribozyme. Not only were the gains localized over cells but also between cells. Furthermore, comparison of the 10 and 30 min time points showed that the ribozyme had progressed from the outer layer of the epithlium to the deeper layers with time.

The degree of ribozyme retention and the increased penetration of the ribozyme into the inner layers of the corneal epithelium suggest that the Carbopol® 974 may have played more of an active role in ocular retention of the ribozyme rather than increasing ribozyme residence time. In vitro uptake studies showed the highest degree of ribozyme uptake was 0.5% with the highest offered dose being 5 μM (unpublished results). The in vivo retention of the unformulated ribozyme gave a similar result. However, the Carbopol® 974 formulated ribozyme yielded between 5 and 15% retention. These observations are consistent with those obtained for Carbopol®934P/pilocarpine applied to rabbit eyes [22]. For this study, ^{111}In-labeled Carbopol®934P showed a rapid clearance rate within 5 min of administration followed by a slower rate of clearance yielding a final 24% of the applied dose retained by the eye 55 min after administration. An efficacy study compared pilocarpine formulated with either Carbopol®934P or polyvinylalcohol. Both formulations had the same viscosity. The Carbopol®934P/pilocarpine was more efficacious than the polyvinyl alcohol formulation suggesting that increased efficacy was due to more than just increased residence time as a result of increased viscosity. Other mechanisms include increased bioadhesiveness, induction of increased permeability to the drug, or induction of paracellular transport. This later mechanism has support from in vitro studies using chelating agents to disrupt gap junctions in epithelial cells. Specifically, in vitro, epithelial cell layers treated with EDTA were shown to have disrupted gap junctions [23] thereby reducing the selective permeability barrier of the epithelium. This process was reversible because removal of the EDTA allowed the gap junctions to reform. Both polyacrylic acid and RNA are capable of chelating divalent cations. The adsorption of the Carbopol and RNA to the epithelial cells may

Based on the above information, a proposed model for the mechanism of increa[illegible]ozyme penetration into the epithelial layers invo[illegible]release of material from both sides of the polymer, the side exposed to the tissue and the side exposed to the external environment. The tear fluid contains cations that erode the formulation from the surface of the eye. At the same time the cell secretes divalent cations causing the collapse of the gel at the cell surface with subsequent release of the ribozyme. This later release mechanism may do more than release the ribozyme at the eye surface. The polyacrylic acid may serve the same function in vivo as observed with EDTA in vitro resulting in paracellular transport of the ribozyme to the inner layers of the corneal epithelium.

The amount of intact ribozyme inside the cells should be sufficient ~~to make~~ for the ribozyme to be in large excess of the target transcript. This conclusion is based on the following calculation. The applied concentration of ribozyme formulated with polyacrylic acid ranged from 42 to 833 μM. If an assumption is made that there are approximately 100 000 cells in the mouse corneal epithelium, 5% uptake of the lowest dose offered yields 2.5×10^7 ribozymes per cell. This amount of intracellular ribozyme easily falls within the therapeutic window for ribozyme therapy.

Another important component in pharmaceutical drug development is the shelf life stability of the product. The shelf life stability for the formulated ribozyme was tested for degradation and ocular retention using a freshly prepared batch of polyacrylic acid/ribozyme vs. a batch that was stored at 4°C. Each was tested over the course of 1 month. No ribozyme degradation was observed over that time and there was no difference in the kinetics of uptake between the freshly prepared batch vs. the batch stored at 4°C (unpublished result). These results have identified a controlled release polymer formulation for ribozymes that should decrease the therapeutic dose compared to the non-formulated ribozyme. Secondly, it has opened the door to a pathway for delivery of small RNA and DNA molecules to epithelial cells that had not been previously identified. This is an important advancement for antisense DNA and ribozyme based therapeutics.

The authors would like to thank Dr. J[illegible]derson at the Institute of Pathology, Case West[illegible]eserve University School of Medicine, Cleveland, OH for advice and making his laboratory available to establish the initial ~~experimental~~ animal protocols.

References

[1] S. Biro, Y.M. Fu, Z.X. Yu and S.E. Epstein, Inhibitory effects of antisense oligodeoxynucleotides targeting c-myc mRNA on smooth muscle cell proliferation and migration, Proc. Natl. Acad. Sci. USA 88 (1993) 1190–1195.

[2] T. Skorski, M. Nieborowska-Skorska, N.C. Nicolaides, C. Szcylik, P. Iversen, R.V. Iozzo, G. Zon and B. Calabretta, Suppression of Philadelphia leukemia cell growth in mice by BCR-ABL antisense oligodeoxynucleotide, Proc. Natl. Acad. Sci. USA 91 (1994) 4504–4508.

[3] H. Sawa, B.E. Sobel and S. Fuji, Inhibition of type-1 plasminogen activator inhibitor production by antisense oligonucleotides in human vascular endothelial and smooth muscle cells, J. Biol. Chem. 269 (1994) 14149–14152.

[4] J.P. Leonetti, G. Degols, J.P. Clarenc, N. Mechti and B. Lebleu, Cell delivery and mechanism of action of antisense oligonucleotides, Prog. Nucleic Acid Res. Mol. Biol. 44 (1993) 143–166.

[5] M. Simons, E.R. Edelman, J.L. DeKeyser, R. Langer and R.D. Rosenberg, Antisense c-myb oligonucleotides inhibit intimal arterial smooth muscle cell accumulation in vivo, Nature 359 (1992) 67–70.

[6] M.R.Bennett, S. Anglin, J.R. McEwan, R. Jagoe, A.C. Newby and G.I. Evan, Inhibition of vascular smooth muscle cell proliferation in vitro and in vivo by c-myc antisense oligodeoxynucleotides, J. Clin. Invest. 93 (1994) 820–828.

[7] J. Abe, W. Zhou, J. Taguchi, N. Takuwa, K. Miki K, H. Okazaki, K. Kurokawa, M. Kumada and Y. Takuwa, Suppression of neointimal smooth muscle cell accumulation in vivo by antisense cdc2 and cdk2 oligonucleotides in rat carotid artery, Biochem. Biophys. Res. Commun. 198 (1994) 16–24.

[8] S. Capaccioli, G. Di Pasquale, E. Mini, T. Mazzei and A. Quattrone, Cationic lipids improve antisense oligonucleotide uptake and prevent degradation in cultured cells and in human serum, Biochem. Biophys. Res. Commun. 197 (1993) 818–825.

[9] C.F Bennett, M.Y. Chiang, H. Chan, J.E. Shoemaker and C.K. Mirabelli, Cationic lipids enhance cellular uptake and activity of phosphorothioate antisense oligonucleotides, Mol. Pharmacol. 41 (1992) 1023–1033.

[10] X.M. Lu, A.J. Fischman, S.L. Jyawook, K. Hendricks, R.G. Tompkins and M.L. Yarmush, Antisense DNA delivery in vivo: liver targeting by receptor-mediated uptake, J. Nucl. Med. 35 (1994) 269–275.

Szczylik, P. Iversen, R.V. Iozzo, G. Zon and B. Calabretta, Suppression of Philadelphia l le[illegible]ll growth in mice by BCR-ABL antisense oligodeoxyn[illegible]ide, Proc. Natl. Acad. Sci. USA 91 (1994) 4504–4508.

[12] J.O. Ojwang, A. Hampel, D.J. Looney, F. Wong-Staal and J. Rappaport, Inhibition of human immunodeficiency virus type I expression by a hairpin ribozyme, Proc. Natl. Acad. Sci. USA 89:(1992) 10802–10806.

[13] M. Yu, J. Ojwang ,O. Yamada, A. Hampel, J. Rapapport, D. Looney and F. Wong-Staal, A hairpin ribozyme inhibits expression of diverse strains of human immunodeficiency virus type 1, Proc. Natl. Acad. Sci. USA 90 (1993) 8303–8307.

[14] D.S. Snyder, Y. Wu, L.W. Quinn, J.J. Rossi, P. Swiderski, B.E. Kaplan and S.J. Forman, Ribozyme-mediated inhibition of *bcr-abl* gene expression in a Philadelphia chromosome-positive cell line, Blood 82 (1993) 600–605.

[15] S.K.Shore, P.M. Nabissa and E.P. Reddy, Ribozyme-mediated cleavage of the BCRABL oncogene transcript: in vitro cleavage of RNA and in vivo loss of P210 protein-kinase activity, Oncogene 8 (1993) 3183–3188.

[16] J.J. Zhao and L. Pick, Generating loss-of-function phenotypes of the fushi tarazu gene with a targeted ribozyme in *Drosophila*, Nature 365 (1993) 448–451.

[17] D.Q.M. Craig, S. Tamburic, G. Buckton and J.M. Newton, An investigation into the structure and properties of Carbopol® 934 gels using dielectric spectroscopy and oscillatory rheometry, J. Control. Release 30 (1994) 213–223.

[18] S.A. Scaringe, C. Franklyn and N. Usman, Chemical synthesis of biologically active oligoribonucleotides using β-cyanoethyl protected ribonucleoside phosphoramidites, Nucleic Acids Res. 18 (1990) 5433–5441.

[19] S.L. Loke, C.A. Stein, X.H. Zhang, K. Mori, M. Nakanishi, C. Suvasinghe, J.S. Cohen and L.M. Neckers, Characterization of oligonucleoitde transport in living cells, Proc. Natl. Acad. Sci. USA 86 (1989) 3474–3478.

[20] L.A. Yakubov, E.A. Deeva, V.F. Zarytova, E.M. Ivanova, A.S. Ryte, L.V. Yurchenko and V. Vlasso, Mechanism of oligonucleotide uptake by cells: involvement of specific receptors, Proc. Natl. Acad. Sci. 86 (1989) 6454–6458.

[21] L. Yakubov, L. Yurchenko, M. Nechaeva, E. Rykova, V. Karamyshev, J. Tonkinson, V. Vlassov and C.A. Stein, Interaction of oligonucleotides with cellular receptors, Nucleic Acids Res. Symp. Ser. 24 (1991) 311.

[22] N.M. Davies, S.J. Farr, J. Hadgraft and I.W. Kellaway, Evaluation of mucoadhesive polymers in ocular drug delivery. I. viscous solutions, Pharm. Res. 8 (1991) 1039–1043.

[23] P. Artursson and C. Magnusson, Epithelial transport of drugs in cell culture. I: Effect of extracellular calcium concentration on the paracellular transport of drugs of different lipophilicities across monolayers of intestinal epithelial (Caco-2) cells, J. Pharm. Sci. 79 (1990) 595–600.

Exhibit 4

A6-409 IDENTIFICATION OF METAL CLEAVAGE SITES IN HUMAN BRAIN TRANSCRIPTS. Daniela Marazziti, Rafaele Matteoni+, Elisabetta Golini, Angela Gallo and Glauco P. Tocchini-Valentini, Istituto Biologia Cellulare CNR, Roma, Italy, +EniChem SpA, Monterotondo, Roma.

Divalent metal ions are involved in ribozyme function, both in promoting proper folding of the RNA and directly participating in catalysis. We have investigated the presence of specific divalent metal cleavage sites in pools of human brain cDNA transcripts. cDNA obtained from a collection of human brain mRNA was cloned into a transcription vector. Pools of cDNA clones of length 250-280 bp were transcribed in vitro and the RNA assayed for the presence of lead-specific cleavage sites. We identified one transcript specifically cleaved in the presence of ≤1 mM Pb^{++}. The cleavage site was mapped by primer extension and direct sequencing of the cleavage product. Secondary structure prediction by computer analysis placed the Pb^{++} cleavage site in the single stranded region of an asymmetric internal loop within an helical hairpin. Similar structural motifs have been reported for in-vitro selected, Pb^{++}-dependent ribozymes. Database analysis with search keys combining sequence and secondary structural elements revealed the presence of homologous motifs in gene transcripts of various metal-binding proteins. We prepared oligonucleotide templates corresponding to the "conserved" putative cleavage motif. The templates were transcribed in vitro and tested for cleavage by metal ions. Specific cleavage at the original site was observed in the presence of Pb^{++}. The effect of other divalent metals was also studied.

A6-410 BIODEGRADABLE POLYMER DEVICES FOR THE SUSTAINED EXOGENOUS DELIVERY OF RIBOZYMES K. J. Lewis, A. Hudson, M.V. Rao* and S. Akhtar. Pharmaceutical Sciences Institute, Aston University, Aston Triangle, Birmingham, UK. B4 7ET, and *Cruachem Ltd, Glasgow, Scotland.

Ribozymes have been shown to inhibit gene-expresion in a sequence-specific manner by causing cleavage of target mRNA. Studies to date suggest that RNA subtsrates are relatively unstablé for exogeous delivery and that for sustained efficacy repeated admistration is likely but clinically undesirable. For these reasons, exogenous delivery systems which can protect ribozymes form ribonuclease digestion and simultaneously provide sustained delivery over extended time periods may be useful for the biopharmaceutical application of RNA ribozyme nucleic acids. Biodegradable polymer matrices offer this potential and have been evaluated for the potentail exogenous delivery of ribozymes in our laboratory. In this preliminary study we have evaluated the potential use of solvent cast films (100μm) of poly L-lactic acid (PLA) polymer of molecular weight 690,000. A 32 mer hammerhead ribozyme antisense to the human *c-myc* oncogene exon 2, was used to demonstrate sustained release of the ribozyme from the PLA film *in vitro* and to confirm that the polymer protects the entrapped ribozyme from degradation prior to release. The ribozyme (Cruachem) was deprotected and 5' end labelled with ^{32}PγATP and bacteriophage T4 polynucleotide kinase. The radiolabelled ribozyme was incorporated into a 2 % polymer-chloroform solution, before casting of the film. Release of the oligonucleotide was monitored using liquid scintillation counting and the stability of the free and polymer entrapped ribozyme in foetal calf serum was monitored using denaturing polyacrylamide gel electrophoresis. The released ribozyme from the polymer matrix was reacted with its substrate to ensure it was still capable of cleaving the active site on *c-myc* sequence. The *in vitro* release profiles suggest that the entrapped ribozyme was released biphasically from the polymer films, characterised by an initial rapid burst of release followed by a more sustained release which extended for several weeks. The polymer entrapped ribozymes were resistant to degradation from serum nucleases over a 14 day period, compared to free ribozyme which was rapidly degraded. The *in vitro* cleavage activity of the polymer released hammerhead was similar to free ribozyme suggesting that the polymer device fabrication procedure did not affect the biological properties of the RNA.

A6-411 Analysis of functional structure of HDV ribozyme by modification interference and in vitro selection strategies Satoshi Nishikawa[1], Yeon Hee Jeoung[1], Penmetcha Kumar[1], Junji Kawakami[1], Fumiko Nishikawa[1], Atsushi Chiba[1,2], Kazuhiro Yuda[1,3], Petri Villjanen[1] & Kazunari Taira[1,3]
[1]National Institute of Bioscience & Human Technology, [2]Ibaraki Univ., [3]Tsukuba Univ., Tsukuba, Ibaraki, 305 Japan.

HDV ribozyme derived from human hepatitis delta virus can catalyze the self-cleavage reaction in the presence of Mg^{2+} ions with the same fashion of hammerhead and hairpin ribozymes. But there are no structural homologies between these ribozymes. In order to elucidate the functional structure of HDV genomic ribozyme we have studied by in-vitro mutagenic analyses and chemical probing method. These results supported pseudoknot secondary structure model and identified important bases for cleavage reaction. These bases are all located in single stranded regions (SSrA, B and C) in this structure and furthermore they are all conserved in HDV antigenomic ribozyme.

Recent several studies on ribozymes have suggested that ribozyme is also one of metal enzymes. To elucidate the binding site of Mg^{2+} ions for catalytic reactions in HDV ribozyme, we generated modification interference analysis with partially thio-substituted HDV ribozyme and Pb^{2+} cleavage analysis in the presence of Mg^{2+} ions. We could identify important phosphates, that is -1, 0 which are located in cleavage site, 21 in SSrC region and 75 in SSrB region. These phosphates seem to be close together for folding of active conformation and agreed with recently proposed tertiary structure model.

HDV ribozyme may have good advantage for therapeutic application because of its origin. *Trans*-acting HDV genomic ribozyme based on pseudoknot secondary structure can cleave 13-nts substrate. Although this *trans*-acting HDV genomic ribozyme was very less active compared to antigenomic one, activity increased 100 fold by extending the stem II base pairings from 5 to 8. Based on this molecule we are now trying to select higher active HDV ribozyme by in vitro selection procedure.

A6-412 EFFECTIVE RIBOZYME DELIVERY IN PLANT CELLS, Rhonda Perriman[1,3], W.J. Peacock[3], E.S Dennis[3] and George Bruening[1,2] ; Centre for Engineering Plants resistant against pathogens (CEPRAP)[1], Dept. of Plant Pathology, University of California, Davis[2], and CSIRO Division of Plant Industry, Canberra Australia[3]

This project investigates the utility of highly expressed linear or tRNA-embedded ribozymes (Rz) as a means of inactivating specific target RNAs in plant cells. Hammerhead Rz and antisense (As) sequences have been incorporated into a tyrosine tRNA and compared with the analogous linear molecules. To further optimise the levels of Rz and As transcripts *in vivo*, we have used an autonomously replicating vector. *In vitro*, the linear Rz was able to induce significantly greater levels of cleavage of the designated target RNA, chloramphenicol acetyl transferase (CAT), than the tRNA-embedded Rz. In contrast to this, *in vivo* CAT activities show that the tRNA-embedded Rz is able to reduce CAT activity to 15% of control levels. This is considerably more effective than the linear Rz and control As sequences. A mutated, non-cleavable CAT target sequence did not exhibit the increased reduction in CAT activity in the presence of the tRNA-embedded Rz. The tRNA Rz construction was initially made with functional RNA polymerase II and III promoter sequences. Mutagenesis of these promoters has revealed the most active Rz transcript is derived from the RNA polymerase III promoter. Finally analysis of CAT mRNA accumulation in the presence of the tRNA Rz indicates that the reduction in CAT activity is consistent with *in vivo* cleavage of the CAT mRNA.

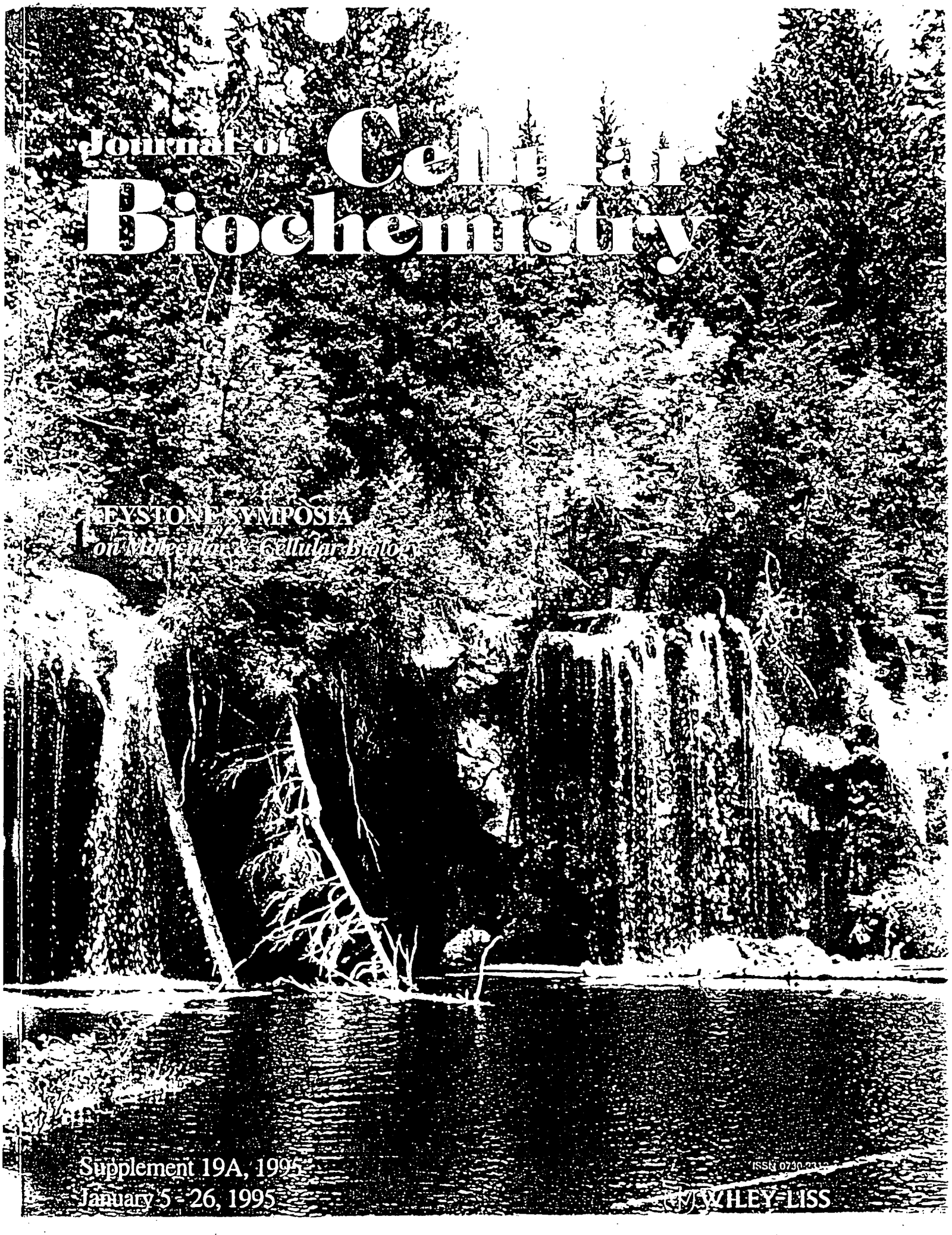
Journal of Cellular Biochemistry
KEYSTONE SYMPOSIA
on Molecular & Cellular Biology
Supplement 19A, 1995
January 5 - 26, 1995
WILEY-LISS

The EMBO Journal vol.13 no.19 pp.4645–4652, 1994

Exhibit 5

Ribozyme-mediated cleavage of the *MDR-1* transcript restores chemosensitivity in previously resistant cancer cells

Michael Kiehntopf, Marion A.Brach, Thomas Licht[1], Simone Petschauer, Leonid Karawajew, Carsten Kirschning and Friedhelm Herrmann[2]

Department of Medical Oncology and Applied Molecular Biology, Freie Universität Berlin, Universitätsklinikum Rudolf Virchow, Robert-Rössle-Cancer Center, and Max-Delbrück-Center for Molecular Medicine, Berlin, Germany and [1]National Cancer Institute, NIH, DCBDC, Labaratory of Molecular Biology, Bethesda, MD, USA
[2]Corresponding author

Communicated by V.A.Erdmann

How cancer cells become resistant to chemotherapy is not completely understood, but it is believed that resistance is usually associated with overexpression of drug resistance genes. Drug resistance mediated by the *MDR-1* gene is the first well characterized form of drug resistance in human cancer. *MDR-1* encodes a phosphoglycoprotein, P-GP, that serves as an energy-dependent drug efflux pump, reducing intracellular drug accumulation and thereby cytotoxicity. We have used ribozymes to reverse the multiple drug resistance phenotype. A hammerhead ribozyme recognizing the GUC sequence at position −6 to −4 close to the translation start site of the 4.5 kb *MDR-1* mRNA was prepared by *in vitro* transcription (MDR-1-RZiv) or chemical synthesis (MDR-1-RZs). Both MDR-1-RZiv and MDR-1-RZs specifically cleaved the *MDR-1* mRNA into two parts of the expected size under physiological conditions in an extracellular system with MDR-1-RZiv being more effective. Site-specific cleavage was dependent on time, temperature and [$MgCl_2$]. To examine the *in vivo* potential of MDR-1-RZ, MDR-1-RZiv and MDR-1-RZs were transfected into a human pleural mesothelioma cell line and into one adriamycin-resistant and one vindesine-resistant subline thereof by liposome-mediated transfer. Incorporation of ribozymes resulted in significantly reduced expression of the *MDR-1* gene, with MDR-1-RZs being more potent than MDR-1-RZiv *in vitro*. MDR-1-RZ reduces P-GP overexpression at the protein level. Liposome-mediated transfer of MDR-1-RZiv or MDR-1-RZs reversed the multiple drug resistance phenotype and restored sensitivity towards chemotherapeutic drugs.
Key words: chemosensitivity/*MDR-1*/ribozyme

Introduction

Conventional chemotherapy of metastatic cancer leads to cure of only a minority of patients. For the majority of patients with disseminated neoplasia, treatment is palliative and prolongation of life is limited. Most of these neoplasias are intrinsically resistant to almost any anti-cancer drug. Other tumors, though originally chemosensitive, recur after successful induction of remission and are then chemoresistant. The molecular basis for the clinical phenomenon of broad spectrum resistance to anti-cancer drugs has been the matter of intensive research (Pastan and Gottesman, 1987; Bradley *et al.*, 1988; Biedler, 1991; Black and Wolf, 1991; Roninson, 1991). Of the various mechanisms by which tumor cells might escape the cytotoxic action of anti-neoplastic drugs, the best characterized form of drug resistance has been ascribed to the expression of the multiple drug transporter phosphoglycoprotein (P-GP). P-GP is a 175 kDa membrane protein which is encoded by the multiple drug resistance 1 (*MDR-1*) gene (Gottesman and Pastan, 1993). Cells expressing the product of the *MDR-1* gene do not appropriately transport and accumulate certain amphipathic pharmacologic agents including DNA intercalators, toxic peptides, antimicrotubule drugs, immunosuppressants (e.g. cyclosporin, FK506 and rapamycin), antibiotics, steroid hormones, synthetic hormone analogs (e.g. tamoxifen), antipsychotics (e.g. phenothiazines) detergents, calcium channel blockers and a variety of anti-cancer drugs (Licht and Herrmann, 1994). The physiological function of P-GP is, however, not yet completely understood. Detoxification of naturally occurring compounds and excretion of endogenous metabolites, e.g. steroid hormones, have both been discussed (Gottesman and Pastan, 1993). In addition, a possible role of P-GP in protecting cells from mutagenic agents has been hypothesized (Ferguson and Baguley, 1993).

As a result of P-GP expression, tumor cells exhibit an increased efflux of cytotoxic agents used for anti-cancer treatment such as anthracyclines, vinca alkaloids, epipodophyllotoxins, actinomycin D, taxol, topotecan and mithramycin, which leads to a reduced intracellular accumulation of these agents insufficient for adequate anti-tumor activity to occur (Pastan and Gottesman, 1987). A decrease in drug influx into multidrug-resistant tumor cells has also been observed (Sirotnak *et al.*, 1986; Ramu *et al.*, 1989) and related to the function of P-GP (Shalinsky *et al.*, 1993).

High concentrations of compounds that compete with anti-cancer drugs for the MDR transporter system, such as immunosuppressants or calcium channel blockers, can increase the intracellular retention of cytostatic agents and thereby enhance their tumoricidal potential (Gaveriaux *et al.*, 1989; Salmon *et al.*, 1991; Arceci *et al.*, 1992). Hence, preclinical experiments using these competitors have been undertaken to interfere with the enzymatic action of P-GP and to reverse MDR by chemosensitizing the malignant cell population. Unfortunately, clinical studies using these compounds have been impeded by the significant toxicity and limited specificity of these 'chemosensitizers'. Therefore, there is a considerable need to find alternative ways of circumventing MDR-1-

mediated drug resistance. Here w. ort on an approach which, rather than tackling P-GP, targets the mRNA from which it is translated by developing an RNA enzyme (ribozyme) directed against the *MDR-1* transcript which abrogates P-GP expression by tumor cells. Furthermore, we provide experimental evidence to suggest that the use of specific ribozymes may represent an effective and specific approach in order to restore cellular sensitivity towards major anti-cancer drugs.

Results

Hammerhead ribozymes require a 'GUC motif' in order to cleave their cognate mRNA (Long and Uhlenbeck, 1993). The *MDR-1* mRNA transcript contains several GUC stretches, one of which has previously been demonstrated to be cleavable by a hammerhead ribozyme in an extracellular system using a truncated, *in vitro* transcribed *MDR-1* mRNA as substrate (Kobayashi *et al.*, 1993). However, *in vitro* and *in vivo*, the secondary structure of the native, full-length *MDR-1* transcript may impede the hybridization of the ribozyme to the target mRNA. Based on the fact that the translation initiation site has previously been targeted successfully by an antisense oligonucleotide (Thiery *et al.*, 1993), and in line with the hypothesis that this site within the *MDR-1* transcript has to be accessible by the translation initiation machinery, we have chosen the GUC sequence at position −6 to −4 with respect to the translation initiation site as a potential target (Figure 1A). The corresponding ribozyme (MDR-1-RZiv) was prepared by *in vitro* transcription. Since this study aimed at elucidating the potential use of an MDR-1 ribozyme *in vivo*, certain requirements regarding the stability of the ribozyme had to be met. Therefore, a synthetic ribozyme, MDR-1-RZs, which is a chimeric DNA−RNA molecule and harbors additional chemical modifications (Figure 1B), was chemically synthesized. These alterations ensure resistance to endogenous and exogenous nucleases (Hendry *et al.*, 1992; Taira and Nishikawa, 1992; Heidenreich *et al.*, 1993).

The next set of experiments was designed to investigate the catalytic potential of both MDR-1-RZiv and MDR-1-RZs in an extracellular system. To this end, *in vitro* transcribed full-length *MDR-1* mRNA was incubated with MDR-1-RZiv or MDR-1-RZs for up to 12 h. In control experiments, *MDR-1* mRNA was also exposed to a mutated, *in vitro* transcribed ribozyme which has no catalytic activity (MDR-1-RZm). The capacity of MDR-1-RZ to cleave *MDR-1* mRNA was time-dependent. A cleavage product of the expected size (184 bp) was detectable within 1 h following exposure of the full-length *MDR-1* mRNA to MDR-1-RZiv (Figure 2A). Lengthening the incubation period to up to 4 h led to cleavage of additional product, but incubation for >4 h did not improve the degree of cleavage (not shown). In contrast, the synthetic ribozyme showed little cleavage within the first hour of incubation. Formation of some cleavage products after 2 h and more after a 4 h incubation was observed (Figure 2A). Moreover, MDR-1-RZs also cleaved a truncated *MDR-1* mRNA transcript of 447 bp in size into the expected 184 and 263 bp fragments (Figure 2B). MDR-1-RZs cleaved most f the target mRNA within 4 h of exposure and prolonging the incubation period to 12 h failed to enhance significantly the degree of cleavage (Figure 2B). A mutated ribozyme containing a single base-pair mutation within the catalytic domain failed to cleave the *MDR-1* mRNA within a 6 h observation period (Figure 2B). The capacity of MDR-1-RZiv to cleave *MDR-1* mRNA was also dependent on the presence of $MgCl_2$ (not shown) as has been described before for hammerhead ribozymes (Haseloff and Gerlach, 1988; Heidenreich *et al.*, 1993; Long and Uhlenbeck, 1993). The K_m and k_{cat} values for MDR-1RZiv and MDR-1-RZs were determined and are shown in Table I.

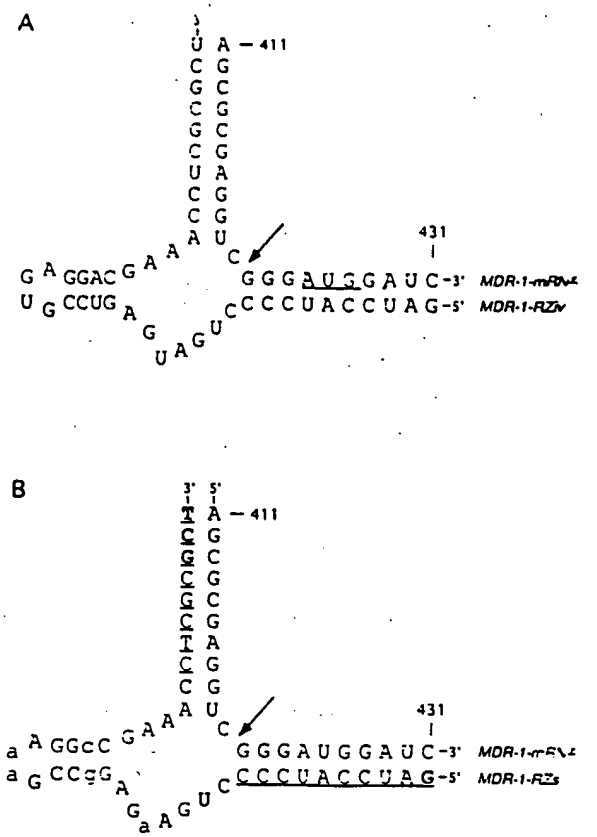

Fig. 1. Design of an *in vitro* transcribed ribozyme and a chemically synthesized ribozyme against the *MDR-1* mRNA. (A) The *MDR-1* mRNA stretch chosen as target sequence and the complementary ribozyme transcribed *in vitro* (MDR-1-RZiv). Positions relative to the transcription inititation site are indicated. The cleavage site is indicated by an arrow and the ATG translation inititation site is underlined. (B) The chemically synthesized ribozyme (MDR-1-RZs) carrying modifications indicated as follows. Underlined letters symbolize deoxynucleotides, which are stabilized by phosphothioate when printed in bold. Shadowed letters indicate 2' fluoro-modified cytidine or uridine ribonucleotides. Lower case letters mark single base-pair exchanges relative to the *in vitro* transcribed ribozyme depicted in panel A.

These findings indicate that the GUC sequence chosen is accessible to ribozyme-mediated cleavage in an extracellular system. Cleavage was specific, because the resulting products were of the expected size, and a mutated ribozyme failed to cut the target mRNA. The chemical modifications introduced into MDR-1-RZs did not impair the specificity of the cleavage reaction but reduced its efficacy. Next, we studied the *in vitro* cleavage potential f both MDR-1-RZiv and MDR-1-RZs. For these experiments a human pleural mesothelioma cell line, PXF1118,

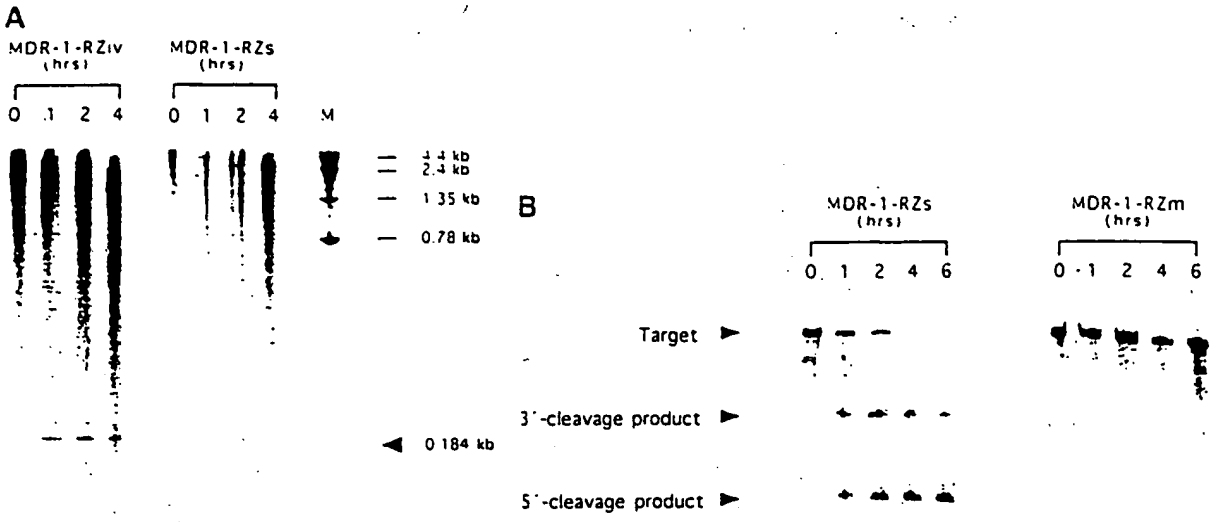

Fig. 2. MDR-1-RZiv and MDR-1-RZs cleave the *MDR-1* mRNA in an extracellular system. (A) Time-kinetics. Full-length *in vitro* transcribed *MDR-1* mRNA (50 pmol) was incubated with MDR-1-RZiv (left panel) or MDR-1-RZs (right panel) (5 pmol each) as detailed in Materials and methods. After the indicated time periods aliquots were collected and samples were separated on a polyacrylamide gel followed by autoradiography. A labeled RNA size marker was run as a standard (M) and the molecular size is indicated. (B) A truncated *MDR-1* transcript was incubated with MDR-1-RZs or with a mutated *in vitro* transcribed ribozyme (MDR-1-RZm) carrying a single base pair mutation in the catalytic domain, as detailed in Materials and methods for up to 6 h. Thereafter, aliquots were collected and samples were separated on a polyacrylamide gel followed by autoradiography.

Table I. K_m and k_{cat} values of MDR-1-RZiv and MDR-1-RZs

Ribozyme	K_m (μM)	k_{cat} (min^{-1})	k_{cat}/K_m (μM^{-1} min^{-1})
MDR-1-RZiv	0.12	0.20	1.7
MDR-1-RZs	3.8	1.4	0.36

The synthetic ribozyme (MDR-1-RZs) or the *in vitro* transcribed ribozyme (MDR-1-1RZiv) was incubated with a 2- to 10-fold excess of the 447 bp truncated *MDR-1* target mRNA as detailed in Materials and methods at 37°C. K_m and k_{cat} values were calculated as described in Materials and methods.

and vindesine- or adriamycin-resistant sublines derived from it (PXF1118VDS and PXF1118ADR, respectively), were instrumental (Licht *et al.*, 1991). The doubling time of PXF1118, PXF1118VDS and PXF1118ADR cells, grown logarithmically in standard culture medium in the absence (PXF1118) or presence of 0.03 μg/ml vindesine (PXF1118VDS) or 0.03 μg/ml adriamycin (PXF1118 ADR), was determined in pilot experiments to be 25.1 ± 0.9, 27.3 ± 1.1 and 28.2 ± 1.0 h, respectively. More than 3% of PXF1118 cells do not express P-GP, while >90% of PXF1118VDS and PXF1118ADR cells displayed P-GP as judged by immunocytochemistry and flow cytometry. Pilot experiments indicated that PXF1118VDS and PXF1118ADR cells do not lose P-GP expression when cultured for 72 h in the absence of vindesine or adriamycin (not shown).

First, the uptake of liposome-complexed and radi labeled MDR-1-RZiv was quantified. As determined in pilot experiments (not shown here), PXF1118 cells and their drug-resistant sublines began to incorporate liposome-complexed radioactive MDR-1-RZiv within 1 h of exposure. Approximately 5% of the radioactivity was taken up by the cells within 4 h. Maximum uptake of 8–9% of radioactivity was achieved within 12 h (not shown). Comparable time-kinetics were observed when intracellular uptake of liposome-complexed MDR-1-RZs or an antisense (MDR-1-AS) oligodeoxynucleotide was analyzed (not shown).

Quantification of ribozyme uptake at the single cell level revealed that ≥98% of cells incorporated radioactively labeled MDR-1-RZiv (Table II). Maximum ribozyme uptake (arbitrarily set as 100%) was achieved in 5–7% of cells scored per experimental point and made up 860 fmol ribozyme. Appoximately 50% of cells incorporated 30–60% of the ribozyme i.e. 258–520 fmol ribozyme. Thereby up to 30% of cells incorporated <258 fmol ribozyme. Comparable results were obtained with MDR-1-RZs (not shown) and MDR-1-AS (Table II).

Uptake of liposome-complexed MDR-1-RZs is associated with intracellular cleavage of the *MDR-1* transcript as demonstrated by reverse transcriptase–polymerase chain reaction (RT-PCR). Amplification of reversely transcribed total cellular RNA isolated from PXF1118VDS cells maintained in the absence of vindesine led to synthesis of a 326 bp cyclophilin product, a 520 bp *MDR-1* product covering the cleavage site and a 118 bp *MDR-1* product corresponding to positions 291–408 5′ of the cleavage site (Figure 3). When PXF1118VDS cells had been exposed to liposome-complexed MDR-1-RZs, amplification of the 520 bp *MDR-1* product spanning the cleavage site f the *MDR-1* RNA was significantly reduced, while amplification of both the cyclophilin product and the 118 bp *MDR-1*

Table II. Uptake of lipsome-complexed ribozyme by PXF1118 cells

% Positive cells (total number)	Cell-type					
	PXF1118		PXF1118 VDS		PXF 1118 ADR	
	RZiv	AS	RZiv	AS	RZiv	AS
	98 ± 2	95 ± 4	96 ± 4	92 ± 5	95 ± 2	96 ± 4
0	2 ± 1	2 ± 1	1 ± 1	2 ± 1	2 ± 1	1 ± 1
1–10	4 ± 2	2 ± 2	3 ± 1	4 ± 1	5 ± 1	2 ± 1
11–20	7 ± 1	5 ± 2	6 ± 2	5 ± 3	6 ± 2	4 ± 2
21–30	9 ± 2	7 ± 1	11 ± 3	8 ± 3	8 ± 2	9 ± 2
31–40	13 ± 3	10 ± 4	14 ± 3	10 ± 2	12 ± 3	9 ± 4
41–50	17 ± 3	12 ± 2	18 ± 2	11 ± 4	17 ± 3	12 ± 2
51–60	18 ± 4	13 ± 4	16 ± 3	15 ± 3	16 ± 3	17 ± 4
61–70	12 ± 3	19 ± 2	13 ± 3	17 ± 3	14 ± 2	20 ± 3
71–80	9 ± 2	15 ± 3	11 ± 2	17 ± 2	10 ± 2	14 ± 3
81–90	7 ± 3	10 ± 2	5 ± 1	8 ± 3	7 ± 3	8 ± 3
91–100	2 ± 1	5 ± 2	2 ± 1	3 ± 2	3 ± 1	4 ± 2

Cells were grown in SCM without (PXF1118) or with 0.03 μg/ml vindesine (PXF1118VDS) or adriamycin (PXF1118ADR), in the presence or absence of equimolar amounts of liposome-complexed radiolabeled ribozyme (RZiv) or liposome-complexed radiolabeled antisense oligonucleotide (AS). Cells were collected after 12 h, plated on coverslips and autoradiographed. The percentage of positive cells was calculated by scoring 100 cells per experimental point. Signal intensity was determined by laser densitometry of each single cell. Values are expressed as relative signal intensity with maximum signal intensity being arbitrarily set as 100%. The number of cells displaying the given ranges of relative signal intensity is indicated ± SD of two independent experiments.

product was unaffected. Similar results were obtained with MDR-1-RZiv; however, the *in vitro* transcribed ribozyme appeared to be less effective in the cell culture than the chemically synthesized ribozyme in cutting the target mRNA (not shown). This may reflect its higher susceptibility to nucleases. When PXF1118VDS cells had been exposed to the liposome-complexed mutated ribozyme (MDR-1-RZm), amplification of the 520 bp *MDR-1* product spanning the cleavage site of the *MDR-1* RNA was unaffected. Taken together, these findings suggest that MDR-1-RZ can still cleave its target mRNA *in vitro* after liposome-mediated transfer into the cells.

The next set of experiments aimed at investigating the effect of MDR-1-RZiv and MDR-1-RZs on P-GP protein expression. In PXF1118 cells cultured in the presence of liposomes, liposome-complexed MDR-1-RZs or MDR-1-RZiv the expression of P-GP was unaffected as shown by flow cytometry (Table III). In contrast, exposure of PXF1118VDS or PXF1118ADR cells to liposome-complexed MDR-1-RZiv or MDR-1-RZs in the absence of vindesine or adriamycin, significantly reduced the number of cells expressing P-GP, while incubation with liposomes alone did not alter P-GP expression in these cells. Synthetic MDR-1-RZs again appeared to be more potent than *in vitro* transcribed MDR-1-RZiv at reducing P-GP expression *in vitro*.

These studies were extended to a functional characterization of P-GP by analyzing rhodamine efflux as previously described (Neyfakh *et al.*, 1988). PXF1118 cells accumulate rhodamine within the cell while PXF1118VDS cells rapidly exclude rhodamine within <1 h (Figure 4). PXF1118 cells cultured for 72 h in the presence of liposome-complexed MDR-1-RZs did not alter their capacity to retain rhodamine. In contrast, PXF1118VDS cells exposed t lipsome-complexed MDR-1-RZs for 72 h displayed a significantly lower capacity to exclude rhodamine during the 1 h observation period. These findings suggest that the transfer of MDR-1-RZ rest res the capacity of *MDR-1*-expressing cells to accumulate compounds which are otherwise expelled.

Finally, the capacity of MDR-1-RZ to restore the chemosensitive phenotype was investigated. PXF1118 cells exposed to liposomes or liposome-complexed MDR-1-RZ do not significantly reduce their viability during a 72 h culture period (Table IV) while exposure of PXF1118 cells to vindesine killed almost all cells during that time (Table IV). PXF1118VDS cells maintained in the presence of vindesine for the same time period were as viable as PXF1118VDS cells cultured in the absence of vindesine. However, exposure of PXF1118VDS cells to vindesine in the presence of liposome-complexed MDR-1-RZs or liposome-complexed MDR-1-RZiv led to significant cell killing, leaving only 3.5% and 27.4%, respectively, of the starting cell population alive. Exposure of PXF1118VDS cells to liposomes alone in the presence of vindesine did not alter cell viability.

Discussion

Ribozymes are small RNA molecules which specifically cleave their target mRNA in a catalytic fashion (Long and Uhlenbeck, 1993). Based on their structural characteristics (Taira and Nishikawa, 1992), different types of ribozymes can be distinguished, among which the hammerhead ribozymes have gained most attention because of their potential usefulness in medical applications. The mechanism by which hammerhead ribozymes act is well understood, and their comparatively small size facilitates their design for various approaches. For example, hammerhead ribozymes have been succesfully used in extracellular systems for cleaving HIV RNA, *bcr–abl* fusion RNA in chronic myelogenous leukemia cells, c-*fos* and c-*ras*-1 RNAs, and the *MDR-1* RNA (Sarver *et al.*, 1990; Scanlon *et al.*, 1991; Kashani-Sabet *et al.*, 1992; K bayashi *et al.*, 1993; Wright *et al.*, 1993). H wever, translati n f this research tool from the extracellular system into the *in vitro*

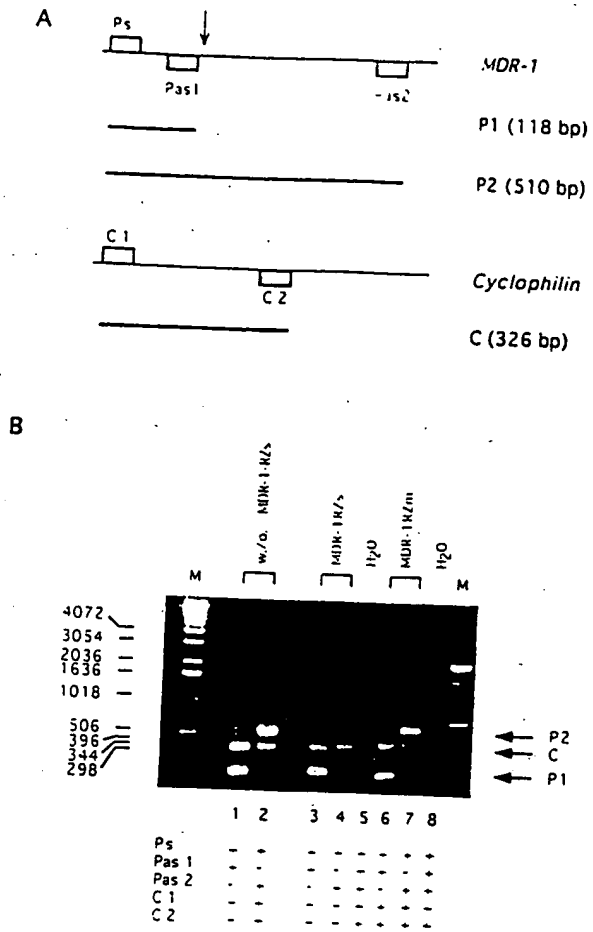

Fig. 3. MDR-1-RZs cleaves the *MDR-1* mRNA in PXF1118VDS cells upon liposomal transfer. (A) Schematic representation of primers used for RT-PCR. For amplification of reverse transcribed *MDR-1* mRNA, a 5' sense PCR primer (Ps), complementary to positions 291–311 of the *MDR-1* mRNA, and two antisense primers, designated Pas1 and Pas2, were used. Pas1 recognizes a 20 bp sequence immediately 5' of the GUC cleavage sequence (positions 389–408), and Pas2 recognizes a 19 bp sequence at positions 792–810 of the *MDR-1* mRNA located 3' of the GUC sequence. The resulting PCR products, P1 and P2, are 118 and 510 bp long, respectively. To amplify the reverse transcribed cyclophilin mRNA one set of primers amplifying a 326 bp product (C) was chosen. (B) RT-PCR analysis of RNA obtained from PXF1118VDS cells mantained in SCM in the absence (lanes 1 and 2) or presence of liposome-complexed MDR-1-RZs (lanes 3 and 4) or liposome-complexed MDR-1-RZm (lanes 6 and 7) for 72 h. The following sets of primers were employed. Lanes 1, 3, and 6, cyclophilin sense/antisense and MDR-1 Ps and Pas1; lanes 2, 4 and 7, cyclophilin sense/antisense and MDR-1 Ps and Pas2. In lanes 5 and 8, all primers were used and H_2O was added to the PCR instead of reverse transcribed RNA (negative control). Co-amplification of cyclophilin in all samples controls for the integrity of RNA and also serves as an internal standard for quantification of the reaction products. A molecular size marker was loaded (M) for size comparison, the molecular weight is shown in bp. Arrows indicate the PCR products P1, P2 and C. Comparable results were obtained for PXF1118ADR cells. The 510 bp PCR product was confirmed to be *MDR-1*-specific by hybridization with an *MDR-1*-specific oligonucleotide probe (not shown).

or even *in vivo* scenario has been hindered by technical obstacles. Unlike antisense oligodeoxynucleotides, which have also been used to eliminate the expression of specific genes (Baserga and Denhardt, 1992), ribozymes are RNA

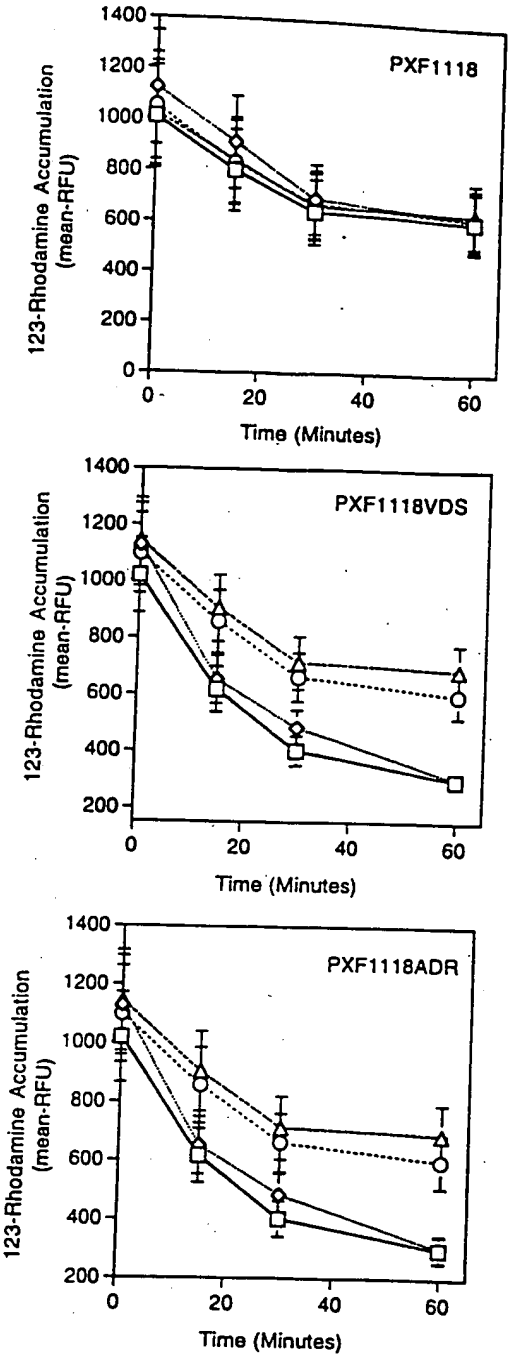

Fig. 4. Liposome-complexed MDR-1-RZ enhances rhodamine retention by PXF1118VDS and PXF1118ADR cells. PXF1118, PXF1118VDS and PXF1118ADR cells were first grown for 72 h in SCM without (PXF1118) or with 0.03 μg/ml vindesine (PXF1118VDS) or adriamycin (PXF1118ADR) present for the last 12 h. Thereafter cells were resuspended in fresh SCM and cultured in the absence ('medium') or presence of liposome-complexed MDR-1-RZ for an additional 48 h. Therafter, rhodamine was added to the cultures after several washings in PBS. Intracellular rhodamine accumulation was analyzed by flow cytometry at the time points indicated. Values are expressed as mean relative fluorescence units (RFU) of three independent experiments (means of individual experiments ± SD). Key: □, medium only; ◇, liposomes + MDR-1-RZm; ○, liposomes + MDR-1-RZiv; △, liposomes + MDR-1-RZs.

Table III. Liposome-complexed MDR-1-RZ reduces P-GP expression by PXF1118VDS and PXF1118ADR cells

Cell type	Exposure to											
	Medium			Liposomes/MDR-1-RZiv			Liposomes/MDR-1-RZs			Liposomes/MDR-1-AS		
	MFI											
	<3.3	3.3–6.9	7–10	<3.3	3.3–6.9	7–10	<3.3	3.3–6.9	7–10	<3.3	3.3–6.9	7–10
PXF1118	95.1 ± 1	2.1 ± 0.4	1.0 ± 0.1	97.4 ± 1.9	1.2 ± 0.5	0.9 ± 0.3	96.5 ± 2.8	2.0 ± 1.2	0.7 ± 0.3	96.9 ± 3.6	1.7 ± 0.7	0.5 ± ...
PXF1118VDS	6.2 ± 2.8	5.1 ± 1.4	88.5 ± 3.4	41.2 ± 2.7	26.7 ± 2.1	31.8 ± 1.9	94.8 ± 4.3	2.5 ± 0.9	1.9 ± 0.4	32.7 ± 2.7	10.8 ± 1.6	58.0 ± 2..
PXF1118ADR	2.7 ± 1.4	6.1 ± 2.0	91.3 ± 3.9	39.5 ± 1.4	24.7 ± 1.2	36.6 ± 2.7	93.4 ± 2.3	3.7 ± 1.5	2.2 ± 1.2	29.5 ± 2.1	12.4 ± 2.5	60.1 ± 3..

Cells were grown in SCM in the absence ('Medium') or presence of liposome-complexed MDR-1-RZiv, MDR-1-RZs or liposome-complexed MDR-1-AS for 72 h. Thereafter, cells were labeled with the 4E3 monoclonal antibody and analyzed by flow cytometry as detailed in Materials and methods. The mean fluorescence intensity (4E3$^+$) was analyzed and the percentage of cells expressing various ranges of mean fluorescence intensity (MFI) (<3.3, 3.3–6.9 and 7–10) is indicated. Values are expressed as the means ± SD of three independent experiments. Analyses with the JSB-1 monoclonal antibody by immunocytochemistry gave comparable results (not shown).

Table IV. Liposome-complexed MDR-1-RZ restores chemosensitivity by PXF1118VDS and PXF1118ADR cells

Cell-type/treatment with:	% viable cells after exposure to				
	Medium	Liposomes/ MDR-1-RZm	Liposomes/ MDR-1-RZiv	Liposomes/ MDR-1-RZs	Liposomes/ antisense
PXF1118	89.1 ± 2.1	87.7 ± 1.9	91.2 ± 3.3	88.3 ± 3.9	86.2 ± 4.1
+ VDS	1.3 ± 0.4	1.9 ± 0.7	2.1 ± 1.1	1.7 ± 0.8	2.4 ± 1.2
+ ADR	1.8 ± 0.3	2.3 ± 0.7	1.9 ± 0.9	2.7 ± 1.3	1.5 ± 0.8
PXF1118VDS					
−VDS	95.2 ± 3.7	91.3 ± 2.9	88.6 ± 4.2	92.3 ± 4.7	88.1 ± 3.9
+VDS	87.5 ± 5.1	86.8 ± 3.9	27.4 ± 4.7	3.8 ± 0.7	47.2 ± 2.9
PXF1118ADR					
−ADR	91.7 ± 2.9	93.2 ± 3.3	90.1 ± 5.1	91.4 ± 4.1	89.3 ± 4.1
+ADR	86.8 ± 3.1	93.8 ± 4.9	33.3 ± 3.7	5.6 ± 0.4	53.3 ± 3.4

Cells were grown in SCM without (PXF1118) or with 0.03 μg/ml vindesine (PXF1118VDS) or 0.03 μg/ml adriamycin (PXF1118ADR) in the absence ('Medium') or presence of liposome-complexed MDR-1-RZ, or liposome-complexed MDR-1-AS for 72 h. Thereafter, cells were stained with propidium iodide and cell viability was determined by flow cytometry as described in Materials and methods. The percentage of viable cells is shown. Values are expressed as means ± SD of three independent experiments.

molecules and as such are highly susceptible to nuclease digestion. Although ribozymes can be transcribed *in vitro* upon genetic transfer of suitable vectors harboring a DNA template of the ribozyme (Cameron and Jennings, 1989; Saxena and Ackermann, 1990), this technique does not allow efficient and specific gene targeting and high level gene expression to be accomplished. In addition, the intracellularly transcribed ribozyme needs to be of a defined length to hybridize specifically to its target mRNA. This can be ensured *in vitro* only by incorporating self-catalytic ribozymes at the 5′ and 3′ ends of the ribozyme of interest (Taira and Nishikawa, 1992). Ribozyme technology has therefore been applied in only very limited ways in *in vitro* and *in vivo* systems. However, the interest in using ribozymes as specific and efficient tools to eliminate gene expression has invited basic research to stabilize riboyzmes through chemical modifications without compromising their catalytic potential (Hendry *et al.*, 1992; Taira and Nishikawa, 1992; Heidenreich *et al.*, 1993). *In vitro* transcribed or chemically synthesized ribozymes have previously been used to target the *bcr–abl* fusion transcript in chronic myelogenous leukemia cells (Snyder *et al.*, 1993; Lange *et al.*, 1994) or the tumor necrosis factor α gene in myelogenous leukemia cells by liposome-complexed transfer (Sioud *et al.*, 1992). Here we report on the development of an *MDR-1*-specific ribozyme, designated MDR-1-RZ, which specifically cleaves the *MDR-1* transcript in an extracellular system. Catalytic efficacy of the *in vitro* transcribed or chemically synthesized *MDR-1* ribozyme has been determined and shown to correspond to the activity of various ribozymes used in previous studies (L'Huillier *et al.*, 1992; Long and Uhlenbeck, 1993). In line with other investigators (Shimayama *et al.*, 1993) we also show that the synthetic *MDR-1* ribozyme displays higher K_m and k_{cat} values than the *in vitro* transcribed ribozyme. MDR-1-RZ can also be effectively placed on tumor cell targets where it cleaves the cognate *MDR-1* RNA and thereby relieves P-GP expression and function when complexed in liposomes. Upon delivery to *MDR-1*-expressing and thus chemoresistant tumor cells, MDR-1-RZ reconstitutes a chemosensitive phenotype leading to efficient killing of previously resistant cells upon exposure to anti-cancer drugs, while not reducing viability of *MDR-1*-non-expressing or *MDR-1*-expressing cells in the absence of drug.

Moreover, we show that in cellular systems, chemically modified ribozymes are preferable to unmodified RNA molecules, most likely because of their increased stability, though the modifications made may reduce their catalytic activity in extracellular systems.

We also demonstrate that the catalytic cleavage of the *MDR-1* target mRNA by a ribozyme is far more effective in restoring a chemosensitive phenotype of tumor cells than an antisense oligodeoxyribonucleotide directed against the same region. The transient delivery of synthetic MDR-1-

RZ may therefore represent a promising approach for reversing drug resistance during anti-cancer chemotherapy.

Materials and methods

Cells and cell culture

The tumor cell line PXF1118 was established from a pleural effusion of a patient with pleural mesothelioma as previously described (Licht *et al.*, 1991). Cells were cultured in Iscove's modified Dulbecco's essential medium (IMDM; Gibco, Long Island, NY) supplemented with 10% heat-inactivated fetal calf serum (FCS; Gibco), 100 U/ml penicillin/streptomycin (Gibco) and 1 mmol/l L-glutamine (Gibco) (referred to as standard culture medium, SCM). Two drug-resistant sublines, designated PXF1118ADR and PXF1118VDS, were derived from parental PXF1118 cells following continuous exposure in culture to 0.03 μg/ml adriamycin (Farmitalia Carlo Erba, Freiburg, Germany) and 0.03 μg/ml vindesine (Lilly, Bad Homburg, Germany), respectively (Licht *et al.* 1991).

Detection of the MDR-1 gene product by immmunocytochemistry and flow cytometry using a specific monoclonal antibody

P-GP, the product of the *MDR-1* gene, was detected by both immunocytochemistry and flow cytometry using the JSB-1 monoclonal antibody (which detects an internal determinant of P-GP; Monosan AM, Uden, The Netherlands) and 4E3 (which detects an external epitope of P-GP; Signet, Dedham, MA) (Scheper *et al.*, 1988; Arceci *et al.*, 1993). For immunocytochemical analysis cells were grown on glass slides and then exposed to monoclonal antibody JSB-1 followed by alkaline phosphatase staining as previously described (Licht *et al.*, 1992). Surface expression of P-GP was examined by indirect immunofluorescence and flow cytometry (FACS Star, Becton Dickinson, Heidelberg, Germany) using monoclonal antibody 4E3 as described (Brach *et al.*, 1992).

RNA extraction and RT-PCR

RNA was prepared as previously described (Brach *et al.*, 1993). Briefly, 10^6 cells were lysed in guanidinium isothiocyanate (Sigma, München, Germany) and extracted with an equal volume of acetate/EDTA-equilibrated phenol (60°C for 25 min with frequent vortexing). The aqueous phase was recovered after centrifugation and extracted once with an equal volume of phenol–chloroform and twice with chloroform. The resulting RNA was precipitated overnight at −20°C with 2.5 vols of ethanol.

RT-PCR was performed essentially as described (Gruss *et al.*, 1992). RNA was digested with RNase-free DNase for 30 min at 37°C and then cDNA was synthesized as follows. Five microliters of total RNA was incubated in a 20 μl reaction volume containing PCR buffer (50 mM KCl, 20 mM Tris–HCl pH 8.4, 2.5 mM $MgCl_2$, 10 μg/ml nuclease-free BSA) using 200 U Moloney murine leukemia virus reverse transcriptase (USB, Cleveland, OH) in the presence of 20 U RNasin (USB) with 10 nmol of each dNTP (Boehringer Mannheim, Mannheim, Germany) and 100 pmol of random hexamer (Pharmacia, Freiburg, Germany). After incubation for 1 h at 37°C, the reaction mixture was denatured by heating to 95°C for 10 min and immediate chilling on ice. The reaction mixture was diluted with 80 μl of PCR buffer containing 5′ and 3′ amplification primers (12.5 pmol each) and 1 U AmpliTaq rTaq DNA polymerase (Perkin Elmer Cetus, Emeryville, CA). Primers used were as follows. *MDR-1* primers: sense (Ps): 5′-TCGAGTAGCGGCTCTTCCAAG-3′; Pas1 antisense: 5′-TTGGAACGGCCACCAAGACG-3′; Pas2 antisense: 5′- GCAGCAACCAGCACCCCAG-3′. Cyclophilin primers: sense: 5′-CTGCAATCCAGCTAGGCATG-3′, antisense: 5′-CATCTGCACTGCCAAGACTG-3′. PCR cycles consisted of denaturation by heating to 94°C for 30 s, annealing of primers at 60°C for 30 s and primer extension at 72°C for 2 min. This cycle was repeated 35 times using a programmable heat block (MWG, Ebersberg, Germany). As a final step, incomplete amplification products were extended at 72°C for 10 min. One-fifth of each reaction mixture was run on 1% agarose gels.

Design and preparation of MDR-1 ribozymes

A hammerhead ribozyme recognizing the GUC sequence at position −6 to −4 to the translation inititation site (MDR-1-RZ) was designed according to criteria previously described (Haseloff and Gerlach, 1988; Heidenreich *et al.*, 1993; Long and Uhlenbeck, 1993). The sequence of MDR-1-RZ is 5′-GAUCCAUCCCCUGAUGAGUCCGUGAGGACGAAACCUCGCGCU-3′, where the sequence complementary to the *MDR-1* transcript is in bold. MDR-1-RZ was either prepared by *in vitro* transcription (MDR-1-RZiv) or synthesized on an oligodeoxynucleotide synthesizer (MDR-1-RZs). For *in vitro* transcription, sense and antisense DNA oligonucleotides complementary to MDR-1-RZ harboring a T7 primer at the 5′ or 3′ end, respectively, were synthesized, annealed and used as templates. *In vitro* transcription was performed as described by the manufacturer (Boehringer Mannheim). In selected experiments, transcripts were radiolabeled by incorporation of [^{32}P]UTP. The amount of *in vitro* transcribed MDR-1-RZiv was quantified spectrophotometrically, and the molar concentration was calculated according to standard procedures. For selected experiments, an MDR-1-RZ was also transcribed from a template containing a single base-pair mutation in the catalytic domain as previously reported (Taira and Nishikawa, 1992) (5′ - GAUCCAUCCCCUAAUGAGUCCGUGAGGACGAAACCUCGCGCU-3′; mutated base is in bold) designated MDR-1-RZm. *In vitro* transcribed MDR-1-RZiv and MDR-1-RZm were stored at −70°C until use. The size of the expected MDR-1-RZiv and its integrity were analyzed by gel electrophoresis of the radiolabeled product followed by Northern blotting and subsequent autoradiography. The chemically synthesized MDR-1-RZs was synthesized by Biometra, Göttingen, Germany. MDR-1-RZs harbors several chemical modifications as shown in Figure 1 according to previously published criteria (Heidenreich *et al.*, 1993). The MDR-1-RZs represents an RNA–DNA chimera with deoxynucleotides forming the sequence complementary to the target transcript while the ribonucleotides constitute the catalytic domain (Hendry *et al.*, 1992). The first 5′ and the last three 3′ deoxynucleotides were stabilized by phosphorothioate. Cytidine and uracil ribonucleotides were replaced by the respective 2′-fluoro-modified ribonucleotides (Heidenreich *et al.*, 1993). In order to enhance the stability of MDR-1-RZs further, several ribonucleotides (Figure 1) were exchanged as previously described (Heidenreich *et al.*, 1993). These modifications are known to increase the stability of the ribozyme (Hendry *et al.*, 1992; Taira and Nishikawa, 1992; Heidenreich *et al.*, 1993).

Design and preparation of MDR-1 antisense oligodeoxynucleotides

An antisense oligodeoxynucleotide (5′-GTCGGGATGGATCTT-3′, MDR-1-AS) covering the translation intitation site of the *MDR-1* mRNA as previously described (Thiery, 1993) was synthesized on a DNA oligodeoxynucleotide synthesizer (Pharmacia) and stabilized by phosphorothioate.

In vitro transcription of target mRNA and extracellular cleavage assay

In order to analyze the capacity of both MDR-1RZiv and MDR-1-RZs to cleave the *MDR-1* transcript, extracellular cleavage assays were performed essentially as previously reported (Haseloff and Gerlach, 1988; Long and Uhlenbeck, 1993). To this end, target mRNA was prepared by *in vitro* transcription. The plasmid pMDR2000XS (kindly provided by Dr M.Gottesmann, NCI, NIH, Bethesda, MD) harboring the full-length *MDR-1* cDNA was linearized by *Xho*I digestion and used as a template for *in vitro* transcription of full-length *MDR-1* mRNA as recommended by the manufacturer (Boehringer Mannheim) using the T7 promoter in the presence of [^{32}P]UTP. In selected experiments, a transcript truncated 447 bp from the transcription initiation site by *Bgl*II digestion was also prepared. The integrity of the transcribed products was confirmed by gel electrophoresis of the reaction products followed by Northern blotting and autoradiography. The amount of *in vitro* transcribed mRNA was quantified spectrophotometrically, and the molar concentration was calculated according to standard procedures. *In vitro* cleavage assays of *in vitro* transcribed target mRNA were performed as follows: 5–10 pmol of radiolabeled target mRNA were incubated with *in vitro* transcribed MDR-1-RZiv or synthetic MDR-1-RZs (1:10 molar ratio) for various time periods, as indicated, in an incubation buffer containing 10 mM $MgCl_2$, 50 mM Tris–HCl (pH 7.4) and RNAsin (1 U) at 37°C. Reaction products were analyzed either on a 5% denaturing polyacrylamide gel or on a 0.8% agarose gel followed by autoradiography. In selected experiments, $MgCl_2$ was added at various concentrations. In order to determine k_{cat} and K_m values, *in vitro* cleavage assays were performed with both the *in vitro* transcribed (MDR-1-RZiv) and the chemically synthesized ribozyme (MDR-1-RZs) using a 2- to 10-fold excess of the 447 bp truncated *MDR-1* mRNA as a target as described above. Steady-state rates of cleavage were measured for each of the two ribozymes and k_{cat} and K_m values were determined from Lineweaver–Burk plots as previously described (L'Huillier *et al.*, 1992).

Liposome-mediated transfer of MDR-1 ribozyme and antisense oligodeoxynucleotides

Transfer of either MDR-1-RZiv or MDR-1-RZs, and of antisense oligodeoxynucleotides into target cells was accomplished by the liposome

technique (Dwarki *et al.*, 1993) as follows. R-1-RZiv, MDR-1-RZm, MDR-1-RZs or MDR-1-AS were complexed with cationic liposomes (Dotap, Boehringer Mannheim) as recommended by the manufacturer. Cells were plated into 24-well plates (10^6 cells/ml) in SCM in the presence or absence of vindesine (0.03 μg/ml) or adriamycin (0.03 μg/ml) and liposomes (45 μg/ml) with or without either MDR-1-RZiv, MDR-1-RZm, MDR-1-RZs or MDR-1-AS, added every 12 h over a total period of 72 h.

Ribozyme and antisense oligodeoxynucleotide uptake studies

In order to quantify the amount of ribozyme and antisense oligodeoxynucleotides (MDR-1-AS) being taken up by the cells upon liposomal transfer, radiolabeled MDR-1-RZiv or radiolabeled antisense oligodeoxynucleotide was complexed with cationic liposomes as detailed above and added to the cell culture. Twelve hours after exposure to MDR-1-RZs, MDR-1-RZiv or MDR-1-AS, cells were washed several times, plated on coverslips and autoradiographed. The percentage of cells containing the radiolabeled ribozyme was determined by scoring 100 cells. The signal intensity within single cells was quantified by laser densitometry using an LKB Ultra Scan XL laser densitometer and LKB Gel Scan XL software (LKB, Pharmacia, Uppsala, Sweden).

Rhodamine analysis

In order to analyze the function of P-GP, efflux of rhodamine was assessed by flow cytometry (Neyfakh *et al.*, 1988). To this end, cells cultured in the presence or absence of vindesine (0.03 μg/ml) or adriamycin (0.03 μg/ml) with or without MDR-1-RZiv, MDR-1-RZm or MDR-1-RZs, were exposed to rhodamine (10 μg/ml) for 20 min at 37°C. Cells were washed several times in PBS followed by flow cytometric analysis.

Determination of cell viability

In order to determine cell viability, cells were incubated with propidium iodide (10 μg/ml) for 15 min at room temperature, washed several times in PBS and assessed by flow cytometry.

Acknowledgements

This work was supported by the Bundesministerium für Forschung und Technologie (to F.H.).

References

Arceci,R.J., Stieglitz,K. and Bierer,B.E. (1992) *Blood*, 80, 1528–1536.
Arceci,R.J., Stieglitz,K., Bras,J., Schinkel,J., Baas,F. and Croop,J. (1993) *Cancer Res.*, 53, 310–317.
Baserga,R. and Denhardt (eds) (1992) *Ann. N.Y. Acad. Sci.*, 660, 1–353.
Biedler,J.L. (1991) *Cancer*, 70 (Suppl.), 1799–1809.
Black,S.M. and Wolf,C.R. (1991) *Pharmacol. Ther.*, 51, 139–154.
Brach,M.A., Buhring,H.J., Gruss,H.J., Ashman,L.K., Ludwig,W.D., Mertelsmann,R.H. and Herrmann,F. (1992) *Blood*, 80, 1224–1230.
Brach,M.A., Gruss,H.J., Kaisho,T., Asano,Y., Mertelsmann,R., Hirano,T. and Herrmann,F. (1993) *J. Biol. Chem.*, 268, 8466.
Bradley,G., Juranka,P.F. and Ling,Y. (1988) *Biochim. Biophys. Acta*, 948, 87–128.
Cameron,F.H. and Jennings,P.A. (1989) *Proc. Natl Acad. Sci. USA*, 86, 9139–9143.
Dwarki,V.J., Malone,R.W. and Verma,I.M. (1993) *Methods Enzymol.*, 217, 644–654.
Ferguson,L. and Baguley,B.C. (1993) *Mutat. Res.*, 285, 79–90.
Gaveriaux,C. *et al.* (1989) *Br. J. Cancer*, 60, 867–871.
Gottesman,M.M. and Pastan,I. (1993) *Annu. Rev. Biochem.*, 62, 385–427.
Gruss,H.J., Brach,M.A., Drexler,H.G., Bonifer,R., Mertelsmann,R.H. and Herrmann,F. (1992) *Cancer Res.*, 52, 3353–3360.
Haseloff,J. and Gerlach,W.L. (1988) *Nature*, 334, 585.
Heidenreich,O., Piechen,W. and Eckstein,F. (1993) *FASEB J.*, 7, 90–96.
Hendry,P., McCall,M.J., Santiago,F.S. and Jennings,P.A. (1992) *Nucleic Acids Res.*, 20, 5737–5741.
Kashani-Sabet,M. *et al.* (1992) *Antisense Res. Dev.*, 2, 3–15.
Kobayashi,H., Dorai,T., Holland,J.F. and Ohnuma,T. (1993) *FEBS Lett.*, 319, 71–74.
Lange,W., Cantin,E.M., Finke,J. and Dolken,G. (1994) *Leukemia*, 7, 1786–1794.
L'Huillier,P.J., Davis,S.R. and Bellamy,A.R. (1992) *EMBO J.*, 11, 4411–4418.
Licht,T. and Herrmann,... (1994) *Frontiers Biotechnol.*, in press.
Licht,T., Fiebig,H.H., Bross,K.J., Herrmann,F., Berger,D.P., Shoemaker,R. and Mertelsmann,R. (1991) *Int. J. Cancer*, 49, 630–...
Licht,T., Bross,K.J., Fiebig,H.H., Schötta,K., Berger,D.P., Dreher,... Löhr,G.W. and Herrmann,F. (1992) *J. Cancer Res. Clin. Oncol.*, 118, 116–122.
Long,D.M. and Uhlenbeck,O.C. (1993) *FASEB J.*, 7, 25–30.
Neyfakh,A.A., Dmitrerskaya,T.V. and Serpinska,A.S. (1988) *Exp. Cell Res.*, 174, 168–174.
Pastan,I. and Gottesman,M. (1987) *N. Engl. J. Med.*, 316, 1388–13...
Ramu,A., Pollard,H.B. and Rosario,L.M. (1989) *Int. J. Cancer*, 43, 539–547.
Roninson,I.B. (1991) *Molecular and Cellular Biology of Multidrug Resistance in Tumor Cells*. Plenum Press, New York.
Salmon,S.E., Dalton,W.S., Grogan,T.M., Plezia,P., Lehnert,M., Roe... and Miller,T.P. (1991) *Blood*, 78, 44–50.
Sarver,N., Cantin,E.M., Chang,P.S., Zaia,J.A., Ladne,P.A., Stephens,D.... and Rossi,J.J. (1990) *Science*, 247, 1222.
Saxena,S.K. and Ackermann,A.J. (1990) *J. Biol. Chem.*, 265, 17...–17109.
Scanlon,K.J., Jiao,L., Funato,T., Wang,W., Tone,T., Rossi,J.J. ... Kashani-Sabet,M. (1991) *Proc. Natl Acad. Sci. USA*, 88, 10591.
Scheper,R.J. *et al.* (1988) *Int. J. Cancer*, 42, 389–394.
Shalinsky,D.R., Jekunen,A.P., Alcaraz,J.E., Christen,R.D., Kim,... Khatibi,S. and Howell,S.B. (1993) *Br. J. Cancer*, 67, 30–36.
Shimayama,T., Nishikawa,F., Nishikawa,S. and Taira,K. (1993) *Nucleic Acids Res.*, 21, 2605–2611.
Sioud,M., Natvig,J.B. and Forre,O. (1992) *Mol. Biol.*, 223, 831–835.
Sirotnak,F.M., Yang,C.H., Mines,L.S., Oribe,E. and Biedler,J.L. (198...) *J. Cell. Physiol.*, 126, 266–274.
Snyder,D.S., Wu,Y., Wang,J.L., Rossi,J.J., Swiderski,P., Kaplan,B.E. ... Forman,S.J. (1993) *Blood*, 82, 600–605.
Taira,K. and Nishikawa,S. (1992) In Erickson,R.P. and Izant,I.G. (eds), *Gene Regulation: Biology of Antisense RNA and DNA*. Raven Press, New York.
Thiery,A.R. (1993) *Biochem. Biophys. Res. Commun.*, 190, 952–960.
Wright,L., Wilson,S.B., Milliken,S., Biggs,J. and Kearney,P. (1993) *Exp. Hematol.*, 21, 1714–1718.

Received on May 26, 1994; revised on July 19, 1994

THE JOURNAL OF BIOLOGICAL CHEMISTRY Vol. 270, No. 43, Issue of October 27, pp. 25702–25708, 1995
Printed in U.S.A.

Chemical Modification of Hammerhead Ribozymes

CATALYTIC ACTIVITY AND NUCLEASE RESISTANCE*

(Received for publication, June 5, 1995, and in revised form, August 9, 1995)

Leonid Beigelman, James A. McSwiggen, Kenneth G. Draper, Carolyn Gonzalez, Kristi Jensen, Alexander M. Karpeisky, Anil S. Modak, Jasenka Matulic-Adamic, Anthony B. DiRenzo, Peter Haeberli, David Sweedler, Danuta Tracz, Susan Grimm, Francine E. Wincott, Varykina G. Thackray, and Nassim Usman‡

From the Departments of Chemistry and Biochemistry, Cell Biology and Enzymology, Ribozyme Pharmaceuticals, Inc., Boulder, Colorado 80301

A systematic study of selectively modified, 36-mer hammerhead ribozymes has resulted in the identification of a generic, catalytically active and nuclease stable ribozyme motif containing 5 ribose residues, 29–30 2′-*O*-Me nucleotides, 1–2 other 2′-modified nucleotides at positions U4 and U7, and a 3′-3′-linked nucleotide "cap." Eight 2′-modified uridine residues were introduced at positions U4 and/or U7. From the resulting set of ribozymes, several have almost wild-type catalytic activity and significantly improved stability. Specifically, ribozymes containing 2′-NH_2 substitutions at U4 and U7, or 2′-*C*-allyl substitutions at U4, retain most of their catalytic activity when compared to the all-RNA parent. Their serum half-lives were 5–8 h in a variety of biological fluids, including human serum, while the all-RNA parent ribozyme exhibits a stability half-life of only ~0.1 min. The addition of a 3′-3′-linked nucleotide "cap" (inverted T) did not affect catalysis but increased the serum half-lives of these two ribozymes to >260 h at nanomolar concentrations. This represents an overall increase in stability/activity of 53,000–80,000-fold compared to the all-RNA parent ribozyme.

Trans-acting ribozymes exert their activity in a highly specific manner and are therefore not expected to be detrimental to non-targeted cell functions. Because of this specificity, the concept of exploiting ribozymes for cleaving a specific target mRNA transcript is now emerging as a therapeutic strategy in human disease and agriculture (Cech, 1992; Bratty *et al.*, 1993). For ribozymes to function as therapeutic agents, they may be introduced exogenously or produced endogenously in the target cells. In the former case, the chemically modified ribozyme must maintain its catalytic activity while also being stable to nucleases. A major advantage of chemically synthesized ribozymes is that site-specific modifications may be introduced at any position in the molecule. This approach provides flexibility in designing ribozymes that are catalytically active and stable to nucleases. In this manuscript we show that using this site-specific, chemical modification strategy, ribozymes can be designed that have wild-type catalytic activity and are not cleaved by nucleases.

A variety of selective and uniform structural modifications have been applied to oligonucleotides to enhance nuclease resistance (Uhlmann and Peyman, 1990; Beaucage and Iyer, 1993; Milligan *et al.*, 1993). Improvements in the chemical synthesis of RNA (Scaringe *et al.*, 1990; Wincott *et al.*, 1995) have led to the ability to similarly modify ribozymes containing the hammerhead ribozyme core motif (Usman and Cedergren, 1992; Yang *et al.*, 1992) (Fig. 1). Yang *et al.* (1992) demonstrated that 2′-*O*-Me modification of a ribozyme at all positions except G5, G8, A9, A15.1, and G15.2 (see numbering scheme in Fig. 1) led to a catalytically active molecule having a greatly decreased k_{cat} value *in vitro*, but a 1000-fold increase in nuclease resistance over that of an all-RNA ribozyme when tested in a yeast extract. In another study (Paolella *et al.*, 1992), a persubstituted 2′-*O*-allyl-containing ribozyme with ribose residues at positions U4, G5, A6, G8, G12, and A15.1 showed a 5-fold decrease in catalytic activity compared to the all-RNA ribozyme (based on k_{cat}/K_m), while the stability of this ribozyme in bovine serum was increased substantially (30% intact material after 2 h compared to a <1-min half-life for the all-RNA ribozyme). Shimayama *et al.* (1993) found it necessary to introduce 2 additional phosphorothioate linkages at positions C3, U4 and to replace U7 by A or G in a phosphorothioate-DNA/RNA chimera containing 21 phosphorothioate (P=S)[1] substitutions (13 P=S DNAs in Stem/Loop II plus 5 and 3 P=S DNAs in Stems I and III, respectively). These ribozymes showed a 100-fold increase in stability relative to the all-RNA ribozyme, but the catalytic activities of these chimeras were reduced 15-fold (U7 → A7) and 42-fold (U7 → G7) compared to the wild-type ribozyme. Substitution of all pyrimidine nucleotides in a hammerhead ribozyme by their 2′-amino or 2′-fluoro analogs resulted in a 25–50-fold decrease in activity and a 1200-fold increase in stability in rabbit serum compared to the unmodified ribozyme (Pieken *et al.*, 1991).

The above data suggest that a strategy of uniform modification cannot be directly applied to ribozymes, since it is necessary to preserve a reasonable level of catalytic activity and therefore to leave some residues, especially in the catalytic core, unmodified. We have constructed a generic, catalytically active, nuclease stable hammerhead ribozyme motif that contains only 5 ribose residues; the remaining residues consist of 2′-*O*-Me nucleotides with one or two other 2′-modified sugars at positions U4 and/or U7 (Figs. 1 and 2). Two of these ri-

* The costs of publication of this article were defrayed in part by the payment of page charges. This article must therefore be hereby marked "*advertisement*" in accordance with 18 U.S.C. Section 1734 solely to indicate this fact.

‡ To whom correspondence should be addressed: Ribozyme Pharmaceuticals, Inc., 2950 Wilderness Pl., Boulder, CO 80301. Tel.: 303-449-6500; Fax: 303-449-6995.

[1] The abbreviations used are: P=S, phosphorothioate; 2′-F, 2′-deoxy-2′-fluorouridine; 2′-NH_2, 2′-deoxy-2′-aminouridine; iT, 3′-3′-linked thymidine; Rz, ribozyme; t_A, time required to cleave 50% of a short matched substrate; t_S, time required to degrade 50% of the full-length ribozyme; k_{cat}^S, maximum ribozyme cleavage rate under single turnover (enzyme excess) conditions; K_M^S, Michaelis constant under single turnover (enzyme excess) conditions.

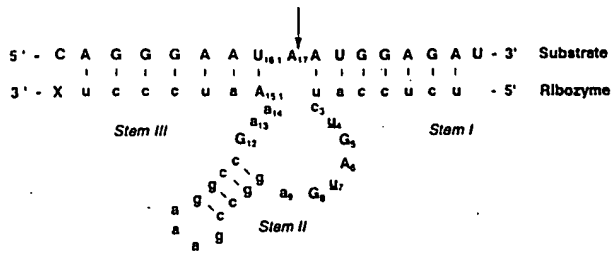

FIG. 1. **Sequences of ribozyme and substrate used in this study.** Conserved nucleotides within the central core are *numbered* according to Hertel *et al.* (1993). *Lowercase letters* represent sites that were substituted with 2'-*O*-methyl nucleotides in the final, nuclease resistant motif. *Underlined letters* at U4 and U7 indicate positions that were replaced by the eight 2'-substituted nucleotides shown in Fig. 2 (compounds 1–8). *Uppercase letters* represent *ribo*nucleotides; five positions (G5, A6, G8, G12, and A15.1) within the nuclease-resistant ribozyme were kept as ribonucleotides to maintain catalytic activity. *X* represents the 3'-3'-linked (inverted) T residue (Fig. 2, compound **9**) that was added to the 3'-end of Rzs **29** and **30**. *Arrow* indicates the site of substrate cleavage.

bozymes (containing 2'-NH_2 modifications at U4 and U7 or 2'-*C*-allyl modifications at U4) have almost wild-type catalytic activity and a 5–8 h half-life in human serum at nanomolar concentrations. The addition of a 3'-3'-linked thymidine nucleotide to these ribozymes maintains their catalytic activity and increases their half-lives in serum to >260 h.

EXPERIMENTAL PROCEDURES

Synthesis of Ribozymes—Automated RNA synthesis and deprotection was carried out on an Applied Biosystems model 394 DNA/RNA synthesizer using the method of Scaringe *et al.* (1990), modified according to Wincott *et al.* (1995). Syntheses were carried out at 2.5 μmol on a derivatized aminomethyl polystyrene solid support (Applied Biosystems). A 5-min coupling step was used for 2'-*O*-silyl protected RNA (Pharmacia Biotech Inc.) and modified phosphoramidites (Fig. 2).[2] A 2.5-min coupling step was used for 2'-*O*-Me RNA (Milligen/Biosearch). Average coupling yields, determined by colorimetric quantitation of trityl fractions, were 97.5–99%. Phosphorothioate linkages at the 3'- and 5'-ends of Rz 5 were introduced by a sulfurization step[3] with Beaucage's reagent (Iyer *et al.*, 1990). Ribozymes were gel-purified, eluted, ethanol-precipitated, rinsed twice with 70% ethanol, dried, and resuspended in TE buffer.

Nucleoside Composition—The nucleoside compositions of the ribozymes were confirmed by nuclease digestion of the ribozyme and analysis by reverse phase high performance liquid chromatography. The ribozymes were converted to nucleosides by incubation of 0.3 A_{260} units of ribozyme with 10 units of P1 nuclease (EC 3.1.30.1; Boehringer Mannheim) and 2 units of calf intestinal alkaline phosphatase (EC 3.1.3.1; Boehringer Mannheim) in 30 mM NaOAc, 1 mM $ZnSO_4$, at pH 5.2 (total volume = 100 μl) overnight at 50 °C. The digested material was injected directly onto a C18 column (Rainin, Dynamax, ODS 4 × 250 mm), and nucleosides were separated by an acetonitrile gradient buffered with 50 mM potassium phosphate, pH 7.0. The retention times were compared with monomer standards.

Radiolabeling of Ribozymes and Substrates—Ribozymes and substrates were 5'-end-labeled using T4 polynucleotide kinase and [γ-^{32}P]ATP. For internal labeling, ribozymes were synthesized in two halves with the junction 5' to the GAAA sequence in Loop II (Fig. 1). The 3'-half-ribozyme portion was 5'-end-labeled using T4 polynucleotide kinase and [γ-^{32}P]ATP, and was then ligated to the 5'-half-ribozyme portion using T4 RNA ligase. Labeled ribozymes were isolated from half-ribozymes and unincorporated label by gel electrophoresis.

Ribozyme Activity Assay—Ribozymes and 5'-^{32}P-end-labeled substrate were heated separately in reaction buffer (50 mM Tris-Cl, pH 7.5, 10 mM $MgCl_2$) to 95 °C for 2 min, quenched on ice, and equilibrated to the final reaction temperature (37 °C or as indicated) prior to starting the reactions. Reactions were carried out in enzyme excess, and were started by mixing ~1 nM substrate with the indicated amounts of ribozyme (5–200 nM, 40 nM for the initial screens) to a final volume of 50 μl. Aliquots of 5 μl were removed at 1, 5, 15, 30, 60, and 120 min, quenched in formamide loading buffer, and loaded onto 15% polyacrylamide, 8 M urea gels. The fraction of substrate and product present at each time point was determined by quantitation of scanned images from a Molecular Dynamics PhosphorImager. Ribozyme cleavage rates were calculated from plots of the fraction of substrate remaining *versus* time using a double exponential curve fit (Kaleidagraph, Synergy Software). The fast portion of the curve was generally 60–90% of the total reaction, so that observed cleavage rates (k_{obs}) and activity half-times ($t_A = \ln(2)/k_{obs}$) were taken from fits of the first exponential. Detailed kinetic analyses of Rzs 1, 2, 25, and 26 were performed in the same way except that reactions were carried out at 25 °C and pH 6.5 to slow down the reactions and to enable more accurate determination of kinetic parameters. Plots of k_{obs} *versus* ribozyme concentration were fit to the Michaelis-Menten equation using a non-linear, least squares routine (Kaleidagraph, Synergy Software) to determine values for k_{cat}^S and K_M^S. Values for the combined parameter, k_{cat}^S/K_M^S, were confirmed by performing cleavage reactions at low ribozyme concentration (5–20 nM), then determining k_{cat}^S/K_M^S from the initial slope of the k_{obs} *versus* ribozyme concentration plot.

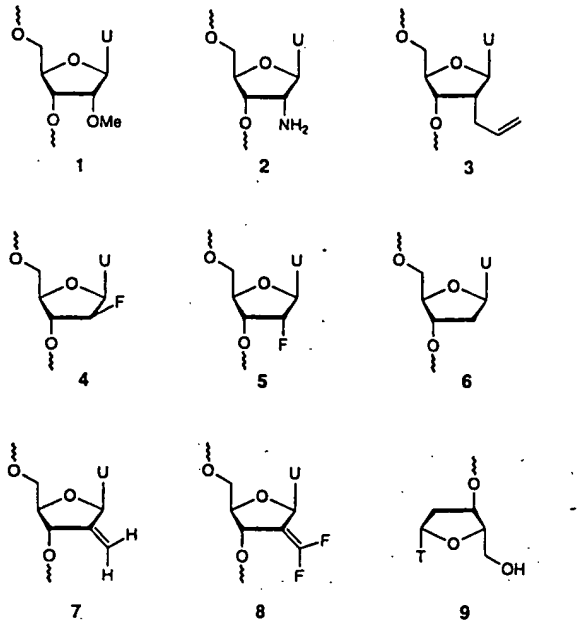

FIG. 2. **Structures of the 2'-modified nucleosides used in this study.** 1, 2'-*O*-Me-U; 2, 2'-amino-U; 3, 2'-*C*-allyl-U; 4, 2'-arabinofluoro-U; 5, 2'-fluoro-U; 6, 2'-deoxy-U; 7, 2'-methylene-U; 8, 2'-difluoromethylene-U; 9, 3'-3' inverted T.

Ribozyme Stability Assay—Five hundred pmol of gel-purified 5'-end-labeled or internally labeled ribozymes were ethanol-precipitated and then resuspended in 20 μl of appropriate fluid (human serum, human plasma, human synovial fluid, or fetal calf serum) by vortexing for 20 s at room temperature. Samples were placed at 37 °C, and 2 μl aliquots were withdrawn after the times indicated in the figures (30 s to 72 h). Aliquots were quenched by the addition of 20 μl of 95% formamide, 0.5 × TBE (50 mM Tris, 50 mM borate; 1 mM EDTA) and were frozen prior to gel loading. Ribozymes were size-fractionated by electrophoresis in 20% acrylamide, 8 M urea gels. Gels were imaged on a Molecular Dynamics PhosphorImager, and the stability half-life (t_S) for each ribozyme was calculated from exponential fits of plots of the percentage of intact ribozyme *versus* the time of incubation.

RESULTS AND DISCUSSION

Modification and Testing Strategy—We focused our efforts on substitutions of the 2'-hydroxyl group since these modifications were considered least likely to perturb the overall structure of the hammerhead ribozyme and were more easily introduced than backbone modifications. Ribozymes were chemically synthesized and gel-purified, and the nucleotide

[2] Beigelman, L., Karpeisky, A., Matulic-Adamic, J., Haeberli, P., Sweedler, D., and Usman, N. (1995) *Nucleic Acids Res.* **23**, in press.

[3] A. D. DiRenzo, K. Levy, P. Haeberli, S. Grimm, C. Shaffer, N. Usman, and F. Wincott, manuscript in preparation.

TABLE I
Cleavage Activity and Nuclease Resistance of Ribozymes 1–5

Rz	Modification[a]	Activity (t_A)[b]	Stability (t_S)[c]	Relative stability/activity $\beta(\text{Rz } n) = \frac{t_S/t_A(\text{Rz } n)}{t_S/t_A(\text{Rz } 1)}$
		min	*min*	
1 All RNA:	UCUCCAU CUGAUGAGGCCGAAAGGCCGAA AAUCCCU	1	0.1	1
2 2′-*O*-Me arms:	ucuccAU CUGAUGAGGCCGAAAGGCCGAA AAucccU	1	0.1	1
3 5+5 P=S arms:	ucucca*U. CUGAUGAGGCCGAAAGGCCGAA Aaucccu	3	0.1	0.3
4 2′-C-Allyl:	ucuccAu cuGAuGAGGCCGAAAGGCCGAA AAucccT	13	120	92
5 2′-Fluoro-Pyr:	ucuccAu cuGAuGAGGccGAAAGGccGAA AAucccT	30	15	5

[a] Uppercase sequences are ribonucleotides. Lowercase, underlined sequences contain the indicated modifications at the sugar or (in the case of Rz 3) at the five phosphodiester linkages *between* the underlined sequences. In Rzs 4 and 5 the "t" at the 3′-end denotes deoxythymidine.
[b] Ribozyme activity expressed as cleavage half-time against the substrate shown in Fig. 1.
[c] Ribozyme stability expressed as half-life of ribozyme in human serum. Times <1 min are estimated and may be shorter.

content was verified by nucleoside composition analysis. The ribozymes were then assayed for *in vitro* cleavage activity, and for nuclease resistance in a range of biological fluids. Activity measurements were made in enzyme excess at concentrations (40 nM ribozyme, ~1 nM substrate) that approach saturating conditions for the all-RNA control ribozyme. Ribozyme activity is reported in Tables I and II as the activity half-time (t_A) at 40 nM ribozyme; a larger number represents a slower cleavage rate and is less desirable. The stability of ribozymes to nuclease digestion was assessed in fetal calf serum, human serum, human plasma, and human synovial fluid using 5′-^{32}P-end-labeled ribozymes. Ribozyme stability is reported in Tables I and II as the stability half-life in human serum (t_S); a larger number represents a slower degradation rate. To compare one ribozyme's activity and stability to another, we have defined a parameter, β, which is the ratio of the stability and activity half-times compared to a reference, Rz 1 (Table I). Thus, in Tables I and II,

$$\beta(\text{Rz } n) = \frac{t_S/t_A(\text{Rz } n)}{t_S/t_A(\text{Rz } 1)} \qquad \text{(Eq. 1)}$$

Larger β values represent an improvement in ribozyme activity and/or stability relative to Rz 1.

5′- and 3′-Modified Ribozymes Are Catalytically Active but Not Stable in Biological Fluids—To establish a base line for ribozyme catalytic activity and stability in biological fluids, ribozymes were synthesized containing RNA only (Rz 1, Table I), or RNA at all positions except in the substrate-binding arms (Stem I, positions 2.2–2.6, and Stem III, positions 15.3–15.7, Fig. 1). Table I shows that 2′-*O*-Me sugar, or phosphorothioate backbone modifications in the substrate-binding arms (Rz 2 and 3, respectively) had minimal effects on catalytic activity. However, ribozyme stability in human serum also remained unchanged with these modifications, and all three ribozymes were rapidly degraded (Fig. 3). No full-length ribozymes were present after 30 s in any of the biological fluids tested; however, stable fragments were observed in ribozymes containing 2′-*O*-Me modifications (Fig. 3). Modification of the Stem I and III backbones with phosphorothioate substitutions did not increase the nuclease resistance of the ribozymes or result in the generation of stable ribozyme fragments (Fig. 3).

The profile of stable fragments generated with the 2′-*O*-Me modified ribozymes varied with the medium and, to a lesser degree, with the base sequence of ribozyme stems (data not shown). At the earliest times, modified ribozymes were digested to fragments between 6 and 10 nucleotides in length whose relative abundance varied somewhat between experiments. Over time, all of the fragments were cleaved at their 3′-termini to generate smaller fragments. The amount of 3′-exonuclease activity was greatest in fetal calf serum, less in human serum and plasma, and least in human synovial fluid. The sensitivity of the 2′-*O*-Me fragments to cleavage by the 3′-exonuclease activity varied between Rz 2 and other ribozymes having the same 2′-*O*-Me content but of different sequence (data not shown). Comparison of nucleoside composition suggests that these patterns of digestion cannot be attributed solely to the primary sequence of the ribozyme fragments.

TABLE II
Cleavage Activity and Nuclease Resistance of Ribozymes 6–30

Rz	2′-Modification[a] (U4/U7)	Activity (t_A)[b]	Stability (t_S)[c]	Relative stability/activity $\beta(\text{Rz } n) = \frac{t_S/t_A(\text{Rz } n)}{t_S/t_A(\text{Rz } 1)}$
		min	*min*	
6	OH/*O*-Me	1	0.1	1
7	*O*-Me/*O*-Me	4	260	650
8	$=CH_2$/*O*-Me	6.5	250	380
9	*O*-Me/$=CH_2$	8	320	400
10	$=CH_2$/$=CH_2$	8.5	250	300
11	$=CF_2$/*O*-Me	4.5	400	900
12	*O*-Me/$=CF_2$	5.5	250	220
13	$=CF_2$/$=CF_2$	>15	380	250
14	F/*O*-Me	3	300	1000
15	*O*-Me/F	8	300	375
16	F/F	3.5	300	850
17	H/*O*-Me	5.5	250	450
18	*O*-Me/H	>10	250	<250
19	H/H	4	280	700
20	araF/*O*-Me	5.5	500	900
21	*O*-Me/araF	4	350	875
22	araF/araF	>15	500	<330
23	NH_2/*O*-Me	10	500	500
24	*O*-Me/NH_2	5.5	500	900
25	NH_2/NH_2	2	300	1500
26	*C*-Allyl/*O*-Me	3	>500	>1700
27	*O*-Me/*C*-Allyl	3	300	1000
28	*C*-Allyl/*C*-Allyl	3	300	1000
29	*C*-Allyl/*O*-Me + iT	3	16,000	53,000
30	NH_2/NH_2 + iT	2	16,000	80,000

[a] Modifications follow the numbering scheme shown in Fig. 1.
[b] Ribozyme activity expressed as cleavage half-time against the substrate shown in Fig. 1.
[c] Ribozyme stability expressed as half-life of ribozyme in human serum. Times <1 min are estimated and may be shorter.

Uniform Modifications in the Ribozyme Core Reduce Catalytic Activity but Enhance Nuclease Resistance—Other researchers have reported increased nuclease resistance of hammerhead ribozymes through uniform substitution of ribopyrimidines with 2′-modified-pyrimidines. For example, Eckstein and co-workers have shown that uniform substitution of all pyrimidine nucleotides by 2′-F or 2′-NH_2 analogs greatly increased the stability of a hammerhead ribozyme, but also

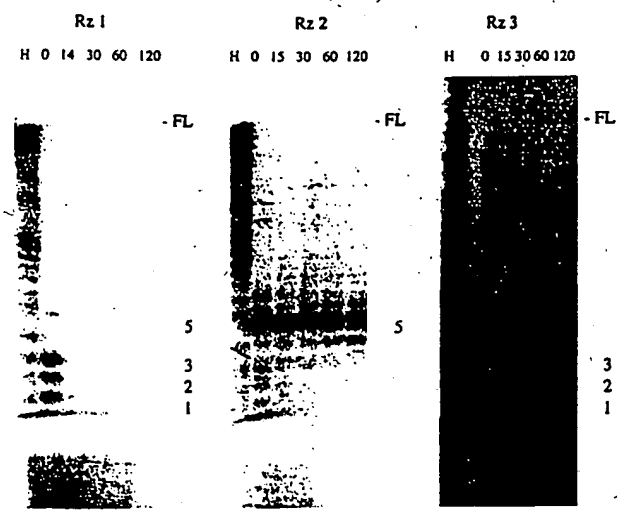

FIG. 3. **Nuclease resistance of minimally modified Rzs 1–3 in human serum.** ^{32}P-5′-End-labeled ribozymes were resuspended in fresh human serum and incubated for the indicated times at 37 °C. After quenching in stop buffer, ribozyme samples were size-fractionated on polyacrylamide gels as described under "Experimental Procedures." Ribozyme 1 is all RNA. Rz 2 contains 2′-*O*-Me arms, and Rz 3 contains P=S (phosphorothioate) arms (see Table I). Times of incubation (minutes) are shown above each panel. *H* = base hydrolyzed ribozyme size markers. *Numbers* to the *right* of each panel show the approximate size, in nucleotides, of the ribozyme fragments generated. *FL*, full-length ribozyme band position.

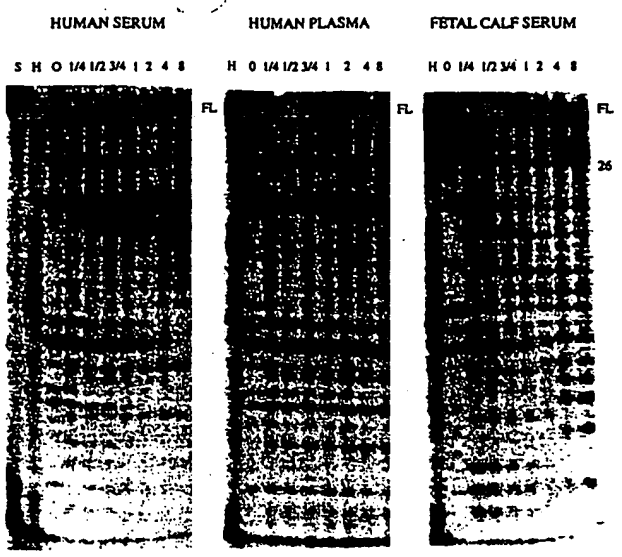

FIG. 4. **Comparative stability of 2′-*C*-allyl substituted, Rz 4, in human serum, human plasma, and fetal calf serum.** Time courses with ^{32}P-5′-end-labeled ribozyme were performed as in Fig. 3 and under "Experimental Procedures." Times of ribozyme incubation (hours) are shown above each panel. *H*, base hydrolyzed ribozyme size marker; *S*, ribozyme resuspended in saline; *FL*, full-length ribozyme band position. Approximate size (in nucleotides) of the major digestion products are shown in the panel margins.

reduced activity by 25–50-fold (Peiken *et al.*, 1991; Heidenreich *et al.*, 1994). We chose to test ribozymes containing uniform 2′-*C*-allyl and 2′-F pyrimidine substitutions. The choice of the 2′-*C*-allyl modification was based on the observation that 2′-*O*-allyl substitutions in hammerhead ribozymes improve stability but cannot be introduced at positions U4 and U7 without a significant detrimental effect on catalysis (Paolella *et al.*, 1992). The 2′-*C*-allyl group should be less bulky than the 2′-*O*-allyl group near the sites required for catalysis, but may still provide sterically and conformationally based nuclease protection.

The uniformly substituted 2′-*C*-allyl-pyrimidine ribozyme showed no activity in the cleavage assay (data not shown), which was likely due to the inability of Stem II to form (De Mesmaeker *et al.*, 1993). Thus, another ribozyme was synthesized that lacked the 2′-*C*-allyl-pyrimidine substitutions in Stem II (Rz 4). Ribozyme 4, showed a 13-fold reduction in cleavage activity relative to Rz 1 (t_A = 13 min), but also exhibited enhanced nuclease resistance in all sera (t_S = 120 min in human serum). A significant amount of full-length ribozyme was present after 4 h (Fig. 4 and Table I). Incubation of Rz 4 in serum resulted in the slow formation of stable oligonucleotide fragments of ~16 nucleotides in length (Fig. 4). This digestion pattern suggested that Stem-Loop II was a primary site of nuclease activity in these ribozymes. Our data and the observations of Eckstein and colleagues (indicating that pyrimidines are the primary sites of endonuclease cleavage in hammerhead ribozymes; Heidenreich *et al.* (1993)) suggested that modification of the pyrimidines in Stem-Loop II might afford even greater nuclease protection.

The 3′-exonuclease degradation of the *C*-allyl modified ribozyme was minimal over the time period. In contrast, the 2′-F-pyrimidine modified Rz 5 showed better protection against endonuclease attack, but gave less protection from 3′-exonuclease activity than the *C*-allyl modifications. The cleavage activity of Rz 5 was reduced 30-fold (t_A = 30 min) relative to Rz 1. Since the 3′-exonuclease degradation of Rz 5 was much more pronounced than the Stem II endonuclease degradation of Rz 4, the overall stability of Rz 5 was ~8-fold lower than Rz 4 (Table I).

It has been shown that 2′-*O*-Me modifications stabilize RNA-RNA duplexes (Inoue *et al.*, 1987) and do not have detrimental effects on the catalytic properties of hammerhead ribozymes when incorporated into the binding arms (Goodchild, 1992). We confirmed this latter observation by comparing the activity of Rz 1 with that of Rz 2. The effect of 2′-*O*-Me substitutions in the catalytic core on catalysis is less predictable (Paolella *et al.*, 1992; Yang *et al.*, 1992) but may be beneficial for stability considering the nuclease resistance of the 2′-*O*-Me fragments generated from Rz 2 (see below).

Selective Ribozyme Modifications Maintain Catalytic Activity and Enhance Nuclease Resistance—We considered two models of essential hydroxyl groups for the hammerhead ribozyme catalytic core in the development of our consensus, nuclease-resistant motif. Yang *et al.* (1992) showed that hammerhead ribozymes containing 2′-*O*-Me nucleosides at all positions except (ribonucleotides) G5, G8, A9, A15.1, and G15.2 resulted in a ribozyme with significantly reduced activity, but with a 10^3-fold increase in nuclease resistance in yeast extracts. Paolella *et al.* (1992) placed 2′-*O*-allyl nucleosides at all positions except U4, G5, A6, G8, G12, and A15.1 and saw better activity (20% of wild type), while maintaining reasonable nuclease resistance (RNase A resistance increased by a factor of 10^2 and t_S in bovine serum increased to ~1 h). These results indicated that a modicum of ribonucleotide positions were required within the ribozyme core to maintain catalytic activity.

Based on the above data, we postulated a consensus motif (Fig. 1) that focused on positions U4 and U7 as pyrimidines within the core that might be 2′-modified without a drastic loss in catalytic activity. To test the importance of the U4 modification, Rz 6 was synthesized using a substitution pattern identical to the one reported by Paolella *et al.* (1992), except that 2′-*O*-Me was used instead of 2′-*O*-allyl at nonessential positions. The choice of 2′-*O*-Me substitutions was based on reports that this 2′-modification (i) confers stability to the hammerhead ribozyme (Yang *et al.*, 1992), (ii) is more stable to nucle-

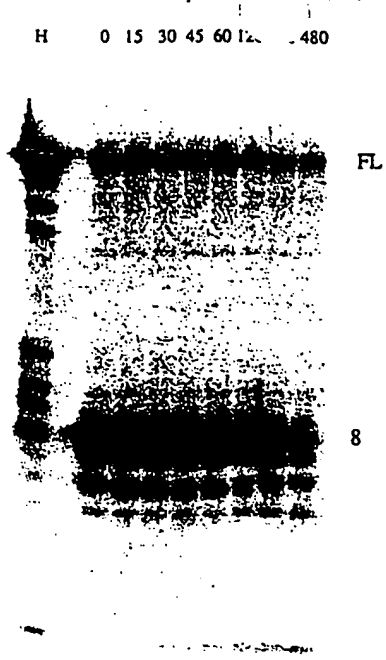

FIG. 5. **Stability of U7 2′-*O*-Me substituted Rz 6 in human serum.** Ribozyme **6** contains 2′-*O*-Me substitutions at all positions shown in lowercase in Fig. 1, with the exception of position U4, which retains the ribose sugar. Time courses with ^{32}P-5′-end-labeled ribozyme were performed as in Fig. 3 and under "Experimental Procedures." Times of ribozyme incubation (minutes) are shown above each panel. *H*, base hydrolyzed Rz **6** size marker; *FL*, full-length ribozyme band position. Approximate size (in nucleotides) of the major digestion products are shown in the panel margins.

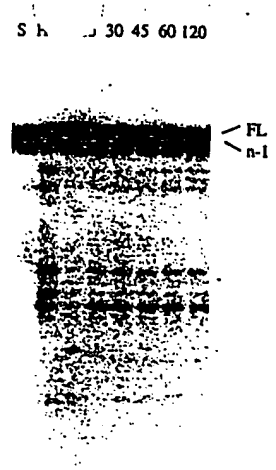

FIG. 6. **Stability of U4/U7 2′-*O*-Me substituted Rz 7 in human serum.** Rz **7** contains 2′-*O*-Me substitutions at all positions shown in lowercase in Fig. 1, including positions U4 and U7. Time courses with ^{32}P-5′-end-labeled ribozyme were performed as in Fig. 3 and under "Experimental Procedures." Medium and times of ribozyme incubation (in minutes) are shown above each panel. *H*, base hydrolyzed Rz **5** size marker; *S*, ribozyme resuspended in saline; *FL*, full-length ribozyme band position; *n-1*, Rz **7** missing the 3′-terminal nucleotide.

ases than either 2′-F or 2′-NH_2 analogs (Kawasaki *et al.*, 1993), (iii) is naturally occurring, thereby reducing the possibility of toxicity *in vivo*, and (iv) is relatively easily synthesized and incorporated. The resulting catalytic activity of Rz **6** was the same as the all-RNA Rz **1** (t_A = 1 min). Unfortunately, Rz **6** showed no improvement in nuclease resistance. In human serum Rz **6** was rapidly cleaved to give smaller fragments that were ~8 nucleotides in length (Fig. 5). The generation of 8-mer cleavage fragments from the 5′-end of Rz **6** suggested that the U4 site (the only unmodified pyrimidine residue within Rz **6**) remained hypersensitive to nucleases. The different stability of Rz **6** compared to the reported 2′-*O*-allyl analog (Paolella *et al.*, 1992) could reflect a different accessibility of position U4 in a more sterically hindered 2′-*O*-allyl core compared to the less bulky 2′-*O*-Me core of Rz **6** and/or different nuclease compositions of bovine and human sera. The stability over time of the intact ribozyme fragment from Rz **6** suggested that the 2′-*O*-Me modification may be as good as the *C*-allyl modification at providing nuclease resistance. Thus, another 2′-*O*-Me substituted ribozyme was made and tested (Rz **7**) that contained the same substitutions as Rz **6** with an additional 2′-*O*-Me substitution at the U4 position. Ribozyme **7** showed a 4-fold reduction in catalytic activity (t_A = 4 min) but also gave a dramatic improvement in the nuclease resistance of the ribozyme (t_S = 260 min, Fig. 6), so that the overall stability/activity ratio, β, improved 650-fold for Rz **7** compared to the all-RNA Rz **1**.

To further elaborate on this model, the seven 2′-modified-uridine nucleotides shown in Fig. 2 were introduced into positions U4 and U7, (ribozymes **8–28**). These modifications were chosen for a variety of reasons. 2′-Fluoro- and 2′-NH_2-U modifications have been successfully applied by Eckstein's group (Heidenreich *et al.*, 1993) but have not been used in a highly 2′-*O*-methylated motif. The 2′-ara-F-U modification was introduced to probe the influence of configuration of the fluoro substituent on activity and stability. 2′-Deoxy-2′-methylene and difluoromethylene nucleotides were introduced under the assumption that imposing conformational restrictions on ribose sugar puckering of these monomers could provide increased nuclease resistance without reducing catalytic activity. Yamagata *et al.* (1992) showed by x-ray analyses that the C1′, C2′, and C3′ carbons in 2′-deoxy-2′-methylene pyrimidine nucleosides are nearly coplanar. Finally, 2′-dU was introduced to probe the effect of removing substituents from the 2′-position. In the case of single U4 or U7 substitutions, the other uridine site contained a 2′-*O*-Me uridine.

The cleavage activity (t_A), human serum half-lives (t_S), and overall stability/activity ratios (β) for Rzs **8–28** are shown in Table II. All modifications to U4 and/or U7 gave significant increases in nuclease resistance for these ribozymes, while varying levels of ribozyme activity were observed. The most dramatic increases in nuclease resistance were seen in Rzs **20**, **22–24**, and **26**, where stability times of greater than 500 min were observed (equivalent to >5000-fold stability increase relative to Rz **1**). Ribozyme **25** gave a less dramatic increase in stability (t_S = 300 min); however, its catalytic activity (t_A = 2 min) made it attractive for further investigation. All of the ribozymes containing U4/U7 modifications were active to some degree, and the majority had activity decreases of less than 5-fold relative to Rz **1**. The best overall ribozymes in terms of combined stability and activity were ribozymes **25** and **26** with β values of 1500–1700.

Certain trends that correlated with the type of 2′-modification and catalytic activity were noted. Modifications that distorted the normal ribose ring pucker resulted in ribozymes with reduced activity; examples included Rzs **8–10** (2′-methylene) and **11–13** (2′-difluoromethylene). Double modification of both U4 and U7 with these nucleotides had an even more pronounced negative effect (Rzs **10** and **13**). 2′-Fluoro substitutions at U4 and U7 were less detrimental to catalysis than the related 2′-arabino-F-substitutions (Rzs **14–16** *versus* Rz **20–**

TABLE III
Single turnover kinetic parameters of ribozymes 1, 2, 25, and 26
Kinetic parameters were determined from single turnover experiments at pH 6.5 and 25 °C.

Rz	k_{cat}^S	K_M^S	k_{cat}^S/K_M^S
	min^{-1}	nM	$\times 10^7\ M^{-1}\ min^{-1}$
1	0.4	13	3
2	0.95	25	4
25	1.2	20	6
26	0.14	56	0.3

22). An especially striking difference was observed for the F/F-modified Rz **16** when compared to araF/araF-modified Rz **22**. Our observations with the F/F-modified Rz **16** are consistent with an earlier proposal (Heidenreich *et al.*, 1993) for a hydrogen bonding network, which includes the 2'-hydroxyl of U4 and U7 and is relatively undisturbed by 2'-F substitutions due to their hydrogen acceptor properties. The greater reduction in activity observed for the araF/araF-modified Rz **22** could then be explained as a significant disruption of these hydrogen bonds due to the altered configuration at the 2'-position. However, this model would suggest that all modifications that remove or shift the position of the 2'-hydroxyl at U4 and U7 should significantly reduce ribozyme activity. In fact, only moderate (4-fold) reductions in activity are observed for H/H-modified Rz **19**, and for a recently tested ara/ara-modified ribozyme (data not shown).

The high activity of Rz **25** (U4/U7 = 2'-NH_2-U) is in agreement with the recently published observation that incorporation of 2'-NH_2-U into both the U4 and U7 positions rescues the activity of uniformly 2'-F-substituted ribozymes at pyrimidine sites (Heidenreich *et al.*, 1994). Interestingly, the combination of 2'-NH_2-U and 2'-*O*-Me substitution at positions U4 and U7 yielded Rz **24** (*O*-Me/NH_2) with moderate and Rz **23** (NH_2/*O*-Me) with low catalytic activity. Only the double modification (NH_2/NH_2) provided a highly active ribozyme. The intrinsic dual role of the amino group as a potential hydrogen bond donor and acceptor could be responsible for the observed effect if both 2'-NH_2 groups are the partners in a hydrogen bonding network. In contrast, the relatively high catalytic activity of the 2'-*C*-allyl modified Rzs **26–28** is not consistent with the hydrogen bonding network proposed by Heidenreich *et al.* (1993) since it is unclear how the 2'-*C*-allyl group could participate in the normal hydrogen bonding or Mg^{2+} coordination networks that create the active catalytic conformation.

Having identified two ribozymes with substantially increased stability (Rzs **25** and **26**), we wanted to confirm that the activity screens were correctly representing the activity of these ribozymes. Thus, more complete activity profiles were determined for Rzs **25** and **26** and were compared to the kinetic parameters of the control Rzs **1** and **2**. Table III shows that Rzs **1**, **2**, and **25** all have similar kinetic behavior. These ribozymes show little difference in the values of the specificity constant, k_{cat}^S/K_M^S, while the less certain estimates of k_{cat}^S and K_M^S vary by only 2-fold. In contrast to these three ribozymes, Rz **26** shows a ~10-fold reduction in k_{cat}^S/K_M^S, which is almost completely due to reductions in k_{cat}^S.

We have attempted to compare our findings with the interactions seen in two recently published and very similar crystal structures (Pley *et al.*, 1994, Scott *et al.*, 1995). However, it is difficult to compare our results to these crystal structures for two reasons. First, most of our substitutions are conservative 2'-*O*-Me sugar substitutions, which should cause a minimum of steric clash with neighboring groups and which can still act as H-bond acceptors, while the remaining, extensive substitutions have focused on the 2'-positions only at U4 and U7. Second, the crystal structures appear to represent a ground-state structure

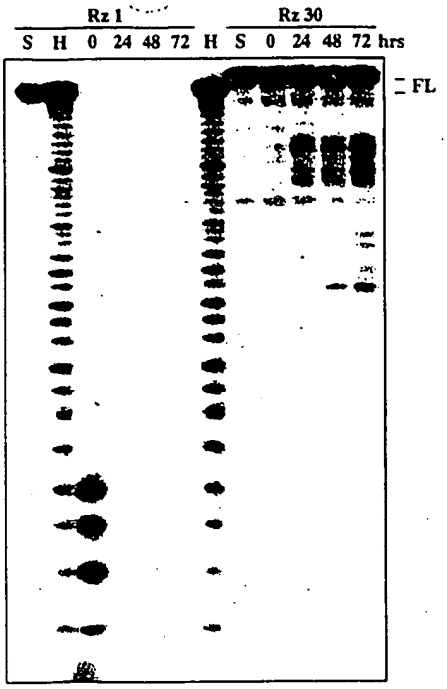

FIG. 7. **Stability of internally labeled Rz 30 in human serum.** Ribozyme **30** (U4/U7 2'-amino with 3'-3' inverted T) was labeled with ^{32}P at the phosphate 5'- to the GAAA sequence in the Stem II loop (Fig. 1) and incubated in human serum as in Fig. 3. For comparison, the all-RNA Rz **1** was 5'-labeled with ^{32}P and incubated under the same conditions. The addition of 3'-3' inverted T to Rz **30** and the absence of a 5'-phosphate makes this ribozyme migrate more slowly than Rz **1** on the acrylamide gel. Times of ribozyme incubation (in hours) are shown above each panel. *H*, base hydrolyzed Rz 1 size marker; *S*, ribozyme resuspended in saline; *FL*, full-length ribozyme band position. *Time 0 h* is actually the time required to add the ribozyme to serum, mix, and quench in stop buffer (~30 s).

that is fairly distant from the transition state. Nevertheless, McKay and colleagues described three positions (U4, G5, and G8) at which H-bond contacts are made with the 2'-hydroxyl. The H-bond contacts at G5 and G8 are in agreement with the observations that these hydroxyl groups cannot be substituted without substantial loss of activity. However, the data for position U4 would suggest that H-bond interactions with this 2'-hydroxyl are not essential for cleavage activity, since substitutions that abolish H-bonds (=CF_2 in Rz **11**, and *C*-allyl in Rz **26**) show the same moderate reductions in activity as do substitutions that maintain H-bonds (F in Rz **14**).

3'-Modifications Maintain Catalytic Activity and Extend Ribozyme Serum Half-life at Nanomolar Concentrations—Ribozymes **7–28** all showed dramatic improvements in nuclease resistance compared to the all-RNA Rz **1**, or even compared to the highly modified Rz **6**, which still contains a ribonucleotide at U4. However, all of these ribozymes still exhibit slow degradation at the 3'-end (*cf.* Fig. 6). Addition of a 3'-3'-linked, inverted T (iT) residue at the 3'-end of DNA oligonucleotides has been reported to inhibit the digestion of DNA by 3'-exonucleases (Ortigão *et al.*, 1992). We therefore added an iT to Rzs **25** and **26** to give Rzs **29** and **30**. The iT residue protected the 3'-terminus of the ribozymes for at least 48 h, when present at 25 nM in either human serum or fetal calf serum (data not shown). We viewed this as a conservative estimate of nuclease resistance due to a low level of phosphatase activity present in both sera.

To eliminate the effect of 5'-phosphatase activity on ribozyme stability measurements, the stability of Rz **30** was

evaluated using ribozymes that contained an internal ^{32}P label (see "Experimental Procedures"). Fig. 7 shows that >75% of internally labeled Rz **30** remained intact after a 72 h incubation in human serum ($t_{\frac{1}{2}}$ = 16,000 min). In contrast, the all-RNA Rz 1 was degraded to small fragments within the 30 s that it took to add ribozyme to serum, mix, and quench the reaction (*time 0 h*, Fig. 1). During the incubation of Rz **30**, a small number of minor bands appeared that have mobilities consistent with digestion at the five remaining ribose sites within the ribozyme. Thus, even greater stabilization of the ribozymes is likely to require substitution of the 5 remaining ribose residues.

To verify that the 3′-exonuclease activity in serum was not significantly diminished during the 72 h assay, Rzs **1** and **2** were added to a sample of the serum after the 72 h incubation period. These nuclease-sensitive ribozymes were degraded immediately (data not shown).

The presence of the inverted T residue at the 3′-end of Rzs **29** and **30** has no effect on catalytic activity. Their activity half-times were identical to the equivalent Rzs **26** and **25**, respectively, which lack the inverted T (Table II). Thus, Rzs **29** and **30** show an overall 50,000–80,000-fold increase in the relative ribozyme stability/activity compared to the all-RNA ribozyme.

Incubation of Nuclease-resistant Ribozymes in Human Serum Does Not Alter Catalytic Activity—To assess the effect on catalytic activity of prolonged incubation of Rzs **29** and **30** in human serum, samples of the Rzs were removed from the serum after 72 h and assayed for activity. To inhibit nuclease digestion of the substrate in serum, yeast tRNA was added to each sample. No diminution in ribozyme catalytic activity was noted in this assay (data not shown).

Conclusions—We have systematically investigated the influence of certain 2′-modifications on hammerhead ribozymes, with the goal of conferring high cleavage activity and increased nuclease resistance in biological sera. We have identified a consensus motif of 2′-hydroxyl groups required to maintain catalytic activity in the context of a persubstituted 2′-*O*-Me hammerhead ribozyme. In this motif, the 5 purine ribonucleotides G5, A6, G8, G12, and A15.1 remain unmodified. Selective modifications, at positions U4 and U7 in the "5-ribose" hammerhead ribozyme, maintain catalytic activity while dramatically increasing the nuclease resistance of the ribozymes in biological sera. The best U4 and U7 modifications for stability and activity were U4/U7 2′-NH_2 and U4 2′-*C*-allyl/U7 2′-*O*-Me, which provided more than a 1500-fold increase in stability/activity ratios (β) over the unmodified all-RNA ribozyme. An additional increase in β values to 53,000–80,000 was achieved by introducing a 3′-3′-linked thymidine to the 3′-end of these ribozymes.

Acknowledgments—We thank Tom Cech, Daniel Herschlag, and Gerald Joyce for suggestions and critical reading of the manuscript.

REFERENCES

Beaucage, S. L. & Iyer, R. P. (1993) *Tetrahedron* **49**, 6123–6194
Bratty, J., Chartrand, P., Ferbeyre, F. & Cedergren, R. (1993) *Biochim. Biophys. Acta* **1216**, 345–359
Cameron, F. H. & Jennings, P. A. (1989) *Proc. Natl. Acad. Sci U. S. A.* **86**, 9139–9143
Cech, T. (1992) *Curr. Opin. Struct. Biol.* **2**, 605–609
De Mesmaeker, A., Lebreton, J., Hoffmann, P. & Freier, S. M. (1993) *Synlett*, 677–679
Goodchild, J. (1992) *Nucleic Acids Res.* **20**, 4607–4612
Heidenreich, O., Pieken, W. & Eckstein, F. (1993) *FASEB J.* **7**, 90–96
Heidenreich, O., Benseler, F., Fahrenholz, A. & Eckstein, F. (1994) *J Biol. Chem.* **269**, 2131–2138
Hertel, K. J., Pardi, A., Uhlenbeck, O. C., Koizumi, M., Ohtsuka, E., Uesugi, S., Cedergren, R., Eckstein, F., Gerlach, W. L., Hodgson, R. & Symons, R. H. (1992) *Nucleic Acids Res.* **20**, 3252
Inoue, H., Hayase, Y., Imura, A., Iwai, S., Miura, K. & Ohtsuka, E. (1987) *Nucleic Acids Res.* **15**, 6131–6148
Iyer, R. P., Phillips, L. R., Egan, W., Regan, J. B. & Beaucage, S. L. (1990) *J. Org. Chem* **55**, 4693–4701
Kawasaki, A. M., Casper, M. D., Freier, S. M., Lesnik, E. A., Zounes, M. C., Cummins, L. L., Gonzalez, C. & Cook, P. D. (1993) *J. Med. Chem.* **36**, 831–841
Milligan, J. F., Matteucci, M. D. & Martin, J. C. (1993) *J. Med. Chem.* **36**, 1923–1937
Ortigão, J. F. R., Rösch, H., Selter, H., Frölich, A., Lorenz, A., Montenarh, M. & Seliger, H. (1992) *Antisense Res. & Dev.* **2**, 129–146
Paolella, G., Sproat, B. S. & Lamond, A. I. (1992) *EMBO J.* **11**, 1913–1919
Pieken, W. A., Olsen, D. B., Benseler, F., Aurup, H. & Eckstein, F. (1991) *Science* **253**, 314–317
Pley, H. W., Flaherty, K. M. & McKay, D. B. (1994) *Nature* **372**, 68–74
Ruffner, D. E., Stormo, G. D. & Uhlenbeck, O. C. (1990) *Biochemistry* **29**, 10695–10702
Scaringe, S. A., Franklyn, C. & Usman, N. (1990) *Nucleic Acids Res.* **18**, 5433–5441
Scott, W. G., Finch, J. T. & Klug, A. (1995) *Cell* **81**, 991–1002
Shimayama, T., Nishikawa, F., Nishikawa, S. & Taira, K. (1993) *Nucleic Acids Res.* **21**, 2605–2611
Uhlmann, E. & Peyman, A. (1990) *Chem. Rev.* **90**, 543–584
Usman, N. & Cedergren, R. J. (1992) *Trends Biochem. Sci.* **17**, 334–339
Wincott, F. E., DiRenzo, A., Shaffer, C., Grimm, S., Tracz, D., Workman, C., Sweedler, D. & Usman, N. (1995) *Nucleic Acids Res.* **23**, 2677–2684
Yang, J.-H., Usman, N., Chartrand, P. & Cedergren, R. J. (1992) *Biochemistry* **31**, 5005–5009
Yamagata, Y., Tomota, K.-I., Marubayashi, N., Ueda, I., Sakata, S., Matsuda, A., Takenuki, K. & Ueda, T. S. (1992) *Nucleosides & Nucleotides* **11**, 835–853

KNH
In Press

Inhibition of Vascular Smooth Muscle Cell Proliferation by Ribozymes that Cleave c-*myb* mRNA

Thale C. Jarvis[1], Laverna J. Alby[1], Amber A. Beaudry[1], Francine E. Wincott[1], Leonid Beigelman[1], James A. McSwiggen[1], Nassim Usman[1], and Dan T. Stinchcomb[1,2]

[1] Ribozyme Pharmaceuticals, Inc.
2950 Wilderness Pl.
Boulder, CO 80301

[2]To whom communications should be addressed. Tel:(303) 449-6500, Fax: (303) 449-6995, Email: stinchdt@rpi.com

Running title: Ribozyme inhibition of cell proliferation

Abstract

Proliferation of injured smooth muscle cells contributes to the reocclusion or restenosis of coronary arteries that often occurs following angioplasty procedures. We have identified and optimized nuclease-resistant ribozymes that efficiently cleave c-*myb* RNA. Three ribozymes targeting different sites in the c-*myb* mRNA were chemically synthesized and delivered to rat aortic smooth muscle cells with cationic lipids; all three significantly inhibited serum-stimulated cell proliferation. RNA molecules with two base substitutions in the catalytic core that render the ribozyme catalytically inactive had little effect on smooth muscle cell proliferation. Ribozymes with scrambled binding arm sequences also failed to affect cell cycle progression of vascular smooth muscle cells. Furthermore, inhibition of rat smooth muscle cell proliferation correlated with a reduction in intact c-*myb* mRNA. Efficacy of the chemically-modified ribozyme was directly compared to phosphorothioate antisense oligodeoxynucleotides (ODNs) targeting the same site in the c-*myb* RNA; the ribozyme had superior efficacy and showed greater specificity than the antisense molecules. Exogenously delivered ribozymes also effectively inhibited porcine and human smooth muscle cell proliferation. Ribozymes targeting c-*myb* or other regulators of smooth muscle cell proliferation may represent novel therapeutics for the treatment of restenosis after coronary angioplasty.

Key words: cell proliferation/c-myb/restenosis/ribozymes/smooth muscle cells/antisense

Introduction

The use of coronary angioplasty to surgically treat atherosclerotic vessels has been accelerating rapidly; over 450,000 procedures were performed in the United States alone in 1994. The procedure is quite effective at opening occluded vessels. However, in spite of a number of technical improvements in the procedure, post-operative occlusion of the arteries, or restenosis, still occurs. Thirty-five to forty-five percent of patients who have undergone a single vessel angioplasty develop clinically significant restenosis within 6 months of the procedure(Popma, et al., 1991, Landau, et al., 1994). Histopathological studies have shown that restenosis after angioplasty is characterized by migration of medial smooth muscle cells to the intima, followed by hyperproliferation and excessive matrix deposition by these neointimal cells (Austin, et al., 1985, Garratt, et al., 1991). Although the underlying mechanisms driving the restenotic process are still a matter of debate, it is widely believed that preventing the injury-induced activation and proliferation of medial smooth muscle cells after angioplasty could prevent intimal thickening and restenosis(Forrester, et al., 1991, Jackson and Schwartz, 1992, Libby, et al., 1992). Towards this goal, we are exploring the use of ribozymes as specific modifiers of smooth muscle cell behavior.

Ribozymes are enzymatic RNA molecules; many of the common, naturally occurring ribozyme motifs can be engineered to cleave specific mRNA sequences (Cech, 1992, Christofferson and Marr, 1995). The hammerhead ribozyme motif is particularly adaptable. First identified in plant virusoids as a *cis*-cleaving motif, the hammerhead ribozyme can be designed to act in *trans* (Symons, 1994). The motif used in this study contains two variable substrate binding arms interrupted by a catalytic core of approximately 22 nucleotides. This ribozyme has simple substrate sequence requirements; hammerhead ribozymes can cleave after any UH sequence (where H = A, C, or U) (Koizumi, et al., 1988, Rufner, et al., 1990). Cleavage of specific mRNA sequences *in vitro* has been repeatedly demonstrated(Cech, 1992). The application of synthetic hammerhead ribozymes to mammalian cells has resulted, in several cases, in a demonstrable reduction in target RNA and a corresponding alteration in cellular phenotype

(Sioud, et al., 1992, Lange, et al., 1993, Snyder, et al., 1993, Kiehntopf, et al., 1994, Sioud, 1994, Leopold, et al., 1995). To date, ribozymes have not been engineered to target mRNA sequences from genes that are critical for normal cell proliferation. In an attempt to inhibit smooth muscle cell proliferation, we designed ribozymes that would cleave c-*myb* mRNA.

The c-*myb* proto-oncogene encodes a protein consisting of a repeated N-terminal DNA binding domain(Tanikawa, et al., 1993), a transcriptional activating domain(Weston and Bishop, 1989), and a C-terminal repressor domain (Sakura, et al., 1989). The consequences of c-*myb* expression have been carefully studied in the hematopoietic lineage, where c-*myb* expression is required for proliferation of early hematopoietic precursors (Mucenski, et al., 1991). Conversely, reduced c-*myb* expression is required for terminal differentiation of hematopoietic cells (Clarke, et al., 1988). Likewise, in cells of other lineages, over-expression of c-*myb* can lead to elevated proliferation (Alitalo, et al., 1984, Griffin and Baylin, 1985, Janssen, et al., 1986, Thiele, et al., 1987) and reduced expression is correlated with differentiation (Thiele, et al., 1988). Thus, in several cell types, c-*myb* is a pivotal regulatory factor, influencing the decision to divide or differentiate.

If c-*myb* plays a similar critical role in the differentiative state of smooth muscle cells, then over-expression should lead to hyperproliferation and reduced expression should promote terminal differentiation. Indeed, when whole serum is added to quiescent smooth muscle cells *in vitro*, expression of a number of cellular proto-oncogenes, including the transcription factor, c-*myb*, is induced (Kindy and Sonenshein, 1986, Brown, et al., 1992) and cell proliferation ensues. Serum-induced c-*myb* expression and proliferation can be blocked with an antisense oligodeoxynucleotide (Brown, et al., 1992). *In vivo*, a c-*myb* antisense oligodeoxynucleotide appears to inhibit restenosis when applied to rat arteries after balloon angioplasty (Simons, et al., 1992). Thus, c-*myb* is required for smooth muscle cell activation and hyperproliferation induced by the multitude of growth factors present in serum or induced by arterial injury *in vivo*.

Herein, we describe the activity of several ribozymes targeting *c-myb*. We find that ribozymes capable f cleaving c-*myb* mRNA can inhibit cell proliferation when applied to smooth

muscle cells as an RNA/cationic lipid complex. RNA molecules that lack catalytic activity or binding activity are much less efficacious than active ribozymes. As expected, the inhibition of smooth muscle cell proliferation by the hammerhead ribozymes correlates with a reduction in c-*myb* mRNA levels. These nuclease-stable ribozymes represent novel therapeutic molecules; their striking efficacy, when delivered exogenously, suggests that they may be used to inhibit the hyperproliferation of smooth muscle cells that occurs in many patients after coronary angioplasty.

Results

Ribozymes targeting c-*myb* inhibit smooth muscle cells

The hammerhead ribozyme motif used in these studies is shown in Figure 1. The consensus sequence that is vulnerable to hammerhead ribozyme cleavage (UH, where H can be A, C, or U) occurs frequently throughout the c-*myb* message. In the intracellular milieu, potential cleavage sites are likely to vary significantly in accessibility to ribozyme binding, depending on protein binding and secondary and tertiary structure in the mRNA. We have determined the optimal sites for ribozyme cleavage of the c-*myb* mRNA by a method described separately (T. Jarvis, et al, in preparation). Hammerhead ribozymes targeting these sites then were synthesized chemically (Wincott, et al., 1995)with modifications designed to confer high levels of nuclease resistance while retaining catalytic activity (Usman, et al., 1994, Beigelman, et al., 1995). The structure is shown in Figure 1. Inactive controls contain two mutations in the catalytic core which abolish cleavage activity. The active and inactive ribozymes have been shown to have equivalent stability with respect to nucleolytic degradation (Beigelman, et al., 1995).

The chemically synthesized ribozymes were delivered to quiescent rat aortic smooth muscle cells (RASMC) using the cationic lipid vehicle, LipofectAMINE. We have shown by flow-cytometric analysis with fluorescently labeled ribozyme, that greater than 90% of the cells are tranfected under these conditions (unpublished data). The cells were then stimulated with serum, and cell proliferation was measured by a bromodeoxyuridine (BrdU) incorporation assay as shown in Figure 2. A high percentage of the serum-stimulated cells underwent DNA replication and therefore stained positively for BrdU (panel A), while a very low percentage of

BrdU positive nuclei were seen in the absence of serum (panel B). Significant inhibition of the proliferative response was seen when cells were treated with an active c-*myb* ribozyme prior to serum stimulation (panel C). By contrast, cells treated with an inactive ribozyme proliferated at levels comparable to the serum control (panel D). Since the inactive ribozyme is expected to bind to the same site in c-*myb* RNA, but is incapable of catalytic cleavage, this result suggests that the inhibition of cell proliferation observed upon treatment with active ribozyme was mediated by cleavage of c-*myb* mRNA.

Data obtained from experiments such as that shown in Figure 2 can be quantified in terms of the percentage of cells proliferating under each treatment condition. Figure 3 shows the activity of ribozymes targeting three different sites in the c-*myb* message. In each case, treatment of the cells with a catalytically active ribozyme resulted in significant inhibition of proliferation, while treatment with the inactive counterpart failed to inhibit. We have also tested active ribozymes containing scrambled binding arms that cannot anneal to the c-*myb* message, and found that they also failed to inhibit proliferation (unpublished data). Several active ribozymes targeting different sites within c-*myb* show comparable levels of inhibition. This suggests that the observed effect is a direct consequence of reduction in c-*myb* expression, and not merely a coincidental "aptamer" effect associated with a particular oligonucleotide sequence or chemistry. The lack of inhibition by three different catalytically inactive ribozymes indicates that the mechanism of the inhibition is sequence-specific cleavage of c-*myb* message.

The ribozyme targeting site 575 of the c-*myb* mRNA was selected for further study. Figure 4 shows the inhibition of proliferation by active ribozyme relative to the serum-stimulated control as a function of offered dose. The ribozyme-mediated inhibition is clearly dose-dependent, with an IC_{50} of approximately 75 nM. The inactive control shows no inhibition except for a modest effect at the highest dose. This result has proven to be highly reproducible. In nine consecutive experiments using this ribozyme, the average specific inhibition (inhibition of proliferation by active ribozyme relative to inactive ribozyme) was 72% ± 16% at a 100 nM dose.

In addition, we have confirmed this result using flow cytometric analysis to measure the proliferative state of the smooth muscle cells (unpublished data).

Treatment with active ribozyme reduces c-*myb* mRNA levels in smooth muscle cells

We have repeatedly shown that active c-*myb* ribozymes inhibit smooth muscle cell proliferation while catalytically inactive ribozyme controls do not. These data strongly suggest that ribozyme cleavage of c-*myb* RNA mediates the observed effect. We attempted to confirm this hypothesis by direct measurement of c-*myb* RNA isolated from cells following ribozyme treatment. Since c-*myb* message is a relatively low-abundance RNA, we chose to measure the RNA by quantitative competitive polymerase chain reaction (QC-PCR) (Thompson, et al., 1992). Each measurement includes a determination of both the c-*myb* RNA level and that of a housekeeping gene, glyceraldehyde phosphate dehydrogenase (GAPDH). The results are displayed as a ratio of c-*myb* to GAPDH to normalize for variations in cell number, RNA yield and integrity, and RNA preparation-specific effects on the PCR analysis. As shown in Figure 5, c-*myb* RNA levels are reduced in smooth muscle cells following treatment with active ribozyme. The ribozyme-mediated reduction in c-*myb* RNA levels is similar in magnitude to the inhibition of proliferation measured in parallel cultures.

The experiment shown in Figure 5 was performed on RNA isolated 12 hours after serum stimulation. In subsequent experiments, we examined the c-*myb* RNA level at earlier and later times following ribozyme treatment. RNA harvested either immediately after ribozyme treatment, 4 hours, 12 hours or 20 hours post serum stimulation showed 72%, 48 ± 15%, 80 ± 6%, or 49 ± 19% reduction in c-*myb* levels by active ribozyme relative to inactive ribozyme, respectively. Thus, ribozyme treatment results in prolonged depression of c-*myb* message in these cells. Since the precise role of c-*myb* in cell cycle progression has not been clearly elucidated, we do not know which time point is the most relevant from the standpoint of proliferation. It is clear, however, that the inhibition in proliferation by active ribozymes correlates with message reduction throughout the assay period.

Comparis n of anti-c-*myb* ribozymes and antisense oligodeoxynucleotides

Several studies have reported inhibition of vascular smooth muscle cell proliferation by antisense oligodeoxynucleotides targeting c-*myb* mRNA (Brown, et al., 1992, Simons, et al., 1992). This gene inactivation strategy utilizes nuclease-resistant phosphorothioate oligodeoxynucleotides. Such molecules can either inhibit translation by steric blocking effects near the site of initiation, or they can activate endogenous RNAse H activity, leading to cleavage of the target RNA. By contrast, the ribozymes used in this study contain 2'-*O*-methyl nucleotides. Hybrids of RNA and 2'-*O*-methyl nucleotides are not substrates for RNAse H cleavage (unpublished data). Since the catalytic activity is intrinsic to the ribozyme itself, cleavage of the target RNA can occur upon hybrid formation, without the additional requirement of ternary complex formation with an endogenous nuclease. Given these differences in mechanism, we wished to compare the relative merits of the antisense and ribozyme approaches in our system.

In Table I, the activity of the ribozyme targeting site 575 is compared to a 15-mer phosphorothioate antisense oligodeoxynucleotide (ODN) that exactly matches the ribozyme binding site, or to a 25-mer antisense oligomer centered around the 575 site. At both doses tested, the active ribozyme showed a high degree of specific inhibition of smooth muscle cell proliferation relative to the inactive or scrambled controls. With the phosphorothioate ODN, non-specific effects exhibited by scrambled sequence controls were much more pronounced. Treatment with the 25-mer ODN gave completely non-sequence-specific inhibition of proliferation. The shorter antisense ODN showed some specificity relative to the scrambled control at both doses, although the overall degree of inhibition was less than that exhibited by the active ribozyme. Thus, under these conditions, the ribozyme approach offered the advantage of both enhanced activity and specificity for the target mRNA.

Brown *et al.*(Brown, et al., 1992) have reported sequence specific effects with two different anti-c-*myb* oligodeoxynucleotides, one targeting the coding region from nucleotides 940 to 959 and one targeting the translational initiation site. In our hands, these oligodeoxynucleotides showed very similar effects to those shown in Table I for the 575 site 15-

mer (unpublished data). In several attempts, we were unable to observe any sequence-specific effects of the oligodeoxynucleotides used by Simons *et al.*(Simons, et al., 1992, Simons and Rosenberg, 1992) In all of the above cases, the scrambled sequence phosphorothioate ODN controls showed significant non-specific inhibition, so the efficacy of the antisense oligodeoxynucleotides had to be assessed against this background.

Ribozymes targeting c-*myb* inhibit porcine and human smooth muscle cell proliferation

In developing oligonucleotide therapeutics, one must consider the sequence conservation of the target gene between humans and each of the relevant preclinical animal species that might be used to evaluate the therapeutic potential of the compound. Recognized animal models for angioplasty include the rat carotid artery injury model, and the porcine iliofemoral or cardiac artery injury model. The complete sequence for human c-*myb* cDNA has been reported (Majello, et al., 1986). Sequencing of selected regions of rat and porcine c-*myb* cDNA has shown that the 575 ribozyme binding site is conserved between rat, pig and human (unpublished data). Figure 6 shows a comparison of the effect of the 575 ribozyme on rat, porcine and human aortic smooth muscle cells. Clearly, the active ribozyme shows specific inhibition relative to the inactive and scrambled-inactive controls in cells originating from each species. The scrambled ribozyme contains an inactive core, and scrambled binding arms and therefore serves as a control for non-specific chemistry effects. We have also verified that an active ribozyme with scrambled binding arms (a control for non-specific cleavage) fails to inhibit (unpublished data). These data suggest that the binding site for the 575 ribozyme must be similarly accessible in rat, pig and human c-*myb* messages, despite the fact that the target mRNAs may have slightly different overall structures. Thus, ribozymes described in these studies may be expected to have similar effects in several well-defined animal models of restensosis and in human clinical trials.

Discussion

We have demonstrated that ribozymes targeting several different sites within the c-*myb* message are highly efficacious in inhibiting the proliferation of vascular smooth muscle cells. The results are reproducible, and have been observed in cells derived from several different species. The inhibition is clearly mediated by a sequence-specific ribozyme cleavage mechanism, as demonstrated by the lack of inhibition by catalytically inactive controls. The observed reduction in intracellular c-*myb* RNA levels following ribozyme treatment lends credence to this mechanistic interpretation.

Using ribozymes as specific probes of c-*myb* function, we have shown that the proto-oncogene c-*myb* is required for cell cycle progression in response to serum stimulation in cultured vascular smooth muscle cells derived from rat, pig and human arteries. Thus, our data illustrate a common role of c-*myb* in potentiating vascular smooth muscle cell proliferation in a variety of species, and is consistent with its role as a pivotal regulatory transcription factor in hematopoetic cells as well. Previously, antisense phosphorothioate molecules have been used similarly to probe the role of c-*myb* in rat and bovine smooth muscle cell proliferation(Brown, et al., 1992, Simons, et al., 1992, Simons and Rosenberg, 1992). The sequence-specificity and the mechanism of action of some of these oligonucletides have been questioned by a number of investigators (Epstein, et al., 1993, Guzman, et al., 1994, Burgess, et al., 1995). The data we present demonstrate the enhanced sequence-specificity of ribozymes as inhibitors of gene expression. RNA molecules with simple substitutions that block catalytic activity and ribozymes with altered sequence recognition properties provide better means of demonstrating sequence-specific effects than "sense" or even "scrambled" antisense oligodeoxynucleotide controls.

Several examples have been reported in which *in vitro* transcribed ribozymes complexed with cationic lipids have shown significant efficacy against their intended target when delivered to mammalian cells in culture (Sioud, et al., 1992, Taylor, et al., 1992, Lange, et al., 1993, Kiehntopf, et al., 1994). In these cases, the cationic lipid complex is thought to protect the RNA from degradation during the assay period. Chemically synthesized ribozymes can be stabilized

additionally by a variety of strategies, including synthesis of DNA/RNA chimeras (Taylor, et al., 1992, Shimayama, et al., 1993) and 2'-substitutions (Pieken, et al., 1991, Usman, et al., 1994, Beigelman, et al., 1995). DNA/RNA chimeric ribozymes delivered as cationic lipid complexes have shown efficacy in reducing MDR-1 expression in pleural mesothelioma cells in culture (Kiehntopf, et al., 1994)and in reducing *bcr-abl* expression in a chronic myelogenous leukemia cell line (Snyder, et al., 1993). However, the DNA moieties in the binding arms of these ribozymes could stimulate RNAseH cleavage and RNA sequences in the catalytic core of the ribozyme are still susceptible to nuclease digestion. In our experiments, we have utilized ribozymes with a unique pattern of 2´-substitutions that maintain the ribozyme catalytic activity while conferring resistance to nucleases present in serum (Usman, et al., 1994, Beigelman, et al., 1995). The enhanced serum stability of the RNA molecules described herein make them ideal for exploring further the utility of ribozymes *in vivo*.

The ribozymes reported here constitute a unique approach to the selective regulation of gene expression, and may be applied *in vivo* to inhibit c-*myb* or other genes critical for smooth muscle cell proliferation. Other oligonucleotides that inhibit smooth muscle cell proliferation have shown promise in animal models of intimal hyperplasia. Antisense ODNs targeting c-*myb*, c-*myc*, cdc2, cdk2 or proliferating cell nuclear antigen (PCNA) have reduced intimal hyperplasia after balloon injury (Simons, et al., 1992, Biro, et al., 1993, Morishita, et al., 1993, Shi, et al., 1993, Simons, et al., 1994). Antisense ODNs targeting PCNA and cdc2 have shown efficacy in an animal model of stenosis after venous graft procedures (Mann, et al., 1995). Other anti-proliferative or cytotoxic strategies have also shown efficacy in animal models of restenosis. For example, treatment of denuded porcine arteries with recombinant adenovirus expressing a constitutively active form of the retinoblastoma that inhibits smooth muscle cell proliferation results in significant reductions in neoinitimal thickening (Chang, et al., 1995). These results indicate that therapies resulting in reduced smooth muscle cell proliferation can ameliorate the intimal hyperplasia associated with balloon injury. Therefore anti-proliferative ribozymes, such as those reported here, may represent promising therapeutics for the treatment of restenosis.

As with antisense or gene therapies, a ribozyme therapy for restenosis will require an effective method for intraluminal delivery. Effective delivery of a synthetic ribozyme would result in prolonged residence of the ribozyme in the arterial wall during the critical time window for smooth muscle cell proliferation following PCTA. Many devices such as microporous balloon catheters, hydrogel catheters, and drug-eluting biodegradable stents that show promise in accomplishing this task are currently under development (Lincoff, et al., 1994, Riessen and Isner, 1994). Ribozymes also may be delivered via a gene therapy approach, expressing the ribozymes from virally encoded transcription units (Christofferson and Marr, 1995, Thompson, et al., 1995). For example, adenovirus has been shown to be highly efficient at infecting smooth muscle cells in denuded arteries(Guzman, et al., 1993, Lemarchand, et al., 1993). Thus, recombinant adenoviruses could be engineered to express c-*myb* ribozymes, providing an alternative approach to achieving inhibition of cell proliferation during the critical period of smooth muscle cell proliferation after coronary angioplasty.

In addition to restenosis, inappropriate expression of c-*myb* is implicated in neoplastic disorders including colon carcinoma(Melani, et al., 1991), small cell lung carcinoma (Griffin and Baylin, 1985), neuroblastoma (Thiele, et al., 1987), melanoma (Hijiya, et al., 1994), and leukemia (Slamon, et al., 1984). Antisense oligodeoxynucleotides targeting c-*myb* have prolonged survival significantly in a SCID mouse model of human leukemia (Ratajczak, et al., 1992), and have suppressed tumor growth in a SCID mouse model of human melanoma (Hijiya, et al., 1994). Thus we believe that ribozymes that are capable of down-regulating c-*myb* expression have considerable therapeutic potential for the treatment of both cardiovascular disease and cancer.

Materials and methods

Ribozyme synthesis and sequences. Ribozymes were synthesized and purified as described by Wincott *et al.* (Wincott, et al., 1995). The active hammerhead motif used in these experiments consists of seven nucleotide binding arms designed to anneal to the c-*myb* message, and a conserved core required for catalytic activity (see Figure 1). A variety of modifications

were introduced to increase nuclease resistance while retaining catalytic activity (Usman, et al., 1994, Beigelman, et al., 1995)as indicated by the following code: lowercase indicates 2'-*O*-methyl nucleotides, uppercase indicates 2'-hydroxyl (ribo) nucleotide, and *U* indicates 2'-*C*-allyl uridine. Inactive versions have the identical binding arm sequences, but have two mutations in the core that eliminate cleavage activity. Scrambled versions contain the inactive core, and the base composition is maintained, but the sequence order of the arms is mixed to eliminate binding to the target sequence. Cleavage site numbering is based on the human c-*myb* sequence (Genbank accession number X52125).

Site 575 active: 5'-guuuucccU GAuGaggccgaaaggccGaaAuucucc-3'

Site 575 inactive: 5'-guuuucccU uAuGaggccgaaaggccGauAuucucc-3'

Site 575 scrambled: 5'-uuccucucU uAuGaggccgaaaggccGauAcgucuu-3'

Site 549 active: 5'-uuggcaacU GAuGaggccgaaaggccGaaAacagac-3'

Site 549 inactive: 5'-uuggcaacU uAuGaggccgaaaggccGauAacagac-3'

Site 1553 active: 5'-accuuuucU GAuGaggccgaaaggccGaaAuagcug-3'

Site 1553 inactive: 5'-accuuuucU uAuGaggccgaaaggccGauAuagcug-3'

Unless otherwise indicated, backbone linkages are phosphodiester. The ribozymes also contain various end-modifications designed to further increase their resistance to exonucleolytic degradation. Two alternative modifications were used in these studies: 1) five phosphorothioate linkages at each end, or 2) four or five phosphorothioate linkages at the 5'-end together with a 3'-3'-"inverted" deoxythymidine linkage at the 3'-end. Each of these end-protected variants showed virtually identical catalytic activity, stability and cell culture efficacy; they were used interchangably in this study. The catalytic cleavage activity of all of the active ribozymes was verified on a matched short substrate by standard methods; inactive ribozymes did not exhibit any detectable cleavage activity under these conditions (unpublished data).

Antisense oligodeoxynucleotides. Phosphorothioate oligodeoxynucleotides were were obtained from Midland Certified Reagent Co. They were designed to anneal to c-*myb* RNA from nucleotide 568 to 582 (15-mer) or from nucleotide 563 to 587 (25-mer).

Antisense 15-mer: 5'-GCTTTCCAATTCTCC

Scrambled 15-mer: 5'-TTCTACACGTCCCTT

Antisense 25-mer: 5'-ACACTGCTTTCCAATTCTCCCTTTT

Scrambled 25-mer: 5'-TTACTCTTCTCGCCCTATATCTCTA

Cell culture. Rat aortic smooth muscle cells (RASMC) were isolated from aortic tissue explants from 69-84 day-old female Sprague-Dawley rats (Harlan Sprague Dawley, Inc.) and assayed through passage six. Porcine aortic smooth muscle cells (PAS) were isolated from aortic tissue explants from adult pigs and assayed through passage ten. RASMC and PAS were grown in Dulbecco's modified Eagle's medium (DMEM) supplemented with non-essential amino acids (0.1 mM of each amino acid), 0.1 mM sodium pyruvate, 100 U/ml penicillin, 100 µg/ml streptomycin, 2 mM L-glutamine, 20 mM Hepes (all from BioWhittaker) and 10% fetal bovine serum (FBS) (Hyclone Laboratories, Inc.). Human aortic smooth muscle cells (AOSMC) were obtained from Clonetics, and grown in SmGM (Clonetics) supplemented with 20 mM Hepes and 2 mM L-glutamine. AOSMC were assayed through passage eight.

Proliferation Assay. Cells were plated in growth medium in 24-well plates at $5x10^3$ cells per well for RASMC and $1x10^4$ cells per well for AOSMC and PAS. After 24 hours, the medium was removed, cells were washed once with Dulbecco's phosphate buffered saline (DPBS) with Ca^{2+}/Mg^{2+}, and refed with starvation medium. Starvation medium is the same as growth medium except the concentration of FBS was reduced to 0.5% FBS for RASMC and AOSMC, and 0.1% FBS for PAS. Cells were starved for 48-72 hours before ribozyme treatment. Ribozymes were diluted in serum-free DMEM with additives as above excluding antibiotics. LipofectAMINE (Gibco-BRL) was added to a final concentration of 3.6 µM DOSPA (= 7.2 µg/ml LipofectAMINE). Lipid/ribozyme mixtures were vortexed, incubated for 15 minutes at

37C and then added to cells which had been washed twice with DPBS with Ca^{2+}/Mg^{2+}. Cells were incubated with the lipid/ribozyme complexes at 37C for 2-4 hours, complexes were aspirated and cells were stimulated by the addition of growth medium. Control wells were treated with lipid only and stimulated with growth medium containing either 10% FBS or 0% FBS. All conditions were run in duplicate. At the time of stimulation, 5-bromo-2'-deoxyuridine (BrdU) (Sigma) was added at a final concentration of 10 μM. Cells were incubated for 20-24 hours, at which point the cells were fixed by the addition of cold 100% MeOH plus 0.3% hydrogen peroxide for 30 minutes at 4C. The following reagents were used at room temperature to stain the BrdU containing nuclei, with two DPBS washes between each step. 1) 2 M HCl for 20 minutes. 2) 1% horse serum in DPBS for 30 minutes. 3) anti-BrdU monoclonal antibody (Bectin-Dickinson) diluted 1:200 in DPBS with 1% BSA and 0.5% Tween 20 for 1 hour. 4) biotinylated horse anti-mouse IgG in DPBS for 30 minutes. 5) ABC reagent (Pierce mouse IgG kit) in DPBS for 40 minutes. 6) DAB substrate (Pierce) DAB buffer for 7 minutes. 7) hematoxylin (Fisher) diluted 1:1 with distilled water for 1 minute. A minimum of 400 cells per well were counted under the microscope and the percent of proliferating cells (BrdU-stained nuclei/total nuclei) was determined. Error bars represent the range of duplicate wells.

Detection of c-*myb* RNA by QC-PCR. The quantitative competitive polymerase chain reaction (QC-PCR) method was performed as described (Beaudry & McSwiggen, 1996). The competitor RNA for c-*myb* was derived from a fragment of rat c-*myb* cDNA covering bases 428 to 753, and containing a deletion of 50 bases from nucleotides 550 to 599. The GAPDH competitor was derived from Ambion plasmid pTRI-GAPDH and also contained a deletion of 50 bases from nucleotides 250 to 299. For RT/PCR 1, the primers were: (i) c-*myb* , R441F 5'-TGGCAGAAAGT(G/A)CT(G/A)AACCCT-3' and R734R 5'-TCCAGTGGTTCTTGATAGCA-3', (ii) GAPDH, Gs123R 5'-CAGCCCCACGGCCATCA-3' and Gs408F 5'-TCACCACCATGGAGAAGGC-3'. For PCR 2, the primers were: (i) c-*myb* , 5'-AACCCTGAACTCATCAAAGG-3' and R720R 5'-ATAGCATTATCAGTCCGTCC-3', (ii) GAPDH, Gs380F, 5'-ACCTGAAGGGTGGGGCCAAA-3' and Gs136R 5'-

CATCACGCCACAGCTTTCC-3'. Primer annealing was at 50°C. The concentration of c-*myb* and GAPDH RNAs in each sample were determined as described (Beaudry & McSwiggen, 1996) from a plot of the percent competitor in the PCR products *versus* the amount of input competitor RNA. All values were reported as a ratio of c-*myb* RNA to GAPDH RNA from the same sample to normalize for the efficiency of RNA isolation, RNA integrity, and PCR amplification efficiency. Each data set contained controls for the following: competitor alone, wild-type alone, negative controls for each step (RT, PCR 1, PCR 2), and "no reverse transcriptase" reactions for each unknown to control for contamination of the starting sample.

Acknowledgements

We dedicate this paper to the memory of Dr. Richard Majack and his work on smooth muscle cell development and differentiation. We gratefully acknowledge Dr. Majack and Dr. James Belknap for their many helpful discussions and experimental protocols. We would also like to thank Carolyn Gonzales for testing all of the ribozymes used in this study in *in vitro* cleavage assays and Dr. Bharat Chowrira for critical reading of the manuscript.

References

Alitalo K, Winquist R, Linn CC, de la Chapelle A, Schwab M, and Bishop JM. 1984. Aberrant expression of an amplified *c-myb* oncogene in two cell lines from a colon carcinoma. Proc. Natl. Acad. Sci USA. 81:4534-4538.

Austin GE, Ratliff NB, Hollman J, Tabei S, and Phillips DF. 1985. Intimal proliferation of smooth muscle cells as an explanation for recurrent coronary artery stenosis after percutaneous transluminal coronary angioplasty. J. Am. Coll. Cardiol. 6:369-375.

Beigelman L, McSwiggen J, Draper K, Gonzalez C, Jensen K, Karpeisky A, Modak A, Matulic-Adamic J, DiRenzo A, Haeberli P, Sweedler D, Tracz D, Grimm S, Wincott F, Thackray V, and Usman N. 1995. Chemical modification of ribozymes: catalytic activity and nuclease resistance. J. Biol. Chem. 270:25702-25708.

Biro S, Fu YM, Yu ZX, and Epstein SE. 1993. Inhibitory effects of antisense oligodeoxynucleotides targeting c-myc mRNA on smooth muscle cell proliferation and migration. Proc Natl Acad Sci U S A. 90:654-8.

Brown KE, Kindy MS, and Sonenshein GE. 1992. Expression of the c-*myb* proto-oncogene in bovine vascular smooth muscle cells. J. Biol. Chem. 267:4625-4630.

Burgess T, Fisher E, Ross S, Bready J, Qian Y-X, Bayewitch L, Cohen A, Herrara C, Hu S, Kramer T, Lott F, Martin F, Pierce G, Simonet L, and Farrell C. 1995. The antiproliferative activity of c-myb and c-myc antisense oligonucleotides in smooth muscle cells is caused by a nonantisense mechanism. Proc Natl Acad Sci USA. 92:4051-4055.

Cech TR. 1992. Ribozyme engineering. Curr. Opinion in Struct. Biol. 2:605-609.

Chang M, Barr E, Seltzer J, Jiang Y-Q, Nabel G, Nabel E, Parmacek M, and Leiden J. 1995. Cytostatic gene therapy for vascular proliferative disorders with a constituively active form of the retinoblastoma gene product. Science. 267:518-522.

Christofferson R, and Marr J. 1995. Ribozymes as human therapeutic agents. J Med Chem. 38:2023-2037.

Clarke FF, Kukowska-Latallo JF, Westin E, Smith M, and Prochownik EU. 1988. Constitutive expression of a *c-myb* cDNA blocks Friend murine erythroleukemia cell differentiation. Mol. Cell. Biol. 8:884-892.

Epstein SE, E. S, and T. F. 1993. Do antisense approaches to the problem of restenosis make sense? Circulation. 88:1351-1353.

Forrester JS, Fishbein M, Helfant R, and Fagin J. 1991. A paradigm for restenosis based on cell biology: clues for the development of new preventive therapies. J Am Coll Cardiol. 17:758-69.

Garratt KN, Edwards WD, Kaufmann UP, Vlietstra RE, and Holmes DRJ. 1991. Differential histopathology of primary atherosclerotic and restenotic lesions in coronary arteries and saphenous vein bypass grafts: analysis of tissue obtained from 73 patients by directional atherectomy. J. Am Coll. Cardio. 17:442-428.

Griffin CA, and Baylin SB. 1985. Expression of the *c-myb* oncogene in human small lung carcinoma. Cancer Res. 45:272-275.

Guzman LA, Garrel CL, Poptic EJ, DiCorleto PE, and Topol EJ. 1994. Despite in vivo cellular and nuclear uptake, antisense oligonucleotides do not have a significant anti-proliferative effect after vascular injury. Circulation. 90:I-47.

Guzman RJ, Lemarchand P, Crystal RG, Epstein SE, and Finkel T. 1993. Efficient and selective adenovirus-mediated gene transfer into vascular neointima. Circulation. 88:2838-48.

Hertel KJ, Pardi A, Uhlenbeck OC, Koizumi M, Ohtsuka E, Uesugi S, Cedergren R, Eckstein F, Gerlach WL, Hodgson R, and et a. 1992. Numbering system for the hammerhead. Nucleic Acids Res. 20:3252.

Hijiya N, Zhang J, Ratajczak M, Kant J, DeRiel K, Herlyn M, Zon G, and Gerwirtz A. 1994. Biologic and therapeutic significance of MYB expression in human melanoma. Proc Natl Acad Sci USA. 91:4499-4503.

Jackson C, and Schwartz S. 1992. Pharmacology of smooth muscle cell replication. Hypertension. 20:713-736.

Janssen JWG, Vernole P, de Boer PAJ, Oosterhuis JW, and Collard JG. 1986. Sublocalization of c-*myb* to 6q21-q23 by *in situ* hybridization and c-*myb* expresion in human teratocarcinoma with 6q rearrangements. Cytogenet. Cell Genet. 41:129-135.

Kiehntopf M, Brach MA, Licht T, Petschauer S, Karawajew L, Kirschning C, and Herrmann F. 1994. Ribozyme-mediated cleavage of the MDR-1 transcript restores chemosensitivity in previously resistant cancer cells. EMBO J. 13:4645-4652.

Kindy MS, and Sonenshein GE. 1986. Regulation of oncogene expression in cultured aortic smooth muscle cells. J. Biol. Chem. 261:12865-12868.

Koizumi M, Iwai S, and Ohtsuka E. 1988. Construction of a series of several self-cleaving RNA duplexes using synthetic 21-mers. FEBS Letters. 2:228-230.

Landau C, Lange RA, and Hillis LD. 1994. Percutaneous transluminal coronary angioplasty. N Engl J Med. 330:981-93.

Lange W, Cantin EM, Finke J, and Dolken G. 1993. In vitro and in vivo effects of synthetic ribozymes targeted against bcr/abl mRNA. Leukemia. 7:1786-1794.

Lemarchand P, Jones M, Yamada I, and Crystal RG. 1993. In vivo gene transfer and expression in normal uninjured blood vessels using replication-deficient recombinant adenovirus vectors. Circ Res. 72:1132-8.

Leopold LH, Shore SK, Newkirk TA, Reddy RMV, and Reddy EP. 1995. Multi-unit ribozyme-mediated cleavage of *bcr-abl* mRNA in myeloid leukemias. Blood. 85:2162-2170.

Libby P, Schwartz D, Brogi E, Tanaka H, and Clinton S. 1992. A cascade model for restenosis. Circulation. 86[suppl III]:III-47-III-52.

Lincoff AM, Topol EJ, and Ellis SG. 1994. Local drug delivery for the prevention of restenosis: Fact, fancy, and future. Circulation. 90:2070-2084.

Majello B, Kenyon LC, and Dalla-Favera R. 1986. Human c-*myb* protooncogene: Nucleotide sequence of cDNA and organization of the genomic locus. Proc. Natl. Acad. Sci. USA. 83:9636-9640.

Mann MJ, Gibbons GH, Kernoff RS, Diet FP, Tsao PS, Cooke JP, Kaneda Y, and Dzau VJ. 1995. Genetic engineering of vein grafts resistant to atherosclerosis. Proc. Natl. Acad. Sci. USA. 92:4502-4506.

Melani C, Rivoltini L, Parmiani G, Calabretta B, and Colombo MP. 1991. Inhibition of proliferation by *c-myb* antisense oligodeoxynucleotides in colon adenocarcinoma cell lines that express *c-myb*. Cancer Res. 51:2897-2901.

Morishita R, H. GG, Ellison KE, Nakajima M, Zhang L, Kaneda Y, Ogihara T, and Dzau VJ. 1993. Single intraluminal delivery of antisense cdc2 kinase and proliferating-cell nuclear antigen oligonucleotides results in chronic inhibition of neointimal hyperplasia. Proc. Natl. Acad. Sci. USA. 90:8474-8478.

Mucenski ML, McLain K, Kier AB, Swerdlow SH, Schreiner CM, Miller RA, Pietryga DW, Scott SJJ, and Potter SS. 1991. A functional *c-myb* gene is required for normal murine fetal hepatic hematopoiesis. Cell. 65:677-689.

Pieken WA, Olsen DB, Benseler F, Aurup H, and Eckstein F. 1991. Kinetic characterization of ribonuclease-resistant 2'-modified hammerhead ribozymes. Science. 253:314-7.

Popma JJ, CAliff RM, and Topop EJ. 1991. Clinical trials of restenosis after coronary angioplasty. Circulation. 84:1426-1436.

Ratajczak F, Kant JA, Lufer SM, Hijita N, Zhang J, Zon G, and Gewirtz AM. 1992. *In vivo* treatment of human leukemia in a *scid* mouse model with c-myb antisense oligodeoxynucleotides. Proc. Natl. Acad. Sci. USA. 89:11823-11827.

Riessen R, and Isner JM. 1994. Prospects for site-specific delivery of pharmacologic and molecular therapies. JACC. 23:1234-44.

Rufner ED, Stormo GD, and Uhlenbeck OC. 1990. Sequence requirements of the hammerhead RNA self-cleavage reaction. Biochemistry. 29:10695-10702.

Sakura H, Kanei-Ishii C, Nagase T, Nakagoshi H, Gonda TJ, and Ishii S. 1989. Delineation of three functional domains of the transcriptional activator encoded by the c-*myb* proto-oncogene. Proc. Natl. Acad. Sci. USA. 86:5758-5762.

Shi Y, Hutchinson HG, Hall DJ, and Zalewski A. 1993. Downregulation of c-myc expression by antisense oligonucleotides inhibits proliferation of human smooth muscle cells [see comments]. Circulation. 88:1190-5.

Shimayama T, Nishikawa F, Nishikawa S, and Taira K. 1993. Nuclease-resistant chimeric ribozymes containing deoxyribonucleotides and phosphorothioate linkages. Nucl Acids Res. 21:2605-2611.

Simons M, Edelman E, and Rosenburg R. 1994. Antisense proliferating cell nuclear antigen oligonucleotides inhibit intimal hyperplasia in a rat carotid artery injury model. J Clin Invest. 93:2351-2356.

Simons M, Edelman ER, DeKeyser J-L, Langer R, and Rosenberg RD. 1992. Antisense c-*myb* oligonucleotides inhibit intimal arterial smooth muscle cell accumulation *in vivo*. Nature. 359:67-70.

Simons M, and Rosenberg RD. 1992. Antisense nonmuscle myosin heavy chain and c-myb Oligonucleotides suppress smooth muscle cell proliferation in vitro. Circ. Research. 70:835-843.

Sioud M. 1994. Interaction between tumour necrosis factor alpha ribozyme and cellular proteins. J. Mol. Biol. 242:619-629.

Sioud M, Natvig JB, and Forre O. 1992. Preformed ribozyme destroys tumour necrosis factor mRNA in human cells. J Mol Biol. 223:831-5.

Slamon DS, deKernion JB, Verma IM, and Cline MS. 1984. Expression of cellular oncogenes in human malignancies. Science. 224:256-261.

Snyder DS, Wu Y, Wang JL, Rossi JJ, Swiderski P, Kaplan BE, and Forman SJ. 1993. Ribozyme-mediated inhibition of bcr-abl gene expression in a Philadelphia chromosome-positive cell line. Blood. 82:600-605.

Symons RH. 1994. Ribozymes. Current Biology. 4:322-330.

Tanikawa J, Yasukawa T, Enari M, Ogata K, Nishimura Y, Ishi S, and Sarai A. 1993. Recognition of specific DNA sequences by the c-*myb* protooncogene product: Role of three repeat units in the DNA-binding domain. Proc. Natl. Acad. Sci. USA. 90:9320-9324.

Taylor NR, Kaplan BE, Swiderski P, Li H, and Rossi JJ. 1992. Chimeric DNA-RNA hammerhead ribozymes have enhanced in vitro catalytic efficiency and increased stability in vivo. Nucl Acids Res. 20:4559-4565.

Thiele CJ, Cohen PS, and Israel MA. 1987. Differential protooncogene expression characterizes histopathologically indistinguishable tumors of the peripheral nervous system. J. Clin. Invest. 80:804-811.

Thiele CJ, Cohen PS, and Israel MA. 1988. Regulation of *c-myb* expressin in human neuroblastoma cells during retinoic acid-induced differentiation. Mol. Cell. Biol. 8:1677-1683.

Thompson J, Brodsky I, and Yunis J. 1992. Molecular quantification of residual disease in chronic myelogenous leukemia after bone marrow transplantation. Blood. 79:1629-1635.

Thompson JD, Macejak D, Couture L, and Stinchcomb DT. 1995. Ribozymes in gene therapy. Nature Medicine. 1:277-278.

Usman N, Beigelman L, Draper K, Gonzalez C, Jensen K, Karpeisky A, Modak A, Matulic-Adamic J, DiRenzo A, Haeberli P, Tracz D, Grimm S, Wincott F, and McSwiggen J. 1994. Chemical modification of hammerhead ribozymes: activity and nuclease resistance. Nucl Acids Symp Series. 31:163-164.

Weston K, and Bishop JM. 1989. Transcriptional activation by the v-*myb* oncogene and its cellular progenitor, c-*myb*. Cell. 58:85-93.

Wincott F, DiRenzo A, Shaffer C, Grimm S, Tracz D, Workman C, Sweedler D, Gonzalez C, Scaringe S, and Usman N. 1995. Synthesis, deprotection, analysis and purification of RNA and ribozymes. Nucl Acids Res. 23:2677-2689.

Legends to figures

Figure 1

Structure of synthetic hammerhead ribozymes used in this study. The consensus sequence for RNA cleavage is U followed by either A, C or G (denoted H). Position 4 contains 2'-*C*-allyl U, a modification that has been shown to increase resistance to endonucleases while retaining significant catalytic activity. The numbering system is based on Hertel *et al.* (Hertel, et al., 1992).

Figure 2

RASMC were treated with 50 nM ribozyme targeting c-*myb* site 575. Ribozymes were complexed with LipofectAMINE as described in Methods. The black arrow indicates a BrdU-positive nucleus that has undergone DNA replication during the assay period. The white arrow indicates a BrdU-negative nucleus. Quantitation of the percentage of BrdU-positive nuclei gave results as follows: Panel A, FBS control, 70 ± 3 % proliferation; Panel B, unstimulated control, 9.5 ± 1.5 % proliferation; Panel C, active ribozyme, 22.5 ± 2.5 % proliferation; Panel D, inactive ribozyme, 68.5 ± 6.5 % proliferation. The ribozymes in this experiment contained five phosphorothioate linkages at the 5'-end and inverted deoxythymidine at the 3'-end.

Figure 3

Active and inactive versions of ribozymes targeting three different sites in c-*myb* were complexed with LipofectAMINE as described in Methods and delivered to rat aortic smooth muscle cells at a 50 nM dose. These ribozymes contained five phosphorothioate linkages at both the 5' and 3'-ends.

Figure 4

The site 575 ribozyme used in Figure 2 was delivered at various doses to rat aortic smooth muscle cells. Percent proliferation relative to the serum-stimulated control is calculated as follows: (%proliferation with ribozyme - %basal proliferation) ÷ (%proliferation with serum - %basal proliferation) * 100. Basal proliferation refers to proliferation in the absence of serum (usually between 5 and 15%).

Figure 5

RASMC were treated with 100 nM of either active or inactive site 575 ribozyme complexed with LipofectAMINE. The ribozymes contained four phosphorothioate linkages at the 5'-end and inverted deoxythymidine at the 3'-end. Cells were stimulated with serum and incubated for 12 hours. Cells were then washed once with DPBS, and the RNA was isolated and analyzed as described in Methods. Parallel cultures were treated identically and assayed for proliferation using the BrdU assay protocol.

Figure 6

Active, inactive and scrambled versions of the site 575 ribozyme were complexed with LipofectAMINE and delivered at 100 nM to rat aortic smooth muscle cells, porcine aortic smooth muscle cells, and at 200 nM to human aortic smooth muscle cells. The ribozymes contained four phosphorothioate linkages at the 5'-end and inverted deoxythymidine at the 3'-end. Proliferation is expressed as a percentage of the serum-stimulated control, as described in Figure 4.

Table I

Comparison of ribozymes and antisense oligodeoxynucleotides targeting c-*myb*

Oligonucleotide treatment of RASMC[a]	% proliferation 100 nM dose	% proliferation 50 nM dose
Active ribozyme	14.5 ± 1.5	17 ± 8
Inactive ribozyme	62 ± 1	65 ± 1
Scrambled ribozyme	58 ± 2	57 ±3
Antisense 15-mer	27 ± .5	37 ± 5
Scrambled 15-mer	42.5 ± 3.5	70 ± 11
Antisense 25-mer	31.5 ± 3.5	44.5 ± 3.5
Scrambled 25-mer	30 ± 4	44.5 ± 7.5

[a] Active, inactive and scrambled-arm inactive versions of the site 575 ribozyme were complexed with LipofectAMINE and delivered to rat aortic smooth muscle cells at either 100 nM or 50 nM. These ribozymes contained five phosphorothioate linkages at both the 5' and 3'-ends. Fully phosphorothioate 15-mer and 25-mer oligodeoxynucleotides that were either complementary to c-*myb* at the 575 site (antisense), or contained the same sequence composition in scrambled order (scrambled) were complexed with LipofectAMINE in the same manner and delivered at either 100 nM or 50 nM. Control levels were 88 ± 1% proliferation for the serum stimulated cells and 8 ± 0.5% proliferation for the unstimulated cells.

Figur 1

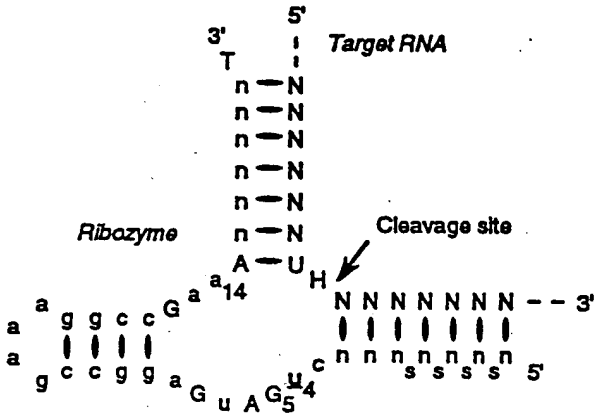

Lower case = 2'-*O*-methyl nucleotides
Upper case = Ribonucleotides
u = 2'-*C*-allyl nucleotide
s = Phosphorothioate linkages
T = 3'-3' inverted thymidine

Inactive version: G5 -> u5 and a14 -> u14

Fig. 2.

A. 10% FBS

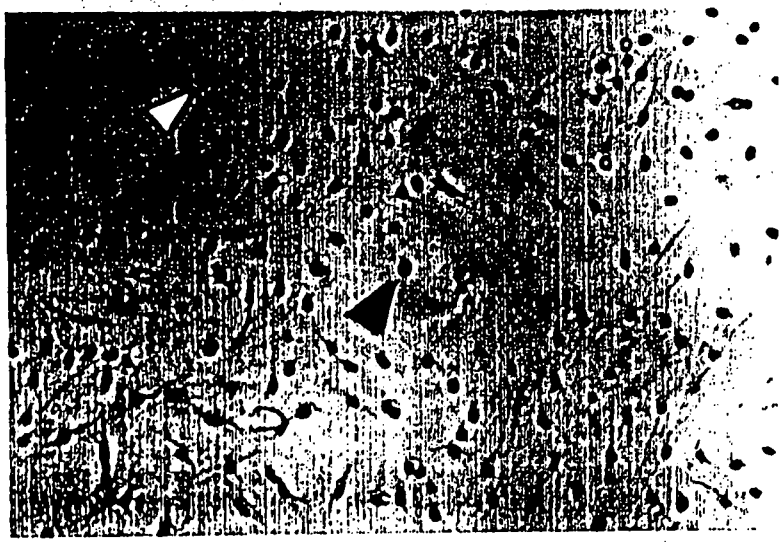

B. 0% FBS

C. Active Ribozyme

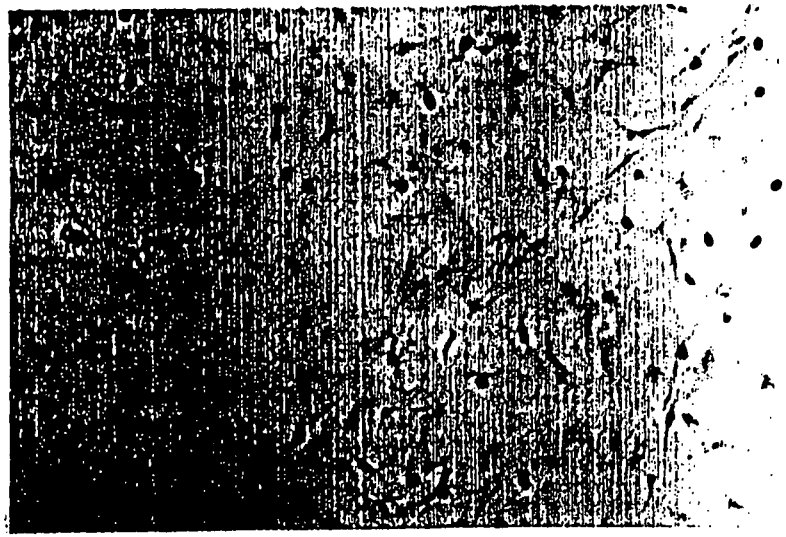

D. Inactive Ribozyme

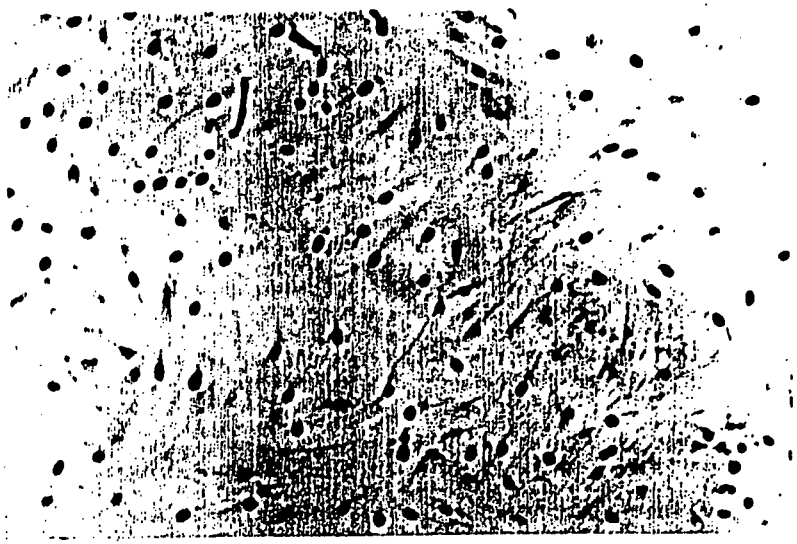

Figure 3

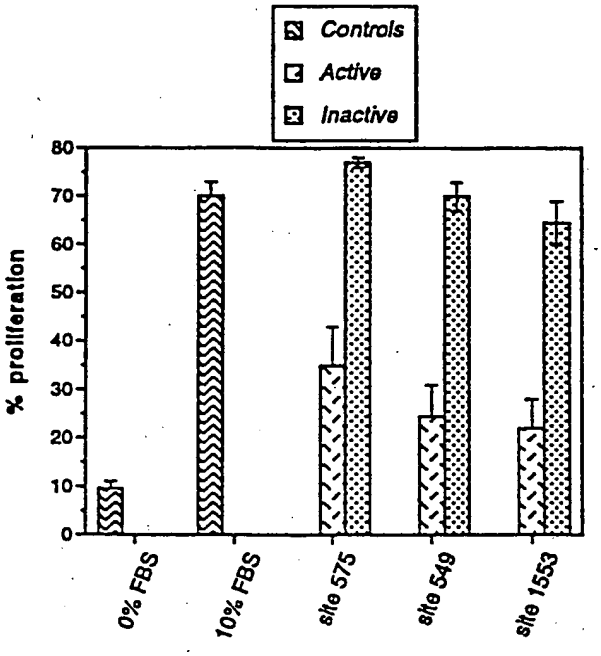
Controls
Active
Inactive
% proliferation
80
70
60
50
40
30
20
10
0
0% FBS
10% FBS
site 575
site 549
site 1553

Figur 4

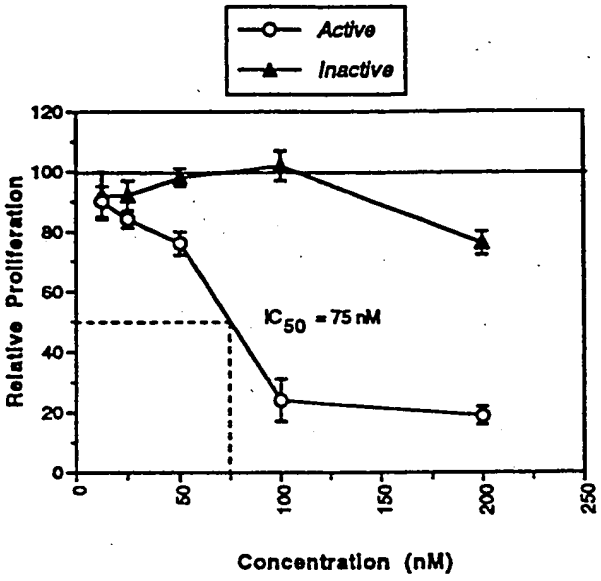
Active
Inactive
120
100
80
60
40
20
0
Relative Proliferation
IC50 = 75 nM
0
50
100
150
200
250
Concentration (nM)

Figure 5

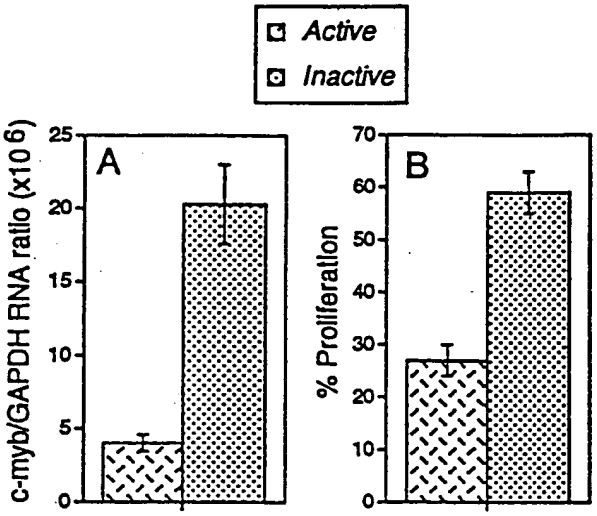
Active
Inactive
A
B
c-myb/GAPDH RNA ratio (x10 6)
% Proliferation
0
5
10
15
20
25
30
40
50
60
70

Figure 6

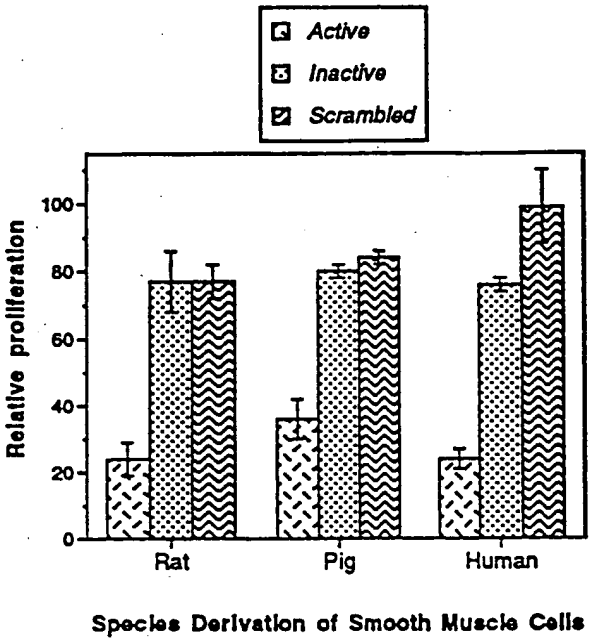
Active
Inactive
Scrambled
Relative proliferation
0
20
40
60
80
100
Rat
Pig
Human
Species Derivation of Smooth Muscle Cells

Exhibit 8

A Synthetic Ribozyme Exhibits Antiviral Activity

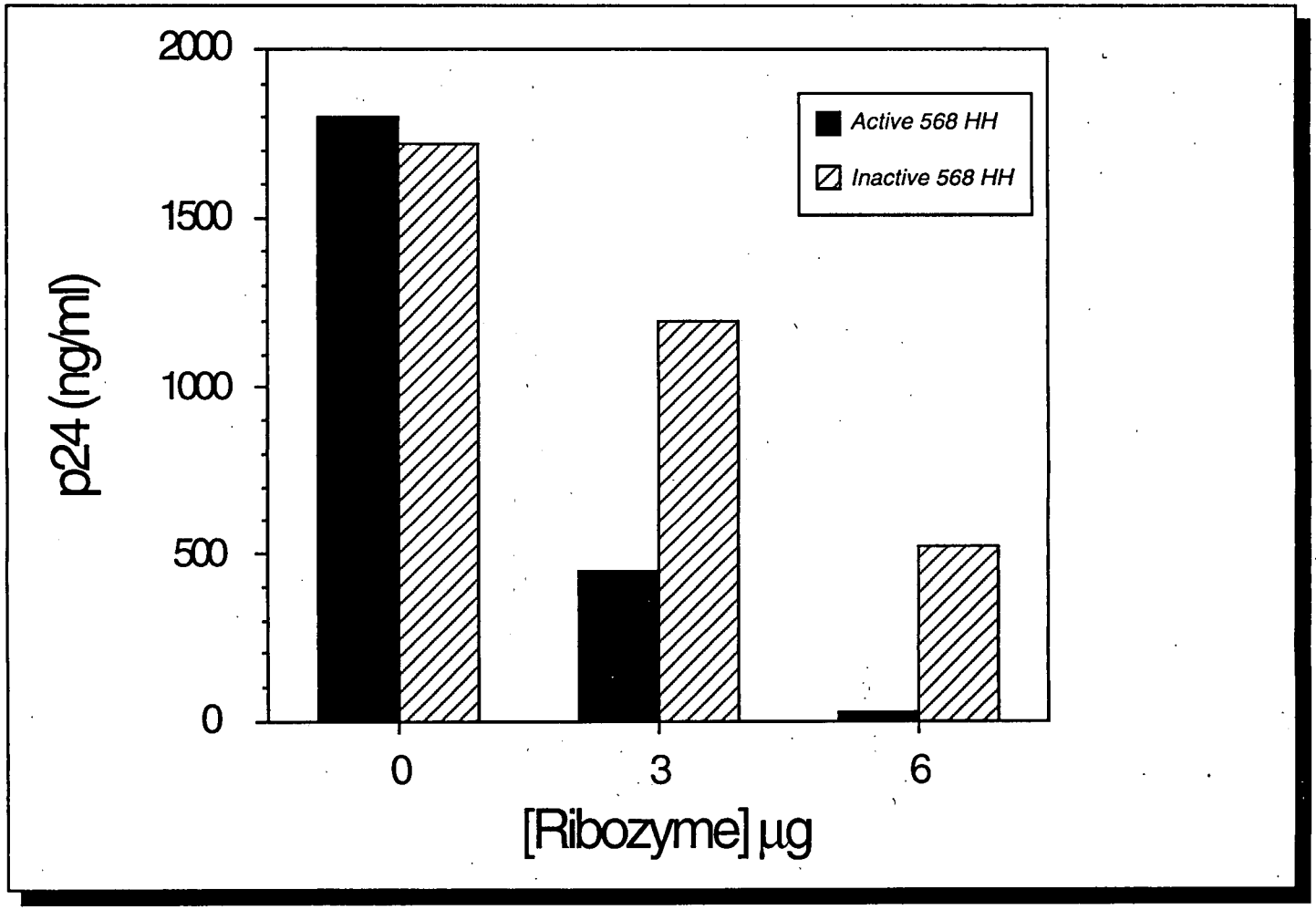

Exhibit 9

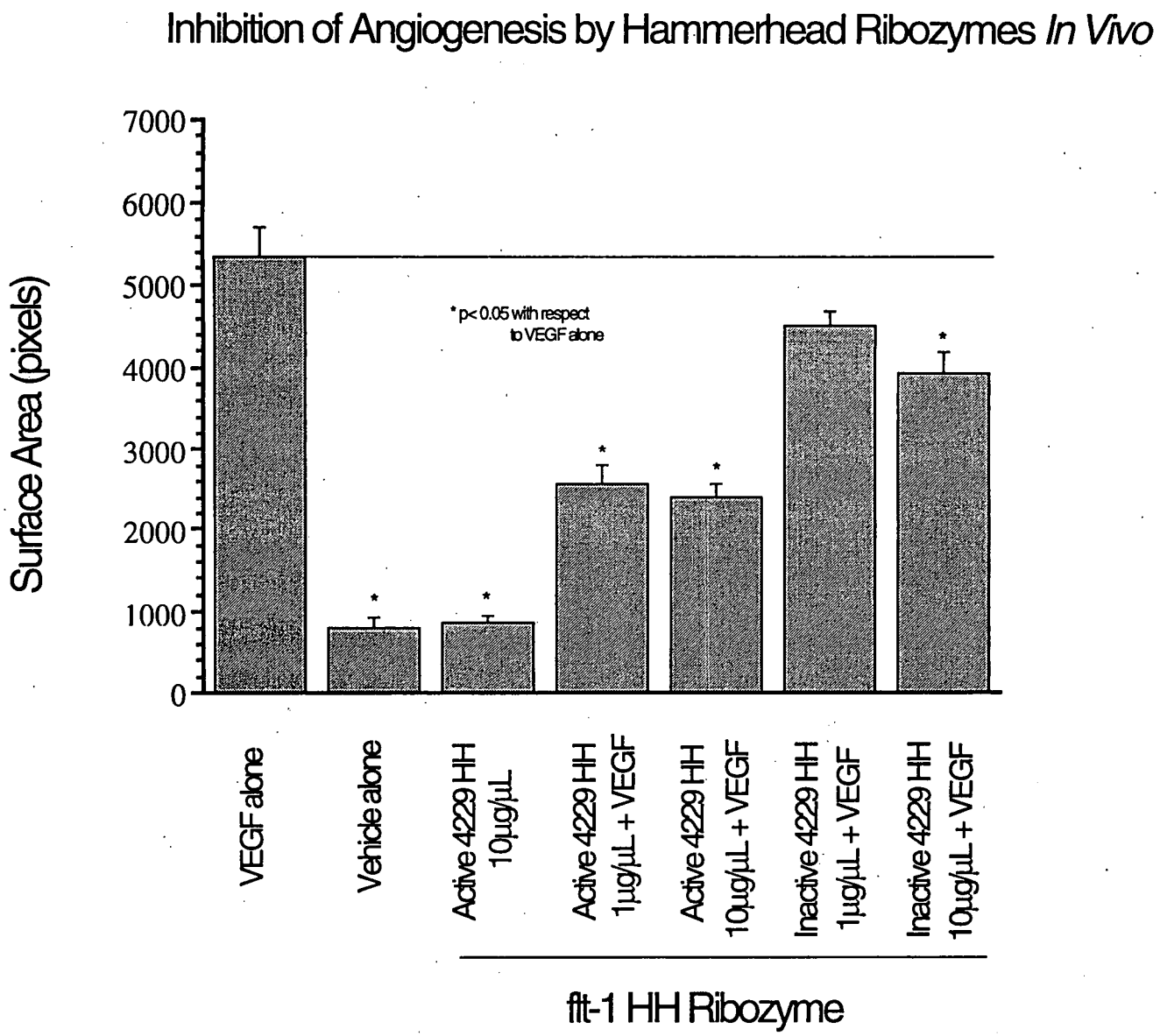
Inhibition of Angiogenesis by Hammerhead Ribozymes *In Vivo*
Surface Area (pixels)
7000
6000
5000
4000
3000
2000
1000
0
* p< 0.05 with respect to VEGF alone
VEGF alone
Vehicle alone
Active 4229 HH 10µg/µL
Active 4229 HH 1µg/µL + VEGF
Active 4229 HH 10µg/µL + VEGF
Inactive 4229 HH 1µg/µL + VEGF
Inactive 4229 HH 10µg/µL + VEGF
flt-1 HH Ribozyme

The EMBO Journal vol.14 no.21 pp.5224–5229, 1995

A synthetic, chemically modified ribozyme eliminates amelogenin, the major translation product in developing mouse enamel *in vivo*

S.P.Lyngstadaas[1,2], S.Risnes[2], B.S.Sproat[3], P.S.Thrane[4] and H.P.Prydz[1,5]

[1]Biotechnology Centre of Oslo and Laboratory Animal Unit, The National Hospital, University of Oslo, PO Box 1125, Blindern, N-0317 Oslo, [2]Department of Oral Biology, Faculty of Dentistry, University of Oslo, PO Box 1052, Blindern, N-0316 Oslo, [4]Department of Pathology, The Norwegian Radium Hospital, Montebello, N-0310 Oslo, Norway and [3]Ribonetics GmbH, Rudolf-Wissel-Strasse 28, D-37079 Göttingen, Germany

[5]Corresponding author

Ribozymes are small RNA structures capable of cleaving RNA target molecules in a catalytic fashion. Designed ribozymes can be targeted to specific mRNAs, blocking their expression without affecting normal functions of other genes. Because of their specific and catalytic mode of action ribozymes are ideal agents for therapeutic interventions against malfunctioning or foreign gene products. Here we report successful experiments to 'knock out' a major translation product *in vivo* using synthesized, chemically modified ribozymes. The ribozymes, designed to cleave amelogenin mRNA, were injected close to developing mandibular molar teeth in newborn mice, resulting in a prolonged and specific arrest of amelogenin synthesis not caused by general toxicity. No carriers were required to assist cellular uptake. Amelogenins are highly conserved tissue-specific proteins that play a central role in mammalian enamel biomineralization. Ultrastructural analyses of *in vivo* ribozyme-treated teeth demonstrated their failure to develop normally mineralized enamel. These results demonstrate that synthesized ribozymes can be highly effective in achieving both timed and localized 'knock-out' of important gene products *in vivo*, and suggest new possibilities for suppression of gene expression for research and therapeutic purposes.

Keywords: 2'-*O*-allylribonucleotides/amelogenin/biomineralization/dental enamel/synthetic hammerhead ribozymes

Introduction

Interference with gene expression at the level of mRNA holds great promise for therapeutic interventions in cases of malfunctioning gene products and infectious diseases. Wagner (1994) recently summarized the available experience of using oligodeoxynucleotides for this purpose and listed the criteria that should be rigorously applied in the evaluation of such experiments. Designed hammerhead ribozymes represent an alternative technology with even greater potential advantages. Hammerhead ribozymes are small RNA structures capable of cleaving an RNA target molecule in a catalytic fashion in the presence of Mg^{2+}(Pyle, 1993). They bear a resemblance to enzymes, and contain a catalytic motif made up of three base paired stems and a core of highly conserved, non-complementary nucleotides essential for catalysis (Cech and Uhlenbeck, 1994). Their three-dimensional (3-D) structure and mode of action have recently been elucidated (Uhlenbeck, 1987; Pley *et al.*, 1994; Tuschl *et al.*, 1994). Hammerhead ribozyme activity can be targeted to specific mRNAs by choosing the sequences flanking the catalytic motif. The two hammerhead ribozymes used here were designed to block expression of amelogenin, the major translation product during mammalian tooth enamel matrix synthesis, in mice. The enamel is a unique tissue due to its hardness, which reflects a high degree of mineralization. The mineral component is mainly hydroxyapatite (HAp) in the form of closely packed ultramicroscopic crystals, larger than those in other mineralized mammalian tissues (bone, dentin and dental cementum). The crystals are organized by differential orientation into a basic pattern of prisms (rods) and interprism (interrod), which is common to all mammals. Amelogenins are the main product of ameloblasts (Termine *et al.*, 1980), the single layered, columnar epithelial cells lining the crown of the tooth anlage (Figure 1), and are expressed only in this organ (Chen *et al.*, 1994). Amelogenins are supposed to play a crucial role in mammalian enamel biomineralization, possibly by forming supramolecular structures that control the HAp crystal growth during enamel formation (Fincham *et al.*, 1994). The primary structure of amelogenin derived from cow, pig, rat, mouse and human demonstrates a high degree of sequence homology between these species (Brooks *et al.*, 1994).

The murine amelogenin gene (AMEL) is located distally

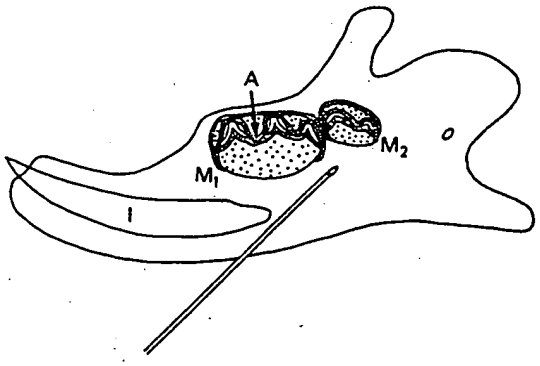

Fig. 1. Lingual view of right mandible of a newborn mouse showing incisor (I) and first (M_1) and second (M_2) molar tooth germs. M_1 where enamel formation has started, and M_2 where enamel formation is about to start (Cohn, 1957; Gaunt, 1964) (M_1 and M_2 depicted as if sectioned). From the tip of the cusps the ameloblasts (A) differentiate in the cervical direction to produce and mature enamel (Sasaki *et al.*, 1990). Needle position during injection is indicated.

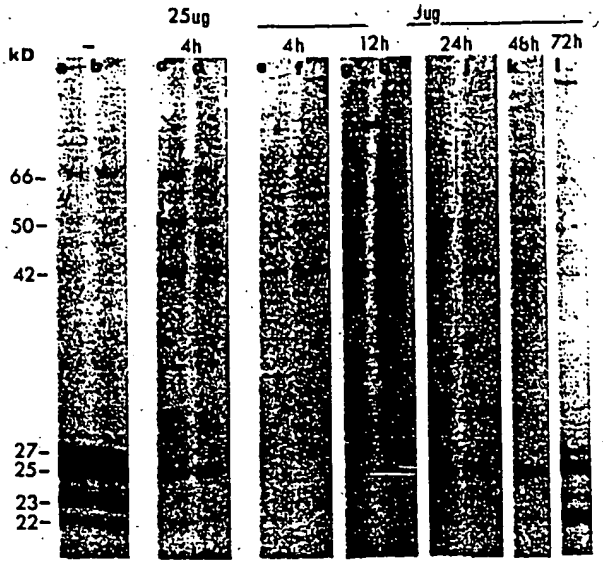

Fig. 2. Autoradiograph of [^{35}S]methionine labelled proteins from normal and ribozyme-treated first molar tooth buds from mandible of newborn mice. Lanes a and b contain proteins from tooth buds of untreated mice. Lanes c and d contain proteins from tooth buds isolated 4 h after injection of 25 µg of the AMEL ribozyme. Lanes e–l contain proteins from tooth buds isolated 4, 12, 24, 48 and 72 h after injection of 50 µg of the AMEL ribozyme. Each lane represents proteins from one half of a first molar tooth bud. The 22, 23, 25 and 27 kDa proteins were identified as amelogenins by protein sequencing. The disappearance of amelogenins indicated a total arrest of their synthesis. All other protein bands appeared unaffected by the ribozyme injection and served as internal controls for the specificity of the AMEL hammerhead ribozyme.

(0.73) on the X chromosome (Lau *et al.*, 1989) and its cDNA has been cloned (Snead *et al.*, 1985). The AMEL gene gives rise to four different polypeptides (Figure 2) caused by differential splicing (Lau *et al.*, 1992). Here we report successful *in vivo* experiments with synthetic hammerhead ribozymes, achieving a specific 'restricted knock out' of the AMEL gene. By local injections (Figure 1) of synthetic ribozyme constructions into newborn mice the major translation product of ameloblasts during the initial stage of enamel formation was eliminated. No carriers were required to assist uptake. The ribozyme effect was monitored both by direct measurement of target protein levels and by loss of biological function. A series of controls demonstrates that the blocking of AMEL expression was specific. Our experiments fulfill the criteria listed by Wagner (1994), and is the first reported study that clearly demonstrates the *in vivo* efficacy of synthesized, chemically modified hammerhead ribozymes.

Results

Effect of the AMEL hammerhead ribozymes

N-terminal amino acid sequences of the 22, 23, 25 and 27 kDa protein bands appearing on SDS–PAGE of molar tooth extracts were revealed by Edman degradation and cyanogen bromide cleavage (Hewick *et al.*, 1981). The protein bands were identified as AMEL proteins when compared with previously reported murine amelogenin protein sequences (Fincham *et al.*, 1991) and were in accordance with the cloned murine AMEL cDNA sequence (Snead *et al.*, 198[illegible]e half-life of amelogenins in molars of newborn mice was determined to be ~210 min in initial pulse–chase experiments where cycloheximide (8 µg/g body weight) and cold methionine (200 µg) were given 100 min after labelled methionine. Amelogenins were isolated and their content of [^{35}S]methionine determined after 100, 200, 300 and 400 min.

When compared with untreated siblings, all ribozyme-injected mice showed a marked decrease in the incorporation of radiolabelled methionine into the amelogenin bands of molar tooth extracts from the injected side after 4 h. Doses of 25 µg ribozyme resulted in a nearly 90% decrease of [^{35}S]methionine in the amelogenin bands. At 50 µg per animal a complete arrest of amelogenin synthesis on the side of injection resulted (Figure 2). This complete arrest of AMEL gene expression lasted ~24 h (Figure 3a). After 3 days amelogenin synthesis was still nearly 50% inhibited. It took 90 h to restore its synthesis to the normal level (100%). After 100 h a brief overexpression (120%) of the AMEL gene was observed. Amelogenin synthesis was back to normal before 120 h and then stabilized at this level.

To see what influence the 3′ terminal phosphorothioate protection of the internucleotide linkages had on ribozyme function and stability, an AMEL hammerhead ribozyme not carrying this modification was applied. Except for a slightly higher and longer lasting efficacy and a slightly more rapid breakdown of the unsulfurized ribozyme, the two AMEL hammerhead ribozymes acted similarly (Figure 3b).

Inhibition of amelogenin synthesis was observed in both the first and the second molar on the side of the injection. In the corresponding contralateral molars a reduction of labelled amelogenins of ~25% was observed at 12 h.

The AMEL hammerhead ribozymes had full activity against all AMEL splice products as none of the four amelogenins appeared in the electrophoresis gels from teeth of ribozyme-treated mice (Figure 2). No other proteins in these gels were affected by the ribozyme injections.

Effect of control injections

Three control oligomers were also designed in order to isolate the ribozyme effects from other oligoribonucleotide effects. One control was an inactive version of the above chemically modified ribozymes in which 'G12' in the conserved hammerhead motif (Haseloff and Gerlach, 1988) was replaced by an 'A', leading to loss of catalytic activity. The second control was a straight antisense oligo(2′-*O*-allylribonucleotide) designed against the same AMEL mRNA region as the ribozymes and applied to distinguish between the ribozyme effect and an ordinary antisense effect. The third control was a randomized oligomer of 18 bases applied for detection of unspecified or toxic actions of the synthetic ribozymes. A fourth control containing only 5 µl sterile saline was included to see whether the injection trauma itself influenced enamel formation.

Injections with the mutated ribozyme gave an immediate inhibition of AMEL expression of >80% (Figure 3c). After 12 h, however, the inhibition was only 40%, and normal levels of amelogenin synthesis were restored within

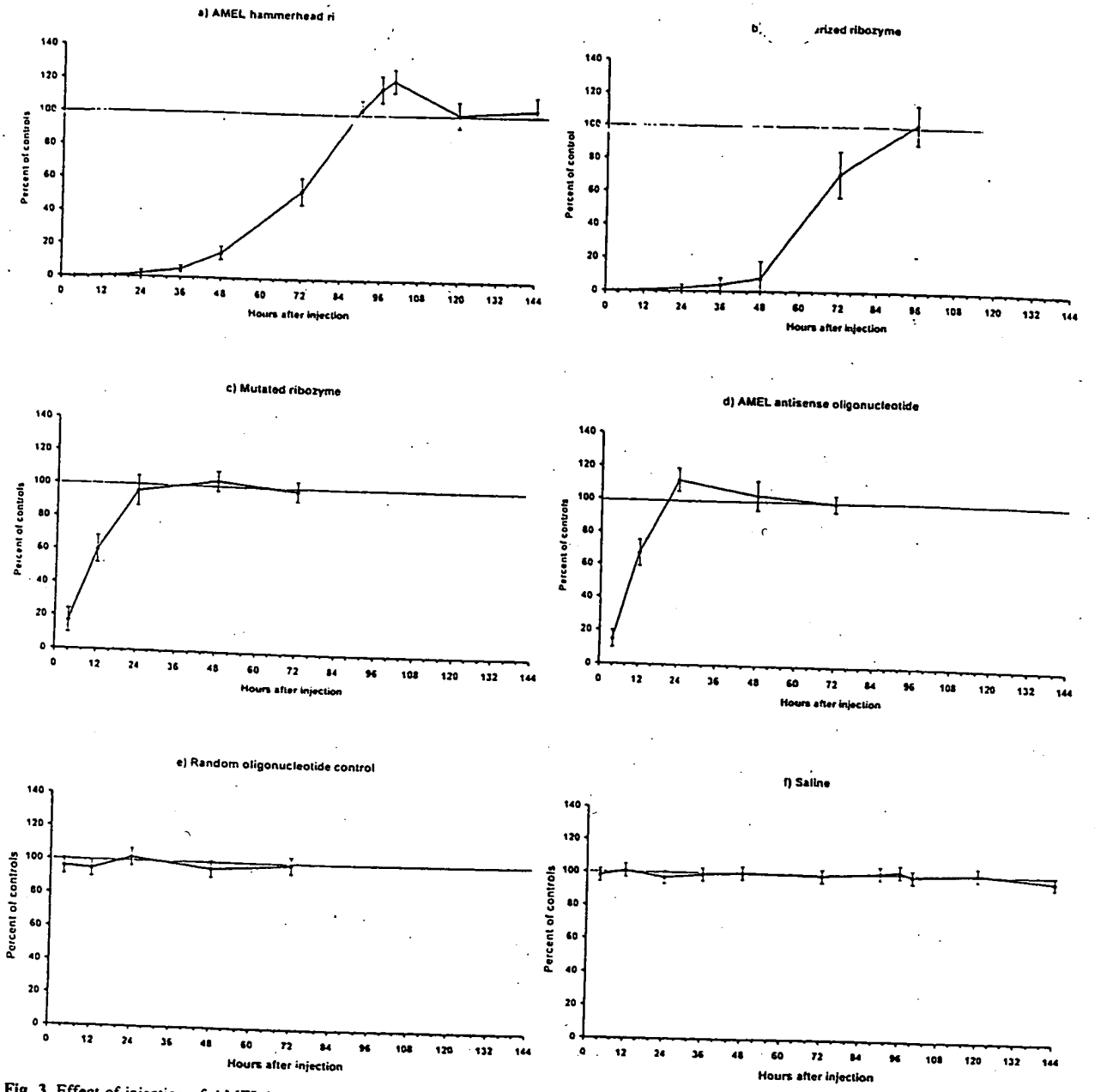

Fig. 3. Effect of injection of AMEL hammerhead ribozymes on [^{35}S]methionine incorporation into amelogenins in newborn mice. Ribozymes and various control oligonucleotides were injected into separate newborn (day 1) mice. Saline injected and untreated litter mates served as controls. The [^{35}S]methionine incorporated into tooth buds was quantitated in a PhosphorImager (Molecular Dynamics). Values are in percent of [^{35}S]methionine incorporated into amelogenins of the corresponding teeth of untreated litter mates, normalized for the size of the available free methionine pool in each tooth bud. These control values are indicated by the 100% line (n = 16 at each time point). (a) AMEL hammerhead ribozyme. Each value is the mean ± SD of four experiments, each with five mice (n = 20). (b) AMEL hammerhead ribozyme without 3′ phosphorothioate protected internucleotide linkages. Each value is the mean ± SD of one experiment with five mice (n = 5). (c) Mutated ribozyme (G12→A). Each value is the mean ± SD of two experiments, each with five mice (n = 10). (d) AMEL antisense oligonucleotide (n = 10). (e) Random oligonucleotide controls (n = 8). (f) Saline controls (n = 8).

24 h. In contrast to earlier *in vitro* experiments with antisense oligo(2′-*O*-allylribonucleotide)s (Johansson *et al.*, 1994), the straight antisense oligoribonucleotide injections produced an effect much like that of the mutated ribozyme, initially inhibiting AMEL expression by 80% (Figure 3d), after 12 h inhibition was only 30%, and normal amelogenin synthesis levels were restored before 24 h. Random oligonucleotide injections or saline injections had essentially no influence on the monitored protein synthesis, and the quantity of incorporated [^{35}S]methionine in these animals did not differ significantly from that of their untreated siblings (Figure 3e and f).

Control injections of 5 µl 0.5% Trypan Blue in saline were used to mark the area of diffusion of the injected fluid. The dye could easily be demonstrated in the mandibular molar tooth buds within 30 min after injection.

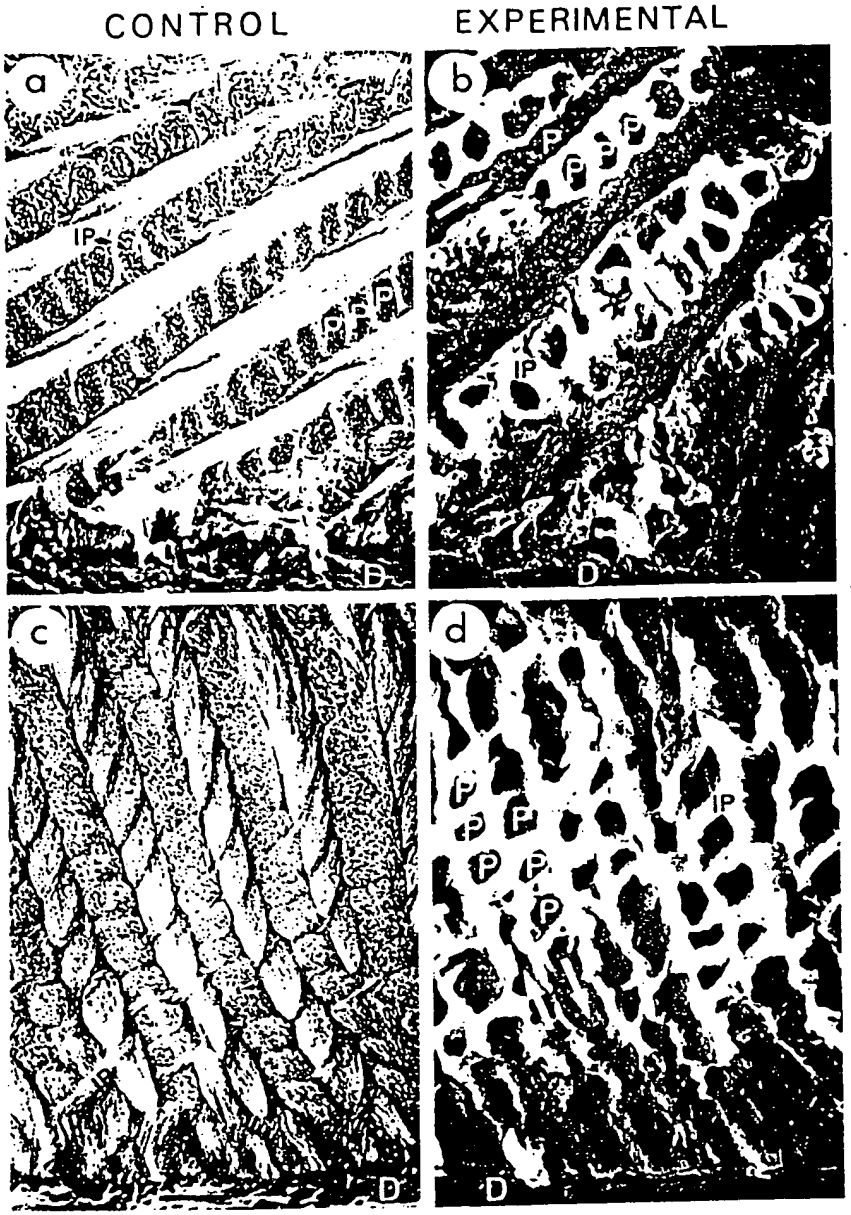

Fig. 4. SEM micrographs of mouse molar inner enamel abutting on dentin (D). (a and c) Normal control enamel with structure similar to rat enamel (Risnes, 1979a,b). (b and d) Corresponding regions of enamel affected by the AMEL hammerhead ribozymes. Prisms (P) of adjacent prism rows are oppositely oriented (unlabelled arrows). The interprism (IP) separates individual prisms. The affected enamel is severely hypomineralized with an accumulation of organic material at the prism periphery–interprism and with no visible HAp crystals within cross-cut prism domains. Magnification bar, 5 μm.

Scanning electron microscopy observations

To look at the effect of the ribozyme on enamel formation, randomly selected mice injected with active ribozyme on day 1 after birth were sacrificed at 5 weeks of age, when their molar teeth were fully developed. Mice injected with the randomized oligonucleotide or saline only and untreated siblings were included as controls. The mandibular molars from these mice were prepared for scanning electron microscopy (SEM) (Risnes, 1985). Molars from ribozyme-treated mice revealed severely disturbed enamel with a pronounced hypomineralization and accumulation of organic material at the prism periphery–interprism, whereas cross-cut prisms appeared as empty holes with no visible HAp crystals present (Figure 4). The general design of the prism pattern and the enamel thickness appeared unaffected. Molars from untreated, saline injected or random oligonucleotide-treated mice showed no such changes. Regions with normal enamel were also observed in teeth from ribozyme-treated animals. Second molars were more severely affected than first molars. No differences were detected in eruption-time or macroscopic tooth morphology between ribozyme-treated, randomized oligonucleotide-treated, saline injected or untreated mice.

Discussion

The AMEL hammerhead ribozyme motif (Haseloff and Gerlach, 1988) was flanked by two AMEL mRNA binding regions (6 and 7 bp, respectively), chosen to optimize the catalytic activity of the ribozyme without losing specificity (Goodchild and Kohli, 1991). Its target was the GUC sequence of the mouse AMEL gene in which the G is at base 86 of the mRNA (Snead *et al.*, 1985). The proposed hammerhead ribozymes were chemically modified (Paolella *et al.*, 1992; Sproat *et al.*, 1994) to contain mostly 2′-*O*-allylribonucleotides and only five ribonucleotides required for catalysis, *viz.* G5, A6, G8, G12 and A15, using the standard numbering system (Hertel *et al.*, 1992), so as to have long term stability *in vivo*. The allylation of U4 is essential to block RNase A attack at this position. In addition, one of the two otherwise identical AMEL hammerhead ribozymes, the mutated ribozyme and the antisense oligoribonucleotide, carried two sulfurized 3′-proximal internucleotide linkages to reduce 3′-exonuclease attack further.

Global 2′-*O*-allylation of oligoribonucleotides confers nuclease resistance, chemical stability, in hybridization high specificity for RNA over DNA and minimal non-specific binding (Iribarren *et al.*, 1990; Lamond and Sproat, 1993), all of which are essential requirements for *in vivo* experiments. Cellular uptake may also be facilitated because of the increased hydrophobicity imparted by 2′-*O*-allylation.

The ribozymes used here totally inhibited expression of the AMEL gene in newborn mice without affecting normal functions of other genes. Apparently, no other proteins were affected by the ribozyme injections (Figure 2), thus constituting a valuable internal control for the specificity of the ribozymes.

The fact that the control dye was detectable in the tooth buds within 30 min, the observed rapid loss of AMEL expression and the fact that amelogenins are produced within ameloblasts only (Chen *et al.*, 1994), provide strong evidence that the modified oligoribonucleotides effectively reach and penetrate these cells, as has been demonstrated for oligodeoxynucleotides when applied to cultured tooth organs (Diekwisch *et al.*, 1993).

The mutated ribozyme and the antisense oligoribonucleotide showed similar effects during the first 12 h. This suggests that the amelogenin-specific hybridizing arms of the mutated ribozyme make it act like an ordinary antisense oligoribonucleotide inhibiting amelogenin synthesis for a short period, possibly by temporary blockage of ribosome progression along mRNA and that the hammerhead motif itself does not affect the specific binding of its flanking regions to amelogenin mRNAs.

Injections containing the randomized oligonucleotide had essentially no influence on AMEL expression (Figure 3d), nor did they produce any structural defects in the mature enamel. This indicates that the observed ribozyme effect was not due to a non-specific or toxic influence of oligonucleotides on AMEL expression. Neither did mice injected with saline show any significant difference from their untreated siblings, indicating that the injections themselves did not affect protein synthesis or function in developing enamel.

The slightly increased efficacy of the ribozyme not protected by 3′ phospl .oate internucleotide linkages might reflect an enhanced cellular uptake of this oligomer. The apparent slightly more rapid cessation of its effect may be due to a more rapid breakdown caused by an increased sensitivity to 3′-exonuclease attack on this ribozyme.

The difference in occurrence of enamel defects among first and second molars reflects the different developmental stages of these teeth at the time of ribozyme injection. The fact that the second molar was more severely affected than the first molar indicates that amelogenin plays a key role at a very early stage in enamel development and may be less important at later stages. Areas with normal enamel formation within each affected tooth represent early (occlusal) and late (cervical) enamel matrix synthesis unaffected by the time-limited ribozyme effect applied here.

Designed hammerhead ribozymes are promising agents for blocking specific gene expression. Chemical modifications enhance their stability, potency and ability to enter cells. As the 3-D structures of the hammerhead motifs are revealed, even more effective ribozymes can be developed. The tooth model lends itself nicely to the study of ribozyme function *in vivo* since the biological consequences of the ribozyme effect are permanently displayed in the mature enamel. We report the first demonstration of *in vivo* efficacy of synthesized, chemically modified ribozymes. Only a few cases of specific gene inhibition caused by antisense oligodeoxynucleotides have been rigorously demonstrated in cultured cells before (Wagner, 1994). Our experiments clearly illustrate the advantages of combining the catalytic activity of a hammerhead motif with the specificity of antisense oligomers in a chemically modified oligoribonucleotide to obtain both enhanced and prolonged specific blocking of gene expression *in vivo*. The strategy used in this model could be highly effective in achieving both timed and localized 'knock-outs' of important gene products *in vivo*, and suggests new possibilities for suppression of gene expression for research and therapeutic purposes.

Materials and methods

Oligoribonucleotide synthesis

The AMEL hammerhead ribozyme (5′-UGUUGACUgaUgAGGCCGUUAGGCCgAAaCAGC*PS*A*PS*C), the unsulfurized ribozyme (5′-UGUUGACUgaUgAGGCCGUUAGGCCgAAaCAGCAC), the mutated ribozyme (5′-UGUUGACUgaUgAGGCCGUUAGGCCaAAaCAGC*P*-*S*A*PS*C), the straight antisense oligo(2′-*O*-allylribonucleotide)(5′-UGUUGAGACAGC*PS*A*PS*C) and the 18mer randomized oligonucleotide (scrambled, unmodified) were synthesized on solid-phase using phosphoramidite chemistry (capital letters are 2′-*O*-allylribonucleotides and lower case letters are ribonucleotides, phosphorothioate protected internucleotide linkages are denoted *PS*, underlined sequences are complementary to the AMEL target sequence). The ribonucleotides carried standard 2′-*O*-*tert*-butyldimethylsilyl protection, which was subsequently removed by treatment of the partially deprotected oligomer with neat triethylamine trihydrofluoride (Gasparutto *et al.*, 1992). The oligonucleotides were purified by HPLC before injection.

Experimental design

Oligoribonucleotides were dissolved in sterile saline to a final concentration of 10 μg/μl each, and 50 μg of each delivered by submandibular injection into live newborn BALB/C (albino) mice without addition of liposomes or other vehicles to enhance cellular uptake. On the first day after birth each animal received an injection of ribozyme or control oligonucleotides on the lingual side of the right mandibular molar area. Other controls received 5 μl saline. A reference group of untreated

siblings of the experimental animals was included to monitor the normal AMEL expression in these mice.

Injections of 5 µl 0.5% Trypan Blue in saline were used to mark the area of diffusion. All injections were carried out using a Hamilton syringe with a 0.3 mm needle at the rate of ~1 µl/s. At 0, 8, 20, 32, 44, 68, 86, 92, 96, 116 or 140 h after the mandibular injections experimental animals and a reference group received a 4 h pulse of 20 µCi [^{35}S]methionine (Amersham) given i.p. The mice were then sacrificed and their mandibular molar tooth buds were dissected out. Each tooth bud was rinsed in sterile saline and boiled in 50 µl 2× SDS–PAGE sample buffer (0.4 g SDS, 1.0 g 2-mercaptoethanol, 0.02 g bromophenol blue and 4.4 g glycerol in 10 ml 0.125 M Tris–HCl, pH 6.8) for 5 min. Half of each sample was then submitted to electrophoresis on 12% SDS–polyacrylamide gels at 80 mA overnight. The gels were dried and placed in a PhosphorImager (Molecular Dynamics) to detect radioactive methionine incorporated into the proteins present. Subsequently, the gels were submitted to ordinary autoradiography for 30 days as a visual control. Proteins in the other half of each sample were precipitated with 0.6 N perchloric acid (PCA) and the supernatant was cleared by centrifugation. The free radiolabelled methionine in the supernatant was measured in a Packard Tricarb Scintillation counter and used to normalize the values from the PhosphorImager so that individual differences in the availability of radiolabelled methionine were adjusted for.

Scanning electron microscopy

Randomly selected mice injected once with the AMEL hammerhead ribozyme on day 1 after birth were sacrificed at 5 weeks of age, when their molar teeth were fully developed and erupted. Mice injected with the randomized 18mer oligonucleotide and with saline only, and untreated siblings were included as controls. The mandibular molars from these mice were dissected out, taking care not to damage enamel structures, and prepared for scanning electron microscopy (SEM) by sectioning and grinding (Risnes, 1985), etching three times for 10 s in 0.1% nitric acid and sputter-coating with gold–palladium. A Phillips 515 SEM was operated at 15 kV.

Protein sequencing

Amelogenin protein bands separated by SDS–PAGE were transferred onto a poly(vinylidene difluoride) membrane by the semi-dry 'sandwich' electroblotting technique (Matsudaira, 1987). The membrane was stained with Coomassie Blue and the four amelogenin bands cut out, separated and submitted to Edman degradation and *in situ* cyanogen bromide cleavage (Hewick *et al.*, 1981).

N-terminal amino acid sequences were analyzed with an Applied Biosystems 477A instrument coupled to a 120A analyzer. After a sufficient number of Edman degradation cycles, the remaining filter-bound polypeptides were cleaved *in situ* with CNBr. The filters with the adhering polypeptides were placed in Eppendorf tubes, 30 µl CNBr solution (0.2 g/ml 70% formic acid) was applied to the filters, and an extra 30 µl was placed in the bottom of each tube, below the filters, to keep them moist. Nitrogen gas was introduced, after which the tubes were sealed and incubated for 24 h in the dark. Following this treatment, the filters were dried under vacuum and reapplied to the sequencer.

Acknowledgements

This work was supported by grants to H.Prydz from the Research Council of Norway and the Norwegian Cancer Society. We are grateful to Professor K.Sletten for sequencing the amelogenins, to D.Sørensen and his staff for the use of the animal facilities and to Dr A.Hogseth for access to the PhosphorImager.

References

Brooks,S.J., Bonass,W.A., Kirkham,C. and Robinson,C. (1994) The human C-terminal sequence is completely homologous to the C-terminal sequence of amelogenin in all species so far studied. *J. Dent. Res.*, **73**, 716.

Cech,T.R. and Uhlenbeck,O.C. (1994) Hammerhead nailed down. *Nature*, **372**, 39–40.

Chen,E. *et al.* (1994) Regulation of amelogenin gene expression during tooth development. *Dev. Dyn.*, **199**, 189–198.

Cohn,S.A. (1957) Development of the molar teeth of the albino mouse. *Am. J. Anat.*, **101**, 295–320.

Diekwisch,T., David,S., Bringas,P.,Jr, Santos,V. and Slavkin,H.C. (1993) Antisense inhibition of AMEL translation demonstrates supramolecular controls ... enamel HAP crystal growth during embryonic molar development. *Development*, **117**, 471–482.

Fincham,A.G., Hu,Y., Lau,E.C., Slavkin,H.C. and Snead,M.L. (1991) Amelogenin post-secretory processing during biomineralization in the postnatal mouse molar tooth. *Arch. Oral Biol.*, **36**, 305–317.

Fincham,A.G. *et al.* (1994) Self-assembly of a recombinant amelogenin protein generates supramolecular structures. *J. Struct. Biol.*, **112**, 103–109.

Gasparutto,D. *et al.* (1992) Chemical synthesis of a biologically active natural tRNA with its minor bases. *Nucleic Acids Res.*, **20**, 5159–5166.

Gaunt,W.A. (1964) The development of the teeth and jaws of the albino mouse. *Acta Anat.*, **57**, 115–151.

Goodchild,J. and Kohli,V. (1991) Ribozymes that cleave an RNA sequence from human immunodeficiency virus: The effect of flanking sequence on rate. *Arch. Biochem. Biophys.*, **284**, 386–391.

Haseloff,J. and Gerlach,W.L. (1988) Simple RNA enzymes with new and highly specific endoribonuclease activities. *Nature*, **334**, 585–591.

Hertel,K.J. *et al.* (1992) Numbering system for the hammerhead. *Nucleic Acids Res.*, **20**, 3252.

Hewick,R.M., Hunkapiller,M.W., Hood,L.E. and Dreyer,W.J. (1981) A gas-liquid solid phase peptide and protein sequenator. *J. Biol. Chem.*, **256**, 7990–7997.

Iribarren,A.M. *et al.* (1990) 2′-*O*-alkyl oligoribonucleotides as antisense probes. *Proc. Natl Acad. Sci. USA*, **87**, 7747–7751.

Johansson,H.E., Belsham,G.J., Sproat,B.S. and Hentze,M.W. (1994) Target-specific arrest of mRNA translation by antisense 2′-O-alkyloligoribonucleotides. *Nucleic Acids Res.*, **22**, 4591–4598.

Lamond,A.I. and Sproat,B.S. (1993) Antisense oligonucleotides made of 2′-*O*-alkylRNA: their properties and applications in RNA biochemistry. *FEBS Lett.*, **325**, 123–127.

Lau,E.C., Mohandas,T.K., Saphiro,L.J., Slavkin,H.C. and Snead,M.L. (1989) Human and mouse amelogenin gene loci are on the sex chromosomes. *Genomics*, **4**, 162–168.

Lau,E.C. *et al.* (1992) Alternative splicing of the mouse amelogenin primary RNA transcript contributes to amelogenin heterogeneity. *Biochem. Biophys. Res. Commun.*, **188**, 1253–260.

Matsudaira,P. (1987) Sequence from picomole quantities of proteins electroblotted onto poly(vinylidene difluoride) membranes. *J. Biol. Chem.*, **262**, 10035–10038.

Paolella,G., Sproat,B.S. and Lamond,A.I. (1992) Nuclease resistant ribozymes with high catalytic activity. *EMBO J.*, **11**, 1913–1919.

Pley,H.W., Flaherty,K.M. and McKay,D.B. (1994) Three-dimensional structure of a hammerhead ribozyme. *Nature*, **372**, 68–74.

Pyle,A.M. (1993) Ribozymes: A distinct class of metalloenzymes. *Science*, **261**, 709–714.

Risnes,S. (1979a) A scanning electron microscope study of aberrations in the prism pattern of rat incisor inner enamel. *Am. J. Anat.*, **154**, 419–436.

Risnes,S. (1979b) The prism pattern of rat molar enamel: a scanning electron microscope study. *Am. J. Anat.*, **155**, 245–257.

Risnes,S. (1985) Multiangular viewing of dental enamel in the SEM: an apparatus for controlled mechanical specimen preparation. *Scand. J. Dent. Res.*, **93**, 135–138.

Sasaki,T., Goldberg,M., Takuma,S. and Garant,P.R. (1990) Cell biology of tooth enamel formation. Functional electron microscopic monographs. *Monogr. Oral Sci.*, **14**, 1–199.

Snead,M.L. *et al.* (1985) DNA sequence for cloned cDNA for murine amelogenin reveal the amino acid sequence for enamel-specific protein. *Biochem. Biophys. Res. Commun.*, **129**, 812–818.

Sproat,B.S., Lamond,A.I. and Paolella,G. (1994) *US Patent 5*, **334**, 711.

Termine,J.D., Belcourt,A.B., Christner,P.J., Conn,K.M. and Nylen,M.U. (1980) Properties of dissociatively extracted fetal tooth matrix proteins. I. Principal molecular species in developing bovine enamel. *J. Biol. Chem.*, **225**, 9760–9768.

Tuschl,T., Gohlke,C., Jovin,T.M., Westhof,E. and Eckstein,F. (1994) A three-dimensional model for the hammerhead ribozyme based on fluorescence measurements. *Science*, **266**, 785–789.

Uhlenbeck,O.C. (1987) A small catalytic oligoribonucleotide. *Nature*, **328**, 596–600.

Wagner,R.W. (1994) Gene inhibition using antisense oligodeoxynucleotides. *Nature*, **372**, 333–335.

Received on June 28, 1995; revised on August 14, 1995

Cell efficacy of Synthetic Ribozymes Targeting the Proto-oncogene c-*myb*: Site Selection and Optimization of Chemical Modifications

Thale C. Jarvis, Francine E. Wincott, Laverna J. Alby, James A. McSwiggen, Leonid Beigelman, John Gustofson, Anthony DiRenzo, Kurt Levy, Melissa Arthur, Jasenka Matulic-Adamic, Alexander Karpeisky, Carolyn Gonzalez, Tod M. Woolf, Nassim Usman, and Dan T. Stinchcomb

Running title- C-*myb* ribozyme site selection and chemistry optimization

Key words: Hammerhead ribozyme/Cell efficacy/C-*myb*/Phosphorothioate/ Smooth muscle cell

Summary

Expression of the proto-oncogene c-*myb* is necessary for proliferation of vascular smooth muscle cells. We have developed synthetic hammerhead ribozymes that recognize and cleave c-*myb*, thereby inhibiting cell proliferation. Herein, we describe a systematic method for the selection of hammerhead ribozyme cleavage sites, and optimization of chemical modifications that maximize cell efficacy. *In vitro* assays were used to determine the relative accessibility of the ribozyme target sites for binding and cleavage. Several ribozymes thus identified showed efficacy in inhibiting smooth muscle cell proliferation relative to catalytically inactive controls. One ribozyme was selected for further characterization. A combination of modifications including several phosphorothioate linkages at the 5'-end of the ribozyme and an extensively modified catalytic core resulted in substantially increased cell efficacy. A variety of different 2' modifications at positions U4 and U7 that confer nuclease resistance gave comparable levels of cell efficacy. These synthetic ribozymes have potential as therapeutics for hyperproliferative disorders such as restenosis and cancer.

Introduction

Since the discovery that certain naturally-occuring RNA motifs were capable of catalytically cleaving other RNAs in a sequence-specific manner, extensive studies have defined the sequence and structural characteristics that control the *in vitro* specificity and kinetics of these RNA enzymes or ribozymes [Cech, 1992 #19] [Symons, 1994 #124] [Tuschl, 1995 #166] [Usman, 1995 #126]. Ribozymes have a broad range of potential *in vivo* applications. These include the use of ribozymes as research tools for probing molecular mechanisms, the use of ribozymes to genetically engineer crops, and the use of ribozymes as therapeutics for human or animal diseases. Each of these applications requires that a ribozyme function efficiently within the intracellular environment. The sequence and structural features that promote potent intracellular activity of ribozymes are currently under study.

Several factors are likely to contribute to the intracellular efficacy of a ribozyme. A ribozyme must co-localize with its molecular target in the appropriate cellular compartment, and must be present at sufficiently high concentration to promote hybridization. In addition, its catalytic cleavage rate must be fast enough and its half-life must be long enough to allow cleavage of a substantial fraction of the target mRNA population. Finally, the cleavage site in the target mRNA must be accessible to ribozyme binding. When the ribozyme is made synthetically, a variety of modifications can be introduced to increase its half-life within the cell, to change its target sequence binding affinity, and possibly also to alter its intracellular trafficking properties. In this study, we have used chemically synthesized hammerhead ribozymes targeting the proto-oncogene c-*myb* to study different chemical modifications and sequence changes that affect cell efficacy. Expression of c-*myb* is necessary for cell-cycle progression in vascular smooth muscle cells [Kindy, 1986 #17] [Brown, 1992 #16]. Therefore, we have used proliferation of rat aortic smooth muscle cells as a measure of the efficacy of the ribozymes targeting c-*myb*.

Unmodified RNA is subject to rapid nuclease degradation upon exogenous delivery to cells or tissues. For example, the half-life of an all RNA hammerhead ribozyme in human serum is

less than 0.1 minute [Beigelman, 1995 #127]. In the literature there are several reports of exogenously delivered synthetic ribozymes showing efficacy in cell culture [Snyder, 1993 #118] [Lange, 1993 #114] [Kiehntopf, 1994 #119] [Sioud, 1994 #143]. Often these studies have utilized DNA/RNA chimeric ribozymes to enhance resistance to exonucleases, leaving large regions of unmodified RNA susceptible to endonucleolytic degradation. Extensive modification of the hammerhead ribozyme motif can give dramatic enhancement of the ribozyme half-life in biological fluids [Beigelman, 1995 #127] [Flory, 1996 #159]. Modifications of this type have been demonstrated to give efficacy *in vivo* [Lyngstadaas, 1995 #162] [Flory, 1996 #159].

Here we report on a systematic method for determining accessible ribozyme target sites, and for determining the optimal hammerhead ribozyme arm length required for cell efficacy. In addition, we explore the effect of chemical modifications such as those reported by Beigelman et al. [Beigelman, 1995 #127] on cell efficacy, using a smooth muscle proliferation assay as the primary endpoint. The result is a c-*myb* ribozyme that, when delivered exogenously to cells, results in substantial and reproducible inhibition of smooth muscle cell proliferation. The inactive ribozyme control has no effect, suggesting that the inhibition by active ribozyme is mediated by cleavage of the target RNA.

Materials and Methods

Ribozyme synthesis and sequences- Ribozymes were synthesized and purified as described [Wincott, 1995 #107] [Beigelman, 1995 #171] [Beigelman, 1995 #170]. The sequences and modifications of all of the active ribozymes used in this study are shown in Figure 1. The cleavage site numbering is based on the human DNA sequence numbering (Genbank accession number X52125; transciption starts at nucleotide 198). The inactive ribozymes contain identical binding arms and chemical modifications except that positions G5 and A14 in the catalytic core were changed to 2'-*O*-methyl uridine, thereby eliminating catalytic activity. The catalytic cleavage activity of all of the ribozymes was confirmed on a matched short substrate by standard methods; inactive ribozymes did not show detectable cleavage activity (data not shown).

Template RNA Transcription- A murine c-*myb* cDNA clone was obtained from Dr. Premkumar Reddy. Full length c-*myb* RNA was prepared by T7 transcription. Reactions contained 40 mM Tris pH 8.3, 10 mM $MgCl_2$,10 mM NaCl, 10 mM DTT[1], 4 mM spermidine, 250 μM each rATP, rGTP and rUTP, and 50 μM rCTP, 40 U RNase inhibitor (Boeghringer Mannheim), 80 μCi of α-CTP (40 μCi/μL; NEN) and 20 units of T7 Polymerase (United States Biochemical Corporation) in a volume of 20 μl and were incubated at 37 °C for two hours. The resulting internally-labeled transcripts were purified over a G50 spin column (Pharmacia).

In Vitro RNAse H Cleavage and Ribozyme Cleavage Reactions- Fifteen nucleotide long antisense DNA oligonucleotides were designed to anneal to potential hammerhead ribozyme binding sites in murine c-*myb*. 4 to 10 ng of internally-labelled murine c-*myb* transcript was incubated with 10 μM oligonucleotide plus 0.8 U RNAse H (Gibco BRL) in 20 mM Tris pH 7.9, 100 mM KCl, 10 mM $MgCl_2$, 0.1 mM EDTA, 0.1 mM DTT) at 37 °C for 60 minutes For the ribozyme cleavage assay, 1.0 μM Rz was incubated with 4 to 10 ng internally-labelled substrate in 75 mM Tris pH 8.0 and

10 mM $MgCl_2$ at 37 °C for 1 hour. Reactions were stopped by addition of formamide gel-loading buffer (95% formamide, 0.1% bromophenol blue, 0.1% xylene cyanol, 20 mM EDTA) and electrophoresed on a 6% denaturing acrylamide gel. Gels were dried and quantified on a phosphorimager.

Cell culture- Rat aortic smooth muscle cells (RASMC) were isolated from aortic tissue explants from 69-84 day-old female Sprague-Dawley rats (Harlan Sprague Dawley, Inc.) and assayed through passage six. RASMC were grown in DMEM supplemented with non-essential amino acids (0.1 mM of each amino acid), 0.1 mM sodium pyruvate, 100 U/ml penicillin, 100 µg/ml streptomycin, 2 mM L-glutamine, 20 mM Hepes (all from BioWhittaker) and 10% FBS (Hyclone Laboratories, Inc.).

Proliferation Assay.- Cells were plated in growth medium in 24-well plates at $5x10^3$ cells per well. After 24 hours, the medium was removed, cells were washed once with Dulbecco's phosphate buffered saline (DPBS) with Ca^{2+}/Mg^{2+}, and refed with starvation medium. Starvation medium is the same as growth medium except the concentration of FBS was reduced to 0.5% FBS. Cells were starved for 48-72 hours before ribozyme treatment. Ribozymes were diluted in serum-free DMEM with additives as above excluding antibiotics. LipofectAMINE (Gibco-BRL) was added to a final concentration of 3.6 µM DOSPA (= 7.2 µg/ml LipofectAMINE). Lipid/ribozyme mixtures were vortexed, incubated for 15 minutes at 37 °C and then added to cells which had been washed twice with DPBS with Ca^{2+}/Mg^{2+}. Cells were incubated with the lipid/ribozyme complexes at 37 °C for 2-4 hours, complexes were aspirated and cells were stimulated by the addition of growth medium. Control wells were treated with lipid only and stimulated with growth medium containing either 10% FBS or 0% FBS. All conditions were run in duplicate. At the time of stimulation, 10 µM BrdU (Sigma) was added. Cells were incubated for 20-24 hours, at which point the cells were fixed by the addition of cold 100% methanol plus 0.3% hydrogen peroxide for 30 minutes at 4 °C. The following reagents were used at room temperature to stain the BrdU

containing nuclei, with two DPBS washes between each step. 1) 2 M HCl for 20 minutes. 2) 1% horse serum in DPBS for 30 minutes. 3) anti-BrdU monoclonal antibody (Becton-Dickinson) diluted 1:200 in DPBS with 1% BSA and 0.5% Tween 20 for 1 hour. 4) biotinylated horse anti-mouse IgG in DPBS for 30 minutes. 5) ABC reagent (Pierce mouse IgG kit) in DPBS for 40 minutes. 6) DAB substrate (Pierce) DAB buffer for 7 minutes. 7) hematoxylin (Fisher) diluted 1:1 with distilled water for 1 minute. A minimum of 400 cells per well were counted under the microscope and the percent of proliferating cells (BrdU-stained nuclei/total nuclei) was determined. Unless otherwise indicated, each experiment was performed two or three times, and a representative experiment is presented. Calculation of % inhibition (AvsI)

Results

Target site selection strategy- Hammerhead ribozymes can recognize and cleave RNA sequences containing U followed by either A, C or U. This consensus sequence occurs very frequently; the murine c-*myb* mRNA contains nearly 500 potential hammerhead ribozyme cleavage sites. We wished to develop a systematic method of selecting sites that were amenable to ribozyme-mediated cleavage *in vivo*. Several criterion must be considered in selecting sites for optimal cleavage. First, the site must be accessible to ribozyme binding. In the intracellular milieu, different cleavage sites are likely to vary significantly in their accessibility to ribozyme binding. Site accessibility is probably determined by both secondary structure in the mRNA and regions of protein binding. In addition, the ribozyme itself must fold into the correct conformation required for binding and cleaving its substrate. Sequences in the substrate binding arms of the ribozyme can affect its propensity to fold correctly and cleave its target [Fedor, 1990 #167].

Hammerhead ribozyme cleavage sites having a high degree of homology between human [Majello, 1986 #59] and murine [Gonda, 1985 #163] c-*myb* sequences. Using a computer folding algorithm, we eliminated from consideration ribozymes that showed a high probability of forming undesirable intramolecular secondary structure[Christoffersen, 1994 #168]. Twenty-seven sites were selected for testing in an oligonucleotide binding assay. We designed DNA oligonucleotides spanning the cleavage sites, annealed these to a full length *in vitro* transcript of murine c-*myb*, and incubated in the presence of RNAse H. This enzyme recognizes DNA/RNA hybrids and cleaves the RNA transcript at the site of hybridization. Sites that are single-stranded and thus readily accessible to oligonucleotide binding are expected to show high levels of cleavage in this assay. Although the structure of the *in vitro* transcript may not mimic exactly the structure of the RNA in the cell, we hoped that this approach would at least allow us to identify and avoid regions of prominent local structure. The ribozyme structures are shown in Figure 1 and the results are shown in Figure 2.

Ribozymes targeting the most accessible sites, as determined by the RNAse H assay, were synthesized and tested for their ability to cleave the *in vitro* transcript under ribozyme excess (single turnover) conditions (Figure 2). In general, the sites that were accessible to oligonucleotide binding in the RNAse H assay are also susceptible to efficient cleavage by ribozymes. There were a few exceptions, such as sites 839 and 1363 in which the ribozyme cleavage is relatively inefficient. Several candidate ribozymes, indicated by the arrows, were selected for testing in cell culture.

Two regions of rat c-*myb* cDNA, encompassing the sites of interest, were sequenced (T. Jarvis, unpublished experiments). A single nucleotide difference between rat and murine c-*myb* was found in the 575 site; the other four sites were conserved. Active and inactive forms of the ribozymes targeting the five sites within rat c-*myb* were synthesized with an unmodified RNA catalytic core and five 2'-*O*-methyl residues in each binding arm. The inactive ribozymes contained two nucleotide changes in the catalytic core that eliminate cleavage activity. The effect of the ribozymes on proliferation of rat aortic smooth muscle cells (RASMC) was assessed (data not shown). Although four of the five active ribozymes did show statistically significant inhibition of proliferation, the degree of inhibition was relatively low (approximately 15-30% inhibition by the active ribozyme compared to the inactive ribozyme control). Poor performance in cell culture could be the result of rapid intracellular degradation. Beigelman et al. have reported extensive modifications designed to enhance the nuclease-resistance of hammerhead ribozymes while retaining catalytic activity [Beigelman, 1995 #127]. We decided to test such modifications, focusing on the ribozyme targeting site 575.

Effect of backbone and 2' sugar modifications on cell culture efficacy- Figure 3 shows the site 575 with and without a nuclease-stable core, and with and without phosphorothioate linkages in the binding arms. Active ribozymes with both a "stabilized" core and phosphorothioate linkages consistently gave enhanced inhibition of smooth muscle cell proliferation. For both the U4 2'-*C*-allyl and the U4,U7 2'-amino variants, there was significantly greater inhibition by the active ribozyme compared to the inactive control, suggesting that the inhibitory effect was mediated by

ribozyme cleavage of c-*myb* RNA. The inactive U4 2'-*C*-allyl ribozyme control showed no inhibition. The inactive U4,U7 2'-amino ribozyme did show some inhibition, although much less than its active counterpart.

Comparison of 5'-end versus 3'-end modifications- The results in Figure 3 indicate that both a nuclease-resistant core and phosphorothioate linkages in the binding arms are necessary for significant cell culture efficacy. Since phosphorothioate linkages are associated with some degree of cytotoxicity and non-specific effects [Sarmiento, 1994 #161] [Uhlmann, 1990 #160], we wished to determine the minimum number of phosphorothioates sufficient for cell efficacy. Figure 4A shows a comparison of ribozymes containing either 5 phosphorothioate linkages at the 5'-end, or 5 phosphorothioate linkages at the 3'-end, or 5 phosphorothioate linkages at both the 5'- and 3'-ends. The ribozyme containing phosphorothioates only at the 3'-end showed no efficacy, while the ribozyme containing phosphorothioates at the 5'-end showed equivalent efficacy to that containing phosphorothioates at both the 5'- and 3'-ends. In this experiment, the inactive ribozyme showed some inhibition relative to the vehicle-treated control. A ribozyme with scrambled sequence binding arms exhibited an equivalent degree of inhibition, indicating that this effect was not mediated by ribozyme binding, but was truly a "non-specific" effect on proliferation. Next, we compared ribozymes with varying numbers of phosphorothioates at the 5'-end (Figure 4B,C). The degree of efficacy gradually decreased as the number of phosphorothioate linkages was reduced. From these experiments we concluded that a minimum of four to five phosphorothioate linkages at the 5'-end is necessary to maintain optimal efficacy.

The ribozymes used in this study contained either 3'-phosphorothioate linkages, or a 3'-3' "inverted thymidine" modification [Seliger, 1994 #164] to protect against 3'-exonuclease activity. We have subsequently shown that the outcome of this assay is not particularly sensitive to the presence or absence of this 3'-protecting group. C-*myb* ribozymes containing various protecting groups including a 3'-3' inverted thymidine, a 3'-3' inverted abasic residue, a 3'- butanediol or no 3' protecting group at all showed equivalent efficacy in inhibiting smooth muscle cell proliferation (data not shown).

Optimization of binding arm length- Ribozymes targeting c-*myb* site 575 were synthesized with arm lengths ranging from five to twelve nucleotides. The effects of these ribozymes on cell proliferation is shown in Figure 5. The data are presented as specific inhibition by active versus inactive ribozyme. The optimal arm length was six to seven nucleotides. We confirmed in five separate experiments that there was no significant difference in efficacy between the 6/6 and 7/7 arm ribozymes (data not shown). We also tested ribozymes with asymmetric arm lengths (StemI/StemIII with 5/10 or 10/5 nucleotides). Both asymmetric variants performed similarly to the 7/7 symmetric ribozyme (data not shown). The symmetric ribozyme containing seven nucleotide binding arms (#2972) was used as a standard for comparison in the experiments that follow.

Effect of 2'-sugar and base modifications- Beigelman et al. [Beigelman, 1995 #127] [Beigelman, 1995 #170] [Beigelman, 1995 #171] have developed a broad spectrum of different modifications in the catalytic core of hammerhead ribozymes that enhance resistance to nuclease degradation while preserving significant catalytic activity. Differences in intracellular stability, cleavage rate and localization properties conferred by these modifications could contribute to the overall cell culture efficacy of the ribozyme. We tested several of these modifications, as shown in Figure 6. The data is presented as the specific inhibition (active versus inactive) of each ribozyme normalized to the specific inhibition of the U4 2'-*C*-allyl ribozyme (#2972). Surprisingly, there was relatively little difference in the cell efficacy exhibited by each of the modified ribozymes. Experiments performed at lower doses supported the conclusion that none of the variants differed by more than two-fold in the dose required to achieve 50% inhibition (data not shown). Some modifications did result in higher levels of non-specific inhibition. For example, inactive ribozymes with the U4,U7 amino modification consistently showed greater inhibition than inactive ribozymes containing any of the other modifications. Although the majority of experiments of performed with this ribozyme chemistry showed greater inhibition by the active version compared to the inactive, we have occasionally observed that the inactive ribozyme inhibition is equal to that of the active [Draper, 1996 #169].

Discussion

Using a systematic site selection strategy, we have identified c-*myb* ribozymes that inhibit cell proliferation when delivered exogenously to cultured vascular smooth muscle cells. The inhibition is mediated by ribozymes containing a catalytically active core, while inactive controls fail to inhibit. The degree of inhibition observed can be affected profoundly by both backbone and 2'-sugar modifications. The optimal ribozyme configuration for inhibition of cell proliferation in this system consists of four phosphorothioate linkages at the 5'-end, six or seven nucleotide binding arms, 30 2'-*O*-methyl residues, and any of a variety of 2'-sugar or base modifications at positions U4 and U7.

The results in Figures 3 and 4 clearly demonstrate the requirement for both a "stabilized" core and several 5'-phosphorothioate linkages in order to achieve significant ribozyme-mediated inhibition of smooth muscle cell proliferation. Beigelman et al. [Beigelman, 1995 #127] have shown that the U4-*C*-allyl and the U4,U7-amino ribozyme motifs increase the serum half-life of the ribozyme >16,000-fold relative to an all RNA ribozyme. Addition of 5'-phosphorothioate linkages increase the resistance to 5'-exonuclease activity [Draper, 1996 #169]. Thus, the enhanced cell efficacy observed with the combination of these two types of modifications could be attributed solely to enhanced resistance to both endonucleases and exonucleases. We cannot rule out the possibility that the phosphorothioate moieties are advantageous for some additional reason, such as conferring altered intracellular localization or trafficking properties. LipofectAMINE delivery results in virtually 100% of the cells taking up ribozyme, with a fairly homogeneous distribution within the population, as demonstrated by flow cytometry using a fluorescently-labeled ribozyme (data not shown). In addition, uptake studies using radioactive ribozymes show that the sheer number of ribozymes delivered to each cell exceeds the c-*myb* mRNA copy number by many orders of magnitude (data not shown). Therefore, a very small percentage of the ribozyme that is taken up could represent the "bioactive" fraction responsible for the observed efficacy. Although ribozyme intracellular localization can be studied using confocal microscopy, or by careful

fractionation, it is difficult to establish a meaningful correlation between cell efficacy and the observed localization of the bulk population.

The optimal hammerhead ribozyme binding arm-length for intracellular activity may be a function of the thermodynamic stability of the duplex formed upon substrate binding, the kinetics of substrate binding and release, or of competing intramolecular ribozyme structures that can compromise substrate binding or conformation of the catalytic core. We have found that there is a distinct arm-length optimum of six or seven nucleotides in each arm for the ribozyme targeting c-*myb* site 575. Depending on the sequence of the binding arms, the optimal arm-length could vary for ribozymes targeting different sites.

We have shown that a variety of different types of modifications at positions U4 and U7 can be tolerated while preserving a similar level of cell efficacy. The *in vitro* catalytic cleavage activities of the ribozymes were determined in single turnover assays on short substrates (data not shown). Although the ribozymes shown in Figure 6 are all catalytically active, the kinetics of substrate cleavage varies. For example, the cleavage rate for the U4,U7-amino c-*myb* site 575 ribozyme is at least ten-fold higher than that of either the U4-*C*-allyl or the U4 6-methyl-U ribozymes. Despite the lower cleavage activity, both the U4-*C*-allyl and the U4 6-methyl-U ribozymes perform as well or better than the U4,U7-amino ribozyme in inhibiting cell proliferation. Thus, there does not appear to be a strict correlation between the k_{obs} measured *in vitro* and the level of efficacy measured in cell culture in this system. This may indicate that some other step besides cleavage is rate limiting in the cell culture assay. Alternatively, the buffer conditions used for the *in vitro* cleavage assays may exacerbate differences between ribozymes that are less significant within the intracellular milieu.

The modified ribozymes used in this study show potential in specifically inhibiting cell proliferation. The combination of efficacy and resistance to nucleolytic degradation suggests that these ribozymes could have therapeutic utility in treating diseases resulting from inappropriate overexpression of c-*myb*. There are several disease conditions in which the disease pathology correlates with upregulation of c-*myb*. For example, in restenosis, vascular smooth muscle cells

hyperproliferate to form a neoinitima following coronary angioplasty, causing re-occlusion of arteries in 30-40% of patients [Landau, 1994 #155] [Jackson, 1992 #139] [Forrester, 1991 #154]. In the rat carotid artery model of restenosis, antisense DNA oligonucleotides targeting c-*myb* inhibit neointimal formation following balloon injury [Simons, 1992 #18]. In addition, c-*myb* has been implicated in the pathology of various cancers including melanoma [Hijiya, 1994 #110], leukemia [Ratajczak, 1992 #54], lymphosarcoma and colon carcinoma [Melani, 1991 #50]. We are continuing to explore new types of ribozyme modifications, as well as a variety of different formulations that can potentially enhance ribozyme delivery, efficacy and residence time in cells and tissues.

Acknowledgements-

We would like to thank Karyn Bouhana for assistance in isolating the primary smooth muscle cells, and Dr. Bharat Chowrira for critical reading of the manuscript.

References

Figure Legends

FIG. 1. **Sequence and structure of synthetic ribozymes used.**

The ribozymes used in this study are uniquely identified in the figure legends and text using the code number in the left column. The alias given in the second column is intended to highlight the salient modification or feature being compared. The last column gives the sequence and chemistry, using the following nomenclature: plain lowercase indicates 2'-*O*-methyl nucleotides, uppercase indicates 2'-hydroxyl (ribo) nucleotides, subscript s indicates phosphorothioate linkages (all other backbone linkages are phosphodiester), T indicates 3'-3' deoxythymidine. *U* at position U4 or U7 indicates either 2'-*C*-allyl uridine, 2'-amino uridine, 2'-fluoro uridine, 2'-hydroxyl 6-methyl uridine,

2'-deoxyabasic ribose, as indicated in the legend. Inactive versions are not shown; they are identical to the active ribozymes except that positions G5 and A14 have been changed to 2'-*O*-methyl uridine. (*) Certain ribozymes used in more than one figure (e.g., 2972) may be listed with a different alias depending on the relevant comparison being made in each figure.

FIG. 2. **Accessibility to binding and cleavage *in vitro*.**

DNA oligonucleotides corresponding to each ribozyme binding site were annealed to a full-length *in vitro* transcript of murine c-*myb*, and mixed with RNAse H as described in Materials and Methods. Ribozymes targeting sites that appeared to be accessible to oligonucleotide binding were synthesized and the cleavage activity against *in vitro* transcript was assessed. Data are expressed as percent of the full length transcript cleaved during a one hour assay. (*) indicates ribozymes that were selected for cell efficacy studies.

FIG. 3. **Cell efficacy of stabilized ribozymes.**

Ribozymes targeting c-*myb* site 575 were complexed with LipofectAMINE and delivered to rat aortic smooth muscle cells at a 100 nM dose. Cell proliferation was measured as described in Materials and Methods. Active and inactive versions of several different chemical modifications were tested. "2'-*O*-Me" indicates an RNA core with five 2'-*O*-methyl residues at the 5'- and 3'-ends (# 2360). "2'-*O*-Me P=S" indicates an RNA core with five 2'-*O*-methyl phosphorothioate residues at the 5'- and 3'-ends (#2557). "U4 *C*-allyl" and "U4 *C*-allyl P=S" indicate U4 2'-*C*-allyl "stabilized" cores without and with phosphorothioate linkages at the 5'- and 3'-ends (#2321, #2550, respectively). "U4,7 NH_2" and "U4,7 NH_2 P=S" indicate U4 and U7 2'-amino "stabilized" cores without and with phosphorothioate linkages at the 5'- and 3'-ends (#2320, #2547, respectively). Data are expressed as proliferation relative to the serum-stimulated control. Relative proliferation is calculated as follows: (%proliferation with ribozyme - %basal proliferation) ÷ (%proliferation with serum - %basal proliferation) x 100; error bars represent the range of duplicate wells.

FIG. 4. **Optimization of phosphorothioate content.**

Ribozymes targeting c-*myb* site 575 were complexed with LipofectAMINE and delivered to rat aortic smooth muscle cells at a 50 nM dose. Each of the ribozymes contained the U4 2'-*C*-allyl "stabilized" core and varying amounts of phosphorothioate. Active and inactive versions of the ribozymes were tested. A. "10 P=S" has five phosphorothioates at both the 5'- and 3'-ends (#2550); "5' P=S" has five phosphorothioates the 5' -end only (#2826); "3' P=S" has five phosphorothioates the 3' -end only (RPI#2828). B. A series of ribozymes containing decreasing number of 5'-phosphorothioate linkages were compared. 5 P=S (#2826), 4 P=S (#2972), 3 P=S (#2974), 2 P=S (#2976), or 1 P=S (#2978). C. Another experiment comparing "10 P=S" (#2550), "5 P=S" (#2826), or "4 P=S" (#2972). The results are expressed as proliferation relative to the serum-stimulated control as described in Fig. 3; error bars represent the range of duplicate wells.

FIG. 5. **Cell efficacy with varying length binding arms.**

Active and inactive versions of ribozymes targeting c-*myb* site 575 were synthesized with different length binding arms, complexed with LipofectAMINE and delivered to rat aortic smooth muscle cells at 50 nM and 100 nM as shown: 5/5 (#3862), 6/6 (#3206), 7/7 (#2972), 8/8 (#3212), 10/10 (#3210), 12/12 (#3208). Data are presented as specific inhibition by active ribozyme relative to inactive ribozyme. Specific inhibition is calculated as follows: (%proliferation with active ribozyme - %basal proliferation) ÷ (%proliferation with inactive ribozyme - %basal proliferation) x 100. Error bars represent the standard error of three to five separate assays.

FIG. 6. **Effects of alternative core modifications.**

Active and inactive versions of ribozymes targeting c-*myb* site 575 were complexed with LipofectAMINE and delivered to rat aortic smooth muscle cells at a 100 nM dose. Different modifications at positions U4 and U7 were compared: U4 2'-*C*-allyl (#2972); U4,U7 2'-*C*-allyl (#3257); U7 2'-*C*-allyl (#3259); U4,U7 2'-amino (#3267); U4 2'-fluoro (#3269); U4 6-methyl U (#3331); U4 deoxyabasic (#3083). All of the ribozymes contained seven nucleotide binding arms and four phosphorothioate linkages at the 5'-end. Ribozyme #2972 (U4 2'-*C*-allyl) was used as a standard of comparison; the specific inhibition of #2972 relative to its inactive counterpart was calculated as described in Fig. 5, and adjusted to 100%. Inhibition by each of the other modified ribozymes was normalized relative to that of #2972. The average inhibition from two to seven experiments with each ribozyme is shown; error bars represent the standard error of the mean.

---

[1] The abbreviations used are: DTT, dithiothreitol; RASMC, rat aortic smooth muscle cells; DMEM, Dulbecco's modified Eagle's medium; FBS, fetal bovine serum; DOSPA, 2,3-dioleyoxy-N-[2(speminecarboxamido)ethyl]-N,N-dimethyl-1-propanaminium trifluroroacetate; BrdU, 5-bromo-2'-deoxyuridine.

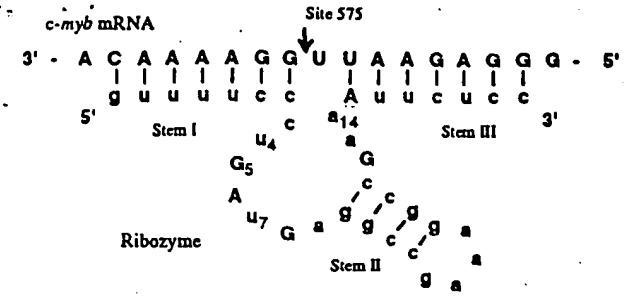

ID#	Alias	5' StemI•Core•StemIII 3'
Figure 1:		
2007	549	uuggcAA•CUGAUGAGGCCGAAAGGCCGAA•AAcagac
2008	551	gcuugGC•CUGAUGAGCGCGAAAGCGCGAA•AUaacag
2009	575	gcuuuCC•CUGAUGAGGCCGAAAGGCCGAA•AUucucc
2010	634	uguccAG•CUGAUGAGGCCGAAAGGCCGAA•AGguuuu
2011	738	uucuuGA•CUGAUGAGGCCGAAAGGCCGAA•AGcauua
2012	839	ucuucUG•CUGAUGAGGCCGAAAGGCCGAA•AAgcuug
2013	936	augugGU•CUGAUGAGGCCGAAAGGCCGAA•AUaggaa
2014	1017	gcuggCU•CUGAUGAGCGCGAAAGCGCGAA•AGggaca
2015	1082	auuccUU•CUGAUGAGGCCGAAAGGCCGAA•AUucgcu
2016	1363	uucug•CUGAUGAGGCCGAAAGGCCGAA•AUucuaa
2017	1553	accuuUU•CUGAUGAGGCCGAAAGGCCGAA•AUagcug
2018	1597	auguuUG•CUGAUGAGGCCGAAAGGCCGAA•AUggugu
2019	1598	cauguUU•CUGAUGAGGCCGAAAGGCCGAA•AAuggug
2020	1635	uucagGG•CUGAUGAGGCCGAAAGGCCGAA•ACcguau
2021	1721	cagcaAC•CUGAUGAGGCCGAAAGGCCGAA•AUuccag
2022	1724	acucaGC•CUGAUGAGGCCGAAAGGCCGAA•ACauuuc
2023	1895	agcuuGU•CUGAUGAGGCCGAAAGGCCGAA•AGauuau
2024	1909	ugccaUU•CUGAUGAGGCCGAAAGGCCGAA•AAacgga
2025	1943	cuuugAG•CUGAUGAGGCCGAAAGGCCGAA•ACauugu
Figure 2:		
2360	2'-*OMe*	guuuuCC•CUGAUGAGGCCGAAAGGCCGAA•AUucucc
2557	2'-*OMe*P=S	gsususususCC•CUGAUGAGGCCGAAAGGCCGAA•AUsusgsusgsc
2321	U4 *C*-allyl	guuuuccc•cUGAuGaggccgaaaggccGaa•AuucuccT
2550	U4 *C*-allyl P=S	gsususususcc•cUGAuGaggccgaaaggccGaa•AususgsusgsC
2320	U4,7 NH_2	guuuuccc•cUGAUGaggccgaaaggccGaa•AuucuccT
2547	U4,7 NH_2 P=S	gsususususcc•cUGAUGaggccgaaaggccGaa•AususgsusgsC
Figures 3 and 4:		
2550	10 P=S	gsususususcc•cUGAuGaggccgaaaggccGaa•AususgsusgsC
2828	3' 5 P=S	guuuuccc•cUGAuGaggccgaaaggccGaa•AususgsusgsC
2826	5' 5 P=S	gsususususcc•cUGAuGaggccgaaaggccGaa•AuucuccT
2972 *	4 P=S	gsusususucc•cUGAuGaggccgaaaggccGaa•AuucuccT
2974	3 P=S	gsususuucc•cUGAuGaggccgaaaggccGaa•AuucuccT
2976	2 P=S	gsusuuucc•cUGAuGaggccgaaaggccGaa•AuucuccT
2978	1 P=S	gsuuuucc•cUGAuGaggccgaaaggccGaa•AuucuccT
Figure 5:		
2972 *	7/7	gsusususucc•cUGAuGaggccgaaaggccGaa•AuucuccT
3206	6/6	ususususcc•cUGAuGaggccgaaaggccGaa•AuucuccT
3208	12/12	asCsasususguuuuucc•cUGAuGaggccgaaaggccGaa•AuucuccccuunnT
3210	10/10	asususgsuuuuucc•cUGAuGaggccgaaaggccGaa•AuucuccccuuT
3212	8/8	usgsususuucc•cUGAuGaggccgaaaggccGaa•AuucuccccT
3216	5/10	usususCsCc•cUGAuGaggccgaaaggccGaa•AuucuccccuuT
3214	10/5	asususgsuuuucc•cUGAuGaggccgaaaggccGaa•AuucuT
3862	5/5	ususususCsCc•cUGAuGaggccgaaaggccGaa•AuucuT
Figure 6:		
2972 *	U4 2'-*C*-allyl	gsususususcc•cUGAuGaggccgaaaggccGaa•AuucuccT
3257	U4,U7 2'-*C*-allyl	gsususususcc•cUGAUGaggccgaaaggccGaa•AuucuccT
3259	U7 2'-*C*-allyl	gsusususucc•cuGAUGaggccgaaaggccGaa•AuucuccT
3269	U4 2'-fluoro	gsusususucc•cUGAuGaggccgaaaggccGaa•AuucuccT
3331	U4 6-methyl U	gsusususucc•cUGAuGaggccgaaaggccGaa•AuucuccT
3267	U4,U7 2'-amino	gsusususucc•cUGAUGaggccgaaaggccGaa•AuucuccT
3083	U4 deoxyabasic	gsusususucc•cUGAuGaggccgaaaggccGaa•AuucuccT

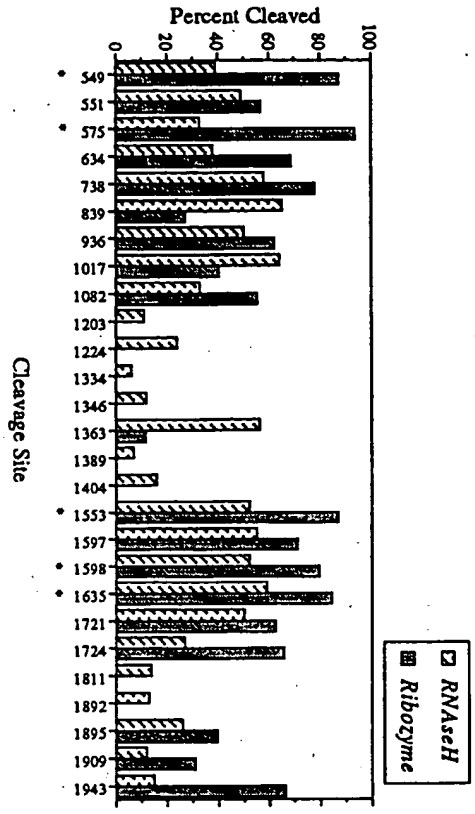
Percent Cleaved
0
20
40
60
80
100
Cleavage Site
549
551
575
634
738
839
936
1017
1082
1203
1224
1334
1346
1363
1389
1404
1553
1597
1598
1635
1721
1724
1811
1892
1895
1909
1943
RNAseH
Ribozyme

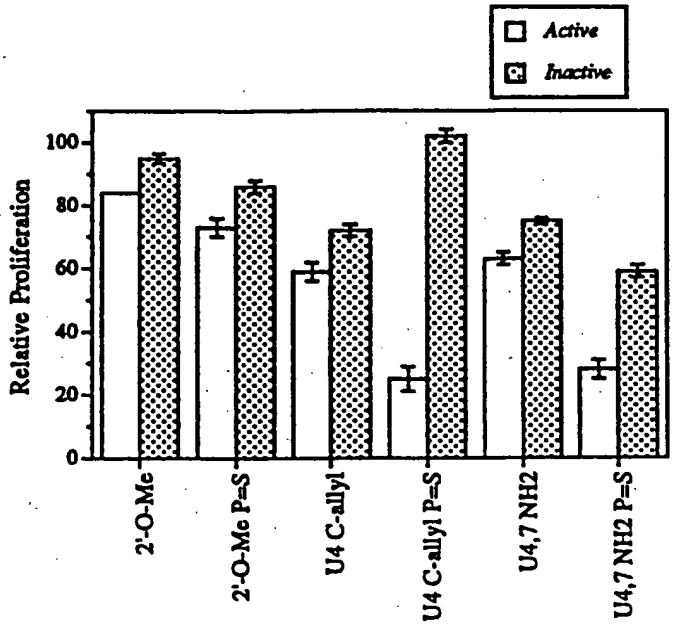
Active
Inactive
Relative Proliferation
100
80
60
40
20
0
2'-O-Me
2'-O-Me P=S
U4 C-allyl
U4 C-allyl P=S
U4,7 NH2
U4,7 NH2 P=S

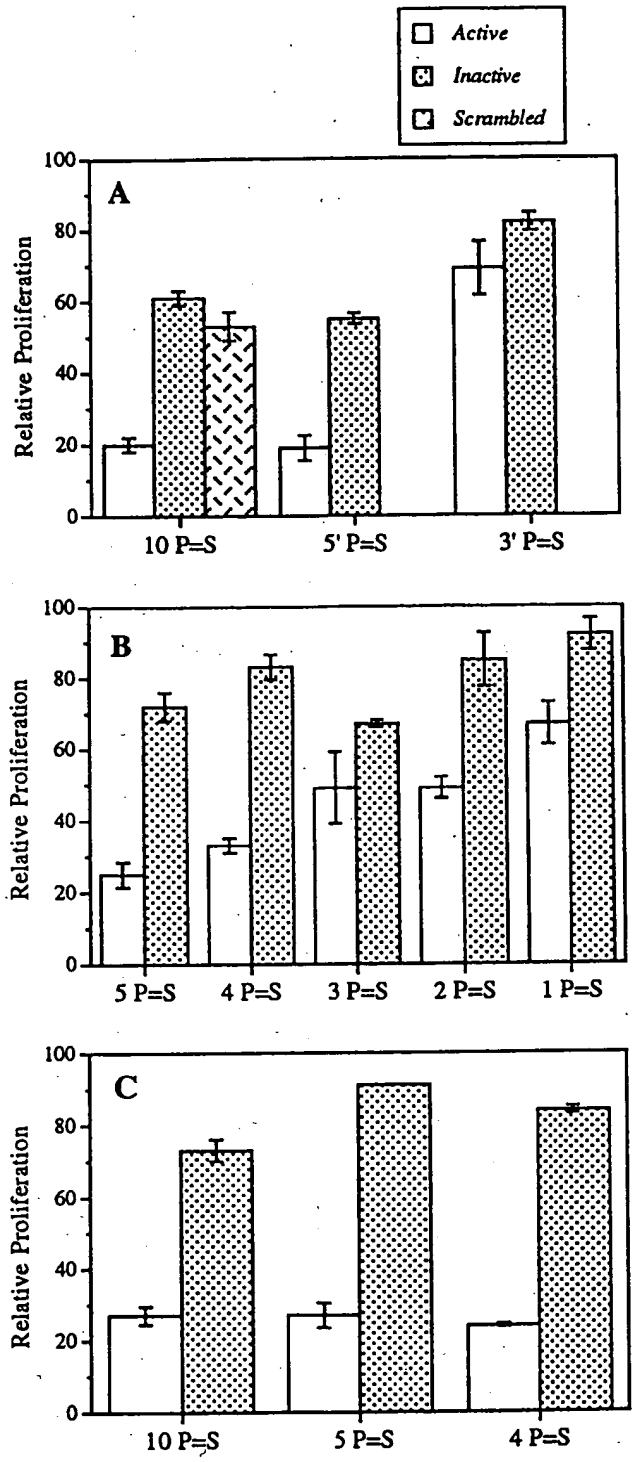
Active
Inactive
Scrambled
A
Relative Proliferation
100
80
60
40
20
0
10 P=S
5' P=S
3' P=S
B
Relative Proliferation
5 P=S
4 P=S
3 P=S
2 P=S
1 P=S
C
Relative Proliferation
10 P=S
5 P=S
4 P=S

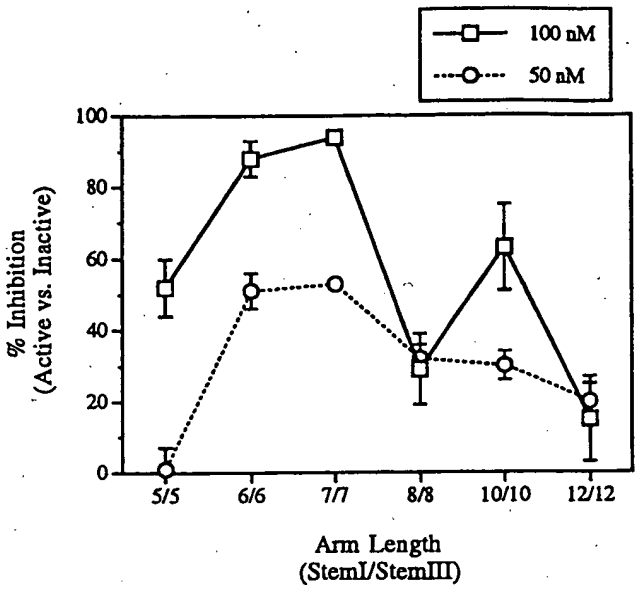
100 nM
50 nM
% Inhibition
(Active vs. Inactive)
100
80
60
40
20
0
5/5
6/6
7/7
8/8
10/10
12/12
Arm Length
(StemI/StemIII)

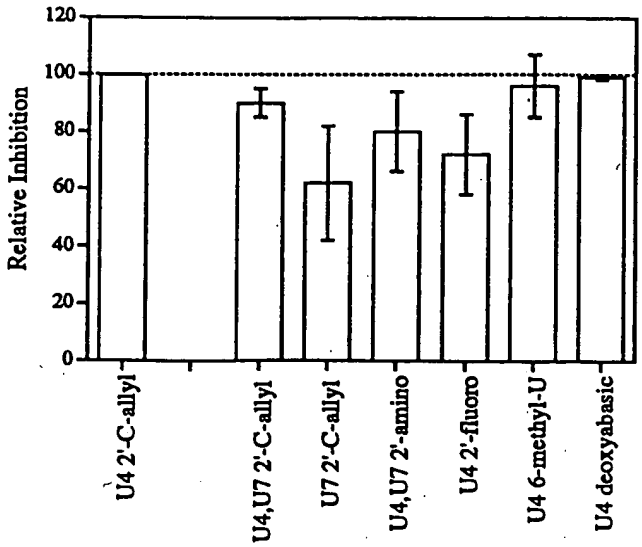
Relative Inhibition
120
100
80
60
40
20
0
U4 2'-C-allyl
U4,U7 2'-C-allyl
U7 2'-C-allyl
U4,U7 2'-amino
U4 2'-fluoro
U4 6-methyl-U
U4 deoxyabasic

Exhibit 12

Anti-flt-1 Ribozyme-Mediated Inhibition of Cell Proliferation